Conjugated organic and organoboron materials

Christopher Donald Entwistle

Conjugated Organic and Organoboron Materials

Christopher Donald Entwistle

Supervisor Professor Todd B. Marder

The University of Durham
Department of Chemistry

2005

Dedicated to the memory of Margay, a faithful and long time companion.

Abstract

A series of compounds containing one or more dimesitylboryl groups (mesityl = 2,4,6-trimethylphenyl) has been synthesised. Triarylboranes were synthesised by reaction of dimesitylfluoroborane with an appropriate lithium reagent. Dimesitylvinyl boranes were synthesised by the hydroboration of an appropriate terminal alkyne with dimesitylborane. Compounds were characterised by standard analytical techniques, and investigated by single crystal X-ray diffraction, optical, thermal and electrochemical methods. The aim of the research was to determine whether such compounds might be useful in the field of organic electronics. In addition, the compound dimesitylborane has been investigated by NMR techniques, which have shown it to exist as a monomer – dimer equilibrium in solution, and the structure of the dimer in the solid state has been more accurately determined using neutron diffraction.

List of Abbreviations

^{n}Bu	*neo*-butyl
^{t}Bu	*tert*-butyl
DCM	dichloromethane
DSC	Differential Scanning Calorimetry
DMF	dimethylformamide
EL	electroluminescence
Et	ethyl
E_{pa}	peak anodic potential,
E_{pc}	peak cathodic potential
EFISH	Electric Field Induced Second Harmonic Generation
EPR	Electron Paramagnetic Resonance
Fc	ferrocene
GC	gas chromatography
GC-MS	gas chromatography – mass spectrometry
GPC	gel permeation chromatography
h	hour/hours
HOMO	highest occupied molecular orbital
HLS	Harmonic Light Scattering
HRS	hyper Rayleigh scattering
LUMO	lowest unoccupied molecular orbital
Me	methyl
Mes	mesityl
MS	mass spectrometry
NLO	non-linear optical
NMR	nuclear magnetic resonance
MLCT	metal to ligand charge transfer
OAc	acetate
OLED	Organic Light-Emitting Diode
Ph	phenyl
PL	photoluminescence
q	8-hydroxyquinolato
SCE	standard calomel electrode
SHG	second harmonic generation
TBAP	tetrabutylammonium perchlorate
TGA	thermogravimetric analysis
THG	third harmonic generation
TMS	trimethylsilyl
TMSA	trimethylsilylacetylene
THF	tetrahydrofuran
UV-Vis	ultraviolet – visible
XRD	X-ray diffraction

Contents

List of Tables	vi
List of Figures and Schemes	viii
Declaration and Statement of Copyright	xvi
Acknowledgements	xvii
Chapter 1. Introduction	1
1.1. Compounds containing three – coordinate boron	1
1.1.1. Three – coordinate boron	1
1.1.2. Compounds containing the dimesitylboryl group	2
1.1.3. Nonlinear optical properties of unsymmetric and symmetric dimesitylboryl compounds	7
1.1.4. Conjugated polymers containing boron in the main chain	14
1.1.5. Electroluminescent and electron transporting properties of dimesitylboryl – containing compounds	25
1.1.6. Other donor-X-B$(Mes)_2$ systems for sensors	33
1.1.7. Triarylboranes as sensors	35
1.1.8. Nonlinear optical properties of boroxine-based octupolar compounds	41
1.2. Compounds containing four-coordinate boron	43
1.2.1. Four - coordinate boron	43
1.2.2. Rigid rods containing four – coordinate boron	43
1.2.3. Blue light emission from molecules containing four – coordinate boron	45
1.2.4. Boron – dipyrrin and dioxaborine – based material	49
1.3. Borane and carborane clusters	53

1.4. Summary 56

1.5 References 57

Chapter 2 Symmetric bis(dimesitylboryl)s: Optical, structural, electrochemical and thermal properties 63

2.1 Introduction 63

2.2. Results and Discussion 64

2.2.1. Synthesis 64

2.2.2. Structural Properties 71

2.2.3. Thermal Properties 83

2.2.4. Optical Properties 96

2.2.5. Electrochemical Properties 114

2.3. Conclusions and further work 121

2.4. Experimental 122

2.4.1. General Manipulations and Synthetic Techniques 122

2.4.2. Preparation of terminal acetylenes 123

2.4.3. Preparation of Bis(dimesitylborylvinyl)organoboranes 128

2.5 References 136

Chapter 3 Compounds Containing a Single Dimesitylboryl Group: Optical and Structural Properties 139

3.1. Introduction 139

3.2. Results and Discussion 139

3.2.1. Synthesis 139

3.2.2. Structural Properties 141

3.2.3. Thermal properties 150

3.2.4. Optical Properties 153

3.3. Conclusions and suggested further work 156

3.4. Experimental 157

3.4.1. General 157

3.4.2. Synthesis 157

3.4.2.1. Synthesis of 2-ethynylthiophene 157

3.4.2.2. Synthesis of dimesitylborylvinylbenzene (4a) 158

3.4.2.3. Synthesis of dimesitylborylvinyl-ortho-carborane (4b) 159

3.4.2.4. Synthesis of 2-dimesitylborylvinylthiophene (4c) 159

3.5. References 160

163

Chapter 4. Reaction of dimesitylborane with 2,5-diethynylpyridine: Unexpected formation of the novel tris-hydroboration product, 1-{dimesitylboryl}-2-{Z-1-dimesitylborylethylidene}-5-{E-dimesitylborylvinyl}-1,2-dihydropyridine.

4.1. Introduction 163

4.2. Results and discussion 164

4.2.1. Synthesis 164

4.2.2. Structural properties. 167

4.2.3. Thermal characteristics. 169

4.2.4. Optical properties. 171

4.2.5. Suggested reaction mechanism and computational analysis. 173

4.3. Conclusions 175

4.4. Experimental section. 175

4.4.1. General considerations 175

4.4.2. Preparation of 2,5-diethynylpyridine 175

4.4.3. Preparation of 1-{dimesitylboryl}-2-{Z-1-dimesitylborylethylidene}-5-{E-dimesitylborylvinyl}-1,2-dihydropyridine (5). 174

4.5. References 178

181

Chapter 5 Dimesitylborane Monomer-Dimer Equilibrium in Solution,the Solid-State Structure of the Dimer by Single Crystal Neutron and X-Ray Diffraction and Structural Comparisons with Related Compounds.

5.1. Introduction 171

5.2. Results and Discussion 184

5.2.1. NMR results 184

5.2.2 Variable concentration NMR study 186

5.2.3 Variable temperature NMR study 188

5.2.4. NMR study of dimesitylborane in supercritical carbon dioxide 189

5.2.5 Neutron and X-ray crystallography 193

5.2.6 Computational studies 195

5.3. Conclusions 199

5.4. Experimental 200

5.4.1. General 200

5.4.2 Synthesis 200

5.4.2.1. Preparation of dimesitylfluoroborane 200

5.4.2.2. Preparation of dimesitylborane 202

5.4.3. NMR experiments in $scCO_2$ 200

5.4.4. Computational methods 203

5.4.5. Neutron Structure Determinations 203

5.4.6. X-ray Structure Determinations 204

5.5. References 206

List of Tables

Table 1.1	Absorption and fluorescence maxima and quantum yields for selected *p*-substituted phenyl(dimesityl)boranes in cyclohexane and dichloromethane.	3
Table 1.2	Absorption maxima and first and second-molecular hyperpolarisibilities for selected D-A organoboranes.	9
Table 1.3	UV-vis absorption and emission maxima, second molecular hyperpolarisibility and reduction potentials for symmetric bis-boryls of the form Mes_2B-X-$BMes_2$	12
Table 1.4	Weight Average Molecular Weight, Number Average Molecular Weight, UV-vis Absorption and Emission Maxima for Selected Organoboron Polymers.	23
Table 1.5	Glass Transition Temperatures (T_g), UV-vis Absorption and Emission Maxima, Quantum Yield (Φ_f) and Oxidation and Reduction Potentials for the Compounds FlAMB-nT	33
Table 2.1	Selected bond lengths and bond angles for 2a.	73
Table 2.2	Selected bond lengths for 2c and 2f.	74
Table 2.3	Selected bond angles for Compound 2c and 2f.	75
Table 2.4	Selected bond torsion angles for Compounds 2a, 2c and 2f	77
Table 2.5	Thermal characteristics of selected bis(boryl)s.	84
Table 2.6	Optical properties of symmetric bisboryls, Mes_2B-X-$BMes_2$	99
Table 2.7	Reduction potentials of compounds containing the dimesitylboryl group.	114
Table 3.1	Selected bond lengths and angles for Compound 4a	141
Table 3.2	Selected bond lengths for Compound 4c	142
Table 3.3	Selected bond angles for Compound 4c	143
Table 3.4	Selected bond lengths and angles for Compound 5	144
Table 3.5	Selected bond torsion angles for Compounds 4a, 4c and 5	145

Table 4.1	Selected bond lengths (Å) and bond angles (°) for compound 6	168
Table 4.2	Calculated energies of Intermediates A-D and of model compound 6.	174
Table 5.1	$^{1}H\{^{11}B\}$ NMR chemical shifts and relative intensities in C_6D_6 at ambient temperature.	185
Table 5.2	Selected bond lengths and angles for the borane dimers $R_4B_2H_2$ by X-ray (R = Mes), neutron (R = Mes) and electron diffraction (R = Me, H) methods.	197
Table 5.3	Selected bond lengths and angles for the MP2/6-31G* optimised dimesitylborane monomer and dimesitylfluoroborane and for the structures of dimesitylfluoroborane and ditripylborane solved by X-ray diffraction.	195
Table 5.4	Total and binding energies for selected boranes at the HF/6-31G* level of theory. A positive sign in the binding energy indicates that the dimer is lower in energy than the separated monomers.	199

List of Figures and Schemes

Figure 1.1.1	Schematic diagram illustrating the shielding of the vacant p-orbital in trimesitylborane (1)	2
Figure 1.1.2	General form of aryldimesitylboranes (2)	3
Figure 1.1.3	Dipolar and ground-state configurations of dimesityl[*p*-(dimethylamino)phenyl]borane (2a)	3
Figure 1.1.4	N-[5-hydroxy-8-(4-dimesitylborylphenylazo)-1-naphthyl]amine (3)	4
Figure 1.1.5	*p*-Bis(dimesitylboryl)benzene (4a)	4
Scheme 1.1	Scheme 1.1.1. Sequential reduction of bis-boryl π–conjugated rods	6
Figure 1.1.6	1,4-bis(dimesitylboryl)-1,4-dihydropyrazine (5a) and 4,4'-bis(dimesitylboryl)-1,1'-4,4'-tetrahydro-4,4'-bipyridiylidene (5b)	7
Figure 1.1.7	General form of (arylalkynyl)dimesitylboranes (6) and arylvinyl)dimesitylboranes (7).	8
Figure 1.1.8	1,4-Bis(dimesitylborylvinyl)benzene (8a, n=1) and 4,4'-bis(dimesitylborylvinyl)biphenyl (8b, n=2).	11
Figure 1.1.9	4-[4'(dimethylamino)phenylazo]phenyldimesitylborane (BNA)	13
Figure 1.1.10	5-(Dimesitylboryl)-5'(pyrrolidin-1-yl)-2,2'-bithiophene (9b) and 5-(dimesitylboryl)-2,2':5',3''-terthiophene (9c).	14
Figure 1.1.11	Polyurethane with pendant boron chromophore (P1).	14
Figure 1.1.12	Boron-containing polymers related to poly(phenylenevinylene) (P2a-g)	17
Figure 1.1.13	General form of poly(*p*-phenylene) (P5) and poly(ethynylene-phenylene-ethynylene) (P6) organoboron polymers	18
Scheme 1.2	Boration copolymerisation between diboron compound and a diisocyanate (P7)	20

Figure 1.1.14	General form of poly(cyclodiborazane) polymers P8-P10.	21
Figure 1.1.15	Nature of the group X for series P9	22
Figure 1.1.16	Nature of the group X in the series P10	23
Figure 1.1.17	Thiophene based boron-containing polymers (P11).	24
Figure 1.1.18	Schematic representation of a typical three-layer OLED	26
Figure 1.1.19	8-hydroxyquinoline and schematic structure of Alq_3	26
Figure 1.1.20	BMB-2T (n = 2) and BMB-3T (n = 3)	27
Figure 1.1.21	TPD	28
Figure 1.1.22	TBB	29
Figure 1.1.23	*o*-TTA	29
Figure 1.1.24	m-MTDATA	29
Figure 1.1.25	TMB-TB.	31
Figure 1.1.26	MB-TTPA.	32
Figure 1.1.27	General form of FlAMB-nT molecules.	33
Figure 1.1.28	General form of *ortho*-substituted (aminoaryl)diarylboranes (10).	34
Figure 1.1.29	*trans*-4'-N,N-diphenylamino-4-dimesitylborylstilbene (11a) and *trans*-2-[(4'-N,N-diphenylamino)styryl]-5-dimesitylborylstilbene (11b).	35
Figure 1.1.30	Trianthrylborane (12) and 9,10-bis(di-9-anthrylboryl)anthracene (13).	36
Figure 1.1.31	Dibenzoborole-containing systems (14).	37
Figure 1.1.32	General form of tris(phenylethynylduryl)boranes (15).	38
Figure 1.1.33	Tris[*p*-(2,2'-dipyridylamino)phenylduryl]borane (16a).	39
Figure 1.1.34	Compounds 17a-e	40

Figure 1.1.35	Compounds 18a-c	41
Figure 1.1.36	Boroxine-based molecules where X = OMe (19a), SMe (19b) or NMe_2 (19c)	42
Figure 1.2.1	{4',-[methyl(diphenyl)phosphonio]biphenyl-4-yl}triphenylborate (PBB) and Me_3N^+-Ph-CH=CH-CH=CH-Ph-$^-BBu_3$ (20)	44
Figure 1.2.2	Stilbazole and stilbazole - borane adducts (21a-c)	45
Figure 1.2.4	Schematic structure of lithium tetra-(8-hydroxyquinolato) boron (22)	46
Figure 1.2.5	General form of BR_2q compounds (23a-c)	47
Figure 1.2.6	7-azaindole and the diborate complex $B_2(\mu\text{-}O)Ph_2(azain)_2$ (24b)	48
Figure 1.2.7	1,6-bis(2-hydroxy-5-methylphenyl)pyridinediyl boron fluoride (25b)	49
Figure 1.2.8	$BPh_2(pybm)$ (26)	49
Figure 1.2.9	*N,N'*-bis(α-naphthyl)-*N-N'*-diphenyl-1,1'-biphenyl-4,4'-diamine (NPB)	49
Figure 1.2.10	General form of the boron-dipyrrin fluorophore (27)	50
Figure 1.2.11	Optically active boron-dipyrrin dye (28)	50
Figure 1.2.12	Bis(dioxaborine) based materials (29a-c)	52
Figure 1.3.1	Precursor to tropyl – cyclopentadienyl substituted dicarbadodecaborane (30)	54
Scheme 2.1	Synthesis of symmetric bis(dimesitylborylvinyl) compounds	65
Figure 2.1	Nature of the π-system, x, in acetylenes and boryl compounds.	65
Scheme 2.2	Synthesis of bis-terminalalkynes via Sonogashira reaction	67

Scheme 2.3	Mechanism for the Sonogashira reaction, showing generation of postulated active catalyst from $(Ph_3P)_2PdCl_2$.	68
Scheme 2.4	Synthesis of *trans*-4,4'-dibromostilbene	69
Scheme 2.5	Preparation of terminal alkyne 1i	69
Scheme 2.6	Synthesis of symmetric bis(dimesitylboryl) compounds.	70
Figure 2.2	ORTEP diagram of the molecular structure of 1,4-bis(dimesitylborylvinyl)benzene (2a) (50 % thermal ellipsoids).	78
Figure 2.3	Unit cell of 1,4-bis(dimesitylborylvinyl)benzene (2a) , showing large void spaces and propeller – like configuration about the boron atoms.	79
Figure 2.4	ORTEP diagram of the molecular structure of 2,5-bis(dimesitylborylvinyl)thiophene (2c) (50 % thermal ellipsoids).	80
Figure 2.5	ORTEP diagram of the molecular structure of 4,4'-bis(dimesitylborylvinyl)biphenyl (2f) (50 % thermal ellipsoids).	81
Figure 2.6	Ball and stick diagrams of (from top) compounds 3a, 3b, 2a, 2f, and 2c (*cisoid* and *transoid* conformations), showing planarity of the compounds (excluding mesityl groups).	82
Figure 2.7	Weight loss as a function of temperature for compound 2a.	86
Figure 2.8	DSC curve for compound 2a.	86
Figure 2.9	Weight loss as a function of temperature for compound 2b	87
Figure 2.10	DSC curve for compound 2b.	87
Figure 2.11	Weight loss as a function of temperature for compound 2c.	88
Figure 2.12	DSC curve for compound 2c.	88
Figure 2.13	Weight loss as a function of temperature for compound 3a.	89
Figure 2.14	DSC curve for compound 3a.	90
Figure 2.15	Weight loss as a function of temperature for compound 3b.	90

Figure 2.16	Weight loss as a function of temperature for compound 2f.	91
Figure 2.17	DSC curve for compound 2f.	92
Figure 2.18	Weight loss as a function of temperature for compound 2h.	92
Figure 2.19	DCS curve for compound 2h.	93
Figure 2.20	DSC curve for compound 2g	94
Figure 2.21	Weight loss as a function of temperature for compound 2g, with a consant heating rate of 10 °C min^{-1}.	95
Figure 2.22	Weight loss as a function of temperature for compound 2g, with sample heated to 150 °C, maintained at this temperature for 1h, cooled to 60 °C and finally heated until decomposition occurred.	95
Figure 2.23	Schematic representation of transitions resulting from absorption (blue), fluorescence (red) and vibrational relaxation.	98
Figure 2.24	Absorption (blue) and fluorescence (red) spectra for 1,4-bis(dimesitylborylvinyl)benzene (2a).	102
Figure 2.25	Absorption (blue) and fluorescence (red) spectra for 1,4-bis(dimesitylborylvinyl)tetrafluorobenzene (2b)	102
Figure 2.26	Absorption (blue) and fluorescence (red) spectra for 2,5-bis(dimesitylborylvinyl)thiophene (2c).	103
Figure 2.27	Absorption (blue) and fluorescence (red) spectra for 1,4-bis(dimesitylboryl)benzene (3a).	104
Figure 2.28	Absorption (blue) and fluorescence (red) spectra for 2,5-bis(dimesitylboryl)thiophene (3b).	104
Figure 2.29	Absorption (blue) and fluorescence (red) spectra for 4,4'-bis(dimesitylborylvinyl)biphenyl (2f)	107
Figure 2.30	Absorption (blue) and fluorescence (red) spectra for 4,4'-bis(dimesitylborylvinyl)fluorene (2g)	107
Figure 2.31	Absorption (blue) and fluorescence (red) spectra for 4,4'-bis(dimesitylborylvinyl)stilbene (2h).	108

Figure 2.32	Absorption (blue) and fluorescence (red) spectra for 4,4'-bis(dimesitylborylvinyl)tolan (2i)	108
Figure 2.33	Absorption (blue) and fluorescence (red) spectra 3-ring all H (2j)	109
Figure 2.34	Absorption (blue) and fluorescence (red) spectra 3-ring-F4 (2k)	109
Figure 2.35	Schematic representation of *cisoid* and *transoid* conformations of 2e, showing relative steric favourability.	111
Figure 2.36	Absorption (blue) and fluorescence (red) spectra for 9,10-bis(dimesitylborylvinyl)anthracene (2d).	112
Figure 2.37	Absorption (blue) and fluorescence (red) spectra for 1,4-bis(dimesitylborylvinyl)naphthalene (2e)	112
Figure 2.38	Absorption (blue) and fluorescence (red) spectra for 9,10-bis(dimesitylboryl)anthracene (3b).	113
Figure 2.39	Cyclic voltammogram of compound 4a.	116
Figure 2.40	Cyclic voltammogram for compound 2a. (THF / 0.1 M $TBABF_4$, 0.2 Vs^{-1})	117
Figure 2.41	Cyclic voltammogram of compound 2b (THF / 0.1 M $TBABF_4$, 0.2 Vs^{-1})	117
Figure 2.42	Cyclic voltammogram of compound 2c (DCM / 0.1 M $TBABF_4$, 0.2 Vs^{-1})	118
Figure 2.43	Cyclic voltammogram of compound 3b (THF, 0.1M $TBABF_4$, 0.2 Vs^{-1})	118
Figure 2.44	Cyclic voltammogram for compound 2h (DCM / 0.1 M $TBABF_4$, 0.2 Vs^{-1})	120
Figure 2.45	Plot of peak current vs. the square root of the scan rate for compound 2h, establishing electrochemical reversibility.	120
Scheme 3.1	Synthesis of dimesitylvinylboranes, 4a-c.	140
Scheme 3.2	Synthesis of *p*-dimesitylborylbromobenzene (5)	140

Figure 3.1	ORTEP diagram of the molecular structure of dimesitylborylvinylbenzene (4a) (50% thermal ellipsoids)	147
Figure 3.2	ORTEP diagram of the molecular structure of dimesitylborylvinylthiophene (4c) (50% thermal ellipsoids)	148
Figure 3.3	ORTEP diagram of the molecular structure of *p*-dimesitylborylvinylbromobenzene (5) (50% thermal ellipsoids)	149
Figure 3.4	Weight loss as a funtion of temperature for Compound 4a (heating rate 10 ^{o}C min^{-1})	151
Figure 3.5	DSC curve for Compound 4a (heating rate 10 ^{o}C min^{-1})	151
Figure 3.6	Weight loss as a funtion of temperature for Compound 4a (heating rate 10 ^{o}C min^{-1})	152
Figure 3.7	DSC curve for Compound 4a (heating rate 10 ^{o}C min^{-1})	152
Figure 3.8	Absorption (blue) and fluorescence (red) spectra for Compound 4a	154
Figure 3.9	Absorption and fluorescence spectra for Compound 4c	155
Figure 3.10	Absorption (blue) and fluorescence (red) spectra for Compound 4b	155
Scheme 4.1	Reaction of dimesitylborane with 1,4-diethynylbenzene, forming compound 2a.	164
Scheme 4.2	The expected and observed reactions of dimesitylborane with 2,5-diethynylpyridine.	165
Scheme 4.3	Reaction of Mes_2BF·pyridine with organolithium reagents (R = Ph (7a), , Bu, (7b) 3-pyridyl (7c)).	166
Figure 4.1	^{1}H-NMR spectrum of Compound 6 (400 MHz, C_6D_6).	167
Figure 4.2	Molecular structure of compound 5, with thermal ellipsoids at 50% probability and hydrogen atoms omitted for clarity.	169
Figure 4.3	Weight loss as a function of temperature for compound 5 (scan rate 10 ^{o}Cmin^{-1}).	170
Figure 4.4	DSC curve for compound 5 (scan rate 10 ^{o}C min^{-1}).	171

Figure 4.5	UV-visible absorption spectrum of compound 5 in cyclohexane solution.	172
Scheme 4.4	Suggested reaction mechanism in the formation of compound 6. For synthesis, X = C≡CH, R = Mes; for calculations, X = H, R = 2,6-$Me_2C_6H_3$.	173
Scheme 5.1	Schematic representation of dimesitylborane dissociation.	183
Figure 5.1	Monomeric boranes ditripylborane, dithexylborane and catecholborane.	183
Figure 5.2	Monomeric forms of boranes known to exist in both monomeric and dimeric forms in solution, bis(pentafluorophenyl)borane and 10-trimethylsilyl-9-borabicyclodecane-H.	183
Figure 5.3	$^1H\{^{11}B\}$ NMR spectrum of dimesitylborane	186
Figure 5.4	Effect of varying dimesitylborane concentration on $^{11}B\{^1H\}$ spectra, normalised to monomer intensity.	187
Figure 5.5	Plot of concentration (monomer)^2 vs. concentration (dimer), ^{11}B-data (▲) and ^1H-data (■).	187
Figure 5.6	Effect of varying temperature on the $^{11}B\{^1H\}$ spectrum of dimesitylborane.	188
Figure 5.7	van't Hoff plot showing variation of K_{diss} with temperature.	189
Figure 5.8	$^{11}B\{^1H\}$ NMR spectrum of dimesitylborane in $scCO_2$ (348 K, 190 bar) showing both monomer and dimer resonances and decomposition products.	192
Figure 5.9	^{11}B NMR spectrum of dimesitylborane in $scCO_2$ (348 K, 190 bar) demonstrating B-H coupling in the monomer.	192
Figure 5.10	ORTEP diagram of the molecular structure of $[Mes_2BH]_2$ (neutron data, 50% thermal ellipsoids) with all hydrogen atoms except the bridging hydrogens omitted for clarity.	194
Figure 5.11	Ball and stick diagram of the optimised geometry of Mes_2BH at the MP2/6-31G* level.	197
Figure 5.12	nd stick diagram of the optimised geometry of Mes_2BF at the MP2/6-31G* level.	198

Declaration

The material contained within this thesis has not been previously submitted for a degree at the Univeristy of Durham or any other institution. Except where indicated in the text, all research was performed by Mr. Christopher D. Entwistle.

Statement of Copyright

Acknowledgements

Firstly I would like to thank my supervisor, Professor Todd B. Marder, for the opportunity to conduct this research, and for his guidance and patience. I would also like to thank the members of the Marder research group, past and present – Jacquie, Jon, Dave, Andrew, Nathan and Ibraheem – for their help and support. Special thanks go to Dr. Rhodri L. Thomas for his excellent tuition and to Dr. R. Ben Coapes for advice, support and many evenings spent putting the world to rights in the various nightspots in and around Durham City. I would also like to thank the technical members of staff that have been associated with the Marder research group; Miss Judith Magee and especially Mr. Brian Hall for his good company and advice and for helping to keep the lab running smoothly. The technical services in the Chemistry department have been of consistently high quality, and I would like to thank all those people who provide the various services and in particular to thank Dr Alan Kenright and Mr. Ian McKeag from the NMR facility. I would also like to thank the members of academic staff who have assisted me during my time at Durham, with special thanks to Dr. Keith Dillon, Dr Andrew Beeby, Dr. Paul Low and Dr. Mark Fox.

On a more personal level, many people have been important to me during my studies; Stephanie Cornet, Kelly Flook and Richard Gover, all of whom studied at the University of Durham at one time. Of course, I am forever grateful for the support of my parents, without whom none of this would have been possible. Lastly, I would like to give my thanks and love to my friend and partner Rachel Woodward, who has been, and still remains, my dearest companion.

Introduction

1.1. Compounds containing three-coordinate boron

1.1.1. Three - coordinate boron

With its vacant p_z orbital, three-coordinate boron is inherently electron poor and is a strong π-electron acceptor, which can lead to significant delocalisation when conjugated with an adjacent organic π-system. Unlike other strong π-acceptors, however, in three-coordinate organoboranes, boron may even function as a σ-donor due to its low electronegativity compared with carbon. [1] The boron p_z orbital is readily attacked by nucleophiles such as water, resulting in either bond cleavage or the formation of a four-coordinate borate species, which can no longer participate effectively in conjugation with adjacent π-systems. As with many other low-coordinate systems, a common strategy in the synthesis of three-coordinate boranes is to provide kinetic stability by blocking the approach of nucleophiles with sterically demanding substituents. Bulky aryl groups, such as the mesityl (2,4,6-trimethylphenyl), fluoromesityl (2,4,6-tris(trifluoromethyl)phenyl) or tripyl (2,4,6-triisopropylphenyl) groups are particularly effective, as steric conjestion around boron results in the formation of propeller-like structures where the *ortho*-substituents on the aryl ligands form a "cage" around the vacant p_z orbital. This is particularly apparent in trimesitylborane (**1**), which is an exceptionally unreactive borane.

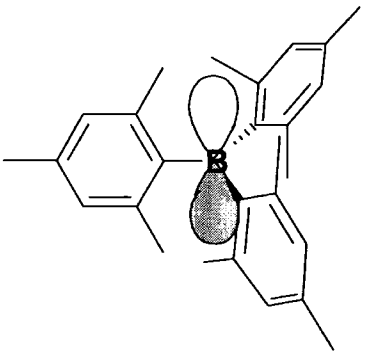

Figure 1.1.1. Schematic diagram illustrating the shielding of the vacant p-orbital in trimesitylborane (1)

1.1.2. Compounds containing the dimesitylboryl group

In 1971, Williams and co-workers, who were investigating the photochemistry of organoboron compounds at Kodak, discovered that whilst triphenylborane was subject to photodegradation in the presence of donor solvents, trimesitylborane was photochemically inert in all solvents. [2] Furthermore, they discovered that two mesityl groups were sufficient to provide an unusual degree of stability, which encouraged them to embark upon a photophysical study of *p*-substituted aryldimesitylboranes (**2**). [3] Quantum yields were measured in a variety of solvents, and were generally increased by the introduction of electron-donating groups. For example, in cyclohexane, dimesityl[*p*-(N,N-diphenylamino)phenyl]borane and dimesityl[*p*-(dimethylamino)phenyl]borane (**2a**) had quantum yields of 0.88 and 0.42 respectively, whereas dimesityl[*p*-cyanophenyl]borane had a quantum yield of only 0.016. It was also noted that although solvent polarity had little effect on the position of the absorption maxima, compounds bearing an electron donor exhibited large bathochromic shifts in their fluorescence maxima on increasing solvent polarity. This indicated that the compounds had low dipole moments in the ground state, but much higher dipole moments in the first excited-singlet state, which were better stabilised

by polar solvents. This dipolar form can only be formed if the boron atom is capable of conjugating with the organic π-system.

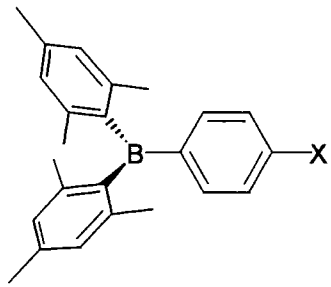

Figure 1.1.2. General form of aryldimesitylboranes (2)

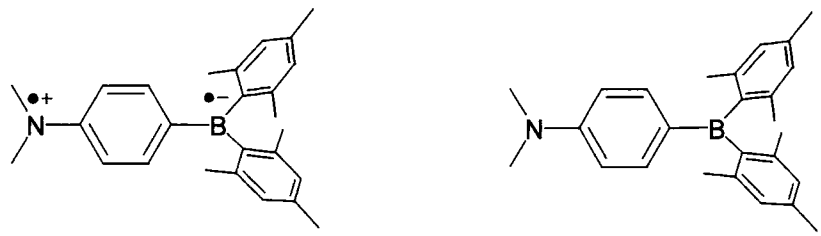

Figure 1.1.3. Dipolar and ground-state configurations of dimesityl[*p*-(dimethylamino)phenyl]borane (2a)

Table 1.1. Absorption and fluorescence maxima and quantum yields for selected *p*-substituted phenyl(dimesityl)boranes in cyclohexane and dichloromethane.

X	λ_{max}(abs) C_6H_{12}	λ_{max}(em) C_6H_{12}	ϕ_f C_6H_{12}	λ_{max}(abs) CH_2Cl_2	λ_{max}(em) CH_2Cl_2	ϕ_f CH_2Cl_2
$N(CH_3)_2$	353	386	0.42	359	491	0.28
$N(C_6H_5)_2$	377	412	0.88	379	469	0.71
$N(CH_2)_5$	354	392	0.43	361	497	0.27
$N(CH_2CH_2)_2O$	345	383	0.43	349	472	0.25
CN	328	394	0.016	326	444	0.032

The group later experimented with the use of the dimesitylboryl moiety as an auxochrome in azonaphthol dyes such as N-[5-hydroxy-8-(4-dimesitylborylphenylazo)-1-naphthyl]amine (**3**) and compared the resulting dyes with analogous nitro-dyes. [4] The results suggested that in addition to possible uses in dye chemistry, the dimesitylboryl group might prove generally useful in chemistry as a substitute for the nitro group where a strong *meta*-directing or highly electron-withdrawing group is required.

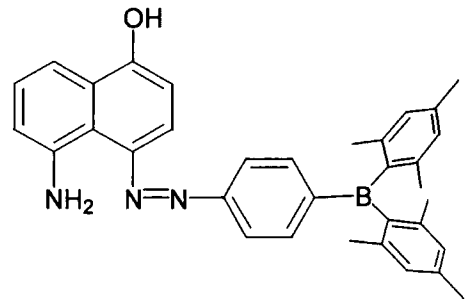

Figure 1.1.4. N-[5-hydroxy-8-(4-dimesitylborylphenylazo)-1-naphthyl]amine (3)

Three-coordinate boron is isoelectronic and isostructural with a carbocation, whereas three-coordinate nitrogen is isoelectronic with a carbanion, so the two are, in effect, inverses of each other. This relationship was explored by Kaim and co-workers, who investigated the electronic structure of diboryl compounds. [5,6]

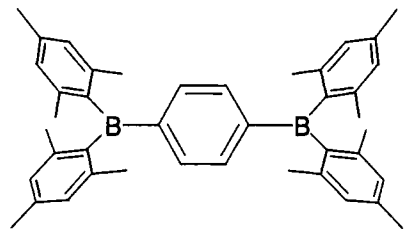

Figure 1.1.5. *p*-Bis(dimesitylboryl)benzene (4a)

The cyclic voltammogram for *p*-bis(dimesitylboryl)benzene (**4a**) exhibited two reversible reductions, to the radical anion and dianion, with reduction potentials of

-1.39 V and -2.08 V respectively (vs. SCE).[7] The first reduction potential is lower in magnitude than that of benzene by approximately two volts, indicating that the presence of one or more dimesitylboryl units greatly facilitates electrochemical reduction. The related compound *4,4'*-bis(dimesitylboryl)biphenyl (**4b**) also exhibits two reversible reductions, at -1.47 and -1.72 V, with the smaller separation indicating weaker coupling between the two boron atoms in this compound. By contrast, *p*-phenylenediamines exhibit two reversible electrochemical oxidations of similar magnitude. These bis-boryls were also investigated by UV-vis/near-IR spectroelectrochemistry. [8] Initially colourless, both compounds exhibited intense absorptions in the visible and near-IR when reduced to the radical anion, with the absorptions of the diborylbiphenyl dianion shifting back to higher energy. The absorption spectra, including vibrational fine structure, were found to resemble closely the absorption spectra of corresponding diamine radical cations, adding further weight to the inverse or "mirror image" analogy between boron and nitrogen. EPR/ENDOR measurements and *ab initio* calculations (using the 6-31G** basis set, and replacing mesityl groups with hydrogen), indicated that the reduced diboron species were subject to a quinoidal distortion, perhaps with a contribution from delocalised B^{II}/B^{III} mixed-valence forms. The π-electron-withdrawing strength of the dimesitylboryl group was re-evaluated, and was found to be closer in magnitude to the cyano than the nitro group.

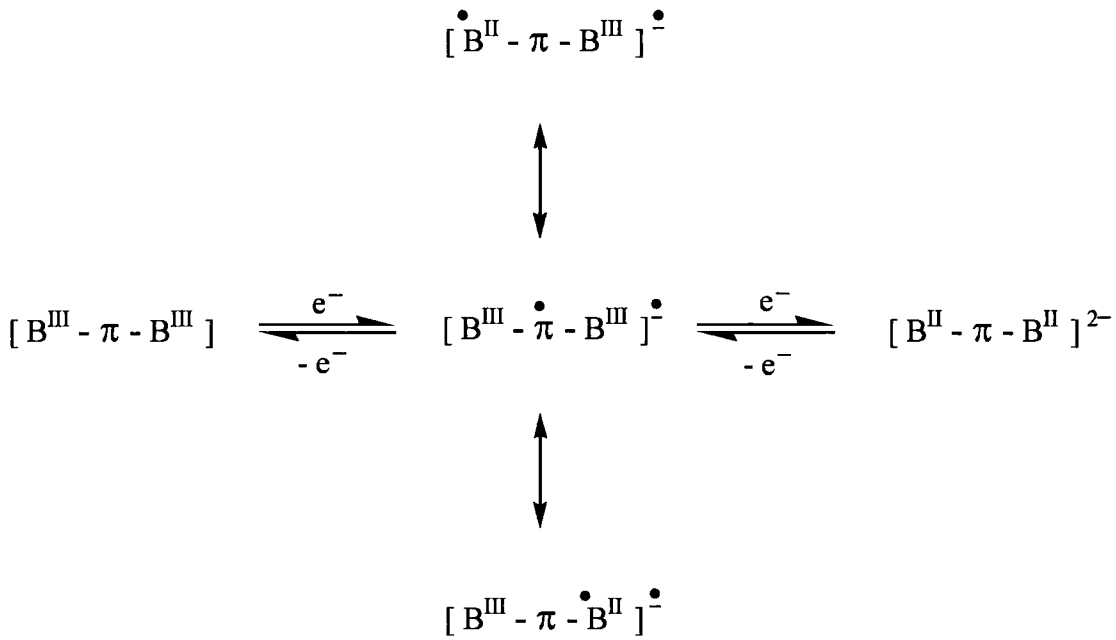

Scheme 1.1. Sequential reduction of bis-boryl π–conjugated rods

The related compound 1,3-bis(dimesitylboryl)benzene (**4c**) has been studied by Okada *et al.* [9] and by Rajca *et al.* [10] The latter group reported that, similar to the 1,4-substituted analogue, this compounds has two reversible reduction potentials at –2.02 and –2.64 V (THF/TBAP, SCE), whereas Oda reported a single reduction potential of –1.98 V (DMF, SCE), with the second reduction being beyond experimental limitations (-2.4 V).[7]

The Kaim group also investigated the radical cations of 1,4-bis(dimesitylboryl)-1,4-dihydropyrazine (**5a**) and 4,4'-bis(dimesitylboryl)-1,1',4,4'-tetrahydro-4,4'-bipyridiylidene (**5b**) (which are isoelectronic with the radical anions of **4a** and **4b** respectively) by EPR and ENDOR spectroscopy in order to investigate the substituent effects of exerted by organoborane groups under different circumstances. [11] Unusually small heteroatom hyperfine splittings indicated a large π-component in the boron-nitrogen bonds, suggesting that the structure of the neutral species may have a large contribution from a quinoid-like form.

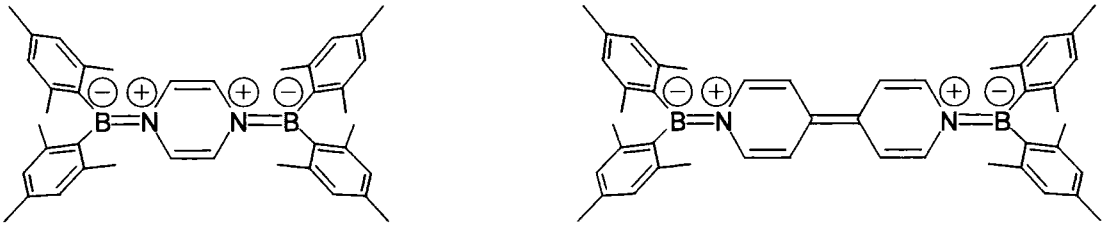

Figure 1.1.6. 1,4-bis(dimesitylboryl)-1,4-dihydropyrazine (5a) and 4,4'-bis(dimesitylboryl)-1,1'-4,4'-tetrahydro-4,4'-bipyridiylidene (5b)

1.1.3. Nonlinear optical properties of unsymmetric and symmetric dimesitylboryl compounds

The work of Williams *et al.* and Kaim *et al.* suggested that the dimesitylboryl unit might be usefully incorporated into organic electronic materials. For example, the change from small dipole moment in the ground state to large dipole moment in the first excited state indicated that donor-acceptor compounds using the dimesitylboryl group as a π-electron acceptor might exhibit nonlinear optical behaviour. The major requirements for a molecule to exhibit a large first molecular hyperpolarisibility are a large change in dipole moment upon excitation and a low energy gap between ground and excited states, both of which are fulfilled by conjugated organic donor-acceptor compounds. The symmetry requirement, that even order nonlinear effects can only be observed in non-centrosymmetric molecules, is also fulfilled. With this in mind, Marder and co-workers set about preparing a series of conjugated donor-acceptor (dimesityl)organoboranes in order to investigate their optical and nonlinear optical behaviour. [12a-c] Aryldimesitylboranes (**2**) were prepared in a similar manner to those previously prepared by Williams *et al.*, by the treatment of an appropriate aryl bromide with butyllithium followed by reaction with dimesitylfluoroborane. A similar synthetic methodology was used to prepare alkynyl(dimesityl)boranes (**6**), but vinyl(dimesityl)boranes required a different approach. Dimesitylborane has been investigated by Pelter and co-workers, who have shown it to be a relatively unreactive

compound. [13] It reacts only slowly with alkenes, is a very weak reducing agent and is tolerant of a large variety of functional groups. However, it reacts rapidly with terminal alkynes at room temperature to give almost exclusively terminal dimesitylboryl groups. Therefore, the reaction of dimesitylborane with appropriate terminal alkynes was employed to produce a series of (arylvinyl)dimesitylboranes (**7**). Donor-aceptor organoboranes incorporating ferrocene and diphenylphosphine moieties were also prepared. [14]

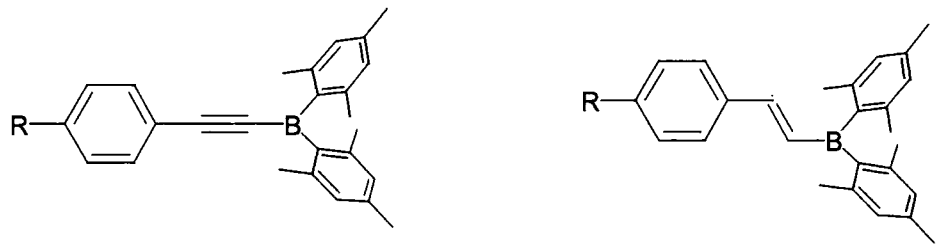

Figure 1.1.7. General form of (arylalkynyl)dimesitylboranes (6) and (arylvinyl)dimesitylboranes (7).

In general, first molecular hyperpolarisibilities were found to increase with increasing π-donor ability of the *para*-substituent, and with increasing conjugation length, and were comparable to those of nitro-substituted analogues: for example, $\beta_{1.907\ \mu m}$ for the compound 4,4'-E-dimesitylboryldimethylaminostilbene was found to be 45 x 10^{-30} esu (EFISH). [12c] Most compounds crystallised in centrosymmetric space groups, however, and thus failed to exhibit second harmonic generation in the solid state (SHG, by the Kurtz powder technique). The third order optical nonlinearities of these asymmetric organoboranes were also measured. As with second order optical nonlinearities, γ_{THG} was enhanced by increased conjugation length and with donor strength: *p*-(dimesitylborylvinyl)(dimethylamino)benzene had a value almost three times larger than that of *p*-(dimesitylborylvinyl)nitrobenzene. In part, this finding may be explained by the increasing planarity of compounds as donor

strength increases, as revealed by the crystal structure determination of several compounds by single crystal X-ray diffraction, although this observation may not relate to solution-phase behaviour. Boron-carbon bond lengths were fairly similar for all compounds with the exception of the ethynylboranes, dimesityl(diphenylphosphinoethynyl)borane and dimesitylboryl(ferrocenylethynyl)borane. [14] In addition, γ_{THG} for compounds containing second-row elements (such as MeS-) was significantly higher than for those containing the corresponding first-row element (such as MeO-), which may be due to the greater polarisibility of second-row elements. Many of the compounds were also highly luminescent, and displayed large solvatochromic shifts in their fluorescence spectra but only small solvatochromic shifts in their absorption spectra.

Table 1.2. Absorption maxima and first and second-molecular hyperpolarisibilities for selected D-A organoboranes.

Compound	X	λ_{max}(abs) (nm)	β EFISH (1.907 μm) (10^{-30} esu)	γ THG (1.907 μm) (10^{-36} esu)
$Mes_2BC_6H_4X$	$N(CH_3)_2$	359	11	24
	SCH_3	335	2.5 ± 0.5	32
	OCH_3	317	3.3	23
$Mes_2BCHCHX$	$C_6H_4N(CH_3)_2$	401	33	93
	$C_6H_4SCH_3$	358	8.6 ± 0.5	81
	$C_6H_4OCH_3$	347	9.3	54

Later, the group prepared some symmetric organoboranes, including two of the compounds previously produced by Kaim *et al.*, in order to examine their linear and third order nonlinear optical properties. [15] Second molecular hyperpolarisibilities (γ_{THG}, 1.907 μm) were relatively large, ranging from 84.2 x 10^{-36} esu for *p*-bis(dimesitylboryl)benzene (over twenty times the measured value for benzene) to 229 x 10^{-36} esu for 4,4'-bis(dimesitylborylvinyl)biphenyl, and increased with increasing conjugation length. Dinitro-compounds with similar conjugation lengths have substantially smaller γ values, which may be explained by the extension of π-conjugation to the vacant p-orbital on boron. The chloroform solutions of these compounds were found to fluoresce when irradiated with UV or near UV light, with the compound 9,10-bis(dimesitylboryl)anthracene (**4d**) exhibiting a particularly bright emission in the blue-green region (496 nm). Single crystals suitable for X-ray diffraction were obtained easily for compound **4a**, but were difficult or impossible to obtain for other compounds in the series. Crystals of **4d** grown from benzene desolvated in seconds, but stable crystals were obtained from mesitylene. The crystal packing diagram for **4d** shows that the bulky mesityl groups prevent close packing, resulting in large void spaces which must be filled with an appropriately sized arene to stabilise the resulting co-crystals. The crystal structures revealed that in each compound, the two boron-centred trigonal planes are coplanar, with very little difference in B-C bond lengths, and the three C-B-C bond angles sum to 360°. The central aryl moieties are also planar, but the central plane is tilted with respect to the boron-centred planes by ca. 24° for **4a** and ca. 53° for **4d**, the difference almost certainly being a result of the greater steric hindrance on replacing phenylenediyl with anthracenediyl. In addition, there is some evidence for a small degree of quinoidal distortion of the central C_6H_4 ring in **4a**, with statistically significant alternation in

bond lengths. It should be noted that although the difficulty in crystallising these compounds is unfortunate from an academic point of view, for many potential applications in organic electronics, it is desirable that materials should be amorphous, thus avoiding crystal grain boundaries and defects which can drastically lower the mobility of charge carriers.

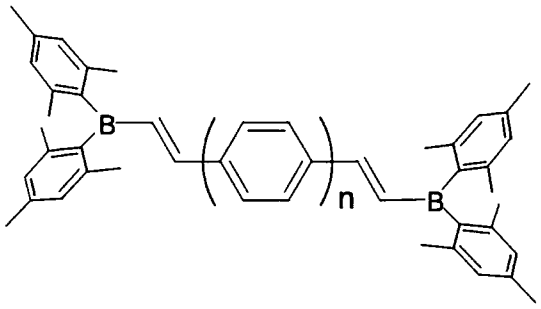

Figure 1.1.8. 1,4-Bis(dimesitylborylvinyl)benzene (8a, n=1) and 4,4'-bis(dimesitylborylvinyl)biphenyl (8b, n=2).

Table 1.3. UV-vis absorption and emission maxima, second molecular hyperpolarisibility and reduction potentials for symmetric bis-boryls of the form Mes_2B-X-$BMes_2$

X		λ_{max}(abs)[a] (nm)	λ_{max}(em)[a] (nm)	γ_{THG} (10^{-36} esu)	$E_{1/2}(1)$[b] (V)	$E_{1/2}(2)$[b] (V)
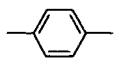	**4a**	338	394[c]	84.2	-1.39	-2.08
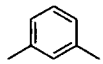	**4c**	x	x	x	-2.02	-2.64
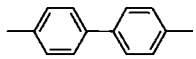	**4b**	342	423[c]	136	-1.47	-1.72
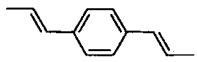	**8a**	372, 386	405, 433	155	x	x
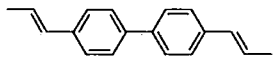	**8b**	370	408, 433	229	x	x
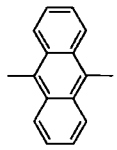	**4d**	[d]	496[c]	x	x	x

[a] Chloroform solution. [b] Measured in THF. [c] Incorrectly reported in reference 14. [d] Complex: λ_{max} = 258, 317, 350, 434, 460 (unpublished data). x = not reported.

Lequan and co-workers have also prepared a number of conjugated donor-acceptor molecules incorporating the dimesitylboryl group and investigated their second order nonlinear optical properties. [16] The first molecular hyperpolarisibilities of the compounds [4'-(dimethylamino)biphenyl-4-yl]dimesitylborane (**BNB**) and 4-[4'(dimethylamino)phenylazo]phenyldimesitylborane (**BNA**) were investigated by both a solvatochromic technique and later by EFISH, which gave values of β (0) of 42 and 72 x 10^{-30} esu respectively. Computational methods estimated that the change in

dipole moment upon excitation was much larger for these compounds than for related nitro-compounds, though measured β-values were similar. The larger value for **BNA** over **BNB** was attributed to more facile charge transfer in the azobenzene backbone than for biphenyl. Crystal structures of these compounds showed that the phenyl groups in **BNA** were almost coplanar, compared to a 26° angle in the biphenyl backbone of **BNB**, but other structural parameters were similar. Again, it was noted that the difference in planarity of the solid-state structures cannot be directly related to the likely planarity in solution for either ground or excited states.

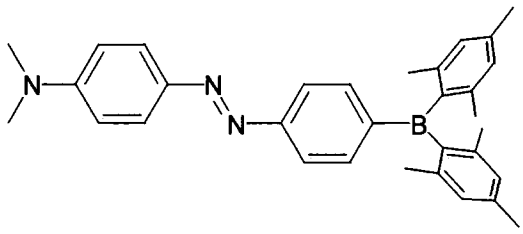

Figure 1.1.9. 4-[4'(dimethylamino)phenylazo]phenyldimesitylborane (BNA)

As electronic transmission through the organic π-system was found to have such a large effect on the first molecular hyperpolarisibility, the Lequan group then prepared a series of compounds where the dimesitylboryl group was linked through a bithiophene group to a strong electron-donating group such as dithianylidene, pyrrolidin-1-yl or 3-thienyl (**9a-c**). Whilst second order molecular hyperpolarisibilities were not found to be significantly improved, the dipole moments were increased, leading to larger values of μβ, a property that is important when NLO active chromophores are incorporated into polymers as pendant molecules. Two such polymers were produced when the group incorporated a modified version of **BNA** as sidechains in polyurethane materials (**P1**). [17] Thin films were produced by spin

coating polymer solutions, which were poled using the Corona technique, and which proved to have high thermal stabilities and large quadratic susceptibilities.

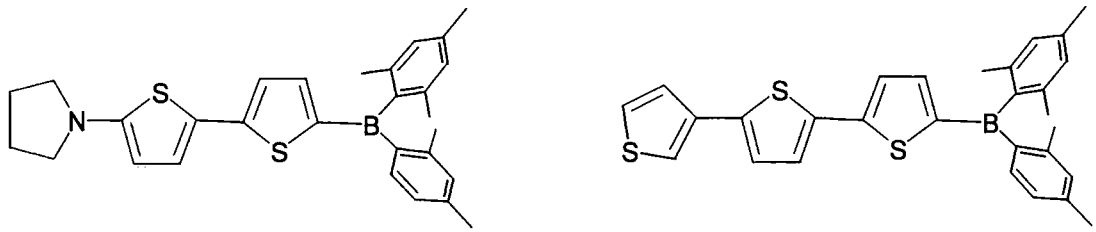

Figure 1.1.10. 5-(Dimesitylboryl)-5'(pyrrolidin-1-yl)-2,2'-bithiophene (9b) and 5-(dimesitylboryl)-2,2':5',3''-terthiophene (9c).

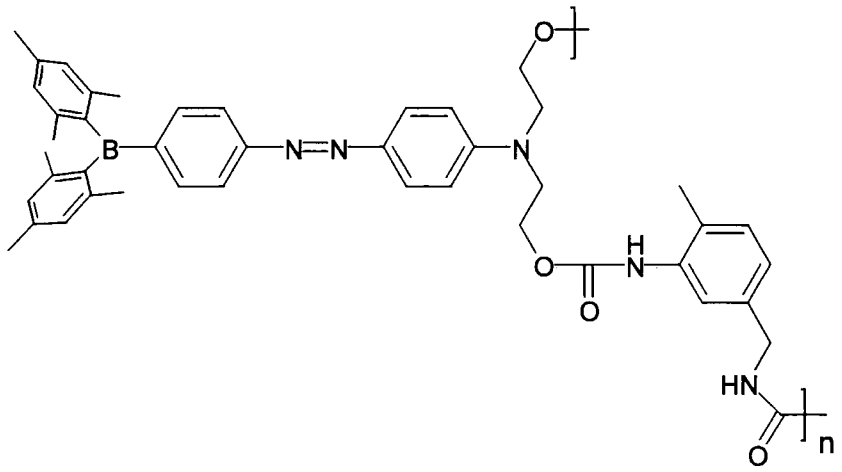

Figure 1.1.11. Polyurethane with pendant boron chromophore (P1).

1.1.4. Conjugated polymers containing boron in the main chain

Chujo and co-workers have synthesised a large number of polymers containing boron in the main chain. [18] Hydroboration polymerisation of aromatic diynes using mesitylborane was used to produce stable π-conjugated, electron-poor polymers related to poly-*p*-phenylenevinylene (Figure 1.1.12, **P2a-d)**, which proved to be highly soluble in common organic solvents and to have high thermal and air stability. [19] Despite having relatively low molecular weights (indicating that the polymerisation process was relatively inefficient), these polymers exhibited strong photoluminescence in the blue region, with large bathochromic shifts compared to the

monomers. This observation indicates that the organic π-systems are substantially extended by conjugation with the vacant p-orbital situated on boron. The third order nonlinear optical properties of these polymers was investigated by degenerate four-wave mixing, [17a] with polymers containing phenyl or fluorenyl units having unusually large bulk third-order susceptibilities ($\chi^{(3)}$ = 6.87 x 10^{-6} and 3.56 x 10^{-7} esu respectively). It is likely that the large values when compared to those for the related bis-boryl small molecules prepared [14] by Marder *et al.* are due mainly to increased conjugation length in the polymers, although bulk and molecular properties may not necessarily be directly linked, and it is difficult to compare values obtained using different techniques. Hydroboration of the heteroaromatic diynes 2,5-diethynylthiophene, 2,5-diethynylfuran and 2,5-diethynylpyridine using mesitylborane was reported to produce related polymers (**P2e-g**). [20] The polymers were highly fluorescent, with the emission wavelengths being dependent on the heteroaromatic unit: **P2e** and **P2f** emitted in the green region, whereas **P2g** had a complex emission spectrum with maxima at 416, 495 and 593 nm, resulting in white light emission. The group also reported having prepared model, monomeric, compounds by the hydroboration of 2-ethynylthiophene and 2-ethynylpyridine in order to investigate further the effect of conjugation length. The UV-vis absorption maximum of the thiophene - containing monomer was virtually unchanged from that of polymer **P2e**, in sharp contrast to polymer **P2a**, which had a large bathochromic shift compared to its monomer, perhaps indicating that electron delocalisation was inefficient in **P2e**. No ground state charge transfer was observed, as shown by the ^{11}B NMR peak position of 31.3 ppm, very similar to that of polymer **P2a** (31.4 ppm). In contrast, polymer **P2c** appeared to have a fairly large ground state interaction and UV-vis absorption was significantly red-shifted compared to the model monomer. TGA

measurements indicated that the heteroaromatic organoboron polymers were significantly more thermally stable than **P2a**, with 10 % weight loss observed at 190 (**P2e**), 209 (**P2f**) and 240 (**P2g**) °C, compared to 128 °C for **P2a**. In later work, the electrical conductivity of the polymers based on phenyl and fluorenyl units, but with the mesityl group replaced by the bulkier tripyl group to improve stability, was investigated by doping with triethylamine or iodine. [21] With $\sigma < 10^{-10}$ S cm^{-1} the undoped polymers function as insulators. Doping with triethylamine, an electron donor, increased the conductivities of both polymers to a maximum of approximately 10^{-6} (fluorenyl) and 10^{-7} S cm^{-1} (phenyl), whereas exposure to an atmosphere of iodine vapour, an electron acceptor, increased the conductivity of both polymers to a maximum of around 10^{-7} S cm^{-1}. The greater increase upon doping with an electron donor may be explained by the electron-poor nature of the polymers, whereby electron transport might be expected to be more facile than transport of positive holes. More recently, hydroboration polymerisation was also used to synthesise organometallic polymers, containing platinum (**P3a**), palladium (**P3b**) or ruthenium (**P4**) in the main chain. [22] The UV-vis absorptions of these polymers were significantly red-shifted with respect to the organometallic monomers from which they were derived, indicating extensive electron delocalisation and, in the case of the ruthenium-containing polymer, possible activation of MLCT in the metal complex, but the exact nature of the electronic interactions in these materials is unclear.

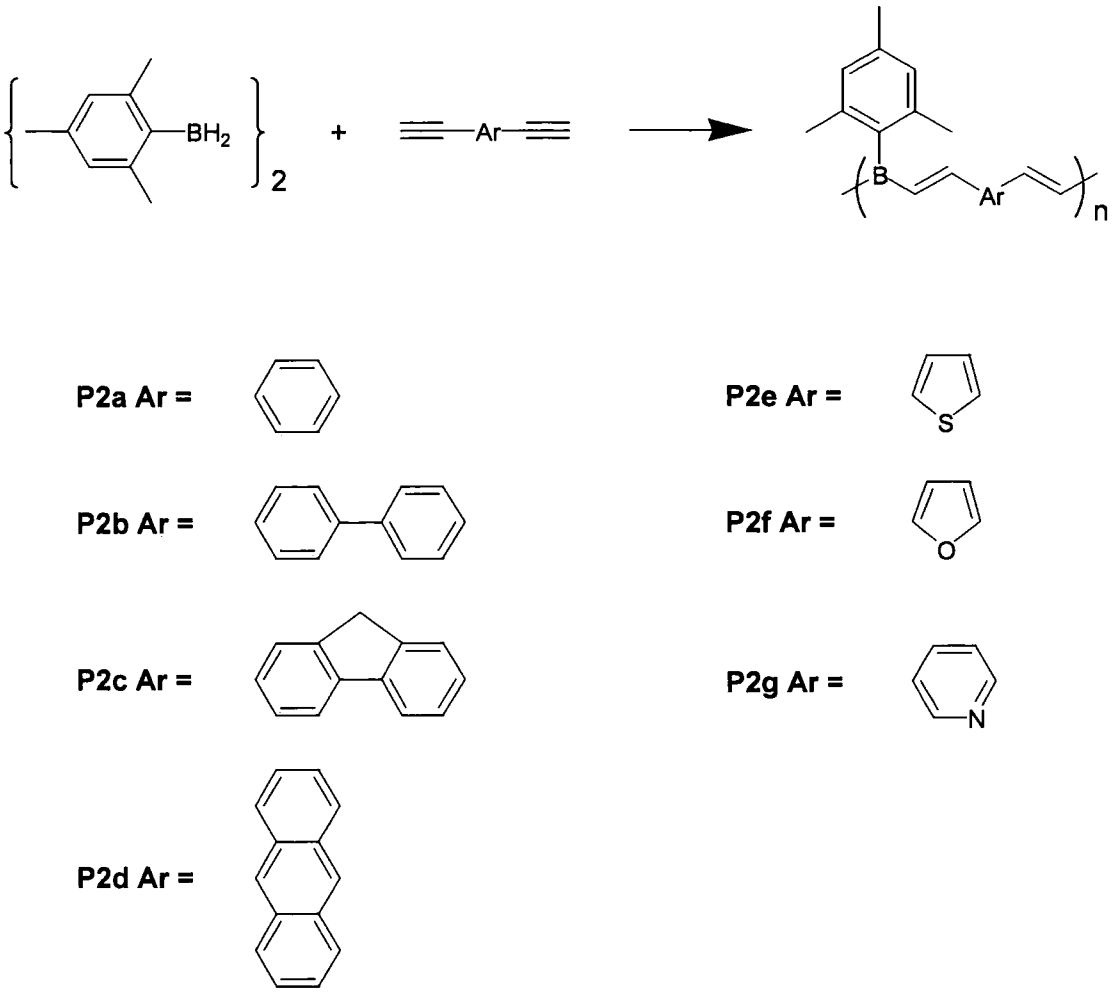

Figure 1.1.12. Boron-containing polymers related to poly(phenylenevinylene) (P2a-g)

Chujo has also synthesised a number of air and moisture stable poly(*p*-phenylene-boranes) (**P5**), [23] via a one-pot procedure, the Grignard reaction of a dibromobenzene derivative and dimethoxyaryl borane, and poly(ethynylene-phenylene-ethynylene-boranes) (**P6**) via polycondensation of bifunctional lithium acetylides with dimethoxyarylborane (aryl = tripyl or mesityl). [24] It was found that for efficient polymer synthesis, it was necessary for the arene starting material to contain long alkoxy chains, which may be due to the increase in solubility such substituents provide. The use of dimethoxytripylborane rather than dimethoxymesitylborane also resulted in higher yields and significantly higher

molecular weight materials. Both classes of polymer were found to be highly luminescent, with emission in the blue or blue-green region.

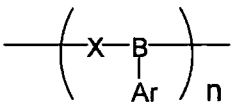

Figure 1.1.13. General form of poly(*p*-phenylene) (P5) and poly(ethynylene-phenylene-ethynylene) (P6) organoboron polymers

Polymers containing B-N bonds in the main chain have also been investigated, these being of interest due to the potential for Npπ - Bpπ interaction and because the N=B bond is isoelectronic with the C=C bond. Copolymers bearing monomeric iminoborane moieties were obtained by of haloboration / phenylboration of diynes and diisocyanates (**P7**), [25] as illustrated in Scheme 1.2. Haloboration (insertion into a boron-halogen bond) of diynes occurs under mild conditions (-78 °C) whereas phenylboration (insertion into a boron-phenyl bond) requires forcing conditions (+70 °C). In contrast, both haloboration and phenylboration of isocyanates occur readily at room temperature. This differing reactivity meant that the Chujo *et al.* were able to use a stepwise method to access the required polymer. First, a diyne was reacted with diphenylbromoborane at room temperature, resulting in the formation of bis(diphenylvinyl)boranes. A diisocyanate was then added to the reaction mixture, resulting in insertion of N-C into one of the boron-phenyl bonds. Boron NMR showed a major broad peak at ca. 29 ppm, with a minor broad peak at ca. 0.5 ppm, and was

compared to the spectra obtained when phenyldichloroborane was reacted with either diethynylbenzene (to give a phenyldi(cholorovinyl)borane, ca. 60 ppm) or with a diisocyanate (to give a phenyldiamidoborane, ca. 5 ppm). This indicated that the likely structure of the polymer was that of a phenyl(bromovinyl)amidoborane. It was postulated that the minor peak at ca. 0.5 ppm was due to diamido(bromovinyl)borane, a result of a second phenylboration reaction at the same boron centre and resulting in a cross-linked structure. To investigate the air stability of these polymers, an air-bubbling experiment was carried out for a THF solution of the polymer obtained from diphenylbromoborane, diethynylbenzene and methyldiisocyanatobenzene. Gel permeation chromatography showed that even after five days of air bubbling, significant degradation did not occur.

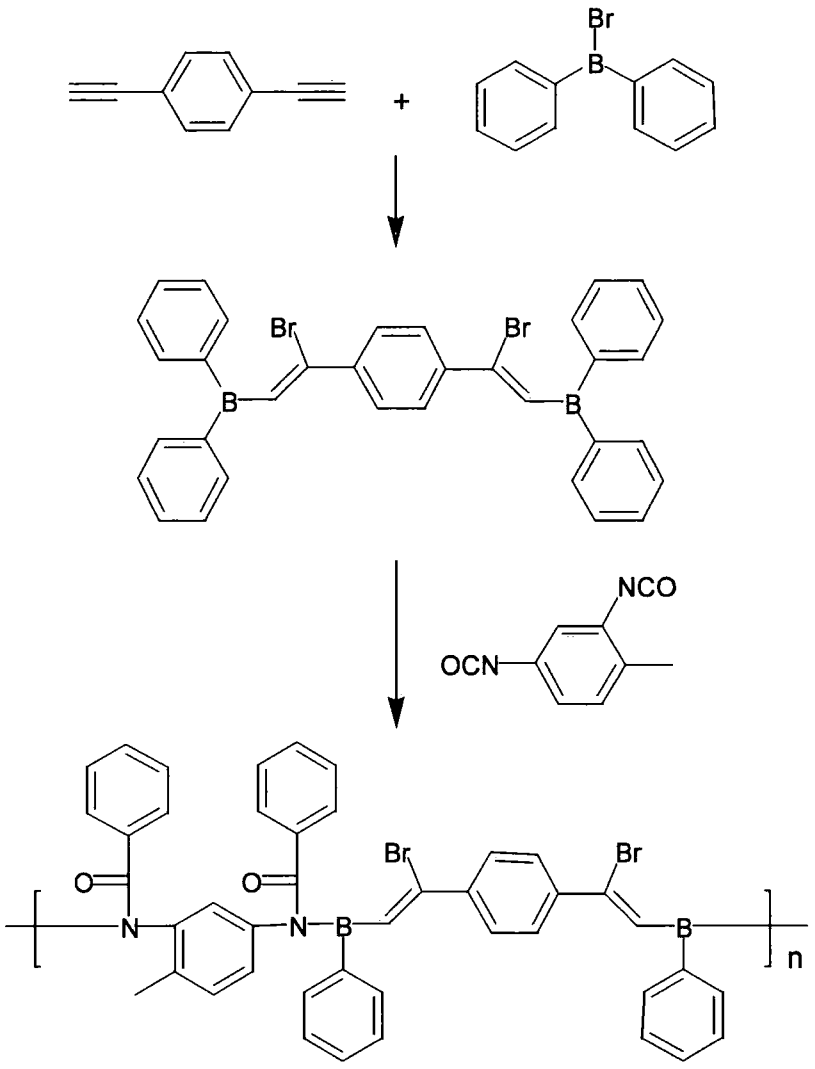

Scheme 1.2. Boration copolymerisation between diboron compound and a diisocyanate (P7)

Chujo *et al.* have also prepared a large number of poly(cyclodiborazanes) (i.e. polymers containing B_2N_2 rings) by the hydroboration of dicyano compounds using various hydroborating agents. [26] For example, polymers have been produced by the hydroboration of aromatic dicyano compounds, including 9,10-dicyanoanthracene, using mesitylborane (**P8**). [27] This polymer was highly fluorescent, with a broad emission in the green region (494 nm, chloroform solution), in contrast to monomeric dicyanoanthracene, which has two sharp emission peaks at 437 and 461 nm, but the

relatively small bathochromic shift in the absorption spectrum indicated that the conjugation length was not greatly increased. However, the authors suggested that the broadness of the emission peak might indicate some energy transfer may be taking place in the polymer. Whilst not involving three – coordinate boron, these are included here for completeness.

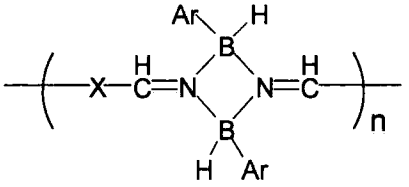

Figure 1.1.14. General form of poly(cyclodiborazane) polymers P8-P10.

They then prepared a number of related polymers containing electron-donating moieties in the backbone in the form of thiophene (**P9a**) or 1,4-dioctyloxybenzene (**P9b**). [28] The resulting polymers were highly fluorescent, emitting in the blue-green region. Although λ_{max}(abs) was not significantly shifted with respect to the monomers for either polymer, the absorption edges and emission maxima were subject to large bathochromic shifts. The emission maxima were also found to be solvent dependent, though solvent effects were not strictly in the order of solvent polarity, indicating that this was due to strength of solvation rather than solvent polarity alone. Model compounds, prepared from mono-cyanothiophene and mono-cyanooctoxybenzene, were found to have similar emission maxima to the parent polymers but no bathochromic shift in the UV-vis absorption edge was observed. The optical data led the authors to suggest that both polymers have an intramolecular charge transferred structure, with π-electron conjugation through the cycloborazane units.

Figure 1.1.15. Nature of the group X for series P9

Poly(cyclodiborazane)s containing oligothiophene moieties in the polymer backbone were prepared by the hydroboration of dicyano-oligothiophenes with mesitylborane or tripylborane (**P10**). [29] As the length of the oligothiophene increased, a bathochromic shift was observed in the absorption and emission spectra of the resulting polymers, indicating an extension of π-conjugation. Fluorescence quantum yields were measured, but were found to be relatively low, ranging from 0.11 to 0.17. Quantum yields did not appear to be affected by the length of the oligothiophene, though it should be noted that polymers consist of a distribution of products of differing length rather than a single discrete product, and that polymer length would also be expected to have an effect upon photophysical properties. The quantum yield did, however, appear to be affected by the choice of either mesitylborane or tripylborane, with polymers prepared from tripylborane having higher quantum yields.

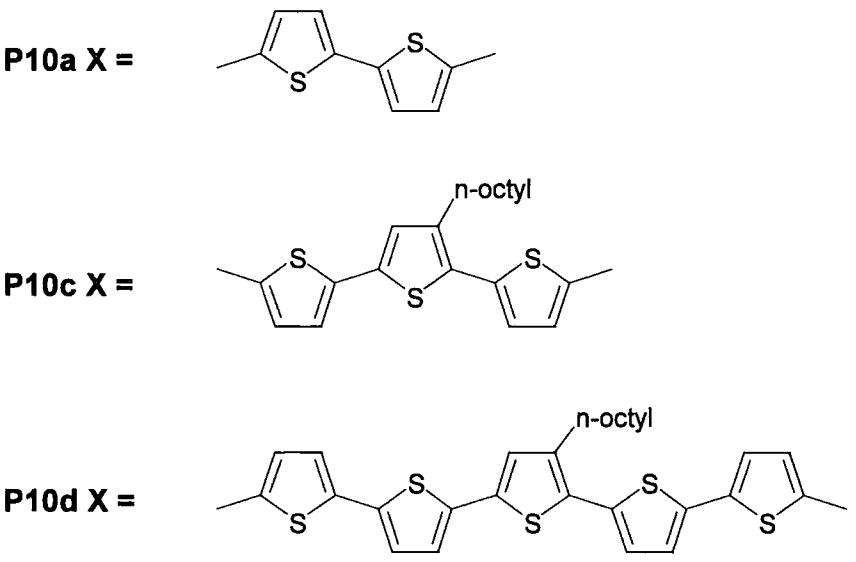

Figure 1.1.16. Nature of the group X in the series P10

Table 1.4. Weight Average Molecular Weight, Number Average Molecular Weight, UV-vis Absorption and Emission Maxima for Selected Organoboron Polymers.

Polymer [a]	Mw	Mn	λ_{max}abs [b] (nm)	λ_{max}em [b] (nm)
P2a	16000	6500	399	441
P2b	10500	5100	390	440
P2c	4200	2800	350, 390, 407	455
P2d	1700	1300	364, 383, 405	412, 436, 462
P2e	4800	3000	350	488
P2f	5900	3000	356	495
P2g	4500	2900	450	416, 495, 593
P3ay	16380	9100	ca. 390	498
P3by	18900	9000	ca. 390	481

P4x	[f]	13000	359, 514	[f]
P5ay [c]	3500	2900	365	481
P5by [d]	3400	3000	367	487
P6ay [d]	3400	2700	397	456
P8y	8800	4400	406	494
P9ax	9400	4700	364	473
P9bx [c]	7900	5800	381	463
P10ax	9300	3300	387	451, 478
P10ay	8700	3200	391	453sh, 492, 518sh
P10cx	6300	4200	415	499, 530sh
P10cy	4700	2500	415	496, 526sh
P10dx	8500	3300	426	536
P10dy	3100	2100	421	532

[a] x = mesityl groups, y = tripyl groups. [b] recorded in chloroform solution; sh denotes shoulder.
[c] octyloxy substituents. [d] dodecyloxy substituents. [f] not reported.

Polythiophenes containing three-coordinate boron have also been reported by Siebert *et al.* **(P11).** [30] The polymers were highly coloured (e.g. R = Ph, turquoise powder), and displayed a large bathochromic shift with respect to the corresponding monomers indicating extensive electron delocalisation through boron. However, the lack of steric protection around boron resulted in limited stability.

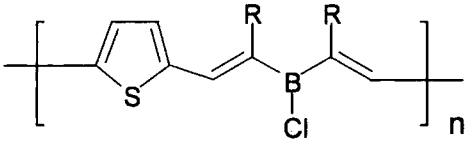

Figure 1.1.17. Thiophene based boron-containing polymers (P11).

1.1.5. Electroluminescent and electron transporting properties of dimesitylboryl – containing compounds

In recent years, there has been a great deal of research into alternatives to traditional inorganic electronic electroluminescent (EL) materials, with conjugated molecular and polymeric organic materials being widely investigated as the basis for organic light emitting diodes (OLEDs).[31] A simplified diagram of a typical multilayer OLED is shown in Figure 1.1.18. Upon application of a potential difference across the device, positive charge carriers (holes) migrate towards the cathode and negative charge carriers (electrons) migrate towards the anode. The recombination of electrons and positive holes takes place in the emitting layer, generating an electronically excited-state molecule (exciton) that either luminesces or transfers its energy to a dopant, which subsequently luminesces. This process generates photons that escape through the transparent indium-tin-oxide (ITO) anode in the form of visible light. Although it is possible to construct OLEDs using only one organic material, it is more common to use several layers (typically three), with the materials used in each of the layers being determined by their different functions. The positive hole-transporting layer is composed of a material that is easily oxidized and forms stable radical cations, with aryl amines being most commonly used. Conversely, the electron-transporting layer is composed of a material that readily form stable radical anions, with the most commonly used example being the aluminium complex Alq_3 (where q = 8-hydroxyquinolato) (Figure 1.1.19). The compound used in the emitting layer must luminesce readily, and should ideally permit the formation of both stable anion and cation radicals in order to prolong the lifetime of the device and improve its efficiency. Efficient green EL from a thin film of Alq_3 was first reported by Tang and van Slyke in 1987,[32] and Alq_3 has also been

used extensively as the emissive layer in OLEDs. Whilst OLEDs emitting in the green to red regions of the spectrum have been developed by doping Alq_3 with various dyes, the blue region has proved harder to attain by this method. Boron – containing materials have been shown to be useful for EL, including blue light emission, and have also been investigated as potential electron transporters.

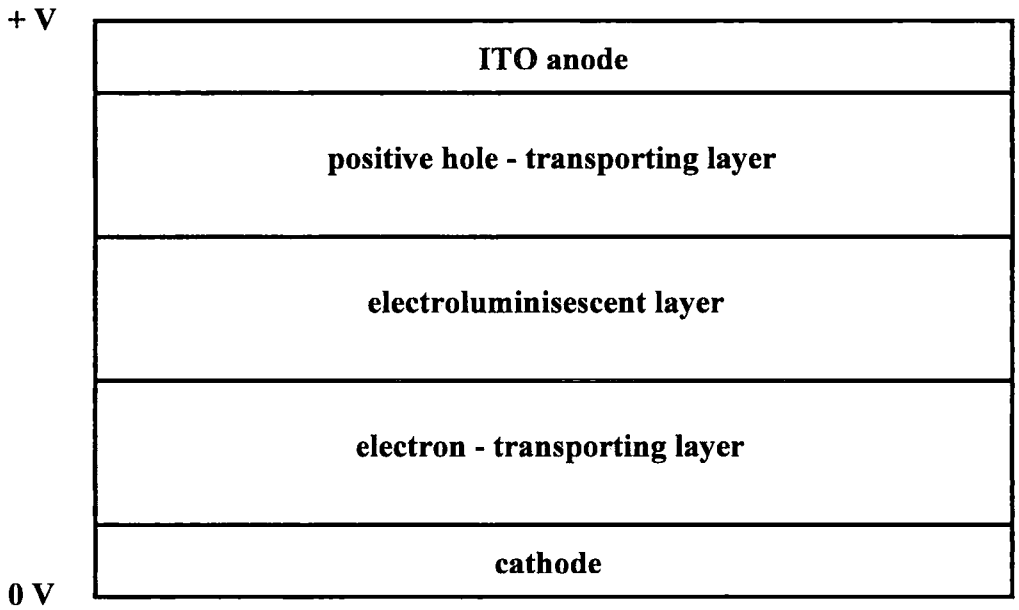

Figure 1.1.18. Schematic representation of a typical three – layer OLED.

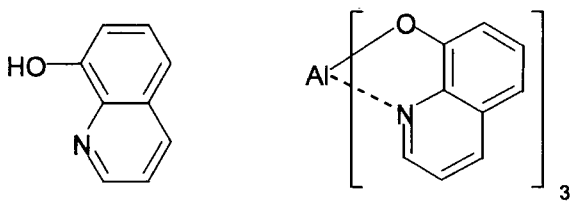

Figure 1.1.19. 8-hydroxyquinoline and schematic structure of Alq_3

Shirota and co-workers have prepared a number of boron-containing amorphous molecular materials for use in organic electronics. [33] Symmetric bis-boryls containing two dimesitylboryl units connected via bithiophene (**BMB-2T**) or terthiophene (**BMB-3T**) moieties readily formed amorphous glasses with high glass transition temperatures (T_g) (T_g for **BMB-2T** = 107 °C), and had good electron transporting properties. [34] **BMB-2T** was also incorporated into OLEDs where it was used as an electron transporter with Alq_3 as an emitter, [34] and also as an electron transporter and emitter.[35] It was found to be highly fluoresecent in THF solution, with fluorescence maxima of 446 and 442 nm and a very high quantum efficiency of 0.86, and was also highly fluorescent when deposited as a thin film.

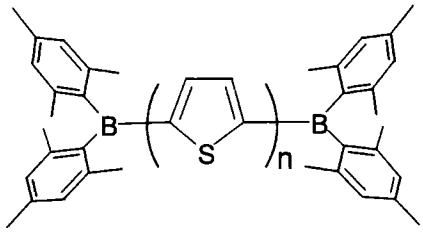

Figure 1.1.20. BMB-2T (n = 2) and BMB-3T (n = 3)

A multilayer device composed of a hole-injection layer (4,4',4''-tris(3-methylphenylphenylamino)triphenylamine (***m*-MTDATA**) in DCM), a hole-transporting layer (N,N'-bis(3-methylphenyl)-N,N'-diphenyl-[1,1'-biphenyl]-4,4'-diamine (**TPD**) in DCM) and **BMB-2T** as an emitting/electron transporting layer was electroluminescent with maxima of 446 and 472 nm attributed to **BMB-2T** and a further intense emission at ca. 560 nm which was attributed to the formation of an exiplex between excited state **BMB-2T** and ground state **TPD**, as demonstrated by the same PL emission maximum from a thin film composed of 1:1 molar ratio **BMB-2T** and **TPD**. Whilst exiplex formation can be used for colour-tuning purposes, it was undesirable in this case as without exiplex emission the OLED would emit intense

blue light. For multicolour visual displays, it is necessary to have components that emit in the red, green and blue regions, the combination of which may be used to produce the full spectrum of visible light. Whilst there are many examples of molecular materials that emit strongly in the green and red regions, blue emitters are much less common, and are an area of much current research. With this in mind, the group added a thin layer of a hole-blocking material (1,3,5-tris(biphenyl-4-yl)benzene (**TBB**)) that would not form an exiplex with **BMB-2T** due to weak electron-donating properties and, when placed between the layers of **BMB-2T** and **TPD**, would effectively prevent their combination. The resulting device was a strong blue emitter, with no sign of green emission. Emission was observed from a starting voltage of 3 V, reaching a maximum intensity of 1100 cd m^{-2} at a driving voltage of 16 V and external quantum efficiency of 0.17 % at a luminance of 300 cd m^{-2}, comparing favourably with devices based on, for example, oxadiazole-materials for blue emission.[36] A similar device, omitting **TBB** and replacing **TPD** with a weaker electron-donor, tri(*o*-terphenyl-4-yl)amine (***o*-TTA**) to prevent exiplex formation, was found to be even more efficient, with a maximum luminance of 1700 cd m^{-2} at a 17 V driving voltage and external quantum efficiency of 0.24% at 300 cd m^{-2}.

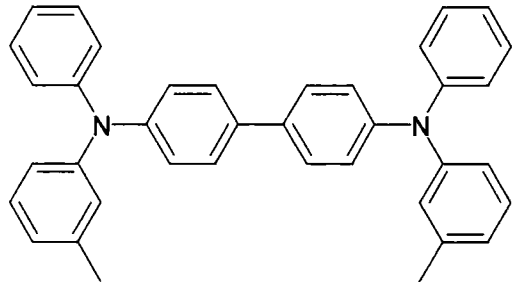

Figure 1.1.21. TPD

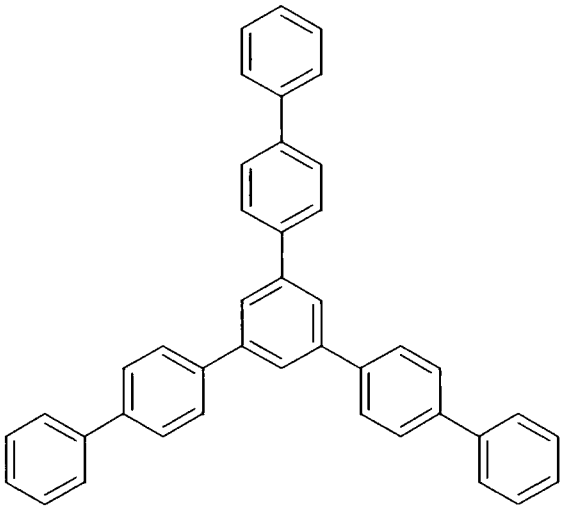

Figure 1.1.22. TBB

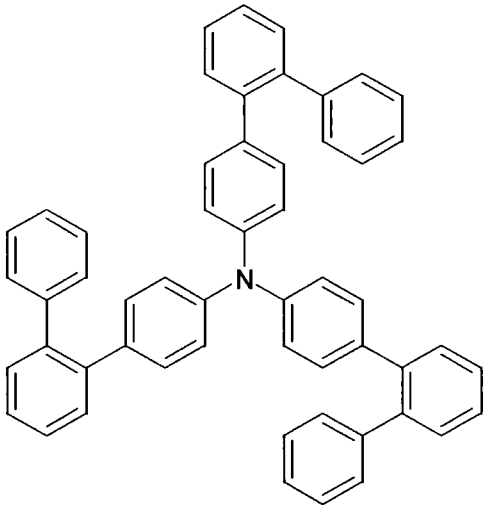

Figure 1.1.23. *o*-TTA

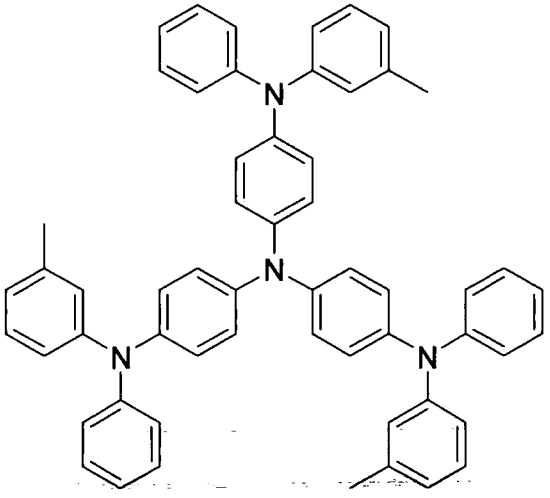

Figure 1.1.24. m-MTDATA

Lee and co-workers have also experimented with OLEDs containing **BMB-2T**, this time doping it in varying concentrations into an electron-transporting layer (a trimer of N-arylbenzimidazoles, **TPBI**) where it functioned as the emitter. This approach was also successful, with the optimised device containing 3 % **BMB-2T** and exhibiting improved colour purity than previous devices. [37] It also had a higher maximum luminance of 2200 cd m^{-2} at 15.3 V driving voltage. Interestingly, Zhou *et al.* have performed some preliminary investigations into the NLO properties of **BMB-2T** using the Z-scan method. [38]

Shirota *et al.* later experimented with donor-acceptor starburst-type oligomers based on bi- or trisubstituted benzene. [39] The compounds 1,3-bis[5-(dimesitylboryl)thiophen-2-yl]benzene (**BMB-TB**) and 1,3,5-tris[5-(dimesitylboryl)thiophen-2-yl]benzene (**TMB-TB**) were investigated as potential electron-transporting, positive-hole blockers. They readily formed stable amorphous glasses, with T_gs of 109 and 160 °C respectively when cooled from the melt in air. Their redox properties were investigated by cyclic voltammetry with two (**BMB-TB**) and three (**TMB-TB**) reversible reductions observed with half-wave reduction potentials ($E_{1/2}^{red}$) very close to that of Alq_3 at –2.03 and –1.98 V respectively (vs. Ag/Ag^+, 0.01 M). This indicated that they should function as efficient electron-transporters. In addition, they were estimated to have a higher HOMO level than Alq_3 and therefore block positive holes more efficiently. This was proven to be the case with the fabrication of devices using the two compounds as both hole-blocker and electron-transporter.

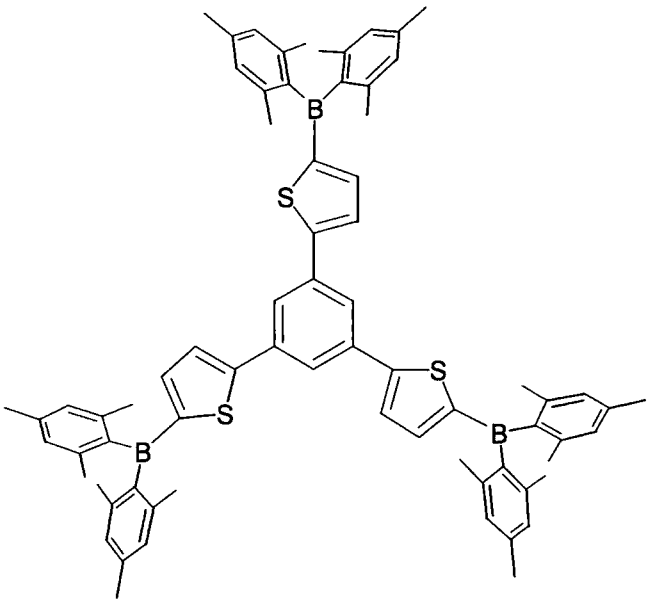

Figure 1.1.25. TMB-TB.

Another starburst-type molecule, the triarylamine 4,4',4''-tris[5-(dimesitylboryl)thiophen-2-yl]triphenylamine (**MB-TTPA**), was investigated for potential use in photovoltaic devices such as photosensors or solar cells. [40] A pn-heterojunction device was fabricated by spin-coating **MB-TTBA** onto an indium-tin-oxide (ITO) coated glass substrate followed by vacuum deposition of a perylene dye and finally vacuum deposition of a silver electrode. A photocurrent flowed when the device was irradiated with white or monochromatic (440 nm) light, with conversion efficiencies of 0.07 and 0.1 % respectively. These values were lower than that of a similar device where **MB-TTBA** was replaced with a nitro-substituted triarylamine compound, though T_g was lower (134 °C, compared to 161 °C for MB-TTPA) for this compound.

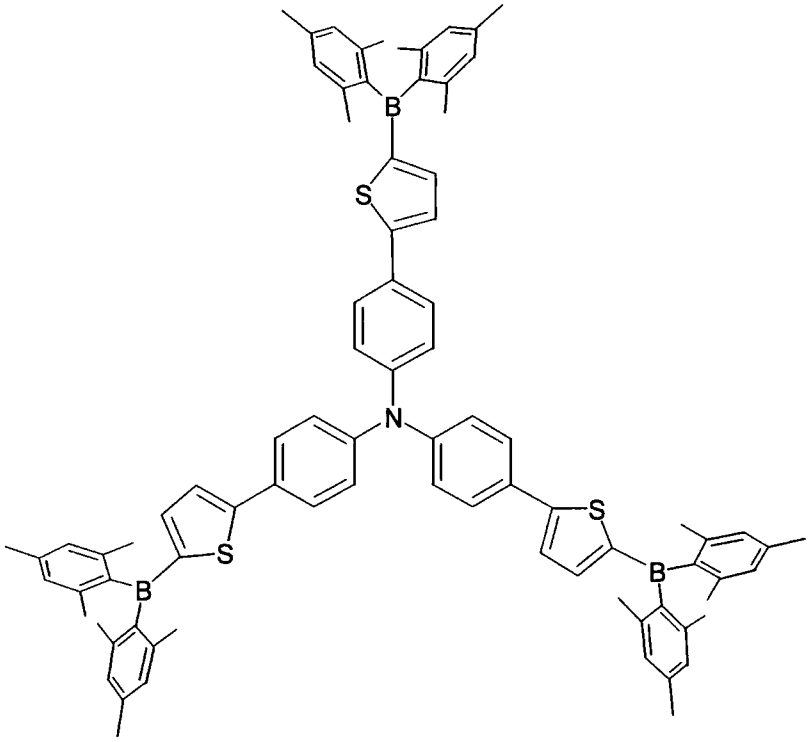

Figure 1.1.26. MB-TTPA.

The group have also prepared a number of donor-acceptor compounds incorporating the dimesitylboryl group with the general form Ar_2N-phenyl-$(thiophendiyl)_nBMes_2$ where Ar = 9,9-dimethylfluoren-2-yl and n = 0 – 3 (**FlAMB-0T, FlAMB-1T, FlAMB-2T** and **FlAMB-3T**). [41] It was suggested that the form of these molecules should permit the formation of both stable anion and cation radicals, which should prolong the lifetime of OLEDs constructed using them. The **FlAMB-nT** series functioned as emissive materials, which were colour-tunable due to the varying backbone length, and were also useful as host materials for other fluorescent dyes. In addition, they readily formed stable amorphous films with T_gs above 120 °C and exhibited reversible oxidation and reductions in solution (by CV). The main properties of these compounds are summarised in Table 1.5. The compounds were used to produce efficient OLEDs of varying colour, with a white-light emitter produced by using a combination of **FlAMB-0T** and **FlAMB-3T**.

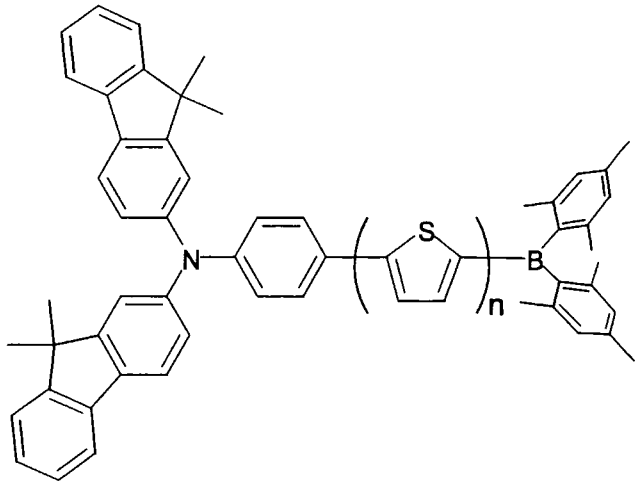

Figure 1.1.27. General form of FlAMB-nT molecules.

Table 1.5. Glass Transition Temperatures (T_g), UV-vis Absorption and Emission Maxima, Quantum Yield (Φ_f) and Oxidation and Reduction Potentials for the Compounds FlAMB-nT

Compound	T_g (^{o} C)[a]	λ_{max}(abs) (nm)[b]	λ_{max}(em) (nm)[b]	ϕ_f[c]	$E_{1/2}^{ox}$ (V)[d]	$E_{1/2}^{red}$ (V)
FlAMB-0T	129	402	505	0.45	0.56	- 2.35
FlAMB-1T	124	435	537	0.50	0.51	- 2.01
FlAMB-2T	127	446	566	0.23	0.48	- 1.95
FlAMB-3T	131	457	582	0.14	0.47	- 1.87

[a] Measured at a scan rate of 5 °C min^{-1}. [b] THF solution. [c] Determined with reference to aqueous acidified quinine sulfate. [d] Measured vs. Ag/Ag^+, with a scan rate of 500 mV s^{-1}.

1.1.6. Other donor-X-B(Mes)$_2$ systems for sensors

Recently, several other groups have prepared donor-acceptor compounds similar to those prepared by the Lequan, Marder and Kodak groups. Kaufmann and co-workers have prepared a number of *ortho*-substituted aminoaryldiarylboranes (**10**) as well as a pyrrolyl- and an indolyl-diarylborane for potential use as sensors. [42] UV-vis and fluorescence spectroscopy showed that λ_{max} (abs) and λ_{max} (em) for the *ortho*-

substituted aminoaryldiarylboranes were all very similar at ca. 415 nm and 488 nm respectively, with high quantum yields ranging from 0.67 to 0.89. The pyrrole and indole-based compounds absorbed and emitted at rather shorter wavelength and had significantly lower quantum yields. Though stable indefinitely in the solid state, dilute solutions were subject to decomposition due to cleavage of the boron-aminophenyl bond.

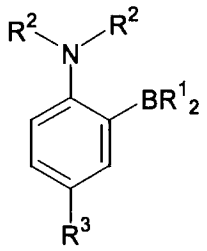

Figure 1.1.28. General form of *ortho*-substituted (aminoaryl)diarylboranes (10).

Fang *et al.* have investigated the structures and the linear and nonlinear optical properties of a series of stilbene and styrylthiophene (**11**) based donor-acceptor compounds containing the dimesitylboryl group. [43] All such compounds were highly fluorescent and, upon excitation with a laser, exhibited intense two-photon excited fluorescence, TPEF, the process whereby two lower energy photons are simultaneously absorbed, followed by emission of a single, higher energy photon. Single – photon excited fluorescence, SPEF, quantum yields were generally higher for stilbene - based compounds than styrylthiophenes, but varied considerably depending upon which solvent they were recorded in, as did the excited-state lifetime. For example, THF solutions of the compound *trans*-4'(N,N-diphenylamino)-4-dimesitylborylstilbene (**11a**) displayed $\Phi = 0.91$ and $\tau = 2.15$ ns, whereas acetonitrile solutions gave $\Phi = 0.65$ and $\tau = 2.82$ ns along with a marked bathochromic shift in the position of fluorescence maximum. TPEF cross - sections were measured relative to

fluorescein (with that assumed as equal to one). As with the single - photon excited quantum yields, the stilbene backbone was found to be more effective than the styrylthiophene π – system in enhancing the efficiency of TPEF. Thus, compound **11a** exhibited a TPEF cross – section of 8.3 with respect to. fluorescein, almost three times higher than that of *tran*-2-[(4'-N,N-diphenylamino)styryl]-5-dimesitylborylstilbene (σ' = 3.0) (**11b**). Perhaps surprisingly, diarylamine groups were found to result in higher fluorescent efficiencies than more strongly electron - donating dialkylamine groups for both single and two – photon processes.

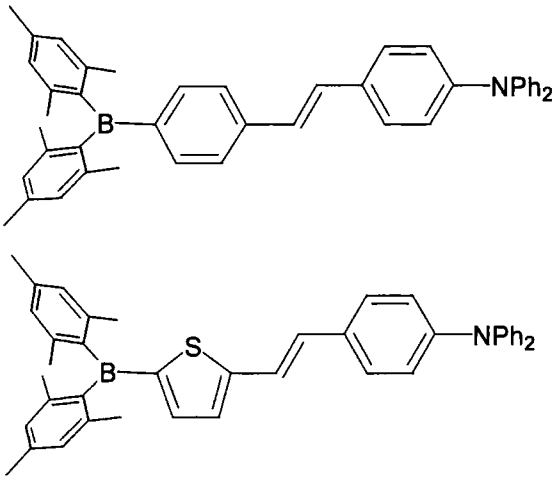

Figure 1.1.29. *trans*-4'-N,N-diphenylamino-4-dimesitylborylstilbene (11a) and *trans*-2-[(4'-N,N-diphenylamino)styryl]-5-dimesitylborylstilbene (11b).

1.1.7. Triarylboranes as sensors

Tamao has prepared a number of anthrylboranes such as tris(9-anthryl)borane (**12**) and 9,10-bis[di(9-anthryl)boryl]anthracene (**13**), in which the anthryl group provides kinetic stability in the same manner as the mesityl group. [44] Starburst oligomers were prepared by adding dimesitylboryl units to the 10-positions on the anthryl ligands. The steric conjestion resulted in propeller-like structures, with large dihedral angles between the boron-centred trigonal plane and anthryl groups, but π-conjugation was extended through boron. UV-vis absorption spectra revealed

structured absorption bands below ca. 390 nm attributed to π-π^* transitions in the anthracene moieties together with an intense broad band at lower energy attributed to a delocalised orbital. Further evidence was provided by calculations at the 6-31 G(d) level, which indicated that the LUMO of tris(9-anthryl)borane is delocalised over the three anthracene moieties via the boron p_z-orbital. The group later investigated the effect of anion complexation on the UV-vis absorption spectra of such compounds.[45] On complexation of fluoride ion, the absorption band situated in the visible region disappeared, resulting in a change from highly coloured to colourless, indicating that complexation of fluoride interrupted the π-conjugation by increasing the coordination number of boron. By contrast, other halide ions and anions such as hydroxide bound only weakly, resulting in little effect on the optical properties and suggesting that these compounds could be used as fluoride-specific chemosensors.

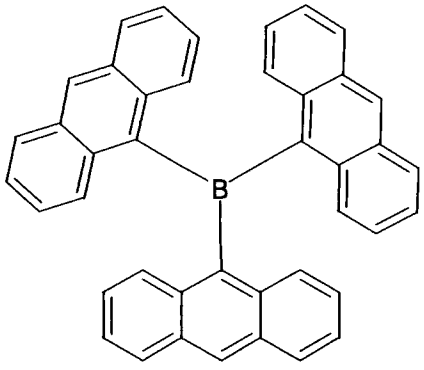

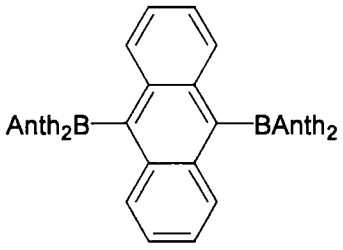

Figure 1.1.30. Trianthrylborane (12) and 9,10-bis(di-9-anthrylboryl)anthracene (13).

The group also investigated a number of dibenzoborole derivatives (**14a-c**) as potential fluoride sensors, this time using the change in fluorescence as an indicator. [46] On changing from THF solution to DMF (a more strongly coordinating solvent), blue-shifts of 100-140 nm were observed, with a dramatic increase (20-30 fold) in quantum yield. Similar effects were observed for THF solutions with increasing amounts of fluoride ion, until the fluorescence spectra resembled those recorded in

DMF. Furthermore, it was found that the fluoride ion could be removed by addition of a stronger fluoride scavenger such as trifluoroborane-diethyletherate, converting the fluoride-bound borates back to the starting dibenzoborole-derivatives.

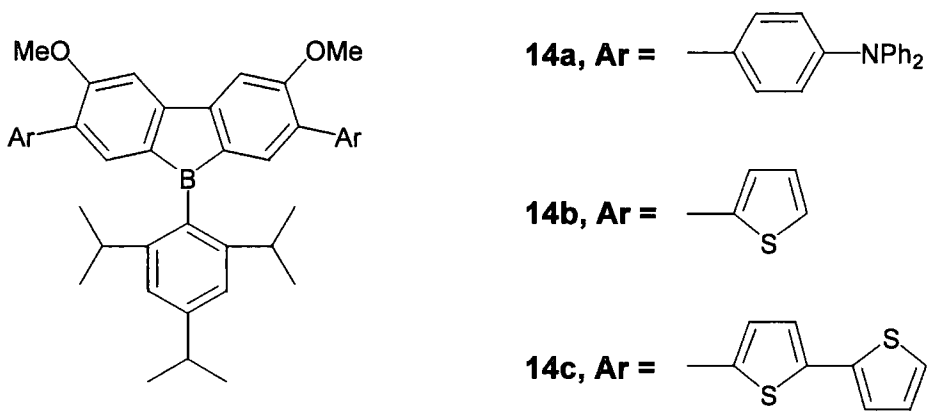

Figure 1.1.31. Dibenzoborole-containing systems (14).

Tamao *et al.* have also prepared [47] a series of tris(phenylethynylduryl)boranes of the form (R-C_6H_4CC-duryl)$_3$B, where R = H, NMe_2, OMe, CN or 4-*n*-BuC_6H_4CC (**15a-e**) and duryl = 2,3,5,6-tetramethylphenyl. The optical properties of the trigonal compounds where R = an electron donor proved to be rather similar to the linear donor-acceptor molecules prepared by other groups: they were highly luminescent, with a strong solvent dependence on the position of the fluorescence maximum but no solvent dependence on the absorption maximum, indicating that both types of compounds have a similar increase in dipole upon excitation. In addition, the incorporation of strong electron-donating substituents resulted in a large bathochromic shift in both absorption and emission spectra. For example, compound **15b** (R = NMe_2) was observed to fluoresce strongly, with λ_{max}(em) = 457 nm (benzene), 512 nm (THF) and 534 nm (DMF), corresponding to a change from blue to green to orange emission, whereas λ_{max}(abs) varied only from 394 to 393 nm. The group also prepared linear molecules of the form (R-C_6H_4-CC-duryl)dimesitylborane (where R =

H or NMe_2). By comparision, λ_{max}(abs) and λ_{max}(em) were blue-shifted with respect to the analagous tridurylboranes by ca. 15-20 nm, indicating that π-conjugation is improved in the tridurylboranes; however, π-conjugation was not significantly increased by extending the length of the arylethynyl moieties (as in **15e**, which had similar optical absorption and emission to **15a**).

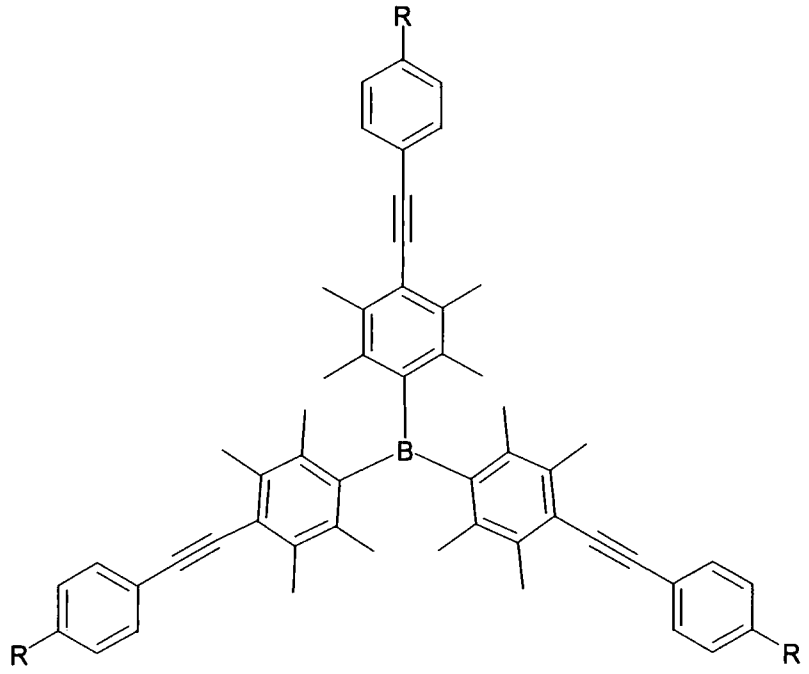

Figure 1.1.32. General form of tris(phenylethynylduryl)boranes (15). R = H (a), NMe_2 (b), OMe (c), CN (d) or 4-*n*-BuC_6H_4CC (e).

The related tridurylboranes tris[*p*-(2,2'-dipyridylamino)phenylduryl]borane and tris[*p*-(2,2'-dipyridylamino)biphenylduryl]borane (**16a,b**) have recently been prepared by Wang *et al.* [48] Both were highly luminescent, with λ_{max}(abs) = 304 nm and λ_{max}(em) = 339 nm (**16a**) and λ_{max}(abs) = 312 nm and λ_{max}(em) = 354 nm (**16b**) (THF). Once again, emission spectra were subject to a strong solvatochromic effect, whereas absorption spectra were unaffected by solvent polarity. Frozen solutions at 77 K displayed new low-energy bands that were attributed to phosphorescence due to their comparatively long decay lifetimes (λ_{max}(em) = 460 nm, τ = 9.1 μs (**16a**) and

λ_{max}(em) =480, 506 nm, τ = 11.0, 9.5 μs (CH_2Cl_2)). The group also investigated the potential of these molecules to act as chemosensors by binding Lewis acids to the dipyridylamino moieties, with the absorption maximum of compound **16a($ZnCl_2$)$_3$** subject to a bathochromic shift of ca. 30 nm with respect to uncomplexed **16a**.

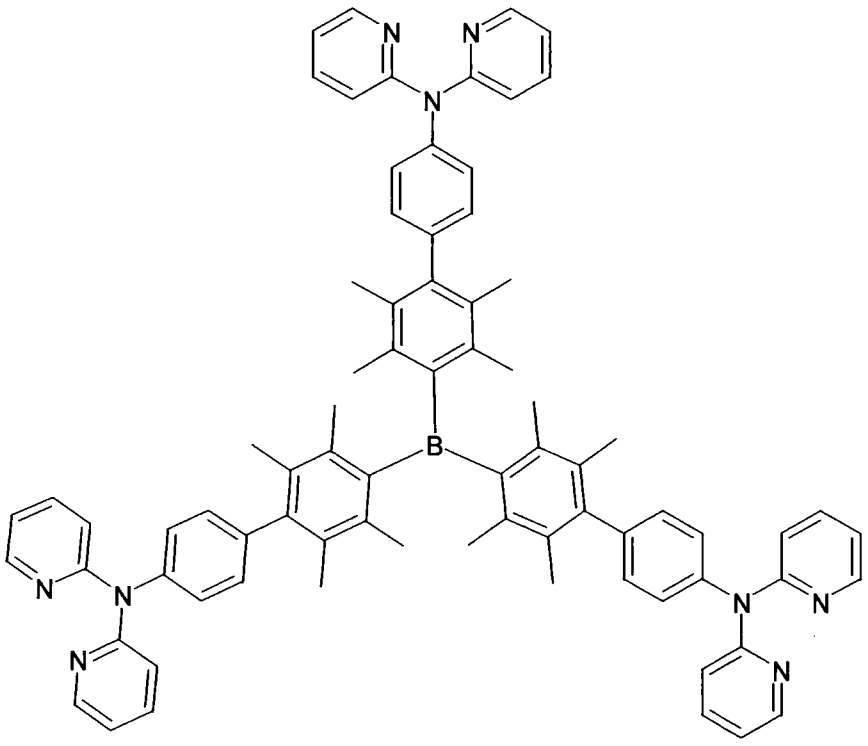

Figure 1.1.33. Tris[*p*-(2,2'-dipyridylamino)phenylduryl]borane (16a).

Although the trigonal molecules had useful optical properties, it was found that their low volatility prevented their use in OLEDs due to the difficulty in vacuum – depositing them onto a substrate. To overcome that problem, the group prepared a series of linear molecules of the general form Mes_2B-X-L, where X = a conjugated aryl or thienyl backbone and L = 2,2'-dipyridylamino (**17**) or 7-azaindolyl (**18**) groups (Figures 1.1.34 and 1.1.35). [49] All of these new molecules were stable in solution and in the solid state, and could be sublimed to form films. Glass transitions were observed for three of the compounds (**17a,b, 18a**), indicating that these are capable of

forming amorphous phases. The compounds had broad absorption bands in the region 300 – 400 nm, assigned to charge – transfer transitions, and sharp absorptions in the 200 – 300 nm region, assigned to ligand – centered $\pi - \pi^*$ transitions. Solutions and films of all compounds fluoresced in the blue region, with a marked solvatochromic effect, and with quantum yields varying widely from 0.06 (**17d**) to 1 (**17e**): in general, the azaindolyl compounds (**18**) had lower quantum yields. The group also found that the Lewis base groups were able to coordinate with either Zn^{II} (**17**) or Ag^{I} ions (**18**). Metal ion complexation had little effect on the position of absorption or emission maxima, but resulted in a decrease in fluorescence intensity attributed to partial quenching, whereas in the solid state interesting extended structures were observed.

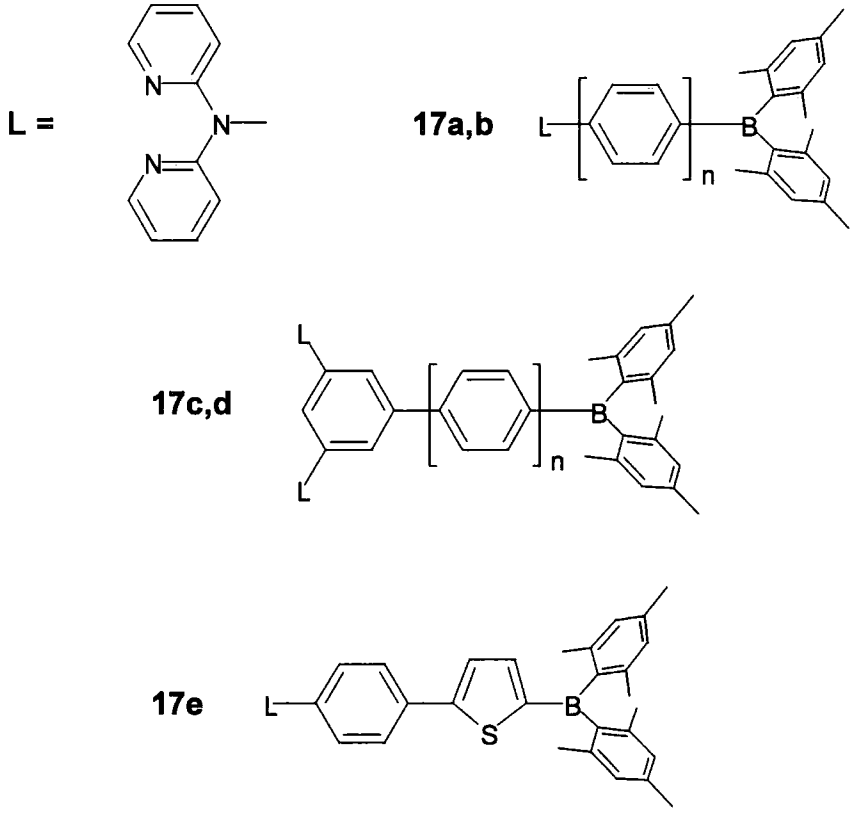

Figure 1.1.34. Compounds 17a (n = 1), 17b (n = 2), 17c (n =0), 17d (n =1) and 17e

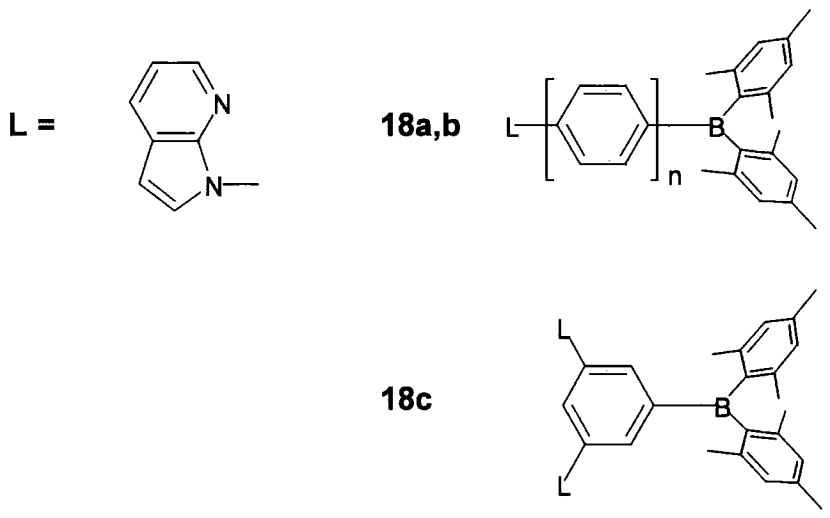

Figure 1.1.35. Compounds 18a (n = 1), 18b (n = 2) and 18c

1.1.8. Nonlinear optical properties of boroxine-based octupolar compounds

The nonlinear optical properties of a series of octupolar molecules based on the boroxine ring (B_3O_3) have recently been investigated. [50] These compounds proved to have intense absorption bands in the UV region but were transparent in the near UV – visible region, a property that is desirable in the construction of practical NLO devices, where optical reabsorption is often a major problem. Harmonic light scattering (HLS) experiments in solution revealed that increasing the electron – donating strength of the aryl substituents led to a significant enhancement of β, indicating that the nonlinear response of these molecules was influenced by intramolecular charge transfer. The authors noted that compound **19c** exhibited a β(0) value of approximately an order of magnitude higher than that of the octupolar molecule 1,3,5-tris(amino)-2,4,6-trinitrobenzene.

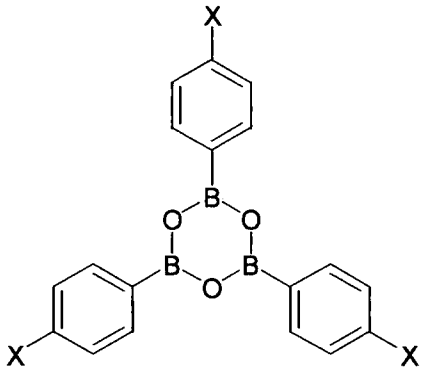

Figure 1.1.36. Boroxine-based molecules where X = OMe (19a), SMe (19b) or NMe_2 (19c)

1.2. Compounds containing four-coordinate boron

A wide variety of compounds containing four-coordinate boron that may potentially prove useful in the field of organic electronics has been synthesised. Although the number of compounds investigated is comparable to that of three-coordinate boron containing species, the field is of less relevance to the work presented here, and so will be discussed in less detail. It should also be noted, however, that a greater number of devices has been constructed with four-coordinate boron materials.

1.2.1. Four - coordinate boron

A fundamental difference between three and four coordinate boron systems is that four - coordinate boron adopts a tetrahedral arrangement, and has no low-lying orbitals through which π - conjugation can be extended. In these systems, therefore, luminescence generally originates from ligand – based orbitals, with the boron moiety providing structural rigidity and / or acting as an electron donating or withdrawing group. In some cases, coordination of heteroatom lone pairs to boron may also discourage $n \rightarrow \pi^*$ transitions, which can lower the fluorescence efficiency since the resulting excited state decays via inter - system crossing.

1.2.2. Rigid rods containing four – coordinate boron

Zwitterionic borates with conjugated π-systems show interesting second-order NLO properties. [51] Upon excitation, these zwitterionic species experience a dipole change in the opposite sense to uncharged D-A molecules, with the excited state having a lower dipole moment than the ground state The organic π – systems are

similarly polarised, but by an inductive (σ) effect rather than a mesomeric (π) effect. The compound {4',-[methyl(diphenyl)phosphonio]biphenyl-4-yl}triphenylborate (**PBB**) was found to exhibit new bands in both absorption and fluorescence spectra upon irradiation, with this band increasing with irradation time whilst the absorption bands attributed to **PBB** irreversibly decreased: it was suggested that photoinduced cleavage of the boron – biphenyl bond, resulting in radical formation and subsequent reaction, was responsible. [51b] When compared to analogous, uncharged D-A molecules, zwitterionic species of the general form Me_3N^+-π-$^-B(n\text{Bu})_3$ show similar β-values but improved transparency and have much higher $\mu\beta_0$ values due to their increased dipole moments; for example, Me_3N^+-Ph-CH=CH-CH=CH-Ph-$^-BBu_3$ (**20**) was found to have $\mu\beta_0$ of approximately 3250 x 10^{-48} esu. [48a] The large dipole moments should favour their alignment in polymer films, thus enhancing macroscopic NLO properties.

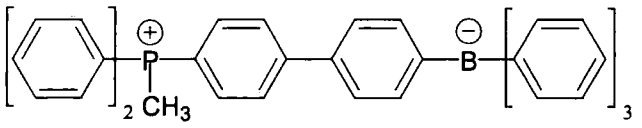

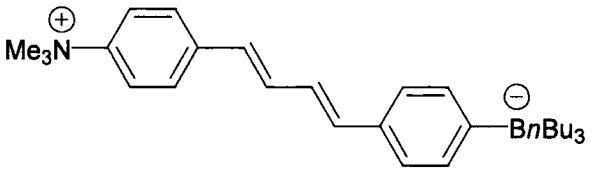

Figure 1.2.1. {4',-[methyl(diphenyl)phosphonio]biphenyl-4-yl}triphenylborate (PBB) and Me_3N^+-Ph-CH=CH-CH=CH-Ph-$^-BBu_3$ (20)

The second order NLO properties of the trifluoroborane and tris(pentafluorophenyl)borane adducts of pyridines and stilbazoles have been investigated by EFISH.[52] Complexation of the Lewis-acidic borane with pyridinyl-N was found to result in a substantial increase in β, with values of $\mu\beta$ increased by a

factor of > 2. For example, whilst the compound trans-4-Me_2N-C_6H_4-C(H)=C(H)-C_5H_4N (**21a**) had $\beta = 45 \times 10^{-30}$ esu and $\mu\beta = 450 \times 10^{-48}$ esu, the borane adducts with BF_3 (**21b**) and $B(C_6F_5)_3$ (**21c**) had β - values of 129 and 155 x 10^{-30} esu and $\mu\beta$ - values of 1520 and 1560 x 10^{-48} esu respectively. Most of the compounds did not, however, display a detectable SHG signal (by the Kurtz powder technique) since they were found to crystallise in centrosymmetric space groups. Although tris(pentafluorophenyl)borane adducts displayed a greater red shift in the UV-vis absorption spectra than BF_3 adducts (consistent with borane acceptor strength), second order effects were generally (but not always) found to be greater in the BF_3 derivatives. A recent theoretical study of these compounds has produced results in good agreement with the experimental data.[53]

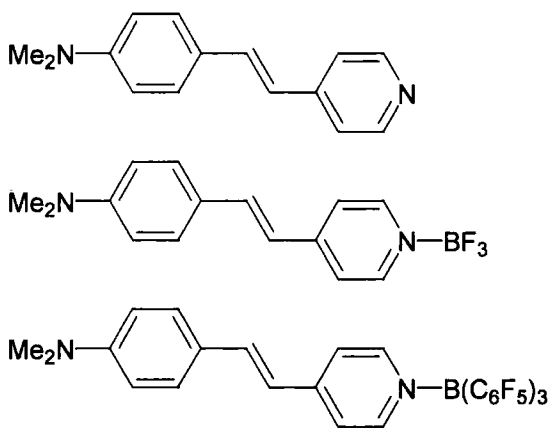

Figure 1.2.2. Stilbazole and stilbazole - borane adducts (21a-c)

1.2.3. Blue light emission from molecules containing four – coordinate boron

There have been a number of studies on boron analogues of Alq_3. Whilst the structure of Alq_3 is octahedral, with bidentate ligands, the smaller size of boron prevents this arrangement. The tetra – quinolato boron compounds Bq_4^- (**22**) and Bq'_4^- (q' = 2-methyl-8-hydroxyquinolato) anions have monodentate coordination through oxygen, [54] whilst compounds of the form BR_2q (**23**) (where R = ethyl,

phenyl or 2–naphthyl) are tetrahedral, with a bidentate quinolato ligand,[55] Generally, the boron compounds emit at shorter wavelengths and are more covalent in nature than their aluminium-based relatives, leading to greater stability towards air and water. The quantum efficiency of emission is higher than that of Alq_3 derivatives, and some of the compounds have also been found to have excellent electron transporting properties. For example, whilst Alq_3 emits with a maximum intensity around 530 nm, devices using $Li^+[Bq_4]^-$ or $Li^+[Bq'_4]^-$ as the emitting layer had strong blue electroluminescence at 466 and 470 nm respectively. The electron affinity of these compounds, however, was lower than that of Alq_3.

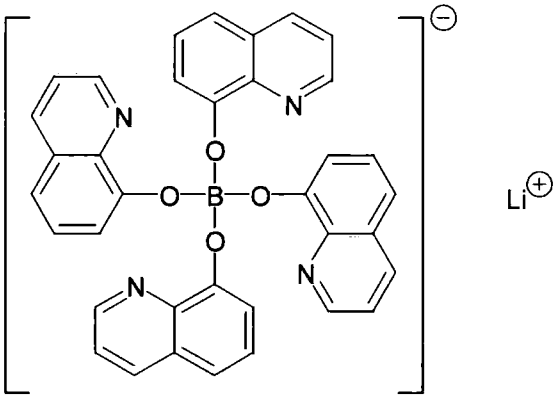

Figure 1.2.4. Schematic structure of lithium tetra-(8-hydroxyquinolato) boron (22)

In contrast, the compounds BR_2q (R = phenyl or 2-naphthyl) were found to be excellent electron-transport materials as well as being highly luminescent. Whilst devices using BR_2q (R = phenyl) as either the emissive or both electron – transport and emissive layer suffered from exiplex formation (resulting in a large red – shift in EL when compared to the PL emission), exiplex formation was not observed in a device using BR_2q (R = 2-naphthyl) in which it functioned as both an electron - transporter and emitter, with λ_{max}(EL) = 514 nm (blue – green). In all cases, the efficiency of these devices was high.

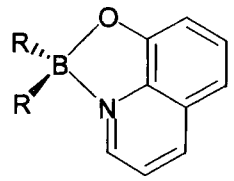

Figure1.2.5. General form of BR_2q compounds (23a-c)

Strong blue EL has also been observed for the air stable diborates $B_2(\mu\text{-}O)R_2(azain)_2$ (R = ethyl or phenyl, azain = 7-azaindole anion)[56] (**24a,b**), and for the complexes BPh_2(2-py-in) and BPh_2(2-py-azain) (2-py-in = 2-(2-pyridyl)indole, 2-py-azain = 2-(2-pyridyl)-7-azaindole).[57] The parent ligand 7-azaindole has no emission in the visible region (λ_{max}(PL) = 357 nm (toluene solution)), but the unstable azaindole anion exhibits bright blue emission in solution and in the solid state; complexation to a central atom such as boron stabilises the anionic ligand whilst maintaining efficient luminescence. In the oxo – bridged diborates, not only was the emission band red shifted from the near – UV to the blue region with respect to. 7-azaindole (λ_{max}(PL) = 419 nm (R = ethyl) and λ_{max}(PL) = 450 nm (R = phenyl)), but the relative intensity of emmision was also greatly increased. It was suggested that this was due to the increase in structural rigidity of the ligand conferred by binding to two boron atoms, thus reducing energy loss via vibrational relaxation of the excited state species. Although the diborates are stable to air and moisture, and have a melting point close to 300 °C, multilayer EL devices were found to have limited long – term stability. A similar oxo-bridged diborate $B_2(O)(Ph_2(q')_2 \cdot H_2O \cdot CH_2Cl_2$, which emits in the blue-green region, has also been reported.[58]

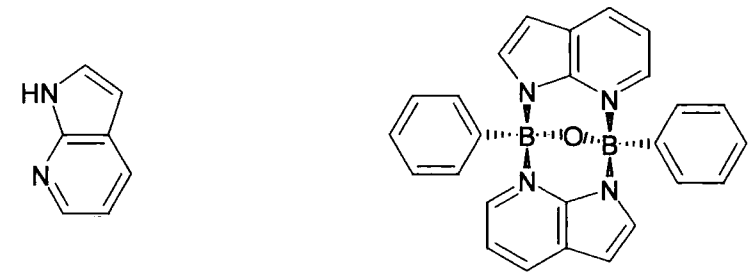

Figure 1.2.6. 7-azaindole and the diborate complex $B_2(\mu\text{-}O)Ph_2(azain)_2$ (24b)

Thin films of the pyridine-phenol complexes 1,6-bis(2-hydroxy-5-R-phenyl)pyridinediyl boron fluoride, ((dppy)BF, R = H) **(25a),** and (mdppy)BF, R = methyl) **(25b)**, have been shown to fluoresce in the blue region and efficiently transport electrons due to intermolecular $\pi\cdots\pi$ stacking interactions in the solid state. [59] When these materials were used to construct multilayer EL devices, however, long wavelength emission bands were observed due to exiplex formation with the hole – transporting material **TPD** (Figure 1.1.21). When the compound *N,N'*-bis(α-naphthyl)-*N*-*N'*-diphenyl-1,1'-biphenyl-4,4'-diamine (**NPB**) was used as the hole transporting layer, devices exhibited a broad emission band due to exiplex formation that resulted in highly efficient white – light emission. It was found that by incorporating a red - emitting layer and varying the relative thickness of the individual layers the emission could be tuned so as to cover the region 500 to 700 nm, and bright white – emitting devices could be constructed. [60] It was suggested that the emission band was the result of overlapping emission bands; interfacial exiplex emission between **NPB** and (dppy)BF, blue emission from bulk **NPB** and bulk (dppy)BF, and red emission from the doped Alq_3 dye.

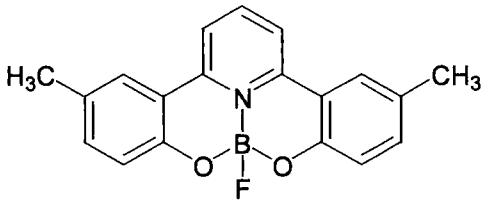

Figure 1.2.7. 1,6-bis(2-hydroxy-5-methyl-phenyl)pyridinediyl boron fluoride (25b)

Another white emitting electroluminescent device has been constructed using the blue light emitting compound $BPh_2(pybm)$ (pybm = 2-(2-pyridyl)benzimidazolate) (**26**). [61] Once again, the boron complex was used as the emitting layer, with a hole - transporting layer of **NPB**, but in this case undoped Alq_3 was used as the electron - transporting layer, resulting in a broad emission band from ca 400 – 750 nm.

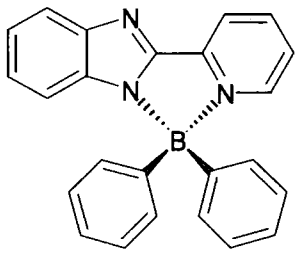

Figure 1.2.8. $BPh_2(pybm)$ (26)

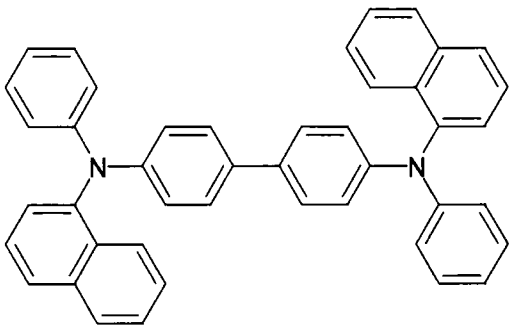

Figure 1.2.9. *N,N'*-bis(α-naphthyl)-*N*-*N'*-diphenyl-1,1'-biphenyl-4,4'-diamine (NPB)

1.2.4. Boron – dipyrrin and dioxaborine – based materials

Fluorophores based on boron dipyrrin, **27**, of the general structure illustrated in figure 1.2.11, have proven to be particularly versatile. [62] Daub and co-workers

have demonstrated that phenolic dyes incorporating this moiety may be deprotonated by organic bases, and have investigated the emissive properties of the phenol / phenolate equilibrium in organic solvents. Successive addition of pyridine resulted in a significant decrease in fluorescent intensity with no change in emission wavelength, whereas reprotonation with trifluoroacetic acid restored fluorescence. Switching between fluorescent on / off states could be repeated with no decomposition or precipitate formation, suggesting that such compounds could be used as novel molecular probes. [63]

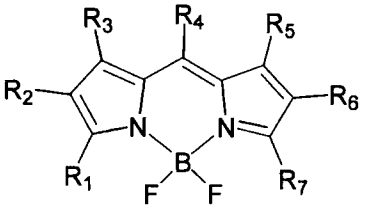

Figure 1.2.10. General form of the boron-dipyrrin fluorophore (27)

The group later investigated an optically active binaphthalene system bearing two boron-dipyrromethene groups **(28),** showing that chiral discrimination towards the enantiomers of 1-phenylethylamine could be achieved by a similar protonation / deprotonation mechanism. [64] In both cases, the fluorescent quenching was due to a photoinduced electron transfer mechanism between the boron-dipyrrin and the naphtholate or phenolate groups.

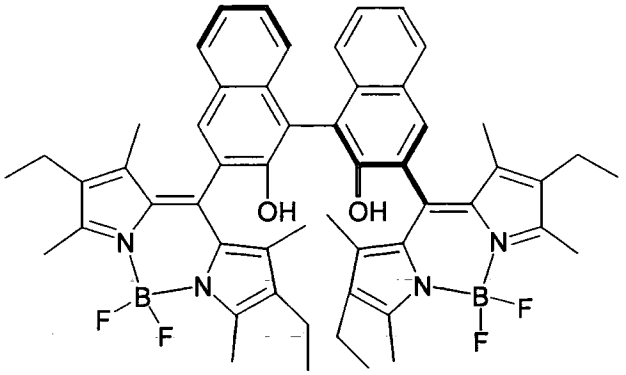

Figure 1.2.11. Optically active boron-dipyrrin dye (28)

Light harvesting arrays comprising a porphyrin and one, two or eight boron-dipyrrin groups have been synthesised using a modular building block approach. [65] Energy transfer from the photoexcited boron-dipyrrin units to the porphyrin energy accepter was found to be highly efficient, and the optical properties of the boron-dipyrrin and porphyrin moieties were found to be complimentary, suggesting that such materials might find use in molecular photonics applications. Light harvesting and photocurrent generation has also been demonstrated for gold electrodes modified with boron-dipyrrin containing mixed monolayers. [66] Monolayers consisting of boron-dipyrrin and porphyrin were shown to exhibit strong energy transfer on the gold surface, but more promising results were obtained when the porphyrin was replaced by a ferrocene (Fc)-porphyrin (P)-fullerene (C_{60}) triad. This system was suggested to be an artificial photosynthetic system, mimicking photoinduced energy transfer (from boron-dipyrrin to the Fc-P-C_{60} triad) as well as multistep electron transfer processes, and additionally provided efficient light to electric current conversion with a quantum yield of 50 ± 8%. The same group has also demonstrated that molecular wires can also be constructed using the boron-dipyrrin group coupled via alternating diphenylacetylene and zinc porphyrin units to an uncomplexed (free base) porphyrin, but here it was found that replacement of the boron-dipyrrin moiety with perylene-based groups gave rise to superior materials. [67]

Compounds similar to the N – based boron dipyrrins, namely dioxaborines, have recently received attention for potential use as electron – transport materials. [68] The single – electron reduction of a phenylene-bridged bis(dioxaborine) (**29**) resulted in a mixed-valence anion with a structured absorption in the near – IR (λ_{max} = 920 nm) that was assigned to the intervalence charge – transfer transition, the nature of which

led to the assignment of **29a**$^{-}$ to Robin and Day's class III (fully delocalised). The authors suggested that the facile reduction and strong electron delocalisation might make this type of compound suitable for incorporation into conjugated polymers, which would be expected to act as efficient electron – transporters. The group later examined the two – photon absorption of **29a** and related materials (**29b,c**) in which the phenylene bridge was replaced by other conjugated units. [69] In compounds **29a** and **30b**, the main peaks in the TPA spectra occurred at significantly less than twice the wavelength of the single – photon absorption maxima, indicating that the most strongly allowed two – photon transition involves a state higher in energy than that which is populated in the single – photon transition. Compound **29c** was investigated for the photodeposition of silver, where it was effectively used to fabricate silver lines by reduction of silver ions at low dye concentrations.

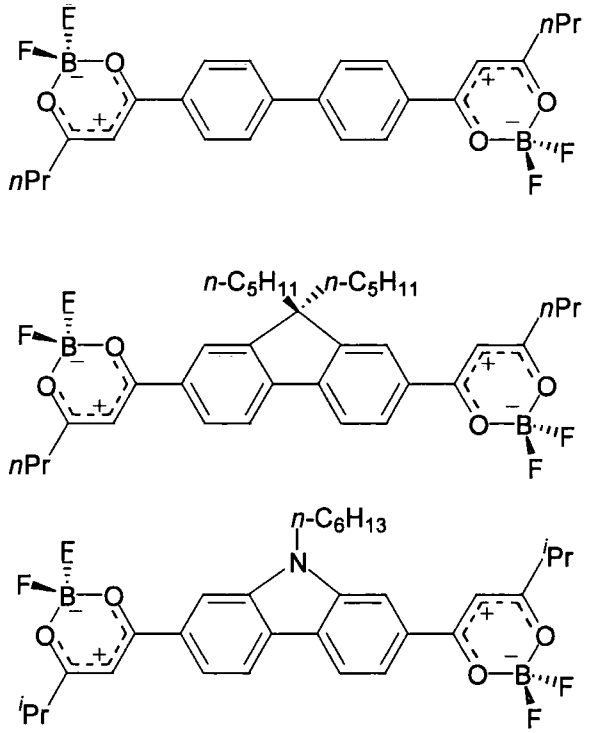

Figure 1.2.12. Bis(dioxaborine) based materials (29a-c)

1.3. Borane and carborane clusters

When compared to the number of three and four – coordinate boron compounds that have been investigated for electrooptical application, polyhedral boranes and carboranes have received little attention. In an early study, the first molecular hyperpolarizibilities of a series of disubstituted icosahedral carboranes have been investigated by SHG and EFISH,[70] but were found to be generally low. Whilst the trend in increasing second order activity with increasing electron donor strength were similar to those found with carbon – based D-A molecules, it was postulated that charge transfer bands in these compounds occur further into the UV, and therefore the band – gaps are larger. Studies of second – order NLO effects were also hindered by the propensity of the carboranes to crystallise in centrosymmetric space groups, and by luminescence of amino – derivatives upon laser excitation. More promising NLO activities have recently been reported for other carborane – based materials. The second order NLO activity of the carborane ylide, $12\text{-}C_7H_6^+\text{-}CB_{11}H_{11}^-$ has been investigated by HRS, and displayed a reasonably high β-value of $236 \pm 50 \times 10^{-30}$ esu; it was also found to be transparent above 400 nm. [71]

Theoretical work has also suggested the potential of boranes and carboranes for second order NLO. *Ab initio* molecular orbital calculations have also suggested that dimeric dodecaborane-dicarbadodecaborane dianions should display NLO properties, with calculated $\beta(0)$ values ranging from $3.4 - 3.6 \times 10^{-30}$ esu for the *ortho*, *meta* and *para* carborane isomers.[72] In these compounds, the dodecaborane group was calculated to act as an electron donor, with the carborane group acting as an electron acceptor, leading to a charge transferred first excited state. The structures and second-order responses for *nido, conjuncto* and *closo* boranes bearing tropylium

($C_7H_6^+$) and cyclopentadienyl ($C_5H_4^-$) substituents have been calculated using semiempirical methods (MOPAC AM1), as have the corresponding carboranes.[73] Some of these clusters were predicted to exhibit surprisingly large β and μβ values. For example, $[(C_7H_6)C_2B_{10}H_{10}(C_5Me_4)]$ was calculated to have $\mu\beta = 12{,}000 \times 10^{-48}$ esu and $\beta = 682 \times 10^{-30}$ esu. A partial explanation for the high (calculated) NLO activities came from a comparison of the HOMOs and LUMOs. In the ground state, the HOMO is located primarily on the cyclopentadienyl ring, with the LUMO located on the tropylium ring leading to high polarisation but without introducing significant strain into the polyhedral spacer: these species may therefore have significant zwitterionic character. The group have reported the synthesis of a precursor (**31**) to one of the compounds for which calculations have been performed, which should hopefully lead to experimental studies to compare with theoretical calculations.[74]

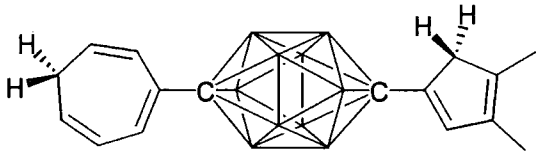

Figure 1.3.1. Precursor to tropyl – cyclopentadienyl substituted dicarbadodecaborane (30)

A recent study of some novel carborane – fullerene dyads linked via phenylacetylene has been reported, which can be thought of as A-π-A systems. [75] These materials exhibited unexpectedly large *β*-values of up to 1189×10^{-30} esu (by HRS), leading to the authors to suggest that in the excited state, the fullerene moieties act as electron donors, though there have been no previous reports of fullerenes behaving in that manner. In the excited state, therefore, electron density is postulated to be transferred through the phenylacetylene linker from fullerene to the linking carbon atom of the carborane cage, leading to a difference in electron density of the

two-carborane carbons, followed by charge transfer between carbons through the σ – aromatic cage. Clearly, more examples of this type of compound will be required to support the proposed mechanism.

The potential use of metallacarboranes in optoelectronics has received very little attention. The hafnium carborane complex $Hf(\eta^5:\eta^1\text{-}CpCMe_2CB_{10}H_{10}C)_2$ displays PL, EL and mechanoluminescence in the blue region, but single layer EL devices incorporating the compound in various percentages into a poly(N-vinylcarbazole) blend displayed a maximum emission at 530 nm, the nature of which was unexplained.[76]

1.4. Summary

Molecular and polymeric boron-containing species exhibit a wide variety of useful properties. Three-coordinate boron has been incorporated into many different systems, where its properties as a strong π – acceptor and its ability to conjugate with adjacent organic π – systems often lead to interesting linear and nonlinear optical effects. Some of these compounds may prove useful in the rapidly expanding field of organic electronics, as has been demonstrated by the construction of a number of optoelectronic devices. Compounds containing four – coordinate boron have also been widely investigated for both electroluminescence and NLO applications, and have proven to be particularly useful as blue light emitters in OLEDs – an area of much current interest. Although polyhedral boranes and carboranes have been less studied, there are recent indications that the unique properties of the boron – based cages may be useful in designing NLO active materials.

1.5. References

[1] Glogowski, M. E.; Williams, J. L. R. *J. Organomet. Chem.* **1981**, *218*, 137 – 146.

[2] Williams, J. L. R.; Grisdale, P. J.; Doty, J. C. *J. Org. Chem.* **1971**, *36*, 544 – 549.

[3] Doty, J. C.; Babb, B.; Grisdale, P. J.; Glogowski, M.; Williams, J. L. R. *J. Organomet. Chem.* **1972**, *38*, 229 – 236.

[4] (a) Glogowski, M. E.; Williams, J. L. R. *J. Organomet. Chem.* **1981**, *216*, 1 – 8. (b) Glogowski, M. E.; Zumbulyadis, N.; Williams, J. L. R. *J. Organomet. Chem.* **1982**, *231*, 97 – 107.

[5] Kaim, W; Schultz, A. *Angew. Chem. Int. Ed.* **1984**, *23*, 615 – 616.

[6] Schultz, A.; Kaim, W. *Chem. Ber.* **1989**, *122*, 1863 – 1868.

[7] (a) Richardson, D.E.; Taube, H.; *Inorg. Chem.* **1981**, *20*, 1278 – 1285. (b) Polcyn, D.; Shain, I.; *Anal. Chem.* **1966**, *38*, 370 – 376.

[8] Fiedler, J.; Zalis, S.; Klein, A.; Hornung, F. M.; Kaim, W. *Inorg. Chem.* **1996**, *35*, 3039 – 3043.

[9] Okada, K.; Sugawa, T.; Oda, M.; *J. Chem. Soc., Chem. Commun.* **1992**, 74 – 75.

[10] Rajca, A.; Rajca, S.; Desai, S. R.; *J. Chem. Soc. Chem., Commun.* **1995**, 1957 – 1958.

[11] Lichtblau, A.; Kaim, W.; Scultz, A.; Stahl, T. *J. Chem. Soc., Perkin Trans. 2* **1992**, 1497 – 1501.

[12] (a) Yuan, Z.; Taylor, N. J.; Marder, T. B.; Williams, I. D.; Kurtz, S. K.; Cheng, L.-T.; *J. Chem. Soc., Chem. Communs.* **1990**, 1489 – 1492. (b) Yuan, Z.; Taylor, N. J.; Marder, T. B.; Williams, I. D.; Cheng, L.-T. in *Organic Materials for Non-linear Optics II, Spec. Publ. No. 91* (Eds.: R. A. Hann and D. Bloor), The Royal Society of Chemistry, Cambridge, **1991**, pp. 190 – 194. (c) Yuan, Z.; Collings, J. C.; Taylor, N. J.; Marder, T. B.; Jardin, C.; Halet, J.-F. *J. Solid State Chem.* **2000**, *154*, 5 – 12. (d) A value of 60 x 10^{-30} esu for $\beta(0)$ was reported for this compound by other workers *vs.* 30 x 10^{-30} esu for the Z-isomer; see reference 15c.

[13] (a) Hooz, J.; Akiyama, S.; Cedar, F. J.; Bennet, M. J.; Tuggle, R.M. *J. Am. Chem. Soc.* **1974**, *96*, 274 (b) Pelter, A.; Singaram, S.; Brown, H. C. *Tetrahedron Lett.* **1983**, *24*, 1433. (c) Entwistle, C. D.; Marder, T. B.; Smith, P. S.; Howard, J. A. K.; Fox, M. A.; Mason, S. A. *J. Organometal. Chem.* **2003**, *680*, 165-172.

[14] Yuan, Z.; Taylor, N. J.; Sun, Y.; Marder, T. B.; Williams, I. D.; Cheng, L.-T. *J. Organomet. Chem.* **1993**, *449*, 27 – 37.

[15] Yuan, Z.; Taylor, N. J.; Ramachandran, R.; Marder, T. B. *Appl. Organomet. Chem.* **1996**, *10*, 305 – 316.

[16] (a) Lequan, M.; Lequan, R. M.; Ching, K. C. *J. Mater.Chem.* **1991**, 1, 997 – 999. (b) Lequan, M.; Lequan, R. M.; Ching, K. C.; Barzoukas, M.; Fort, A.; Lahoucine, H.; Bravic, B.; Chasseau, D.; Gaultier, J. *J. Mater. Chem.* **1992**, *2*, 719 – 725. (c) Lequan, M.; Lequan, R. M.; Chane-Ching, K.; Callier, A.-C.; Barzoukas, M.; Fort, A. *Adv. Mat. Opt. Electron.* **1992**, *1*, 243-247. (d) Branger, C.; Lequan, M.; Lequan, R. M.; Barzoukas, M.; Fort, A. *J. Mater. Chem.*, **1996**, *6*, 555 – 558.

[17] Branger, C.; Lequan, M.; Lequan, R. M.; Large, M.; Kajzar, F. *Chem. Phys. Lett.* **1997**, *272*, 265 – 270.

[18] (a) Matsumi, K.; Chujo, Y. in *Contemporary Boron Chemistry, Spec. Publ. No. 253* (Eds.: M. G. Davidson, A. K. Hughes, T. B. Marder, K. Wade), The Royal Society of Chemistry, Cambridge, **2000**, pp. 51 – 58. (b) Chujo, Y.; Takiza, N.; Sakurai, T. *J. Chem. Soc. Chem. Commun.* **1994**, 227 – 228. (c) Chujo, Y. *J. Macromol. Sci. Pure* **1994**, *A3,* 1647 – 1655. (d) Chujo, Y.; Sakarai, T.; Takizawa, N. *Polym. Bull.* **1994**, *33*, 623 – 628. (e) Chujo, Y.; Morimoto, M.; Tomita, I. *Polym. J.* **1994**, *27*, 90 – 97. (f) Matsumi, N.; Chujo, Y. *Polym. Bull.* **1997**, *39*, 295 – 302. (g) Matsumi, N.; Chujo, Y. *Polym. Bull.* **1997**, *38*, 531 – 536. (h) Chujo, Y. *Macromol. Symp.* **1997**, *118*, 111 – 116. (i) Matsumi, N.; Chujo, Y. *Macromolecules* **1998**, *31*, 3155 – 3157. (j) Miyata, M.; Matsumi, N.; Chujo, Y. *Polym. Bull.* **1999**, *42*, 505 – 510. (k) Chujo, Y.; Sasaki, Y.; Kinomura, N.; *Polymer* **2000**, *41*, 5047 – 5051. (l) Miyata, M.; Meyer, F.; Chujo, Y. *Polym. Bull.* **2001**, *46*, 23 – 28. (m) Matsumi, N.; Chujo, Y. *Polym. J.* **2001**, *33*, 383 – 386. (n) Miyata, M.; Chujo, Y. *Polym. J.* **2002**, *34*, 967 – 969.

[19] Matsumi, N.; Chujo, Y. *J. Am. Chem. Soc.* **1998**, *120*, 5112 – 5113.

[20] Matsumi, N.; Miyata, M.; Chujo, Y. *Macromolecules* **1999**, *32*, 4467 – 4469.

[21] Kobayashi, H.; Sato, N.; Ichikawa, Y.; Miyata, M.; Chujo, Y.; Matsuyama, T. *Syn. Met.*, **2003**, 393 – 394.

[22] (a) Matsumi, N.; Chujo, Y.; Lavastre, O.; Dixneuf, P. H. *Organometallics* **2001**, *20*, 2425 – 2427. (b) Matsumoto, F.; Matsumi, N.; Chujo, Y. *Polym. Bull.* **2001**, *46*, 257 – 262. (c) Matsumoto, F.; Matsumi, N.; Chujo, Y.*Polym. Bull.* **2002**, *34*, 119 – 120.

[23] Matsumi, N.; Naka, K.; Chujo, Y. *J. Am. Chem. Soc.* **1998**, *120*, 10776 – 10777.

[24] Matsumi, N.; Umeyama, T.; Chujo, Y. *Polym. Bull.* **2000**, *44*, 431 – 436.

[25] (a) Matsumi, N.; Kotera, K.; Naka, K.; Chujo, Y. *Macromolecules* **1998**, *31*, 3155 – 3157. (b) Matsumi, N.; Kotera, K.; Chujo, Y. *Macromolecules* **2000**, *33*, 2801 – 2806.

[26] (a) Chujo, Y,; Tomita, I.; Murata, N; Mauermann, H.; Saegusa, T. *Macromolecules* **1992**, *25*, 27. (b) Chujo, Y.; Tomita, I.; Saegusa, T. *Polym. Bull.* **1993**, *31*, 553. (c) Chujo, Y.; Tomita, I.; Saegusa, T. *Polym. Bull.* **1993**, *31* 547. (d) Chujo, Y.; Tomita, I.; Saegusa, T.; *Macromolecules* **1994**, *27*, 6714. (e) Chujo, Y.; Tomita, I.; Asano, T.; *Polym. J.* **1994**, 26, 85 – 92. (f) Chujo, Y.; Tomita, I. *Macromol. Symp.* **1997**, *122*, 83 – 88. (g) Matsumi, N.; Chujo, Y. *Polym. Bull.* **1999**, *43*, 117 – 120. (h) Matsumi, N.; Chujo, Y. *Polym. Bull.* **1999**, *43*, 151 – 155. (i) Naka, K.; Umeyama, T.; Chujo, Y. *Macromolecules*, **2000**, *33*, 7467 – 7470. (j) Matsumi, N.; Chujo, Y.; *Macromolecules* **2000**, *33*, 8146 – 8148. (k) Matsumi, N,; Umeyama, T.; Chujo, Y. *Macromolecules*, **2001**, *34*, 3510 – 3511. (l) Matsumi, N.; Chujo, Y. *J. Organometal. Chem.* **2003**, *680*, 8047 – 8050.

[27] (a) Matsumi, N.; Naka, K.; Chujo, Y. *Polym. J.* **1998**, *30*, 833. (b) Matsumi, N.; Naka, K.; Chujo, Y. *Macromolecules*, **1998**, *31*, 8047 – 8050. (b)

[28] Matsumi, N.; Umeyama, T.; Chujo, Y. *Macromolecules*, **2000**, *33*, 3956 – 3957.

[29] Miyata, M.; Matsumi, N.; Chujo, Y. *Macromolecules*, **2001**, *34*, 7331 – 7335.

[30] Corriu, R. J. P.; Deforth, T.; Douglas, W.E., Guerrero, G.; Siebert, W. S.; *J. Chem. Soc., Chem. Commun.* **1998**, 963 – 964.

[31] For a more thorough discussion of light emitting electrochemical processes, see, for example, Armstrong, N.R.; Wightman, R.M.; Erin, M. *Annu. Rev. Phys. Chem.* **2001**, *52*, 391 – 422.

[32] Tang, C. W.; van Slyke, S. A. *Appl.Phys. Lett.* **1987**, *51*, 913-915.

[33] Shirota, Y. *J. Mater. Chem.* **2000**, *10*, 1 – 25.

[34] (a) Noda, T.; Shirota, Y. *J. Am. Chem. Soc.* **1998**, *120*, 9714 – 9715. (b) Makinen, A. J.; Hill, I. G.; Noda, T.; Shirota, Y.; Kafafi, Z. H. *Appl. Phys. Lett.* **2001**, *78*, 670 – 672.

[35] (a) Noda, T.; Ogawa, H.; Shirota, Y. *Adv. Mater.* **1999**, *11*, 283 – 285. (b) Noda, T.; Shirota, Y. *J. Luminescence* **2000**, 1168 – 1170.

[36] Hamada, Y.; Adachi, C.; Tsutsui, T.; Saito, S. *Jpn. J. Appl. Phys.* **1992**, *31*, 1812 – 1813.

[37] Chen, B. J.; Zhang, X. H.; Lin, X. Q.; Kwang, H. L.; Wong, N. B.; Gambling, W. A.; Lee, S.T. *Syn. Met.* **2001**, *118*, 193 – 196.

[38] Zhou, J.; Pun, E. Y. B.; Chung, P. S.; Zhang, X. H. *Optics Commun.* **2001**, *191*, 427 – 433.

[39] Kinoshita, M.; Shirota, Y. *Chem. Lett.* **2001**, 614 – 615.

[40] Kinoshita, M.; Fujii, N.; Tsuzuki, T.; Shirota, Y. *Syn. Met.* **2001**, *121*, 1571 – 1572.

[41] (a) Shirota, Y.; Kinoshita, M.; Noda, T.; Okumoto, K.; Takahiro, O. *J. Am. Chem. Soc.* **2000**, *122*, 11021 – 11022. (b) Doi, H.; Kinoshita, M.; Okumoto, K.; Shirota, Y. *Chem. Mater.* **2003**, *15*, 1080 – 1089.

[42] Allbrecht, K.; Kaiser, V.; Boese, R.; Adams, J.; Kaufmann, D. E. *J. Chem. Soc., Perkin Trans. 2* **2000**, 2153 – 2157.

[43] (a) Liu, Z.-Q.; Fang, Q.; Wang, D.; Xue, G., Yu, W.-T.; Shao, Z.-S.; Jiang, M.-H.; *J. Chem. Soc. Chem. Commun.* **2002**, 2900 – 2901. (b) Liu, Z.-Q.; Fang, Q., Wang, D.; Cao, D.-X.; Xue, G.; Yu, W.-T.; Lei, H. *Chem. - Eur. J.* **2003**, *9*, 5074 – 5084.

[44] Yamaguchi, S.; Akiyama, S.; Tamao, K. *J. Am. Chem. Soc.* **2000**, *122*, 6335 – 6336.

[45] (a)Yamaguchi, S.; Akiyama, S.; Tamao, K. *J. Am. Chem. Soc.* **2001**, *123*, 11372 – 11375. (b) Yamaguchi, S.; Akiyama, S.; Tamao, K. *J. Organomet. Chem.* **2002**, *652*, 3 – 9.

[46] Yamaguchi, S.; Shirasaka, T.; Akiyama, S.; Tamao, K. *J. Am. Chem. Soc.* **2002**, *124*, 8816 – 8817.

[47] Yamaguchi, S.; Shirasaka, T.; Tamao, K. *Org. Lett.* **2000**, *2*, 4129 – 4132.

[48] Jai, W.-L.; Song, D.; Wang, S. *J. Org. Chem.* **2002**, *68*, 701 – 705.

[49] Jia, W.-L.; Bai, D.-R.; M^{c}Cormick, T.; Liu, Q.-D.; Motala, M.; Wang, R.-Y.; Seward, C.; Wang, S. *Chem. Eur. J.* **2004**, *10*, 994 – 1006.

[50] Alcaraz, G.; Euzenat, L.; Mongin, O.; Ledoux, I.; Zyss, J.; Blanchard-Desce, M.; Vaultier, M. *Chem. Commun.* **2003**, 2566 – 2567.

[51] (a) Lambert, C.; Stadler, S.; Bourhill, G.; Bräuchle, C. *Angew. Chem.* **1996**, *108*, 710-712; *Angew. Chem. Int. Ed. Engl.* **1996**, *35*, 644-646. (b) Ching, K.C.; Lequan, M.; Lequan, R. M.; Grisard, A.; Markovitsi, D. *J. Chem. Soc. Faraday Trans.* **1991**, *87*, 2225 - 2228.

[52] Lesley, M. J. G. ; Woodward, A.; Taylor, N. J. ; Marder, T. B.; Cazenobe, I. ; Ledoux, I.; Zyss, J.; Thornton, A.; Bruce, D. W.; Kakkar, A. K. *Chem. Mater.* **1998**, *10*, 1355-1365.

[53] Su, Z. M.; Wang, X. J.; Huang, Z. H.; Wang, R. S.; Feng, J. K.; Sun, J. Z. *Synthetic Metals* **2001**, *119*, 583-584.

[54] (a) Tao, X. T.; Suzuki, H.; Wada, T.; Miyata, S.; Sasabe, H. *J. Am. Chem. Soc.* **1999**, *121*, 9447-9448. (b) Tao, X. T.; Suzuki, H.; Wada, T.; Sasabe, H.; Miyata,

S. *App. Phys. Lett.* **1999**, *75*, 1655-1656. (c) Miyata, S.; Sakuratani, Y.; Tao, X. T. *Optical Materials*, **2002**, *21*, 99-107.

[55] (a) Anderson, S.; Weaver, M. S.; Hudson, A.J. *Syn. Lett.* **2000**, *111-112*, 459-463. (b) Wu, Q.; Esteghamation, M.; Hu, N.-X.; Popovic, Z.; Enwright, G.; Tao, Y.; D'Iorio, M.; Wang, S. *Chem. Mater.* **2000**, *12*, 79-83.

[56] (a) Hassan, A.; Wang, S. *Chem. Commun.* **1998**, 211-212. (b) Esteghamation, M.; Hu, M. X. Popovic, Z.; Enright, G.; Breeze, S. R.; Wang, S. *Angew. Chem. Int. Ed. Engl.* **1999**, *38*, 985-988.

[57] Wang, S. *Coord. Chem. Rev.* **2001**, *215*, 79-98.

[58] Son, H. .; Jang, H.; Jung, B.-J.; Kim, D.-H.; Shin, C. H.; Hwang, K.Y.; Shim, H.-K.; Do, Y. *Syn. Met.*, **2003**, *137*, 1001 – 1002.

[59] (a) Li, Y.; Liu, Y.; Guo, J.; Wang, Y. *Chem. Commun.* **2000**, 1551-1552. (b) Liu, Y.; Guo, J.; Zhang, H.; Wang, Y. *Angew. Chem. Int. Ed. Engl.* **2002**, *41*, 182-184.

[60] Feng, J.; Liu, Y.; Li, Y.; Wang, Y.; Liu, S. *Opt. and Quant. Electronics* **2003**, *35*, 259-265.

[61] Liang, F. S.; Cheng, Y. X.; Su, G. P.; Ma, D. G.; Wang, L. X.; Jing, X. B.; Wang, F. S. *Sythetic Metals*, **2003**, *137*, 1109-1110.

[62] Rurack, K.; Kollmannsberger, M.; Daub, J. *New J. Chem.* **2001**, *25*, 289-292.

[63] Gareis, T.; Huber, C.; Wolfbeis, O. S.; Daub, J. *Chem. Commun.* **1997**, 1717-1718.

[64] Beer, G.; Rurack, K.; Daub, J. *Chem Commun.* **2001**, 1138-1139.

[65] Li, F.; Yang, S. I.; Ciringh, Y.; Seth, J.; Martin, C. H.; Singh, D. L.; Kim, D.; Birge, R. R.; Bocian, D.F.; Holten, D.; Lindsey, J. S. *J. Am. Chem. Soc.* **1998**, *120*, 10001-10017.

[66] Imahori, H.; Norieda, H.; Yamada, H.; Nishimura, Y.; Yamazaki, I.; Sakata, Y.; Fukuzumi, S. *J. Am. Chem. Soc.* **2001**, *123*, 100-110.

[67] Amroise, C. Kirmaier, R. W. Wagner, R. S. Loewe, D. F. Bocian, D. Holten, J. S. Lindsey, *J. Org. Chem.*, **2002**, *67*, 3811-3826.

[68] Risko, C.; Barlow, S.; Coropceanu, V.; Halik, M.; Brédas, J.-L.; Marder, S. R. *Chem. Commun.*, **2003**, 194-195.

[69] Halik, H.; Wenseleers, W.; Grasso, C.; Stellacci, F.; Zojer, E.; Barlow, S.; Brédas, J.-L.; Perry, J. W.; Marder, S. R. *Chem. Commun.*, **2003**, 1490-1491.

[70] (a) Murphy, D. M.; Mingos, D. M. P.; Forward, J. M. *J. Mater. Chem.* **1993**, *3*, 67-76. (b) Murphy, D. M.; Mingos, D. M. P.; Haggit, J. L.; Rowell, H. R.; Westcott, S. A.; Marder, T. B.; Taylor, N. J.; Kanis, D. R. *J. Mater. Chem.* **1993**, *3*, 139-148.

[71] Grüner, B.; Janoušek, Z.; King, B. T.; Woodford, J. N.; Wang, C. H.; Všetecka, V.; Michl, J. *J. Am. Chem. Soc.* **1999**, *121*, 3122-3126.

[72] Abe, J.; Nemoto, N.; Nagase, Y.; Shirai, Y.; Iyoda, T. *Inorg. Chem.* **1998**, *37*, 172-173.

[73] (a) Littger, R.; Taylor, J.; Rudd, G.; Newlon, A.; Allis, D.; Kotiah, S.; Spencer, J. T. in *Contemporary Boron Chemistry*, M. G. Davidson, A. K. Hughes, T. B. Marder, K. Wade (Eds.) Spec. Publ. No. 253, The Royal Society of Chemistry, Cambridge **2000**, 67-76. (b) Allis, D. G.; Spencer, J. T. *J. Organomet. Chem.* **2000**, *614*, 309-314. (c) Allis, D. G.; Spencer, J. T. *Inorg. Chem*, **2001**, *40*, 3373-3380.

[74] Taylor, J.; Caruso, J.; Newlon, A.; Englich, U.; Ruhlandte-Senge, K.; Spencer, J. T. *Inorg. Chem.* **2001**, *40*, 3381-3388.

[75] (a) Lamrani, M.; Hamasaki, R.; Mitsuichi, M.; Miyashita, T.; Yamamoto, Y. *Chem. Commun.* **2000**, 1595-1596. (b) Hamasaki, R.; Ito, M.; Lamrani, M.; Mitsuishi, M.; Miyashita, T.; Yamamoto, Y. *J. Mater. Chem.*, **2003**, *13*, 21-26.

[76] Hong, E.; Jang, H.; Kim, Y.; Jeoung, S. C.; Do, Y.; *Adv. Materials* **2001**, *13*, 1094-1096.

Chapter 2

Symmetric bis(dimesitylboryl)s: Optical, structural, electrochemical and thermal properties

2.1. Introduction

The bonding of three-coordinate boron may be described by three sp^2 hybrid orbitals situated in a trigonal plane, with a vacant boron p_z orbital orthogonal to the plane. The vacant orbital can participate in conjugation with adjacent organic π-systems, which has been shown to result in interesting optical properties. Low valent boron is usually thought of as being unstable, with the vacant p_z orbital readily attacked by nucleophiles such as water, which can result in either bond cleavage or the formation of a four-coordinate borate, which can no longer participate effectively in π-conjugation. Kinetic stabilisation can be provided by sterically demanding groups, with bulky aryl groups bearing *ortho*-substituents being particularly effective. The mesityl (2,4,6-trimethylphenyl, Mes) group is commonly used, and compounds containing two or more such groups bound to boron exhibit significant stability towards air and moisture. The resulting molecules have twisted, propeller-like configurations, with the *ortho*-methyl groups forming a "cage" around the p_z orbital. The dimesitylboryl group is a π-electron acceptor, comparable in strength to the cyano group, but unlike other π-acceptors, however, it is a weak σ-electron acceptor, and since the electronegativity of boron is less than that of carbon, it may even function as a σ-electron donor when bonded to organic systems. [1] In addition to its electronic effects, the dimesitylboryl group has a powerful influence upon solid-state properties; compounds with two or more dimesitylboryl moieties are often inherently non-crystalline, as close-packing of molecules is inhibited, and readily form either films or

powders. Since the presence of crystal defects and grain boundaries can severely reduce the mobility of charge-carriers, it is important that materials used in organic light emitting diodes (OLEDs) can be deposited in a non-crystalline form.

Compounds containing three – coordinate boron, many using the dimesitylboryl group, have been shown to have interesting optical, electronic and structural properties with a wide range of potential applications. [2] Some examples include fluoride ion sensors,[3,4] nonlinear optically active materials,[5,6,7,8,9] and both single [1,10,11] and two-photon[12] fluorescence applications. There are relatively few reports, however, of symmetric bis(dimesitylboryl) compounds.[7,13,14,15,16,17,18,19] We therefore decided to prepare and investigate the properties of a range of symmetric compounds of the general form $Mes_2B - \pi - BMes_2$.

2.2. Results and Discussion

2.2.1. Synthesis

Compounds of the general form *trans, trans*-Mes_2B-(CH=CH)-X-(CH=CH)-$BMes_2$ (where X = a conjugated organic π-system) (Figure 2.1) were prepared by the reaction of a bis-terminal alkyne with one equivalent of dimesitylborane dimer [20] in THF, as illustrated in Scheme 2.1. The compounds **2a** (X = C_6H_4) and **2f** (X = C_6H_4-C_6H_4) have been previously prepared. [7]

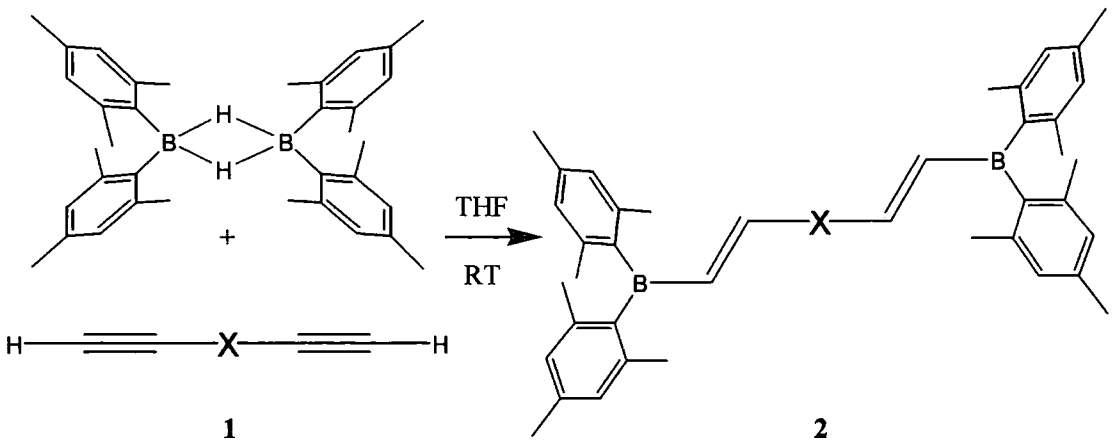

Scheme 2.1. Synthesis of symmetric bis(dimesitylborylvinyl) compounds

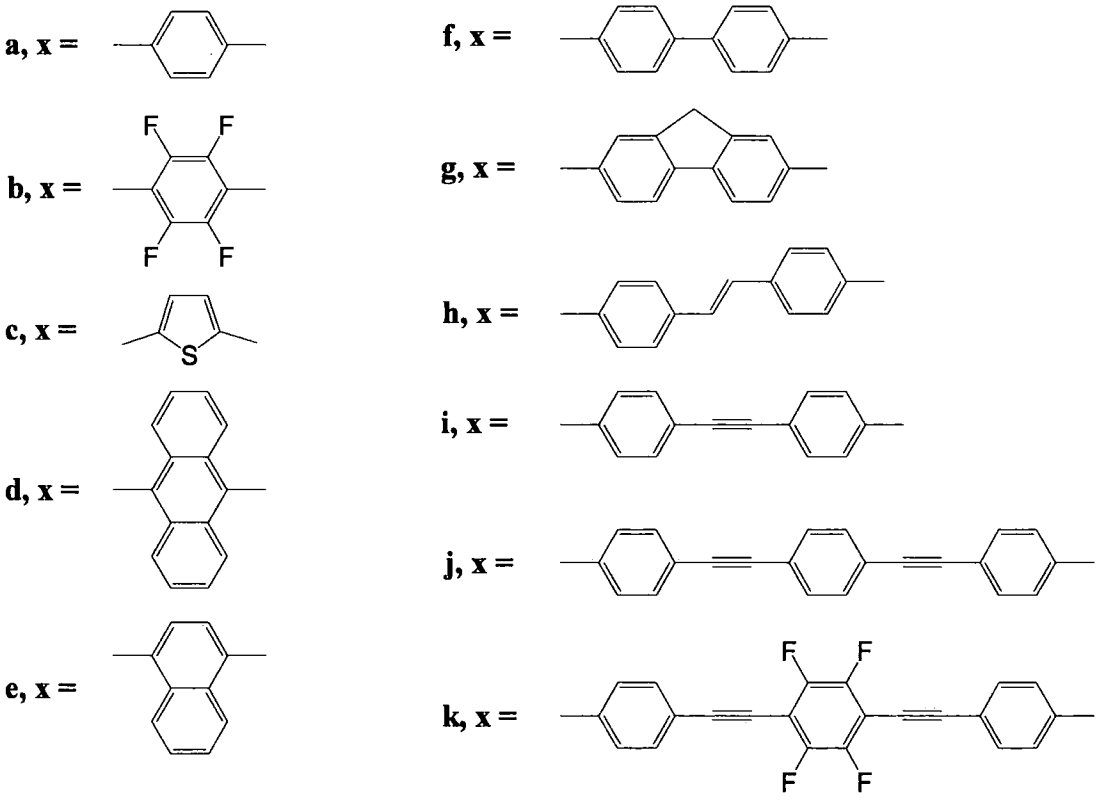

Figure 2.1. Nature of the π-system, x, in acetylenes and boryl compounds.

Protected alkynes were prepared by palladium-catalysed cross-coupling reactions (Sonogashira reaction), followed by deprotection to furnish the bis-terminal alkynes (Scheme 2.2.). The Sonogashira reaction is a versatile and facile process for the formation of ethynylarenes from aryl halides and terminal acetylenes. It is catalysed by a wide variety of palladium compounds in the presence of a base, and usually in the presence of a copper (I) salt. [21] The accepted mechanism of the Sonogashira reaction is illustrated in Scheme 2.3. [22] Efficient reaction occurs in a variety of solvents, and amines are often used as both the solvent and the base. In the present work, the catalytic system used was usually $(Ph_3P)_2PdCl_2$ (1-2 mol% with respect to aryl halide) with a small amount of cuprous iodide ($Cu^{(I)}I$) in triethylamine. Where this was found to be ineffective, for example in the preparation of 1,4-diethynylnaphthalene (**1e**), the palladium catalyst was instead generated in situ from a mixture of $(PhCN)_2PdCl_2$ and 1.5 molar equivalents of $^tBu_3P$ in toluene. The $Si(CH_3)_3$ protecting group was removed by stirring over sodium carbonate in methanol/water, with a co-solvent such as DCM sometimes added to improve solubility. The $C(CH_3)_2OH$ protecting group required more forcing conditions, and was removed (as acetone, $O=C(CH_3)_2$) by heating a toluene solution of the alkyne under a nitrogen atmosphere with NaOH or $KOBu^t$. Whilst all protected alkynes were stable under ambient conditions, some terminal alkynes (**1d,e**) were found to be unstable; in these cases, it was necessary to prepare the alkyne immediately before use. The compound *trans*-4,4'-diethynylstilbene (**1h**) was synthesised via Pd/Cu catalysed cross-coupling of TMSA and *trans*-4,4'-dibromostilbene. Attempts to synthesis this compound via a Wittig procedure resulted a mixture of two isomers (ca. 9:1 by GC-MS): after isolation and purification of the major component, XRD revealed this to be the *cis*-

isomer. A different procedure,[23] the Pd catalysed reaction of vinyltriethoxysilane with two equivalents of 4-bromophenyldiazonium tetrafluoroborate, gave the desired *trans*-4,4'-dibromostilbene in high yield, with very small amounts of the *cis*-isomer (Scheme 2.4). The compound 4,4'-diethynyltolan [24] (**1i**) was synthesised in a stepwise manner, as illustrated in Scheme 2.5.

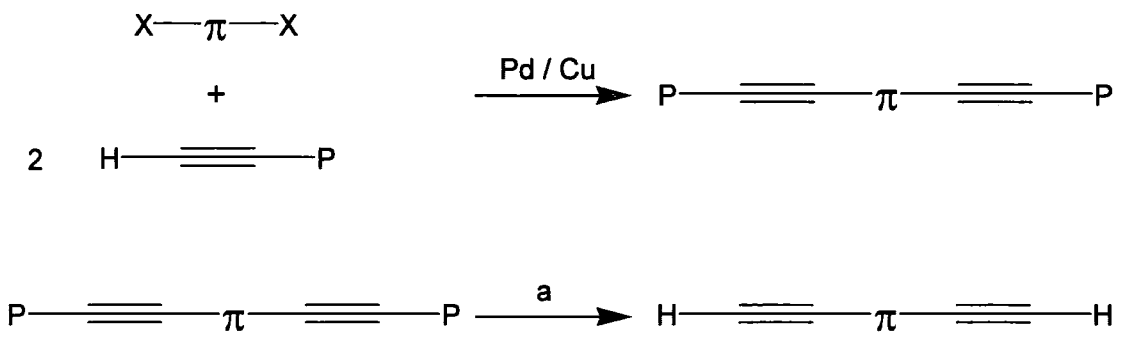

Scheme 2.2. Synthesis of bis-terminalalkynes via Sonogashira reaction (a = Na_2CO_3 / MeOH / H_2O for P = $SiMe_3$; a = NaOH or $KOBu^t$ / $C_6H_5CH_3$ for P = $C(CH_3)_2OH$; X = Br or I.

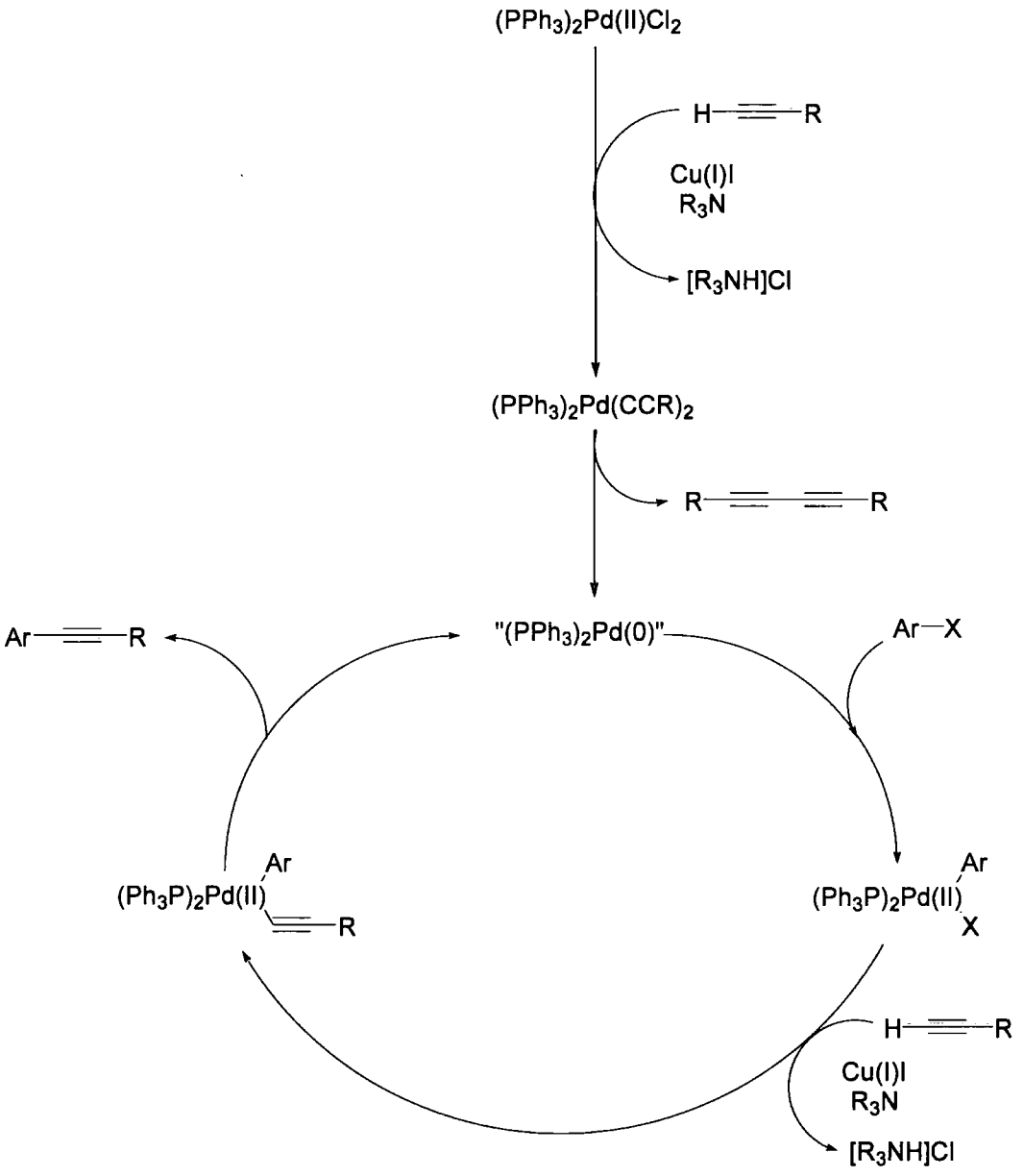

Scheme 2.3. Mechanism for the Sonogashira reaction, showing generation of postulated active catalyst from $(Ph_3P)_2PdCl_2$.

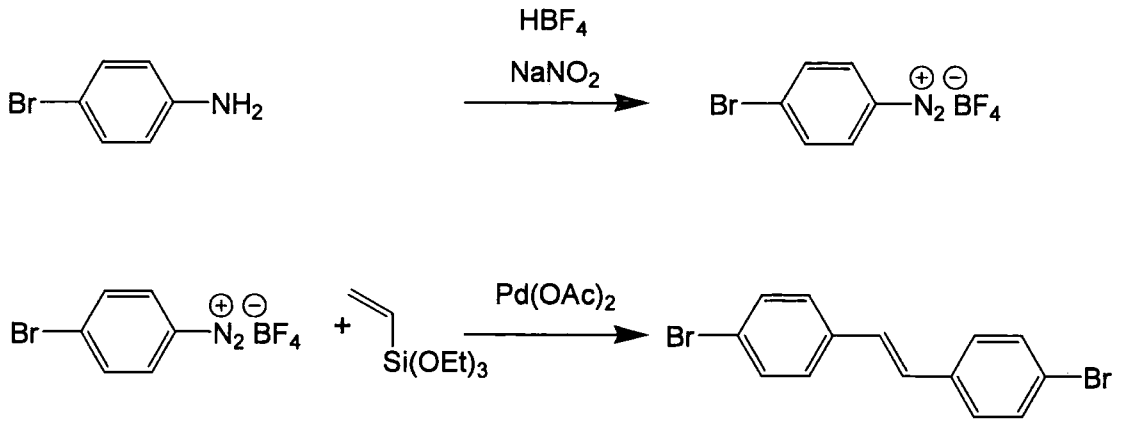

Scheme 2.4. Synthesis of *trans*-4,4'-dibromostilbene

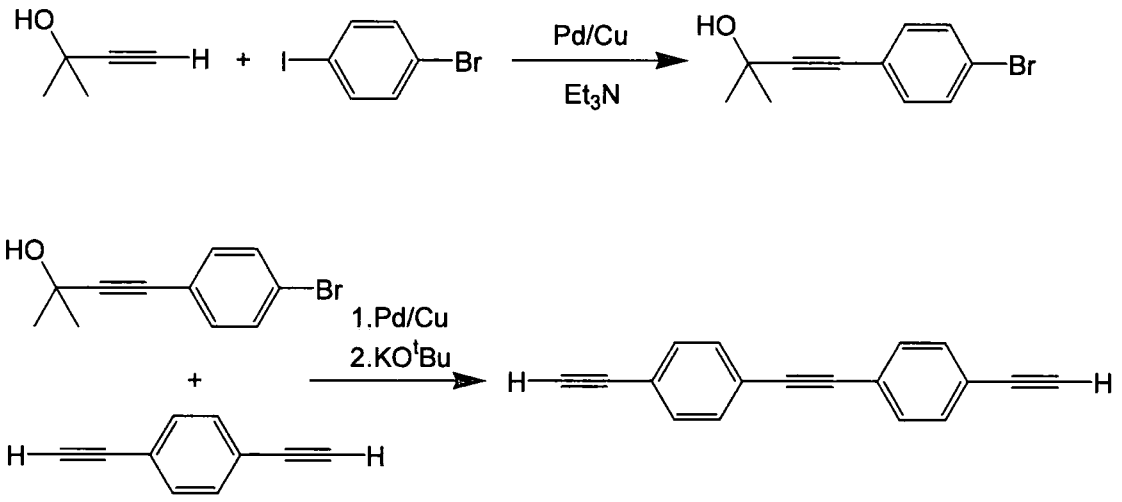

Scheme 2.5. Preparation of terminal alkyne 1i

Compounds of the form Mes_2B-X-$BMes_2$ were prepared by the dilithiation of the appropriate aryl dibromide followed by reaction with dimesitylfluoroborane, as illustrated in Scheme 2.6. The compounds **3a** and **3c** have been prepared previously via di-Grignard (**3a**)[13] and dilithio- species (**3a,c**), but the conditions reported [7] for the preparation of **3a** were found to be ineffective, resulting in mainly *p*-(dimesitylboryl)bromobenzene (**5**) with very small amounts of the desired compound. Attempts to lithiate this compound using either ^{t}BuLi or ^{n}BuLi, followed by reaction

with $FBMes_2$ to generate **3a,** were unsuccessful, as were attempts to generate the Grignard reagent $Mes_2BC_6H_4MgBr$. In order to determine an effective procedure for generating 1,4-dilithiobenzene, a series of small – scale reactions were carried out using varying amounts of ^{n}butyl- or ^{t}butyllithium with dibromobenzene or diodobenzene in different solvent combinations. The reactions were quenched with a large excess of trimethylsilyl chloride, and the proportions of bis(trimethylsilyl)benzene and byproducts were assessed by GC-MS. The most effective conditions were found to be addition of three equivalents of ^{n}BuLi (1.6 M in hexane) to a solution of dibromobenzene in toluene at room temperature, which, after overnight stirring and quenching with trimethylsilylchloride revealed the formation of bis(trimethylsilyl)benzene in >80% yield. Dilithiothiophene was prepared in a similar manner, and reacted with $FBMes_2$ to furnish Compound **3c**, but attempts to prepare other aryl dilithium reagents in sufficient purity and yield were unsuccessful.

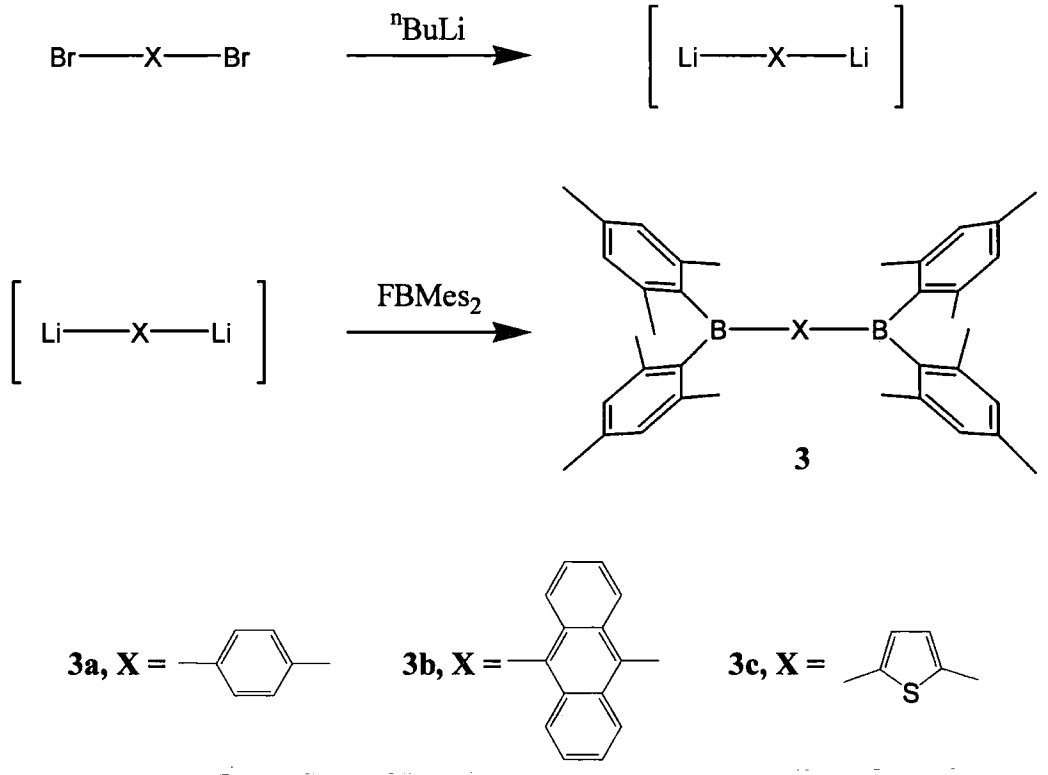

Scheme 2.6. Synthesis of symmetric bis(dimesitylboryl) compounds.

2.2.2. Structural Properties

Crystal structures of the compounds **2a**, **2c** and **2f** were determined by single-crystal X-ray diffraction at 120 K. Single crystals of **2a** formed by cooling a solution of hexane / DCM desolvated within seconds, but crystals obtained by cooling a toluene solution desolvated in minutes and were stable once covered in perfluorinated oil. Single crystals of **2a** were also obtained from an equimolar solution of **2a** and 1,4-bis(N,N-dimethylamino)benzene in hexane / DCM: these crystals contained neither solvent nor the diamine, and were indefinitely air-stable. Whilst crystals grown from toluene required several months to form, in the presence of the diamine large crystals of **2a** formed overnight at room temperature inside a sealed vial. Whilst it is clear that the diamine somehow induced crystallisation, the nature of this involvement is unclear and numerous attempts to grow crystals of other symmetric diboryls in the presence of various diamines were unsuccessful. Since there were no statistically significant differences between the bond lengths and angles of the two structures, which differed only in unit cell parameters and the presence or absence of disordered toluene, only the higher quality structure will be discussed.

Crystals of **2c** were grown by cooling a solution of **2c** in hexane / DCM, with one molecule of DCM per unit cell retained in the lattice. Though these crystals desolvated rapidly, they were sufficiently stable once covered in oil for the analysis to be completed. Single crystals of **2f** were obtained by cooling a toluene solution, and contained disordered toluene molecules, desolvating relatively slowly (ca. 10 – 20 minutes). It proved impossible to obtain crystals suitable for XRD of any other bis(boryl)s despite repeated attempts. In general, cooling resulted in the formation of powders, whereas solvent evaporation resulted in amorphous films. Structures of the

compounds **3a** and **3b** have been previously reported. Selected bond lengths and angles are presented in Tables 2.1 – 2.3.

In all structures, the boron atoms are trigonal planar, with the three C-B-C bond angles adding up to 360°. Boron-carbon bond lengths are similar for all compounds (ca. 1.58 Å for B-mesityl bonds and ca. 1.56 Å for boron-vinyl bonds), with the greater steric demands of the mesityl group probably accounting for the slight bond-lengthening when compared with the boron-vinyl bonds. All structures are approximately planar except for the mesityl groups, which are strongly twisted out of the BC_3 plane in propeller-like configurations, as shown in the unit cell diagram of Compound **2a** (Figure 2.3). Interplanar angles between the BC_3 planes and attached mesityl groups are typically around 45° for one mesityl group and 60° for the other. The twisted mesityl groups inhibit close-packing of the molecules, so that all unit cells are characterised by large void-spaces: this explains why solvent molecules are often incorporated in the crystal lattices, and why these compounds are so difficult to crystallise.

Table 2.1. Selected bond lengths and bond angles for 2a.

Bond Lengths (Å)		Bond angles (°)	
B(1)-C(8)	1.5476(19)	C(8)-B(1)-C(11)	120.20(12)
B(1)-C(11)	1.580(2)	C(8)-B(1)-C(21)	118.51(12)
B(1)-C(21)	1.582(2)	C(11)-B(1)-C(21)	121.28(11)
B(2)-C(10)	1.5458(18)	C(10)-B(2)-C(31)	118.23(11)
B(2)-C(31)	1.5858(19)	C(10)-B(2)-C(41)	119.63(11)
B(2)-C(41)	1.5814(19)	C(31)-B(2)-C(41)	121.89(11)
C(1)-C(2)	1.3970(17)	B(1)-C(8)-C(7)	122.97(13)
C(1)-C(6)	1.4006(18)	B(2)-C(10)-C(9)	121.34(12)
C(1)-C(7)	1.4664(17)	C(1)-C(7)-C(8)	127.09(12)
C(2)-C(3)	1.3776(17)	C(4)-C(9)-C(10)	128.30(12)
C(3)-C(4)	1.4007(17)		
C(4)-C(5)	1.3999(17)		
C(4)-C(9)	1.4626(17)		
C(5)-C(6)	1.3824(17)		
C(7)-C(8)	1.3446(18)		
C(9)-C(10)	1.33442(18)		

Table 2.2. Selected bond lengths for 2c and 2f.

Bond Lengths (Å)					
2c				2f	
S(1)-C(3)	1.7339(19)	S(2)-C(53)	1.727(2)	B-C(8)	1.552(4)
S(1)-C(6)	1.7305(19)	S(2)-C(56)	1.732(2)	B-C(11)	1.590(4)
B(1)-C(1)	1.552(3)	B(3)-C(51)	1.556(3)	B-C(21)	1.585(4)
B(1)-C(11)	1.578(3)	B(3)-C(61)	1.575(3)	C(1)-C(2)	1.384(4)
B(1)-C(21)	1.585(3)	B(3)-C(71)	1.571(3)	C(1)-C(6)	1.392(4)
B(2)-C(8)	1.554(3)	B(4)-C(58)	1.551(3)	C(1)-C(7)	1.464(4)
B(2)-C(31)	1.576(3)	B(4)-C(81)	1.578(3)	C(2)-C(3)	1.388(4)
B(2)-C(41)	1.573(3)	B(4)-C(91)	1.582(3)	C(3)-C(4)	1.387(4)
(C1)-C(2)	1.341(3)	(C51)-C(52)	1.340(3)	C(4)-C(4')	1.488(5)
C(2)-C(3)	1.449(3)	C(52)-C(53)	1.451(3)	C(4)-C(5)	1.393(4)
C(3)-C(4)	1.371(3)	C(53)-C(54)	1.383(3)	C(5)-C(6)	1.380(4)
C(4)-C(5)	1.414(3)	C(54)-C(55)	1.411(3)	C(7)-C(8)	1.343(4)
C(5)-C(6)	1.368(3)	C(55)-C(56)	1.370(3)		
C(6)-C(7)	1.445(3)	C(56)-C(57)	1.449(3)		
C(7)-C(8)	1.341(3)	C(57)-C(58)	1.344(3)		

Table 2.3. Selected bond angles for Compound 2c and 2f.

Selected Bond Angles (°)					
2c				2f	
C(1)-B(1)-C(11)	118.18(2)	C(51)-B(3)-C(61)	113.71(2)	C(8)-B-C(11)	118.2(2)
C(1)-B(1)-C(21)	118.52(2)	C(51)-B(3)-C(71)	119.30(2)	C(8)-B-C(21)	117.4(2)
C(11)B(1)-C(21)	123.30(2)	C(61)-B(3)-C(71)	126.91(2)	C(11)-B-C(21)	124.4(2)
B(1)-C(1)-C(2)	123.18(2)	B(3)-C(51)-C(52)	124.97(2)	B-C(8)-C(7)	124.2(3)
C(1)-C(2)-C(3)	127.33(2)	C(51)-C(52)-C(53)	124.21(2)	C(8)-C(7)-C(1)	128.2(3)
C(8)-B(2)-C(31)	118.09(2)	C(58)-B(4)-C(81)	118.21(2)		
C(8)-B(2)-C(41)	116.46(2)	C(58)-B(4)-C(91)	116.0(2)		
C(31)-B(2)-C(41)	125.42(2)	C(81)-B(4)-C(91)	125.78(2)		
B(2)-(C8)-C(7)	123.99(2)	B(4)-C(58)-C(57)	123.8(2)		
C(8)-C(7)-C(6)	126.51(2)	C(58)-C(57)-C(56)	126.6(2)		

Compound **2a** (Figure 2.2) crystallised in space group $P2_1/c$. The two dimesitylborylvinyl moieties in this molecule are unsymmetric, with markedly different torsion angles. This difference in torsion angles is also a feature in the structure of **2c** (space group $P\bar{1}$), which is interesting in that the unit cell contains both *cisoid* and *transoid* configurations (Figure 2.4). Whilst the *transoid* form is thermodynamically favoured in these compounds, as it allows for better electronic conjugation, the *cisoid* form reduces steric hindrance of the thiophene and vinyl hydrogen atoms. Since both forms are present, it suggests that these factors are quite finely balanced for this compound. It is noticeable that the *transoid* conformation is

considerably less planar. Compound **2f** crystallised in space group *I2/a*, with the result being that the biphenyl moiety is completely planar since the molecule contains an inversion centre (Figure 2.5). In addition, other relevant torsion angles are considerably smaller than for compounds **2a** and **2c**, so that this compound has a far greater overall planarity.

In assessing the conjugation of these compounds, it is useful to measure the interplanar angle between the two BC_3 planes. In the triarylboranes **3a** and **3b**, these are coplanar, with angle exactly equal to 0 °. This is also the case for **2h**, but the other vinyldiarylboranes differ significantly: the compounds **2a** and **2c**(*cisoid*) have similar interplanar angles (ca. 19.6 ° and ca. 20.4 ° respectively), whilst **2c**(transoid) has an interplanar angle of ca. 27 °. The differing planarities of these molecules, illustrated in Figure 2.6, may be interpreted as resulting from (1) minimisation of steric effects, with the most significant of these being the interactions of the mesityl groups, which are minimised in compounds containing vinyl units; and (2) maximisation of electronic conjugation. The compounds **2a** and **2c** may be described as having a relatively planar unit, Mes_2B-CHCH-X (where X = C_6H_4 or C_4H_2S) with the second dimesitylborylvinyl unit being considerably more twisted, which may indicate that these compounds are not fully delocalised. Crystal packing effects should not be underestimated, however, and may be the cause of these compounds asymmetric conformations. It seems likely that crystal packing is also the major cause of the high planarity of **2h** (this will be discussed further in Section 2.2.4). It should be noted that solid-state structures can only be a guide to conformations in the solution phase, since all of these compounds would be expected to exhibit a large number of rotational and vibrational modes in solution.

Table 2.4. Selected bond torsion angles for Compounds 2a, 2c and 2f

Selected Torsion Angles (Å)			
2a		2f	
C(11)-B(1)-C(8)-C(7)	-170.48	C(11)-B-C(8)-C(7)	9.47
C(21)-B(1)-C(8)-C(7)	8.84	C(21)-B-C(8)-C(7)	-171.42
B(1)-C(8)-C(7)-C(1)	-177.30	B-C(8)-C(7)-C(1)	-179.46
C(8)-C(7)-C(1)-C(2)	-11.27	C(8)-C(7)-C(1)-C(2)	171.95
C(8)-C(7)-C(1)-C(6)	165.63	C(8)-C(7)-C(1)-C(6)	-8.39
C(31)-B(2)-C(10)-C(9)	-19.04		
C(41)-B(2)-C(10)-C(9)	155.34		
B(2)-C(10)-C(9)-C(4)	-164.77		
C(10)-C(9)-C(4)-C(3)	175.77		
C(10)-C(9)-C(4)-C(5)	-0.17		
2c (cisoid)		2c (transoid)	
C(11)-B(1)-C(1)-C(2)	14.29	C(61)-B(3)-C(51)-C(52)	-152.39
C(21)-B(1)-C(2)-C(3)	-165.96	C(71)-B(3)-C(51)-C(52)	24.61
B(1)-C(1)-C(2)-C(3)	-176.90	B(3)-C(51)-C(52)-C(53)	172.66
C(1)-C(2)-C(3)-C(4)	178.87	C(51)-C(52)-C(53)-C(54)	20.07
C(1)-C(2)-C(3)-S(1)	4.73	C(51)-C(52)-C(53)-S(2)	-158.05
C(31)-B(2)-C(8)-C(7)	-30.70	C(81)-B(4)-C(58)-C(57)	-15.27
C(41)-B(2)-C(8)-C(7)	150.98	C(91)-B(4)-C(58)-C(57)	163.82
B(2)-C(8)-C(7)-C(6)	179.20	B(4)-C(58)-C(57)-C(56)	-175.77
C(8)-C(7)-C(6)-C(5)	174.30	C(58)-C(57)-C(56)-C(55)	177.67
C(8)-C(7)-C(6)-S(1)	-10.33	C(58)-C(57)-C(56)-S(2)	-3.10

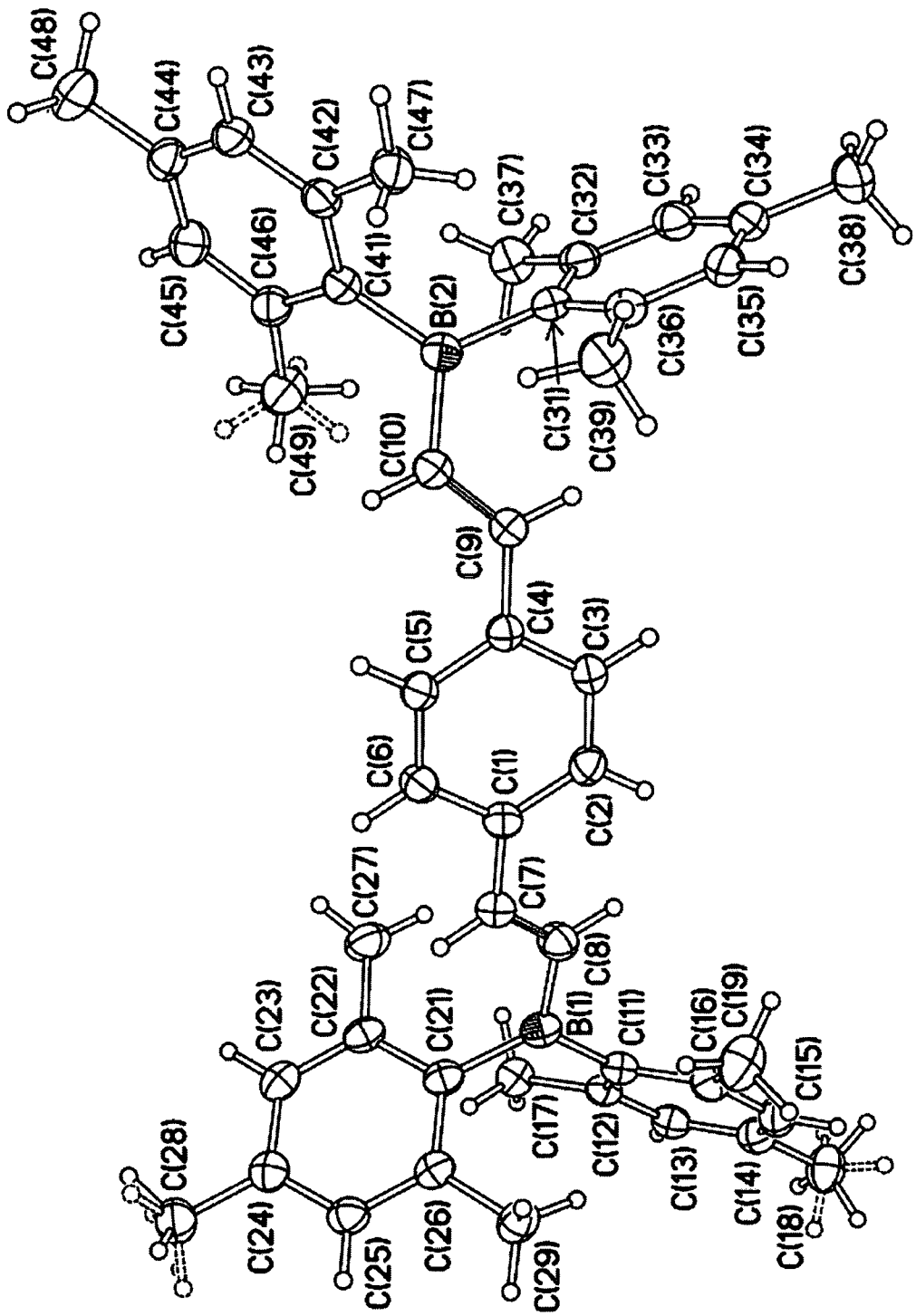

Figure 2.2. ORTEP diagram of the molecular structure of 1,4-bis(dimesitylborylvinyl)benzene (2a) (50 % thermal ellipsoids).

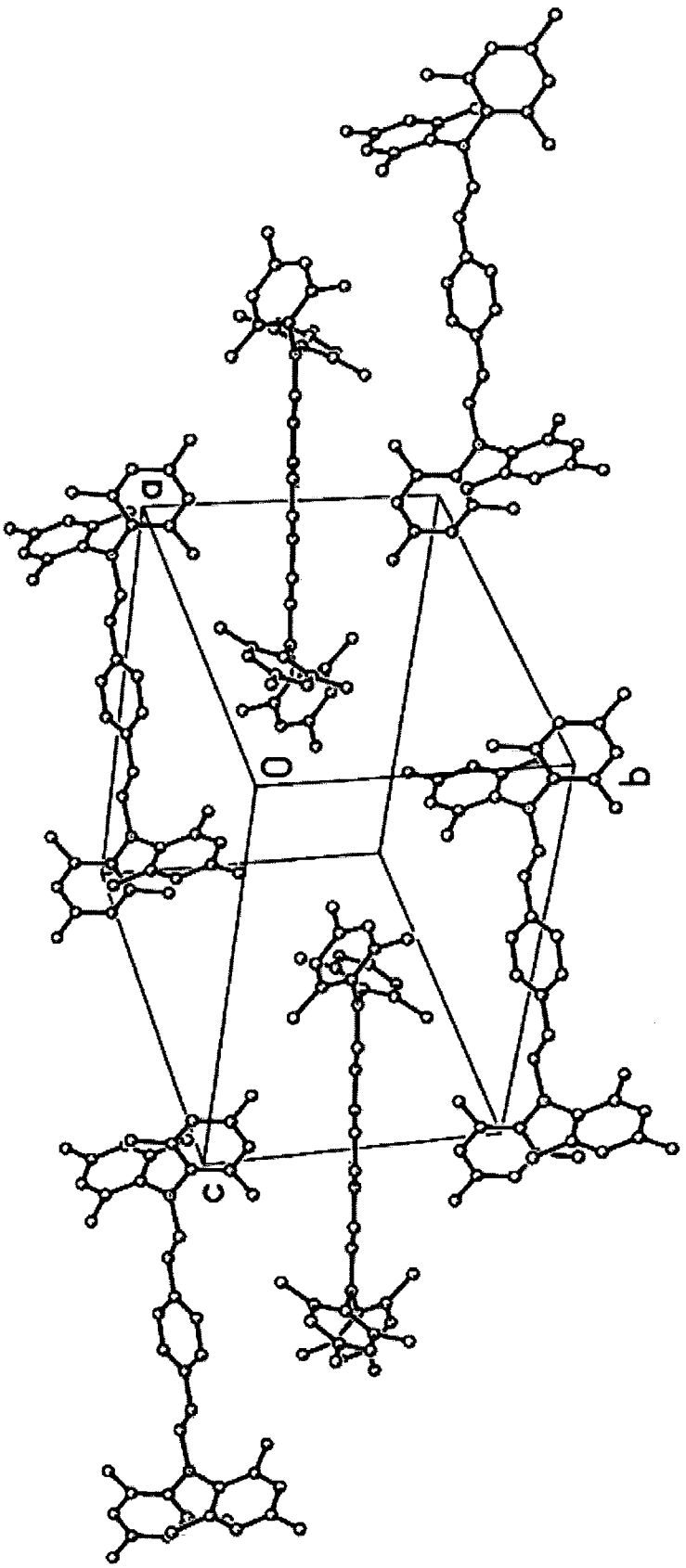

Figure 2.3. Unit cell of 1,4-bis(dimesitylborylvinyl)benzene (2a) , showing large void spaces and propeller – like configuration about the boron atoms.

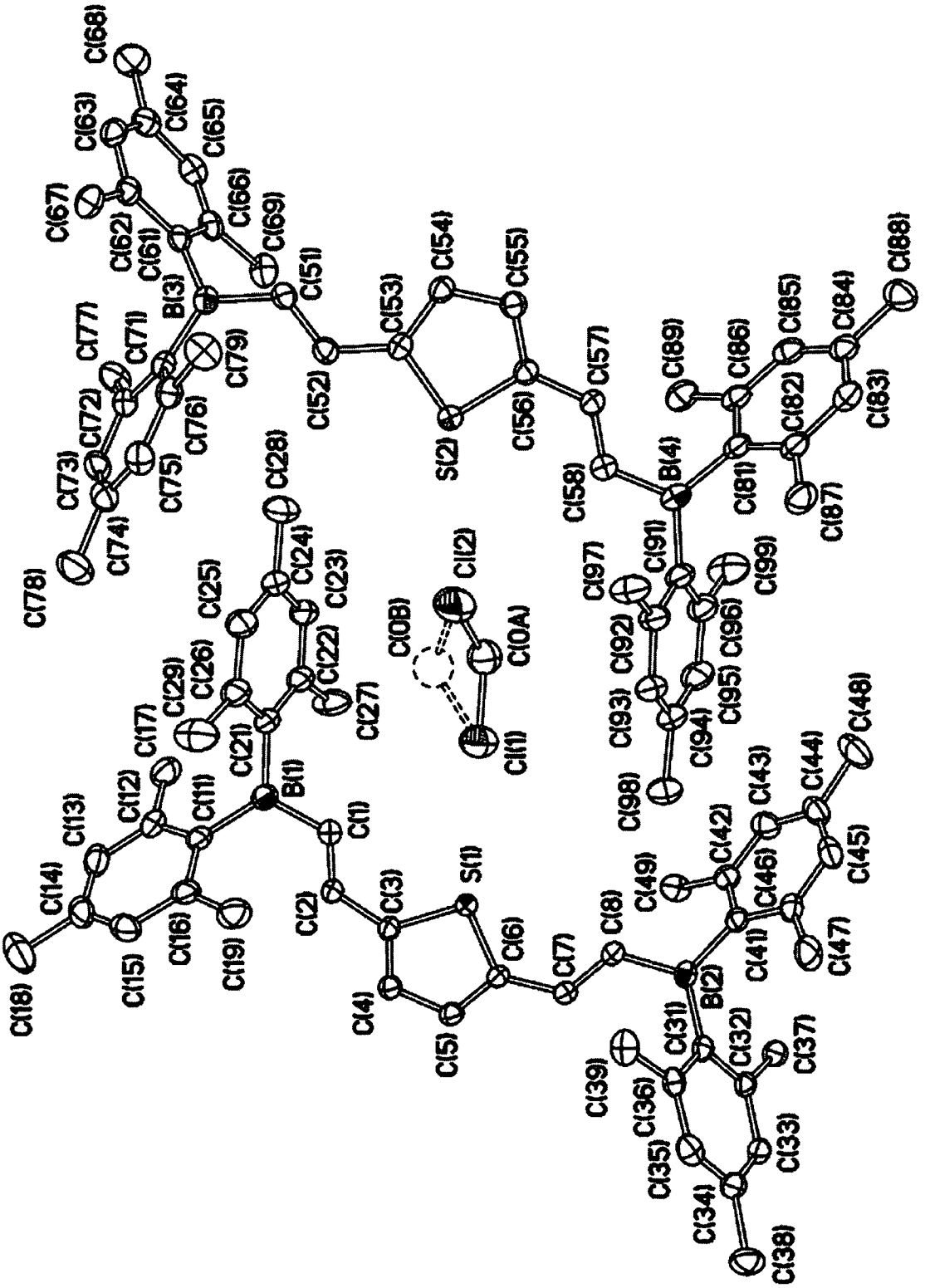

Figure 2.4. ORTEP diagram of the molecular structure of 2,5-bis(dimesitylborylvinyl)thiophene (2c) (50 % thermal ellipsoids).

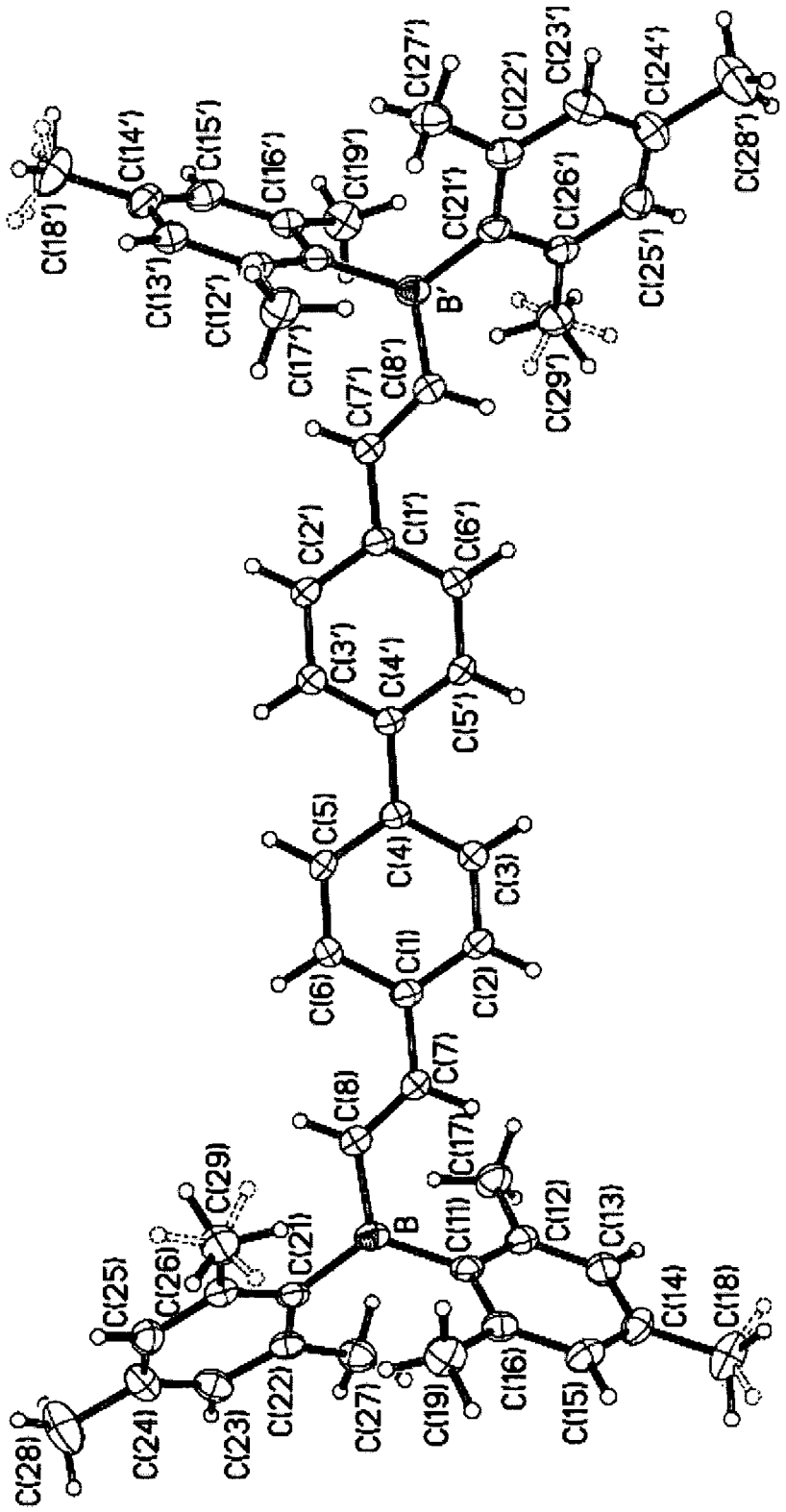

Figure 2.5. ORTEP diagram of the molecular structure of 4,4'-bis(dimesitylborylvinyl)biphenyl (2f) (50 % thermal ellipsoids).

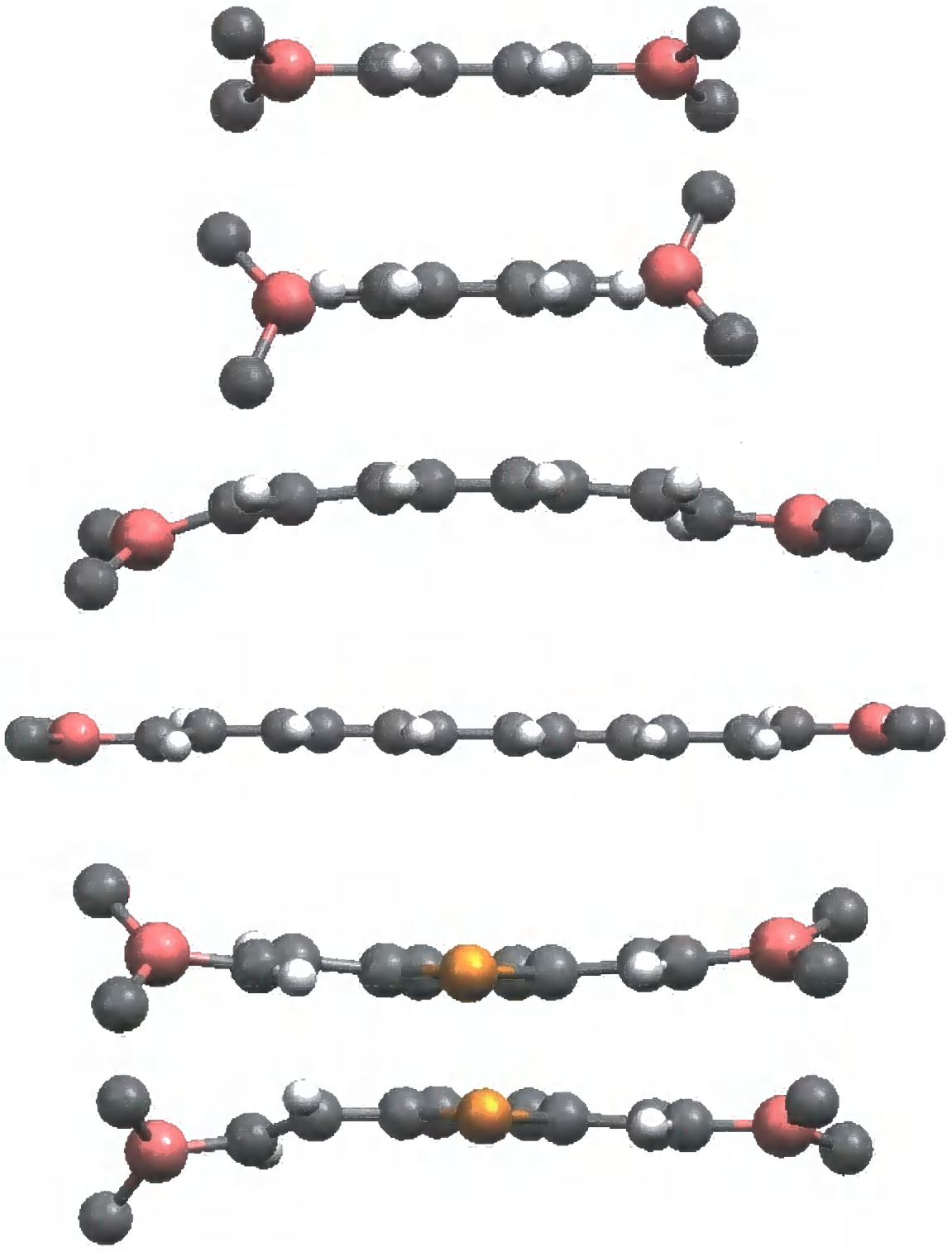

Figure 2.6. Ball and stick diagrams of (from top) compounds 3a, 3b, 2a, 2f, and 2c (*cisoid* and *transoid* conformations), showing planarity of the compounds (excluding mesityl groups).

2.2.3. Thermal Properties

In order to investigate properties such as thermal stability and melting temperature, selected compounds were examined by Thermogravimetric Analysis (TGA) and Differential Scanning Calorimetry (DSC). These properties are important when considering the suitability of materials for inclusion in electronic devices, since in order to form useful devices, the materials used in their construction must be thermally stable under the manufacturing conditions and the temperature range the device will be subject to. In addition, DSC reveals the presence or absence of glass transitions, (T_g), which may be defined as the temperature above which the material changes from crystalline to an amorphous state (which usually exhibit superior charge mobilities).

Most compounds did not have an observable melting point since, with the exception of **2a**, thermal decomposition (observed by TGA) occurred before melting. In some cases it was possible to observe a melting point above the decomposition temperature using DSC, since the decomposition rate was slow compared to the heating rate: in these cases, impurities introduced by partial decomposition of the sample may be responsible for the rather broad range over which melting occurs. In the compounds where TGA or DSC were not undertaken, the decomposition temperature was estimated using standard melting point apparatus, with the sample sealed inside a tube in the drybox. The accuracy of these measurements was limited, since decomposition occurred over a wide temperature range, and the onset was not obvious. All compounds exhibited an initial weight loss due to adsorbed solvent or moisture. Since compounds were stored in sealed tubes in the drybox, this is thought to be the result of water adsorption occurring when the samples were loaded into the instrument. With the exception of Compound **2a**, which crystallised as a 1 : 1 DCM

solvate, NMR spectroscopy confirmed that neither organic solvents or water were present in the stored samples. A summary of the thermal characteristics is presented in Table 2.5.

Table 2.5. Thermal characteristics of selected bis(boryl)s.

Compound	m.p. (°C)	Tg (°C)	Decomposition[a] (°C)
2a	236-242	141	255
2b	b	b	270
2c	c	b	205
2f	b	b	155
2g	b	135[d]	225
2h	240-250	108[d]	250
3a	215-222	b	240
3c	b	b	230

a Decomposition temperature defined as the temperature by which 2% weight loss has occurred, excluding weight loss due to adsorbed water / solvents.
b Not observed or not present.
c Sublimes at T > 350 °C.
d Tentative assignment.

Compound **2a** exhibits a gradual desolvation, starting at ca. 130 °C and resulting in a total weight loss of ca. 20%, with decomposition commencing at 235 °C. The compound has a broad melting point from 236 – 242 °C, with no recrystallisation observed on cooling. A glass transition is observed at 141 °C, indicating that this compound is microcrystalline at lower temperatures and changes to a glassy state at higher temperatures. The exothermic event at 160 °C is thought to be the result of a rearrangement.

The TGA curve of Compound **2b** also shows loss of adsorbed moisture, but thermal decomposition is unclear; whilst TGA indicates that the onset is ca. 250 °C, the compound begins to change colour from yellow to brown at temperatures greater than 200 °C. It seems likely that this compound is unstable at T > 200 °C, with the rate of decomposition increasing as the temperature rises. The DSC curve is featureless, with no evidence for either glass transitions or melting. Attempts were also made to examine this compound by powder X-ray diffraction, but no peaks were observed above the level of instrumental noise; in conjunction with the DSC results, this suggests that this compound is amorphous at room temperature and above. The difference in behaviour with that of **2a** is probably due to the larger size of the fluorine atoms, resulting in a less planar configuration.

The DSC results for **2c** again show no evidence for melting or glass transitions. TGA results appear to show that after loss of adsorbed water (commencing at ca. 65 °C), both decomposition and sublimation occur: sublimation was confirmed by deposition of analytically pure **2c** in the chimney of the TGA instrument. Since this was not observed when the temperature was kept at below 350 °C, it is clear that decomposition occurs at T > 200 °C, and that remaining **2c** sublimes at T > 350 °C. This result indicates that it should be possible to deposit films of this compound under vacuum.

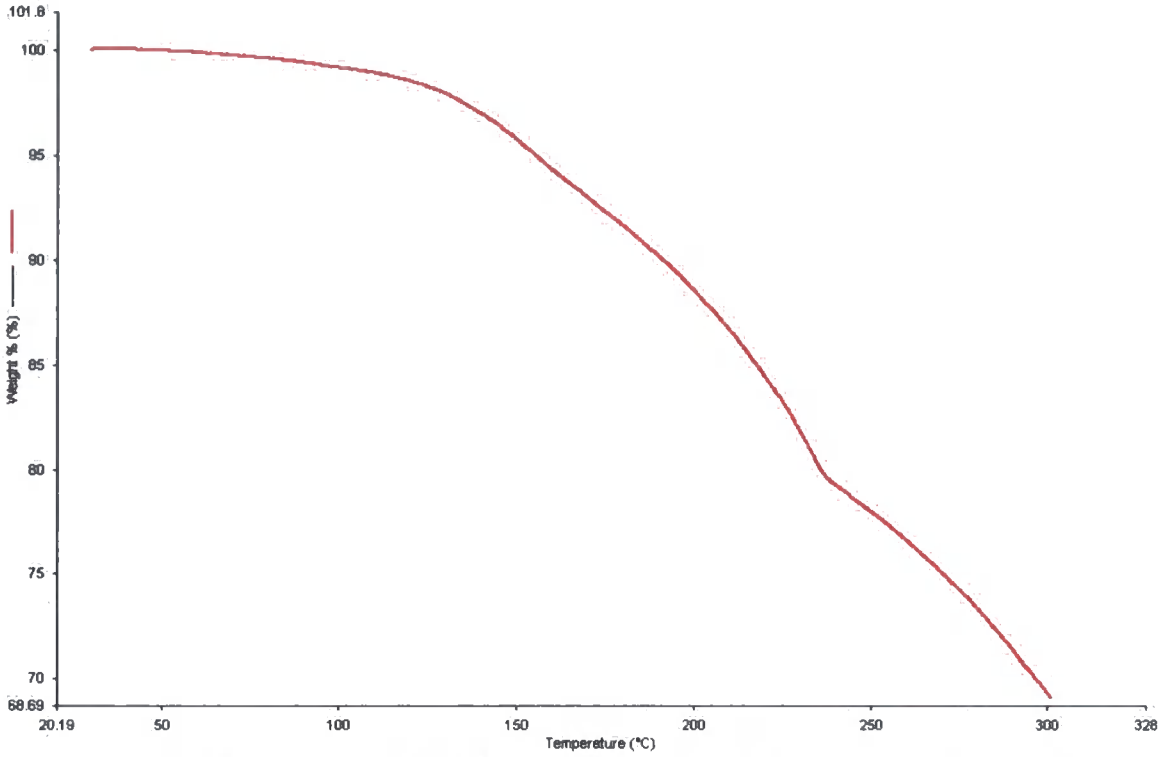

Figure 2.7. Weight loss as a function of temperature for compound 2a.

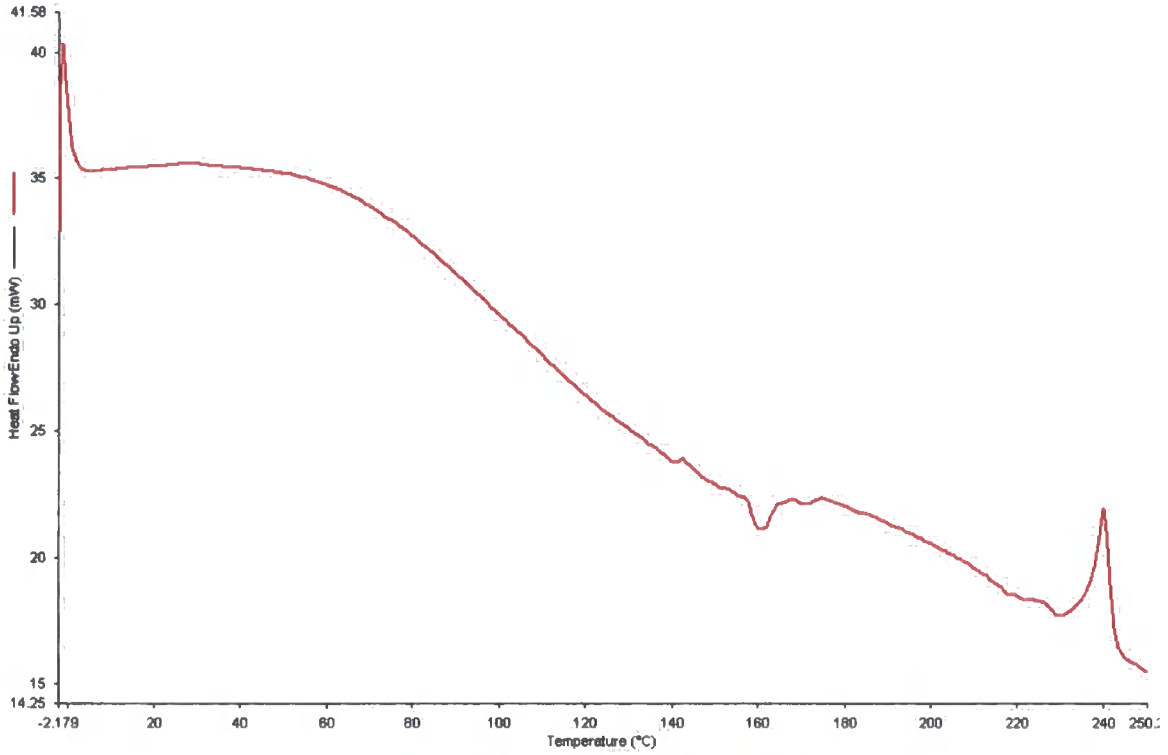

Figure 2.8. DSC curve for compound 2a.

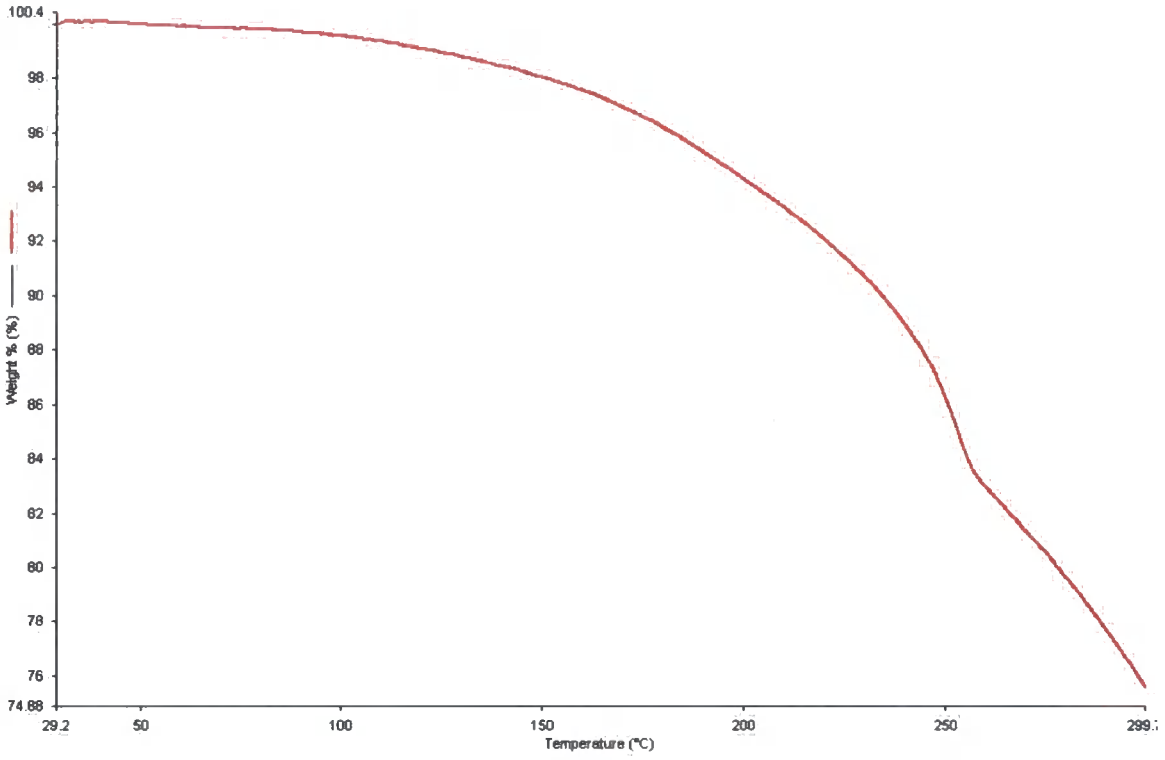

Figure 2.9. Weight loss as a function of temperature for compound 2b.

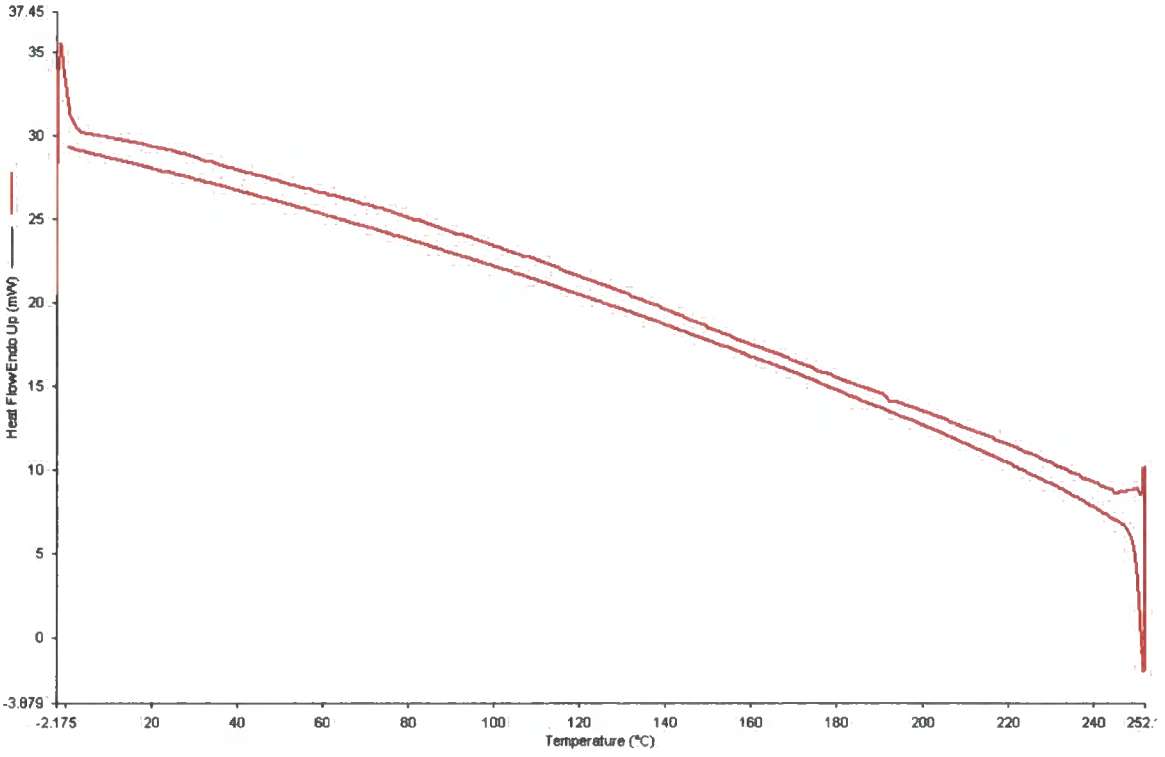

Figure 2.10. DSC curve for compound 2b.

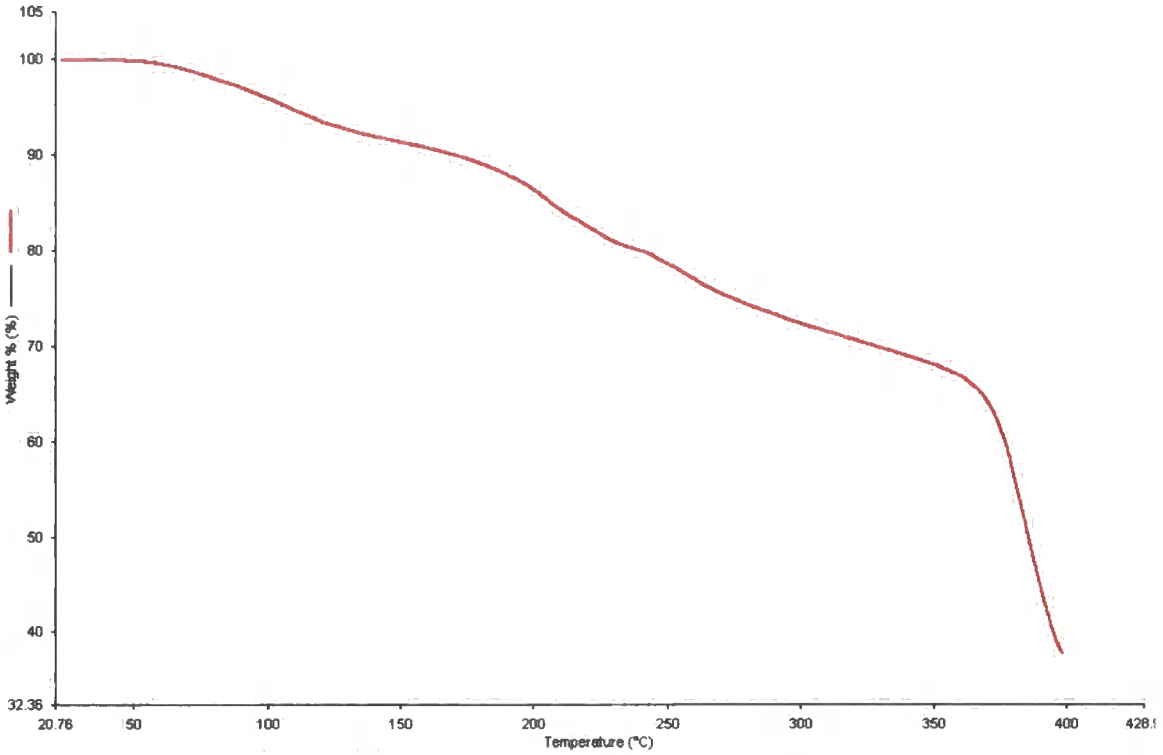

Figure 2.11. Weight loss as a function of temperature for compound 2c.

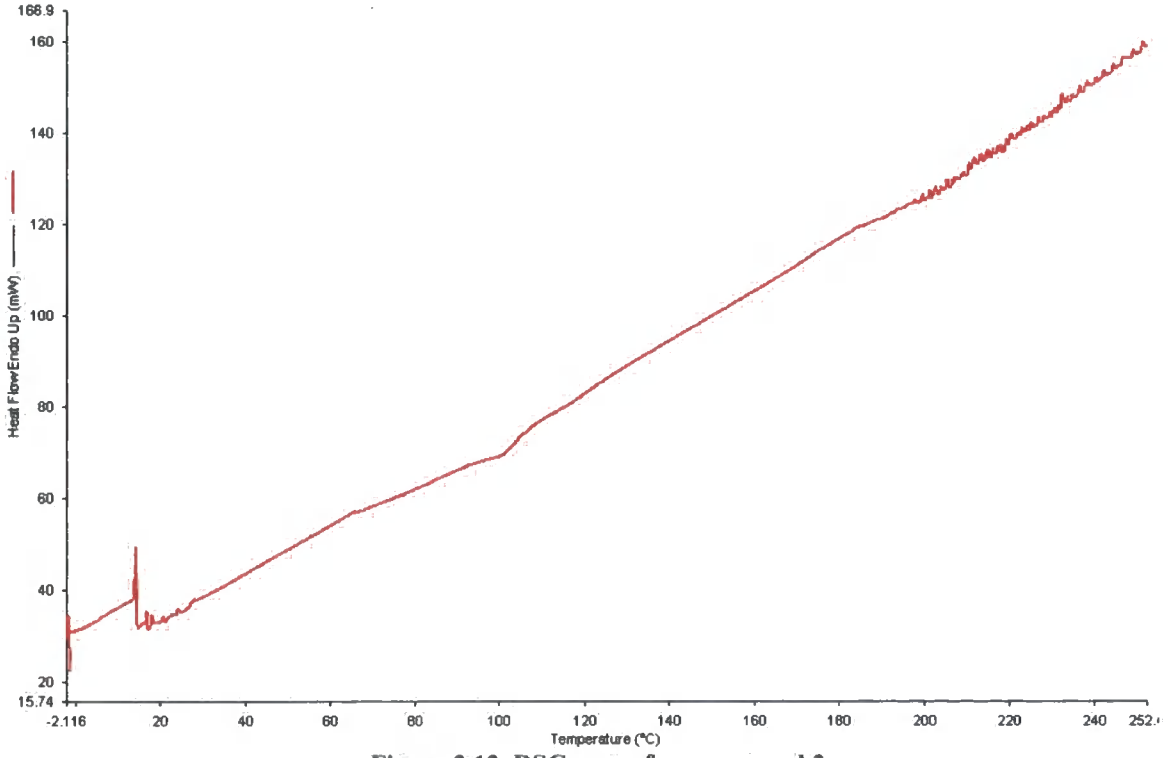

Figure 2.12. DSC curve for compound 2c.

The triarylborane **3a** exhibits a somewhat broad melting point at ca. 215 °C. Upon cooling, there was evidence for recrystallisation at ca. 145 °C. Decomposition occurs at T > 240 °C, and no glass transitions were observed. Compound **3b** decomposes at similar temperature, but DSC revealed neither glass transitions nor melting.

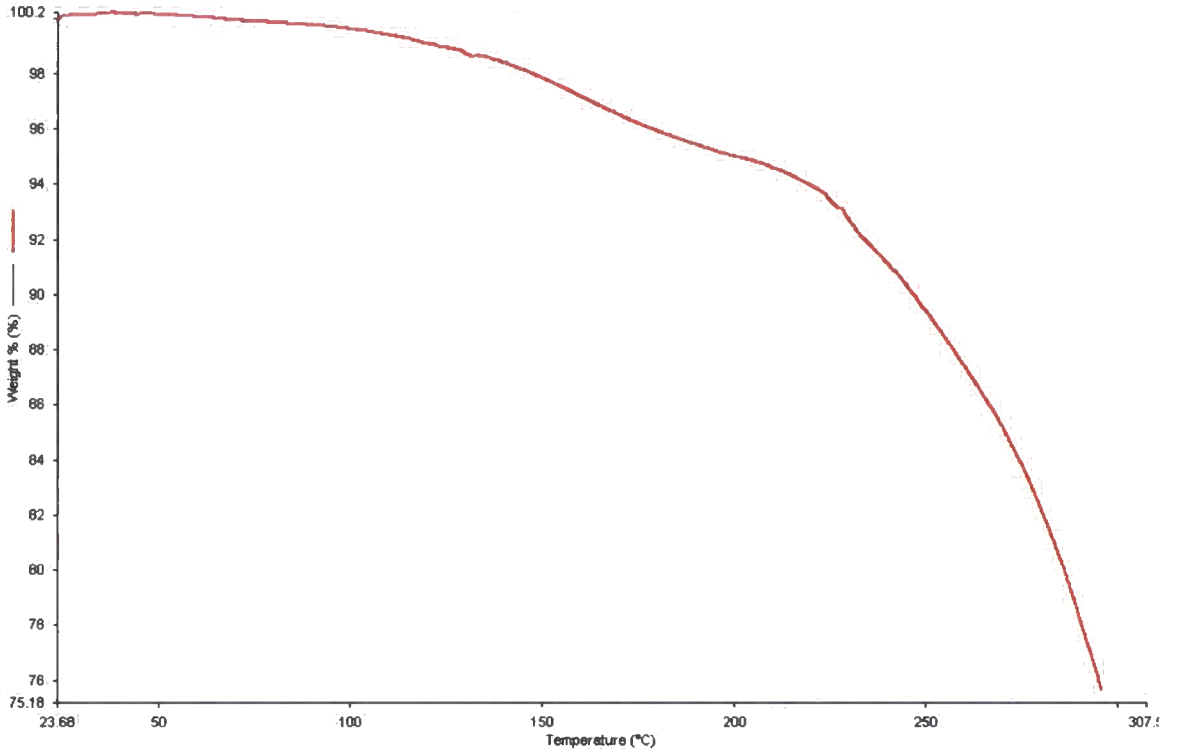

Figure 2.13. Weight loss as a function of temperature for compound 3a.

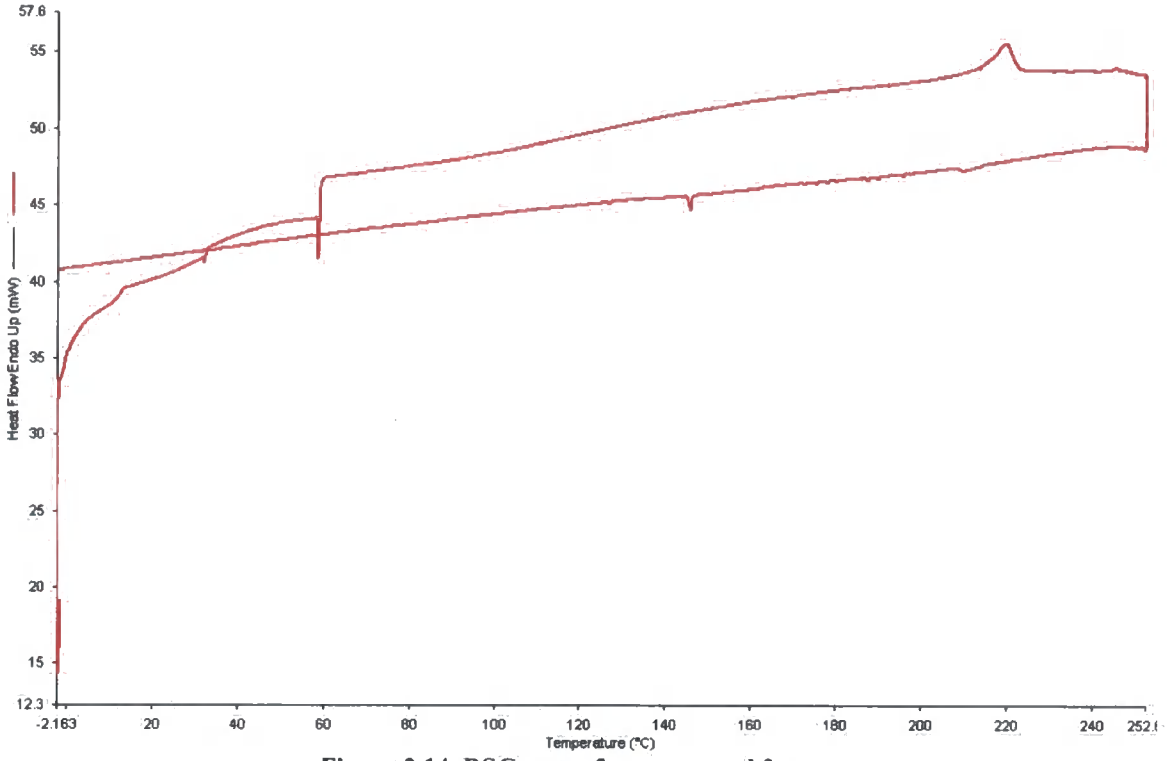

Figure 2.14. DSC curve for compound 3a.

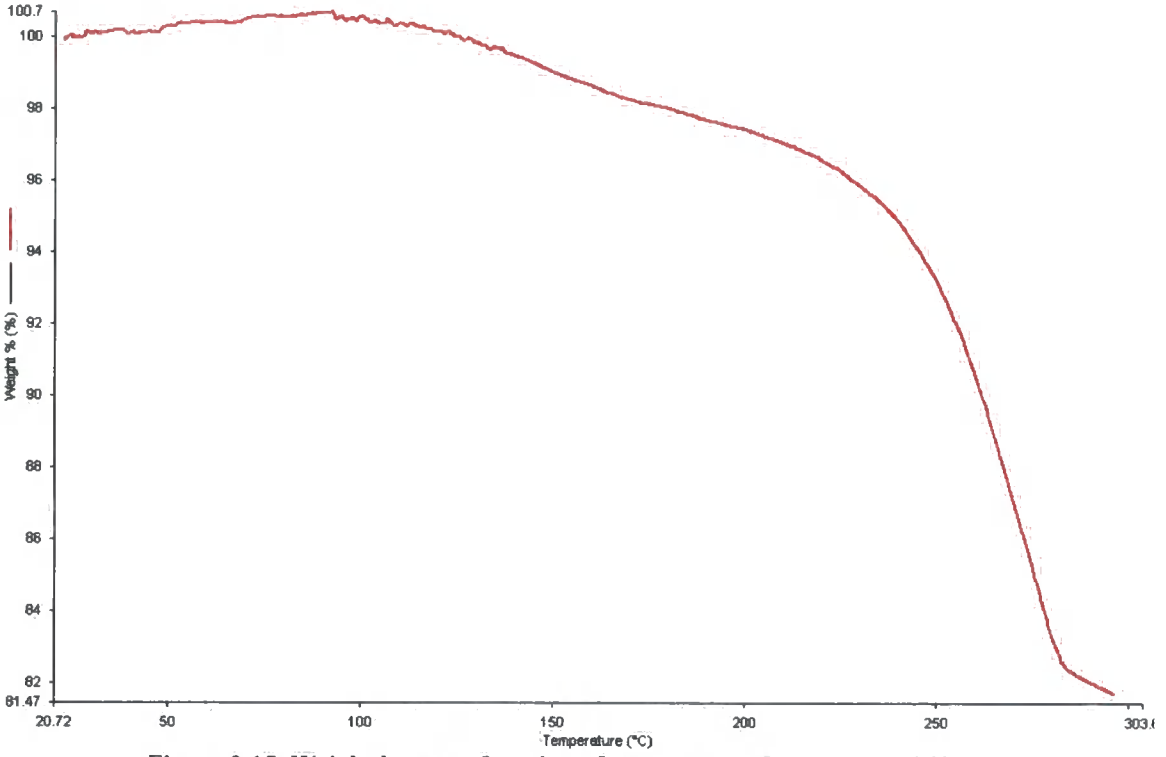

Figure 2.15. Weight loss as a function of temperature for compound 3b.

Compound **2f** loses adsorbed moisture between 100 and 150 °C, at which temperature the onset of thermal decomposition was observed. There was no evidence for either melting or glass transitions. Compound **2h** loses adsorbed moisture at the surprisingly high temperature of ca. 180 °C, with thermal decomposition occurring at T > 250 °C. A broad melting point was observed in the DSC, commencing at ca. 240 °C and was confirmed by measuring the melting point in a sealed tube. The sample started to liquefy to a viscous yellow oil at ca. 242 °C (uncorrected value) and at ca. 260 °C the colour began to noticeably darken, eventually forming a dark brown oil. Unfortunately, it was impossible to record the DSC at T > 250 °C, since decomposition of the sample may have caused damage to the instrument. A possible glass transition occurs at 108 °C, but the changes in energy are smaller than expected and thus this can only be a tentative assignment.

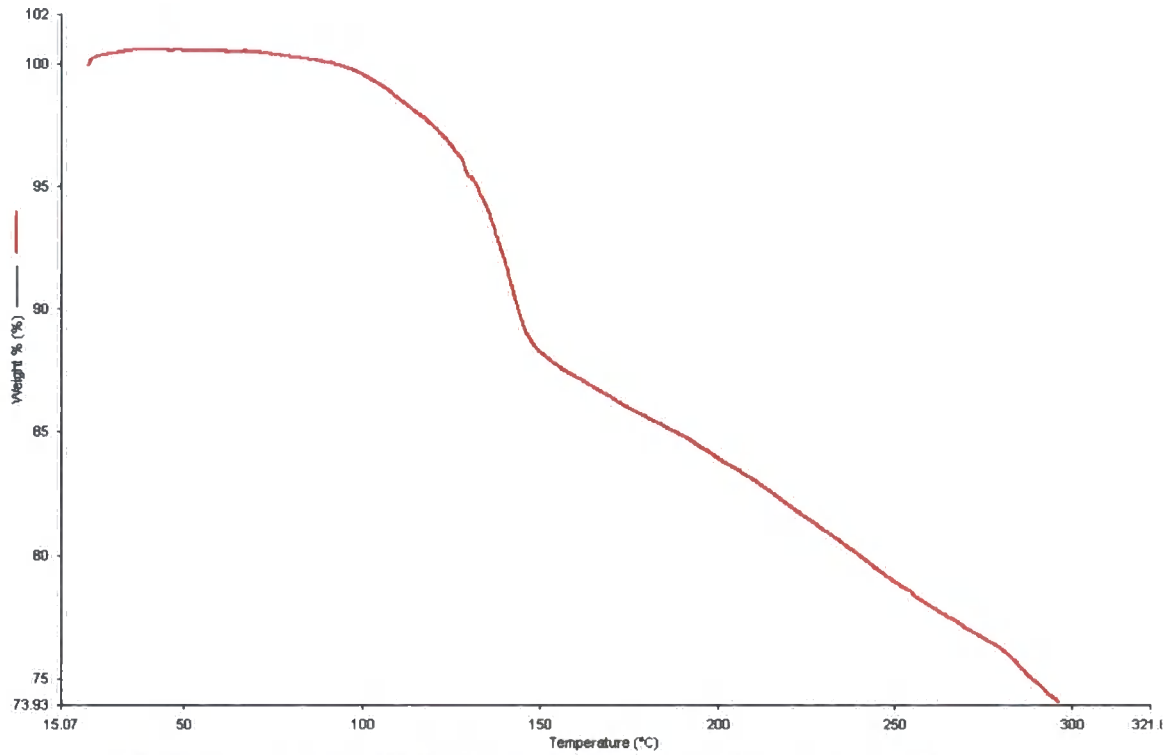

Figure 2.16. Weight loss as a function of temperature for compound 2f.

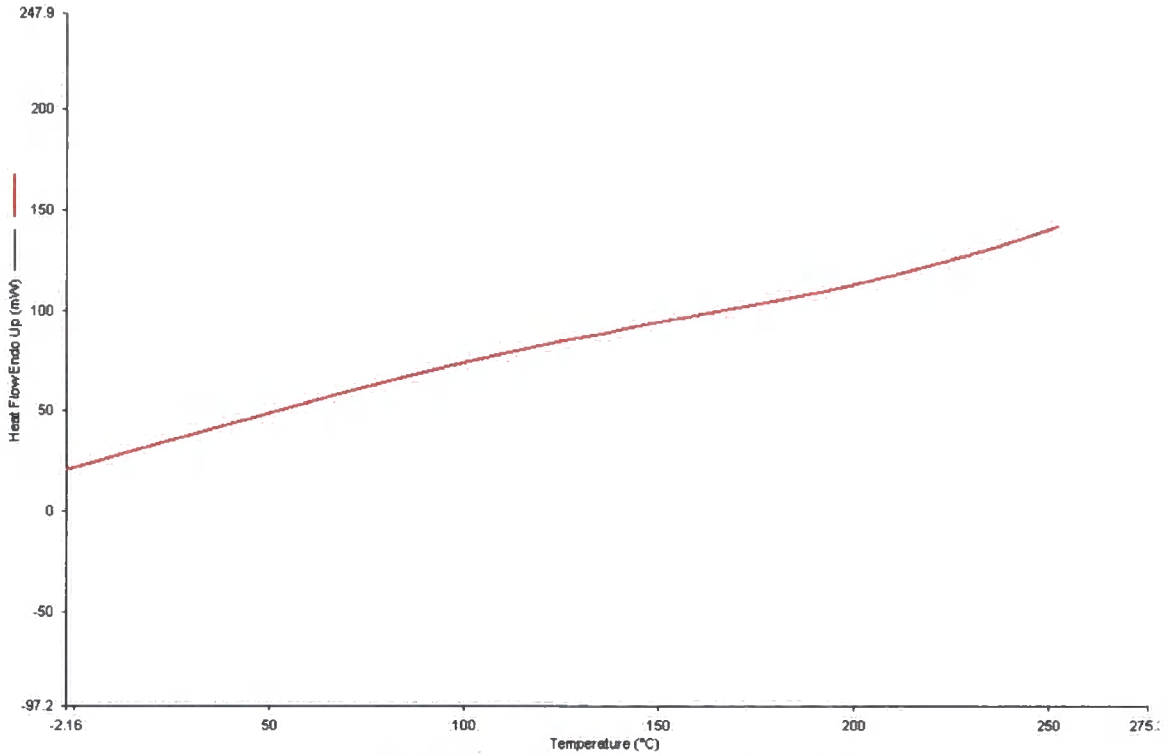

Figure 2.17. DSC curve for compound 2f.

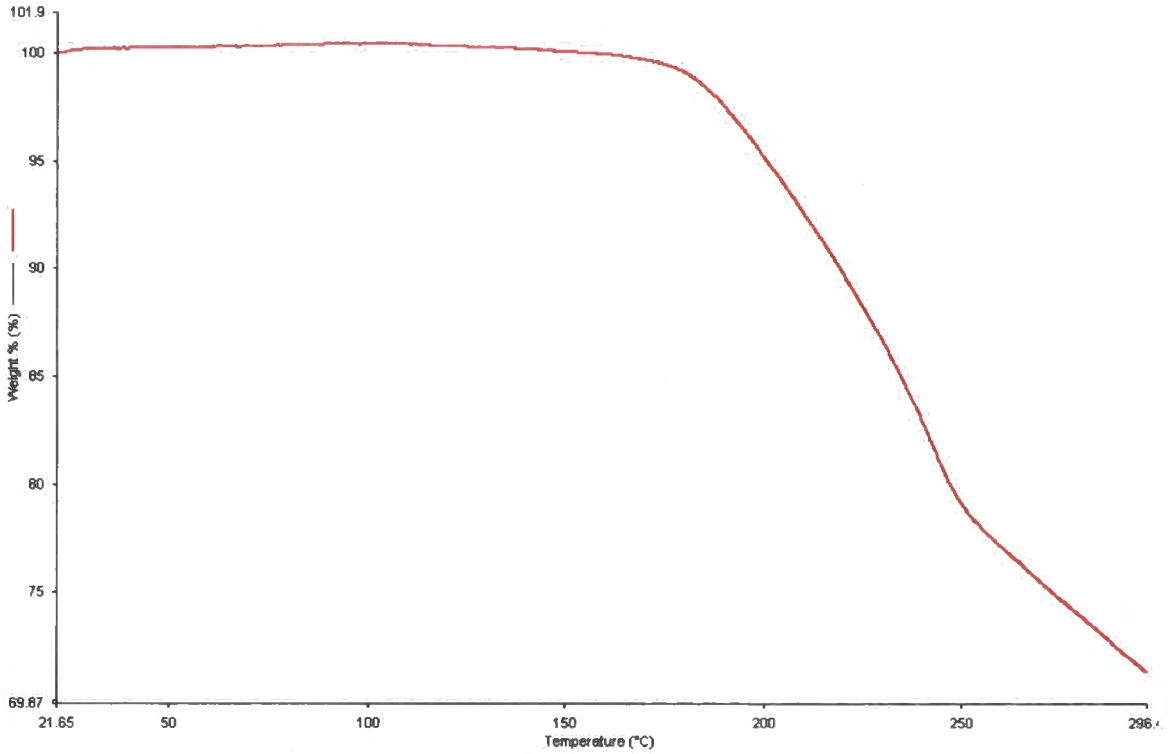

Figure 2.18. Weight loss as a function of temperature for compound 2h.

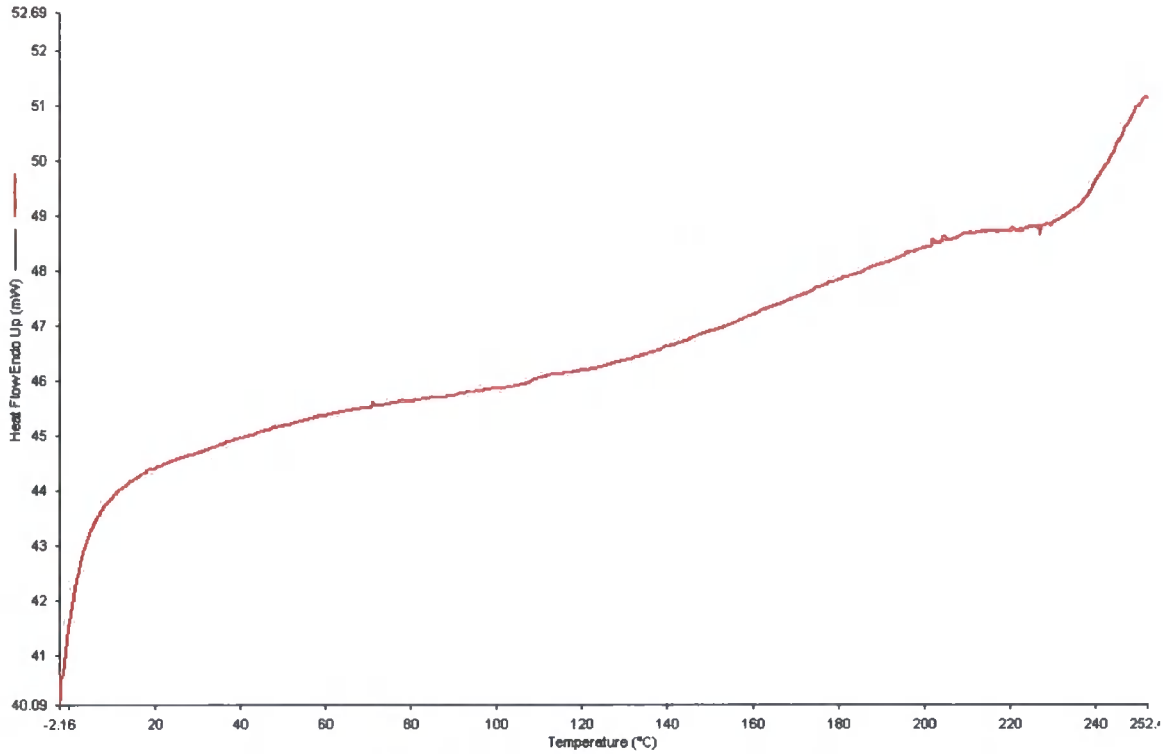

Figure 2.19. DSC curve for compound 2h.

Compound **2g** appears to have a T_g at ca. 135 °C. TGA reveals a gradual weight loss in the region of ca. 5% at 50 – 150 °C, followed by a plateau from 145 – 200°C where weight is approximately constant. The sample again loses weight when T > 200°C, as shown in Figure 2.21. It is unclear why the thermal properties of this compound are so different from the properties of the similar compound **2f**, but may be a reflection of the enforced planarity of the fluorene system, though structural data suggest that in the solid state, the biphenyl moiety is completely planar. It seems unlikely, however, that the presence of a bridging methylene group in **2g** should result in major structural differences.

In order to confirm that the initial weight losses of this and the other compounds investigated were due to desorption of moisture or solvents, and not simply the result of a complex decomposition pattern, a second sample of **2g** was held at 150°C for 60 minutes to drive off adsorbed water, then cooled and reheated to 300°C. As expected, no loss of weight was observed before the onset of

decomposition (2% weight loss at 225°C), confirming that the compound was thermally stable below that temperature (Figure 2.22). This pattern was the same for all other compounds examined, and reflects the hygroscopic nature of these materials. All compounds were stored in the glovebox and transported for analysis in sealed vials, but were open to the atmosphere during sample loading: NMR spectroscopy confirmed that neither organic solvents nor water were present in the stored compounds. The high temperatures required to remove adsorbed water may be in part due to coordination with the vacant p_z orbitals on the boron atoms.

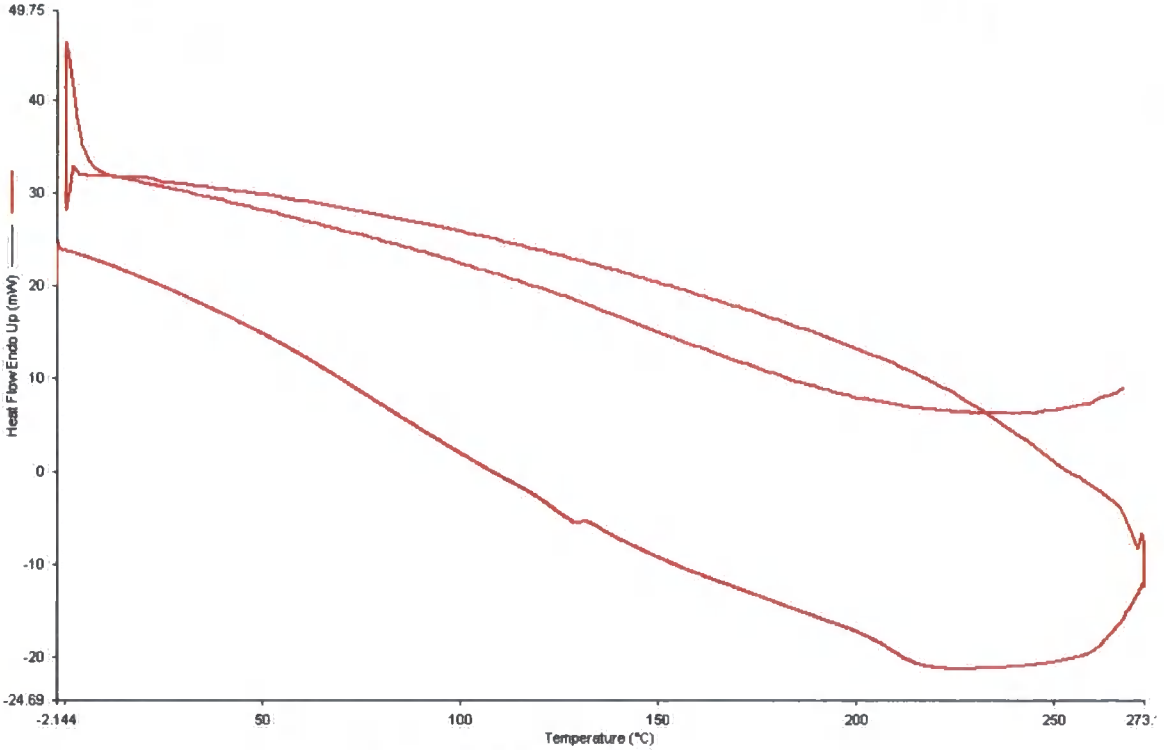

Figure 2.20. DSC curve for compound 2g.

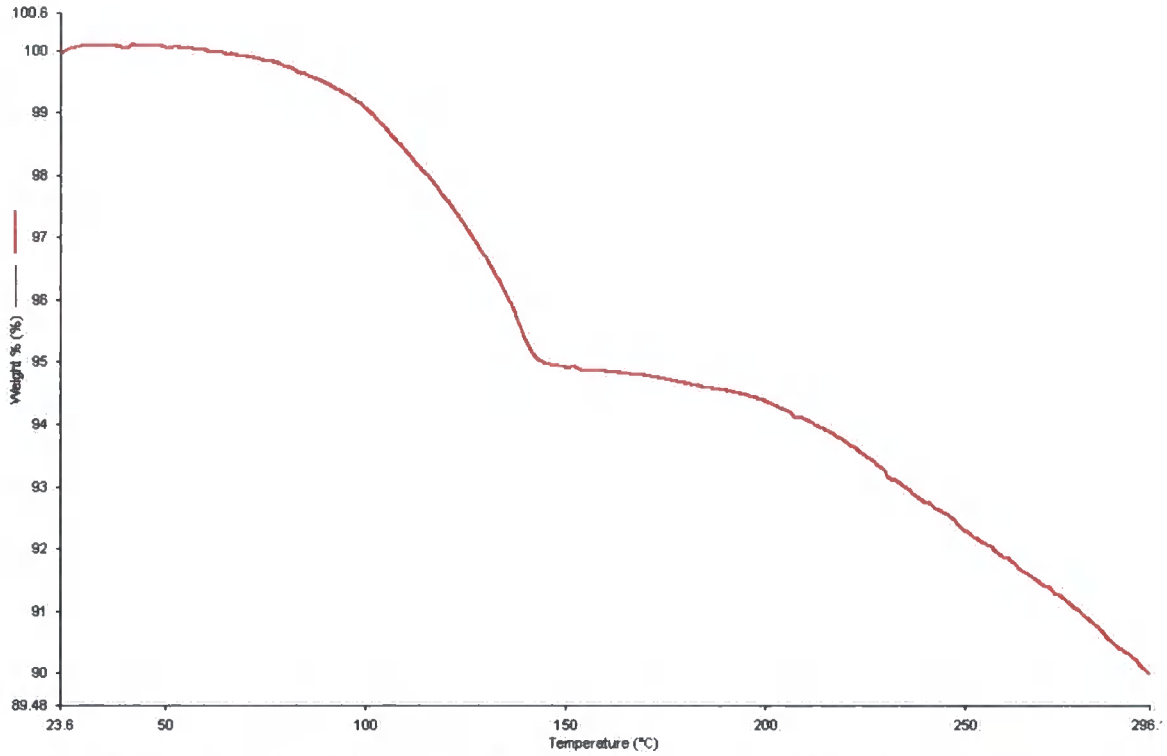

Figure 2.21. Weight loss as a function of temperature for compound 2g, with a consant heating rate of 10 °C min^{-1}.

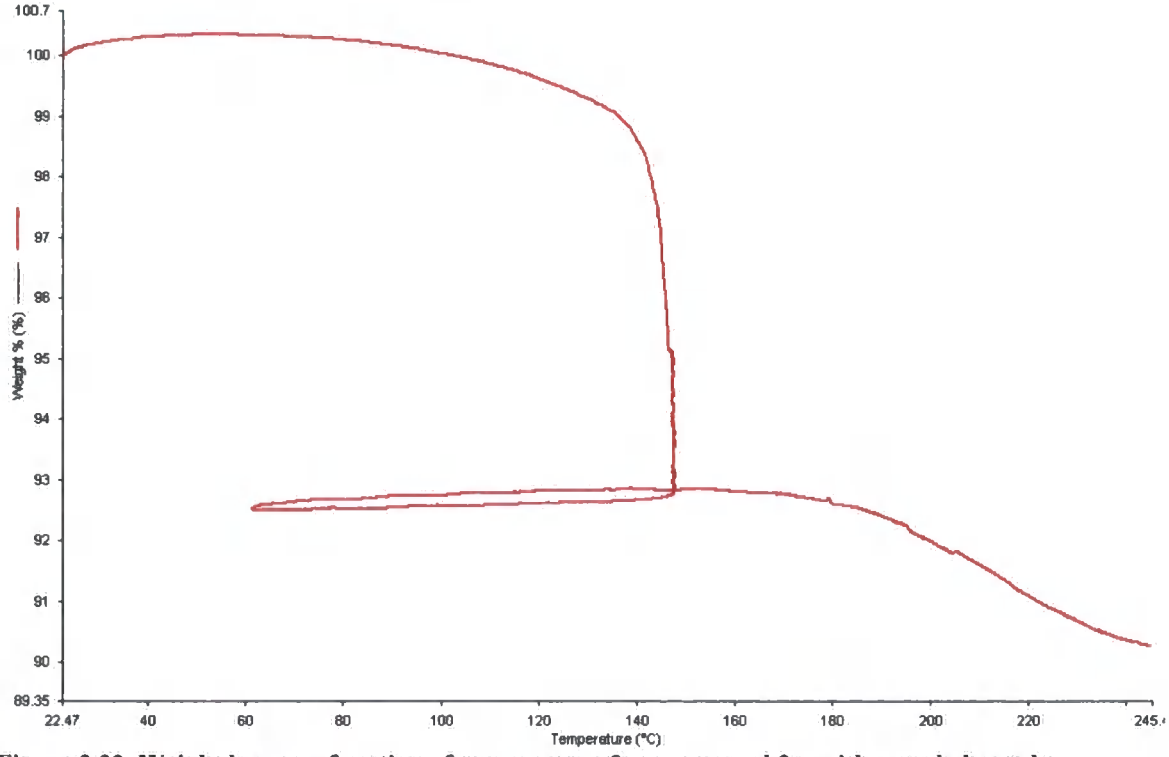

Figure 2.22. Weight loss as a function of temperature for compound 2g, with sample heated to 150 °C, maintained at this temperature for 1h, cooled to 60 °C and finally heated until decomposition occurred.

2.2.4. Optical Properties

UV-visible absorption and emission data, including absorptivity (ε) and fluorescence quantum yield (Φ_F), were collected for all compounds. All spectra were recorded in cyclohexane since absorption and emission maxima were found to be largely independent of solvent. Quantum yields were measured by comparison with double matched standards of quinine sulphate / 1 M H_2SO_4 and norharmane / 0.1 M H_2SO_4, according to Equation 1.[25]

From the definition of Φ_F;

$$\Phi_F = \frac{\text{no. of photons emitted}}{\text{no. of photons absorbed}} = \frac{\text{intensity of fluorescence}}{\text{intensity of absorption}} = \frac{I_F}{I_A}$$

By rearrangement; $I_F = \Phi_F I_A$ **(1)**

Therefore a plot of integrated fluorescent intensity vs. absorbance should result in a straight line, with a gradient proportional to quantum yield and an intercept of zero. Provided that instrumental parameters such as excitation wavelength and slit widths are constant, and the experiment is run under conditions approximating optical transparency (to minimise effects such as optical reabsorption),[26] the quantum yield of a sample (x) may be calculated relative to that of a sample with known quantum yield (st) according to Equation 2;

$$\Phi_F(x) = \Phi_F(st)\left(\frac{\text{Grad (x)}}{\text{Grad (st)}}\right)\left(\frac{\eta^2(x)}{\eta^2(st)}\right) \qquad \textbf{(2)}$$

where η is the refractive index of the solvent.

In practice, two standard samples are used and cross calibrated with each other by calculating the quantum yield for Standard A assuming a literature value of Standard B, and then repeating the calculation with Standard A assumed as being correct; if the quantum yields thus determined are found to be within ± 10% of the literature values, then reliable quantum yields for unknown samples may be calculated against each standard. The error in the measurement comes from the difference in quantum yield determined from the two standards.

A summary of optical properties is presented in Table 2.6. All compounds exhibited an intense absorption in the UV region (λ_{max} = 205 nm); the position of this band was constant for all compounds investigated, and is thought to be associated with $\pi - \pi^*$ transitions of electrons localised on the mesityl groups. This high energy band is not further discussed since it occurred near the limits of detection for the spectrometer, in a region where cyclohexane weakly absorbs. A lower energy absorption band was also observed for all compounds, and is assigned to $\pi - \pi^*$ transitions from the conjugated π - system extending throughout the backbone; λ_{max} varied from the near UV region (**3a,** λ_{max} = 338 nm) to the blue-green region (**3b** λ_{max} = 458 nm). Fluorescence occurred in the blue region with the exception of compounds containing an anthracene moiety, which emitted in the blue-green to green region, but quantum yields varied widely. Fine structure, observed in the absorption and/or emission spectra for many of the compounds, is a result of vibrational energy levels (Figure 2.23). Upon absorbing a photon of appropriate energy, molecules are promoted from the ground vibrational and electronic level (S_0) to a vibrational level in a higher electronic level (usually S_1), followed by rapid radiationless relaxation to the lowest vibrational level in the S_1 state. With the fluorescent emission of a photon, the

molecule relaxes to a vibrational level in the S_0 electronic state and rapidly returns to the ground vibrational state.

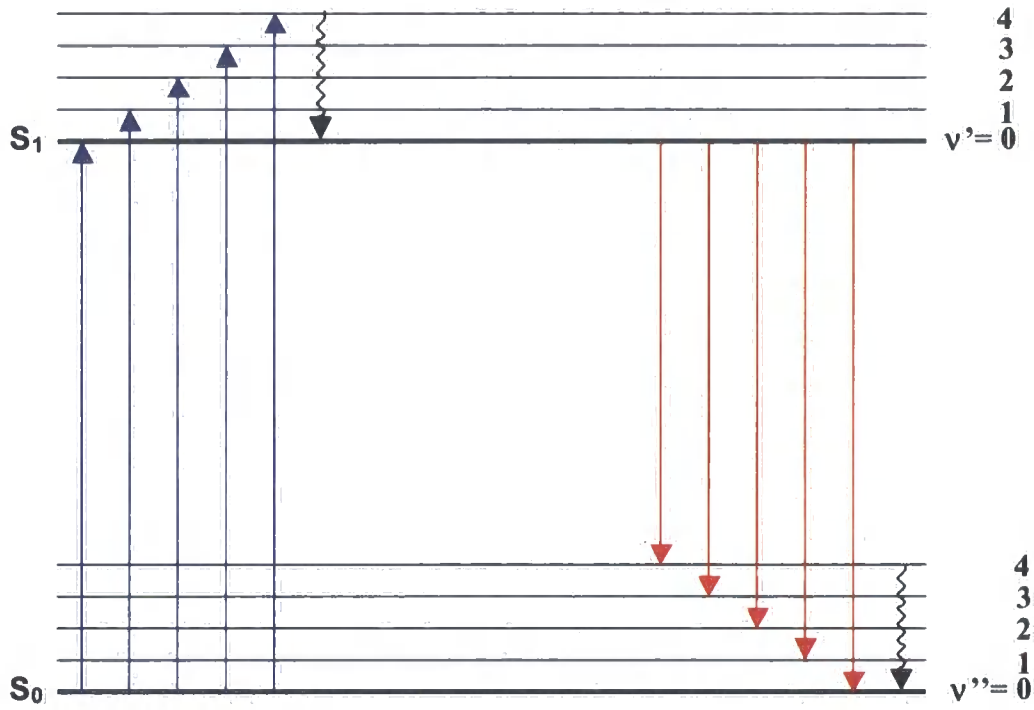

Figure 2.23. Schematic representation of transitions resulting from absorption (blue), fluorescence (red) and vibrational relaxation.

Table 2.6. Optical properties of symmetric bisboryls, Mes_2B-X-$BMes_2$ (cyclohexane solutions, ε calculated at the most intense absorption)

X	number	λ_{max} (abs) / nm	ε / $dm^3cm^{-1}mol^{-1}$	λ_{max} (em) / nm $\lambda_{(excitation)}$ = 340 nm	ϕ_F
(CHCH)-C_6H_4-(CHCH)	2a	372,390	42000	406,428,460(sh)	0.015±0.002
(CHCH)-C_6F_4-(CHCH)	2b	362	47000	420(sh), 440	0.073±0.002
(CHCH)-thiophenediyl-(CHCH)	2c	411,433	48000	452,478,516(sh)	0.010±0.002
(CHCH)-anthracenediyl-(CHCH)	2d	330, 436	70000	565	< 0.005
(CHCH)-naphthalenediyl-(CHCH)	2e	340(sh), 396	67000	454, 484, 520(sh)	0.038±0.002
(CHCH)-C_6H_4-C_6H_4-(CHCH)	2f	365	58000	408,433,472(sh)	0.054±0.002
(CHCH)-fluorenediyl-(CHCH)	2g	386,406	75000	417,441 470(sh)	0.098±0.002
(CHCH)-C_6H_4-(CHCH)-C_6H_4-(CHCH)	2h	397,418(sh)	83000	434,460,493(sh)	0.38±0.01
(CHCH)-C_6H_4-CC-C_6H_4-(CHCH)	2i	377, 397	64000	410, 435	0.22±0.01
(CHCH)-C_6H_4-CC-C_6H_4-CC-C_6H_4-(CHCH)	2j	380	89000	412, 437, 475(sh)	0.16±0.01
(CHCH)-C_6H_4-CC-C_6F_4-CC-C_6H_4-(CHCH)	2k	376	85000	410, 436,	0.21±0.01
C_6H_4	3a	338	25000	385	0.062±0.002
anthracenediyl	3b	346,432,458	65000	496	0.68±0.02
thiophenediyl	3c	364	48000	395	< 0.005

One-ring systems

The absorption spectra of compounds containing one central aromatic ring reveal a number of trends. The compound **2c** is significantly bathochromically shifted (by ca. 40 nm) with respect to **2a** and **2b**, indicating that conjugation is improved, probably because of the lower aromaticity of the thiophendiyl unit. Despite having similar extinction coefficients, this red shift results in the appearance of **2c** (bright yellow as a solid and intensely coloured in solution) being dramatically different from that of **2a** and **2b**; these compounds absorb only weakly in the visible region, resulting in pale yellow powders and solutions, whereas **2c** absorbs strongly in the violet - blue region. The effect of replacing hydrogen atoms with fluorine in the compounds **2a** and **2b** results in a slight hypsochromic shift of the absorption maximum but also results in a broader absorption band with weaker fine structure, which tails into the visible region so that the compound appears more highly coloured to the naked eye. The absorption band of **3a**, which has no vinyl spacers and therefore a shorter conjugation length, occurs at significantly higher energy (λ_{max} (abs) = 338 nm) and this compound has no significant absorption in the visible region.

The emission spectra reveal similar trends, with **3c** having a significantly lower energy emission maximum. It is interesting to note that in contrast to their absorption spectra, the emission maximum of **2b** appears at lower energy than that of **2a**. All of these compounds fluoresce weakly in the blue region. Compound **2c** appears to have a significantly lower quantum yield than **2a**, perhaps due to the presence of the heavy sulphur atom; this effect has been noted in related donor-accepter compounds containing the dimesitylboryl group.[12] It should be noted, however, that it is difficult to measure quantum yields with such a low magnitude, and the errors are relatively large (20 % for compound **2c**). Compound **2b** has a

significantly higher quantum yield (ca. five times that of **2a**), though it is not known what causes this effect. Whilst **3a** has a significantly higher quantum yield that of **2a**, perhaps as a result of greater structural rigidity, the fluorescence of the thiophene – based compound **3c** was unexpectedly weak, such that it was impossible to measure a quantum yield. Since this compound was prepared via the reaction of dilithiothiophene with $FBMes_2$, eliminating LiF, it was initially thought that the fluorescence might be being quenched by traces of fluoride; organoboranes are very susceptible to this effect, and have been investigated as possible fluoride ion sensors.[3,4] Passing a solution of **3c** through silica gel (to which fluoride binds very strongly) followed by recrystallisation had no effect on the remeasured fluorescence spectrum, however, so this can be discounted. The reason for the extremely weak fluorescence of this compound is presently unexplained, and is particularly surprising in comparison with the related compounds Mes_2B-(C_4H_2S)n-$BMes_2$ (n = 2, **BMB-2T**, n = 3, **BMB-3T**), which have been used as the emitting layer in OLEDs.[16-18] It should be noted, however, that the synthesis and properties of compound **3c** have not been reported, possibly because of its unfavourable optical properties.

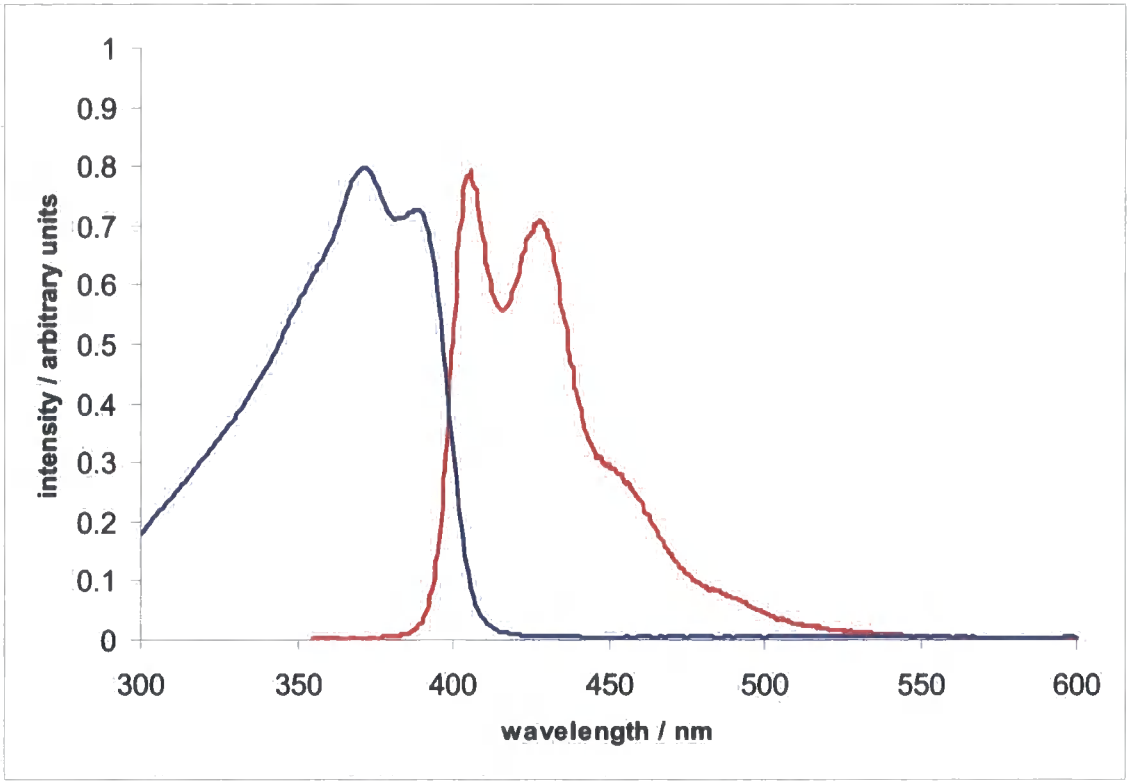

Figure 2.24. Absorption (blue) and fluorescence (red) spectra for 1,4-bis(dimesitylborylvinyl)benzene (2a).

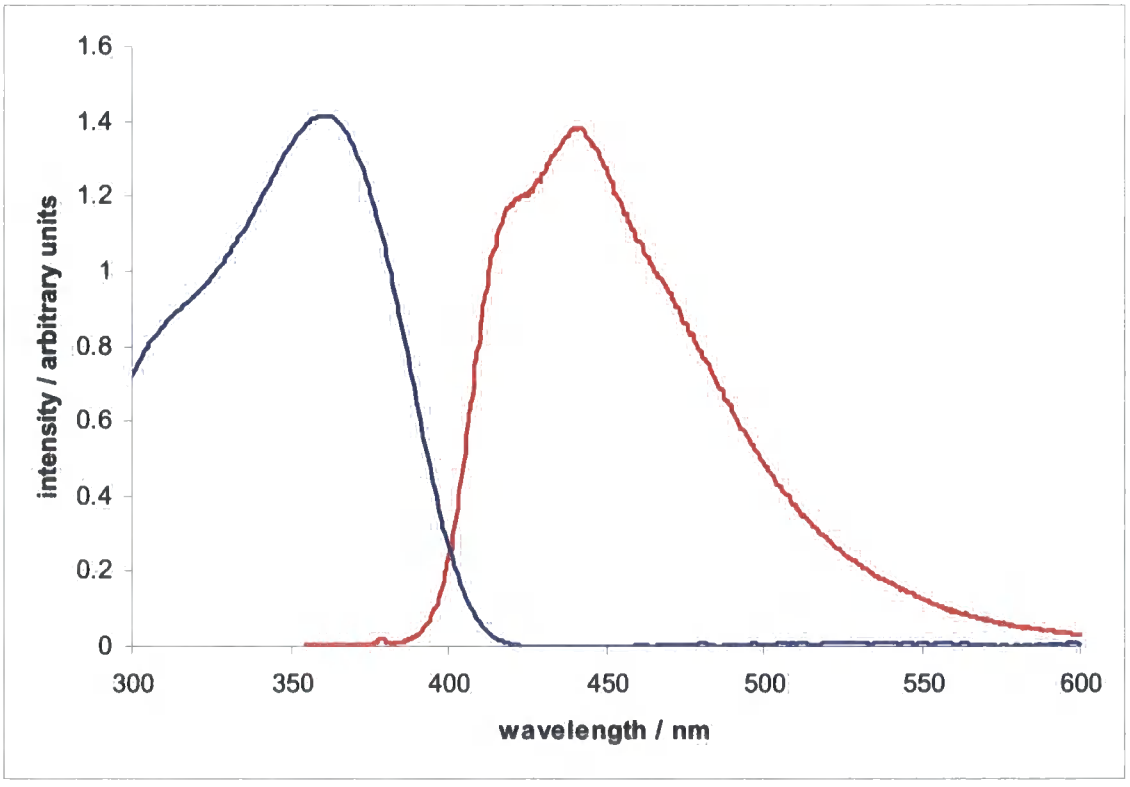

Figure 2.25. Absorption (blue) and fluorescence (red) spectra for 1,4-bis(dimesitylborylvinyl)tetrafluorobenzene (2b)

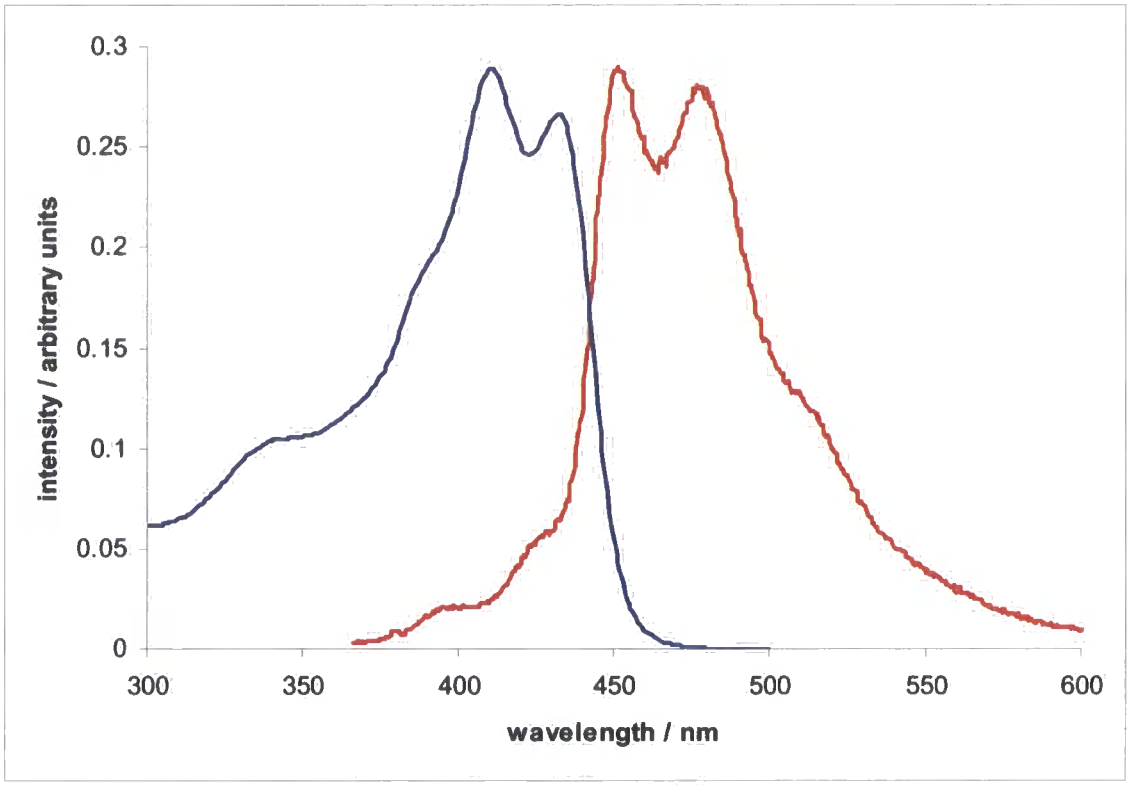

Figure 2.26. Absorption (blue) and fluorescence (red) spectra for 2,5-bis(dimesitylborylvinyl)thiophene (2c).

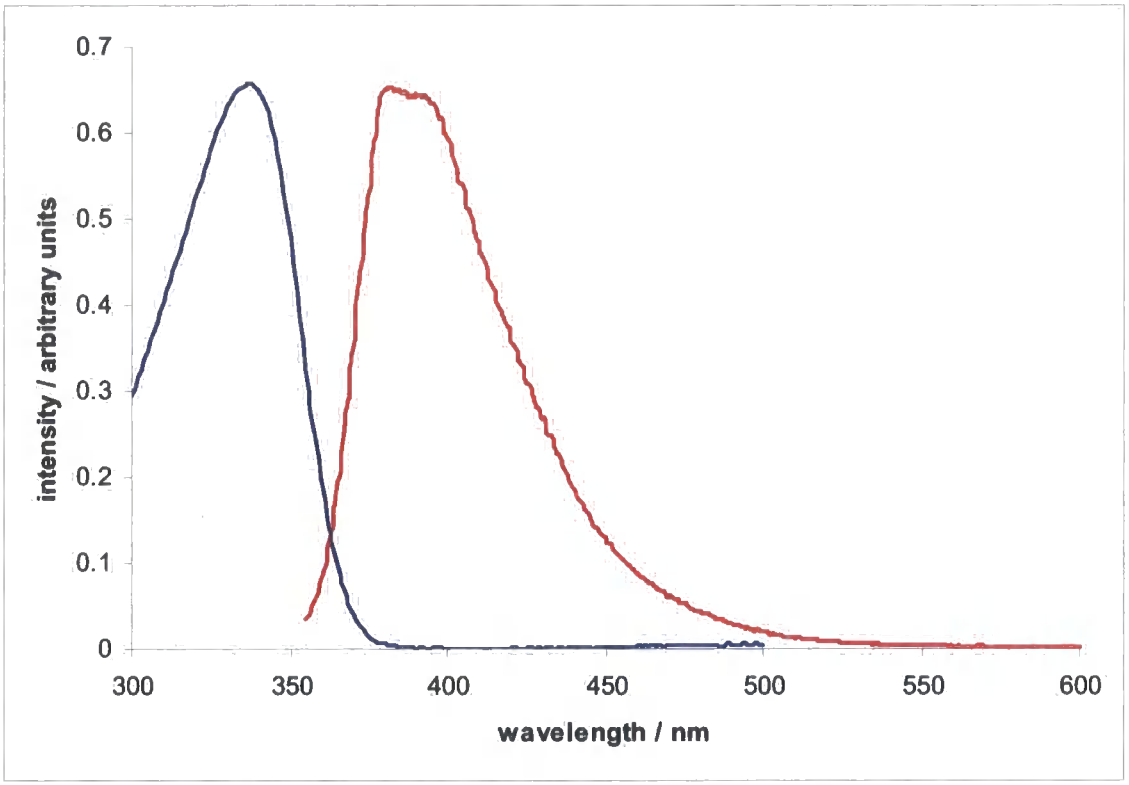

Figure 2.27. Absorption (blue) and fluorescence (red) spectra for 1,4-bis(dimesitylboryl)benzene (3a).

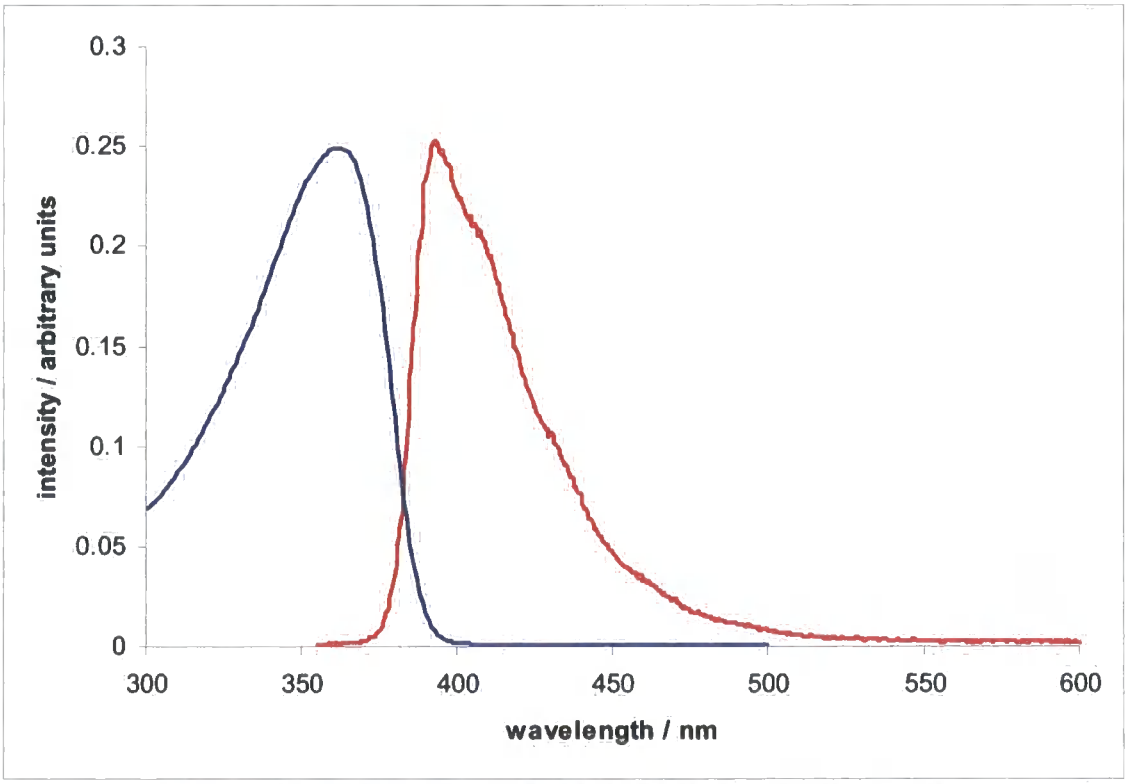

Figure 2.28. Absorption (blue) and fluorescence (red) spectra for 2,5-bis(dimesitylboryl)thiophene (3b).

Two and three-ring systems

Compounds with more extended π-systems illustrate a number of different factors. The biphenyl moiety in **2f** is planar in the solid state (as demonstrated by the molecular structure), but comparison of the optical properties with that of **2g** suggest that this is not the case in solution. The fluorenyl moiety in **2g** is forced to be planar in both the solid state and in solution due to the restraint imposed by the central methylene bridge, and since any electronic effects due to the methylene bridge are expected to be unimportant, the optical properties of the two compounds should be similar if the molecular conformations were similar. In fact, both the absorption and emission maxima of **2g** are significantly red-shifted with respect to. **2f**, indicating that the conjugation is more efficient, resulting in a lowering of the HOMO-LUMO energy gap. The quantum yield of **2g** is also significantly higher than that of **2f** (0.10 and 0.055 respectively).

Compounds **2h** and **2i** have the same conjugation length, but differ in that **2h** contains a vinyl group whereas **2i** has an alkynyl group. Both compounds have a broad and relatively featureless absorption band and an emission band that displays fine structure, with the absorption and emission bands occurring at lower energy in **2h**, indicating that the vinyl group is superior to the alkynyl group for improving conjugation in this type of molecule. The fluorescence quantum yield of **2h** is also much higher, which may be attributed to the difference in rotational motions about the molecular axis. Cis-trans isomerisation of alkenes involves breaking and reforming the C=C bond, which requires relatively high energies, and in conjugated systems there is often evidence of restricted rotation of allylic bonds since this disrupts the favourable overlap of p-orbitals; a planar conformation of **2h** would therefore be expected to be, on average, the most likely to exist at any given time. In contrast,

rotation about C-C triple bonds does not require bond breaking. The alkynyl spacer also aids rotation of the benzene rings relative to one another, since hydrogen atoms on adjacent rings are relatively distant. The result is that in tolan-type systems, there is a very low energy barrier to rotation of the rings, and this is thought to result in very rapid twisting of these molecules in solution. Since fluorescence is expected to occur from a planar conformation, (which allows for conjugation of the p-orbitals), and greater structural rigidity tends to favour a high quantum yield, it is not surprising that Φ_F for **2i** is lowered relative to **2h**.

The three compounds containing alkyne moieties have very similar optical properties. Absorption and emission spectra of all three are virtually identical, with the exception of small differences in vibrational fine structure. This indicates that conjugation is not significantly affected by increasing the length of the backbone by one phenylethynyl unit, and may hint at a saturation effect, though this seems unlikely with such small molecules. It is interesting to note that whilst quantum yields are similar for the two-ring compound **2i** and the three-ring compound **2k**, the quantum yield of compound **2j** is lower. This may be explained by two factors; the lesser probability of compounds containing three benzene rings of attaining a conformation in which all the ring systems are coplanar, and the apparent increase in fluorescence efficiency resulting from replacement of hydrogen atoms with fluorine atoms, as observed in the compounds **2a** and **2b**. This latter effect does not, however, appear to modify the molar extinction coefficient to a great degree.

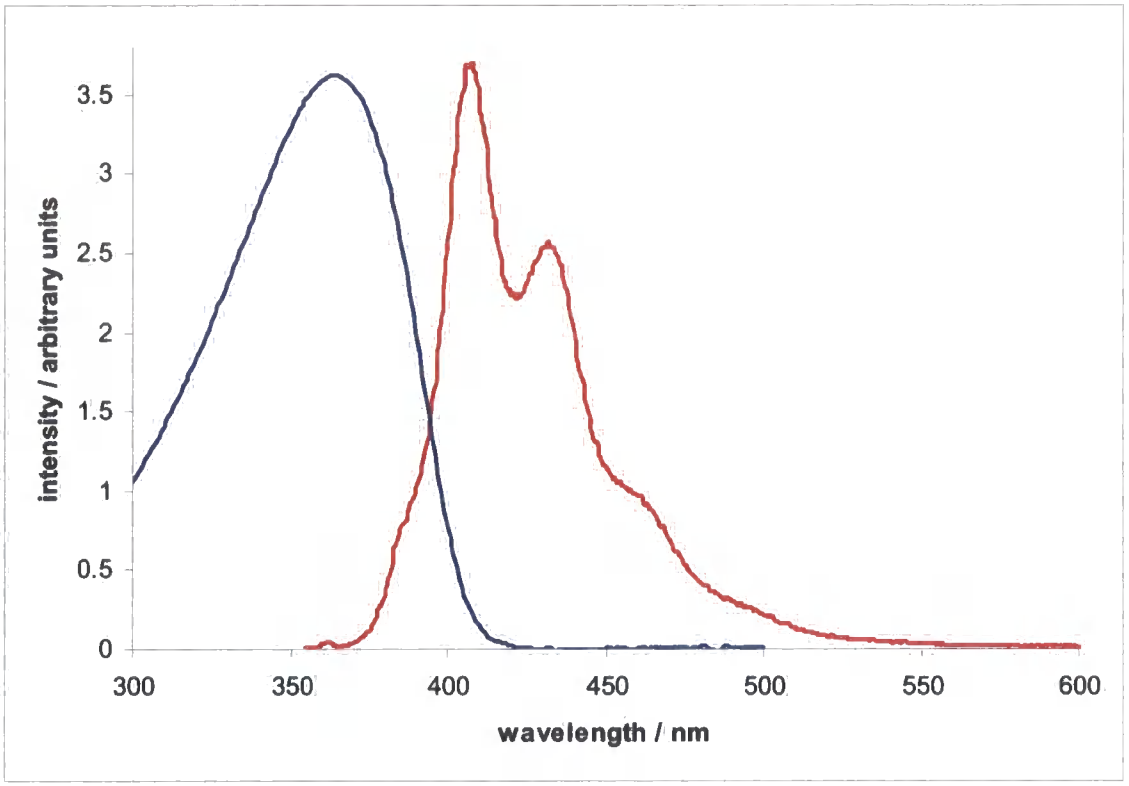

Figure 2.29. Absorption (blue) and fluorescence (red) spectra for 4,4'-bis(dimesitylborylvinyl)biphenyl (2f)

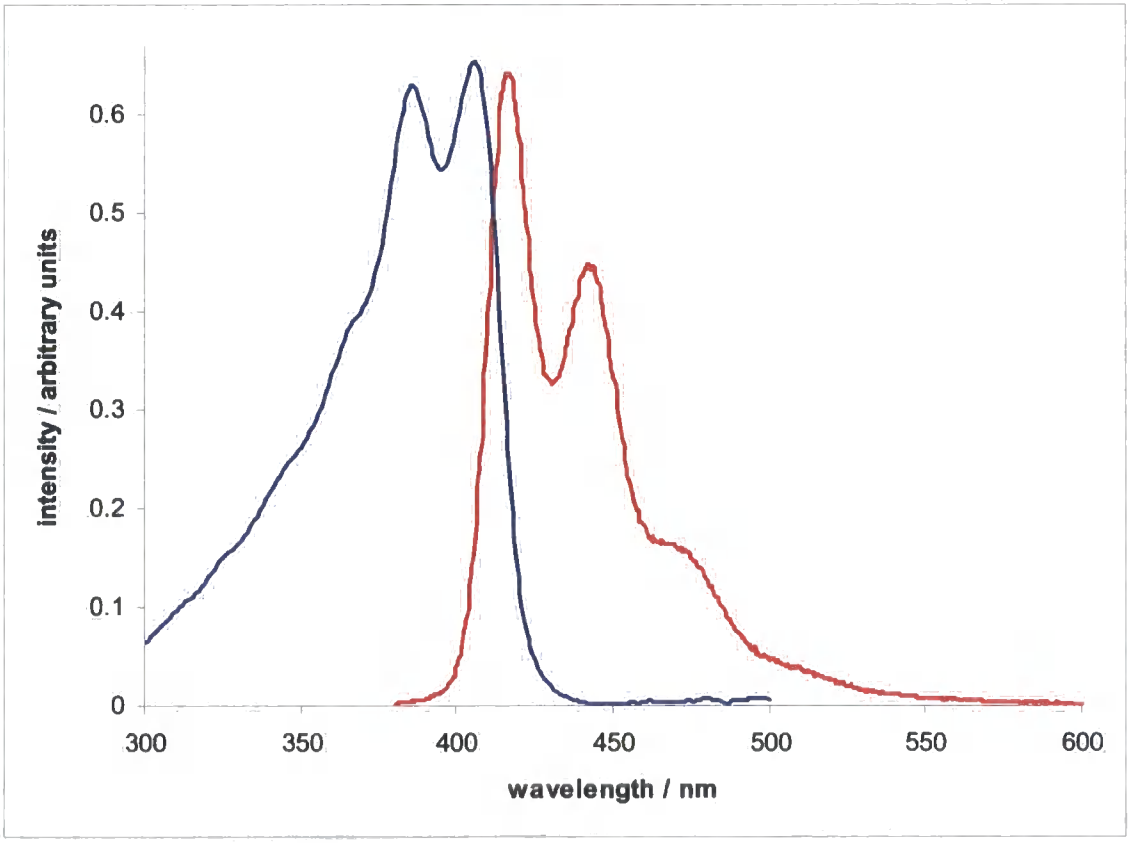

Figure 2.30. Absorption (blue) and fluorescence (red) spectra for 4,4'-bis(dimesitylborylvinyl)fluorene (2g)

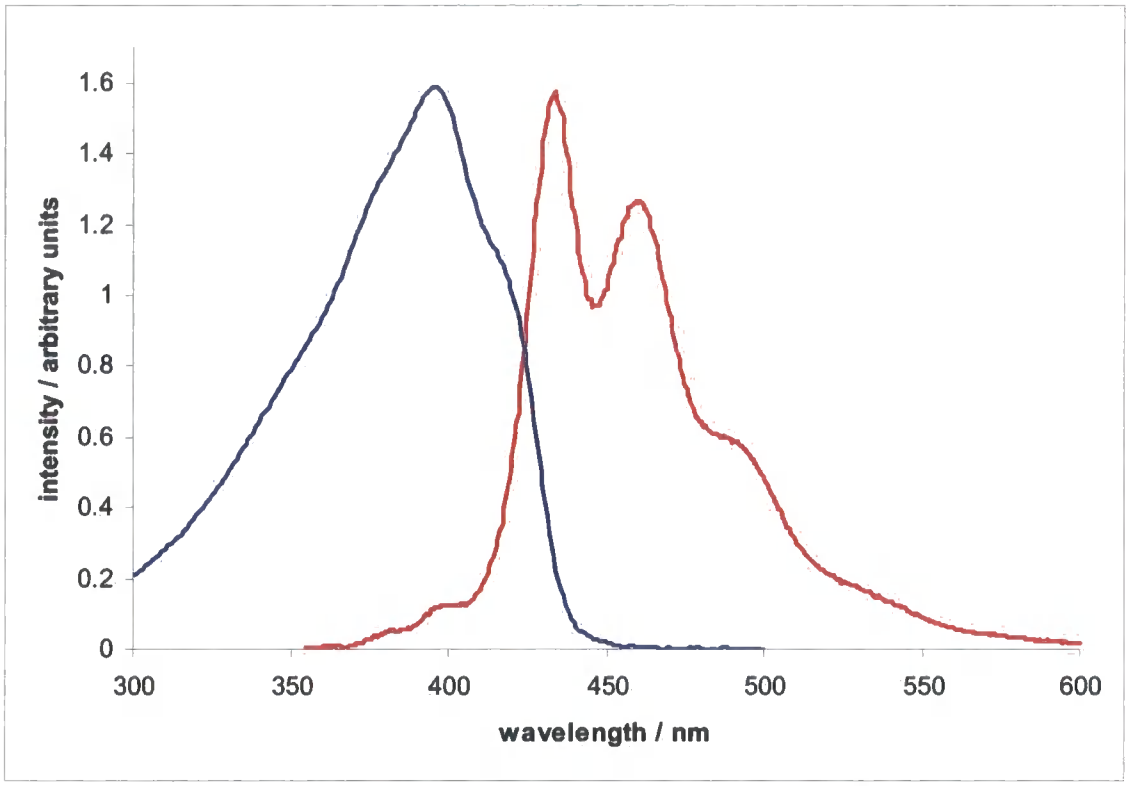

Figure 2.31. Absorption (blue) and fluorescence (red) spectra for 4,4'-bis(dimesitylborylvinyl)stilbene (2h)

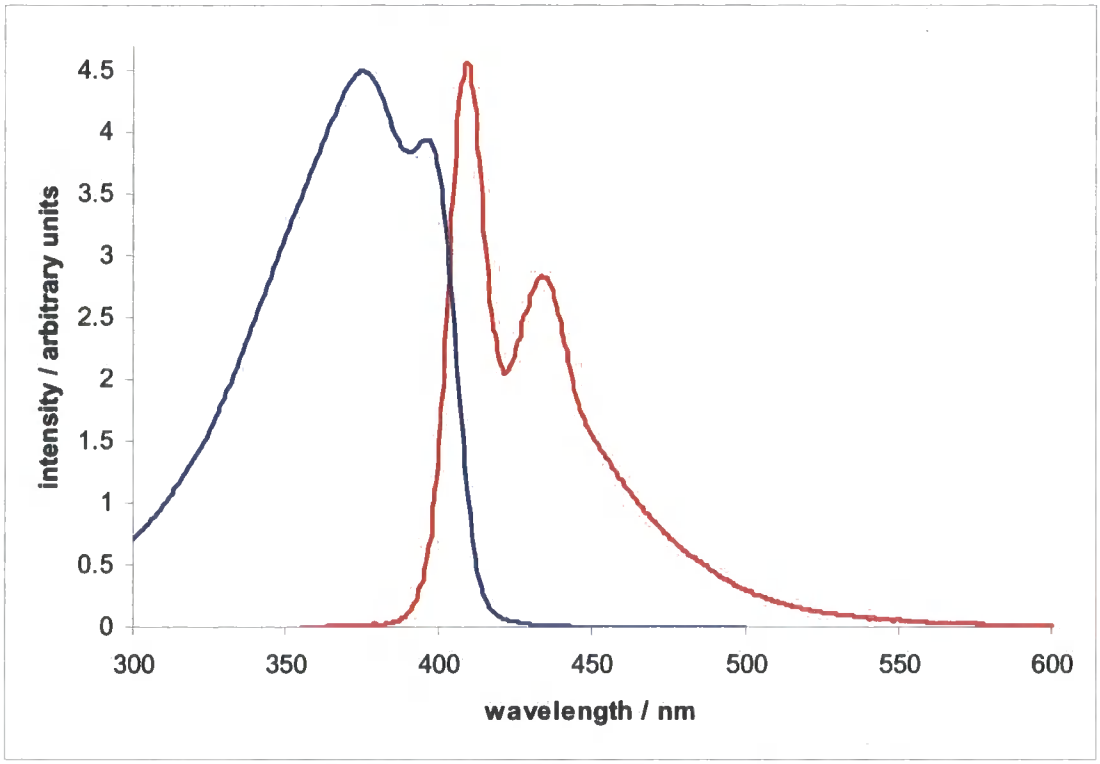

Figure 2.32. Absorption (blue) and fluorescence (red) spectra for 4,4'-bis(dimesitylborylvinyl)tolan (2i)

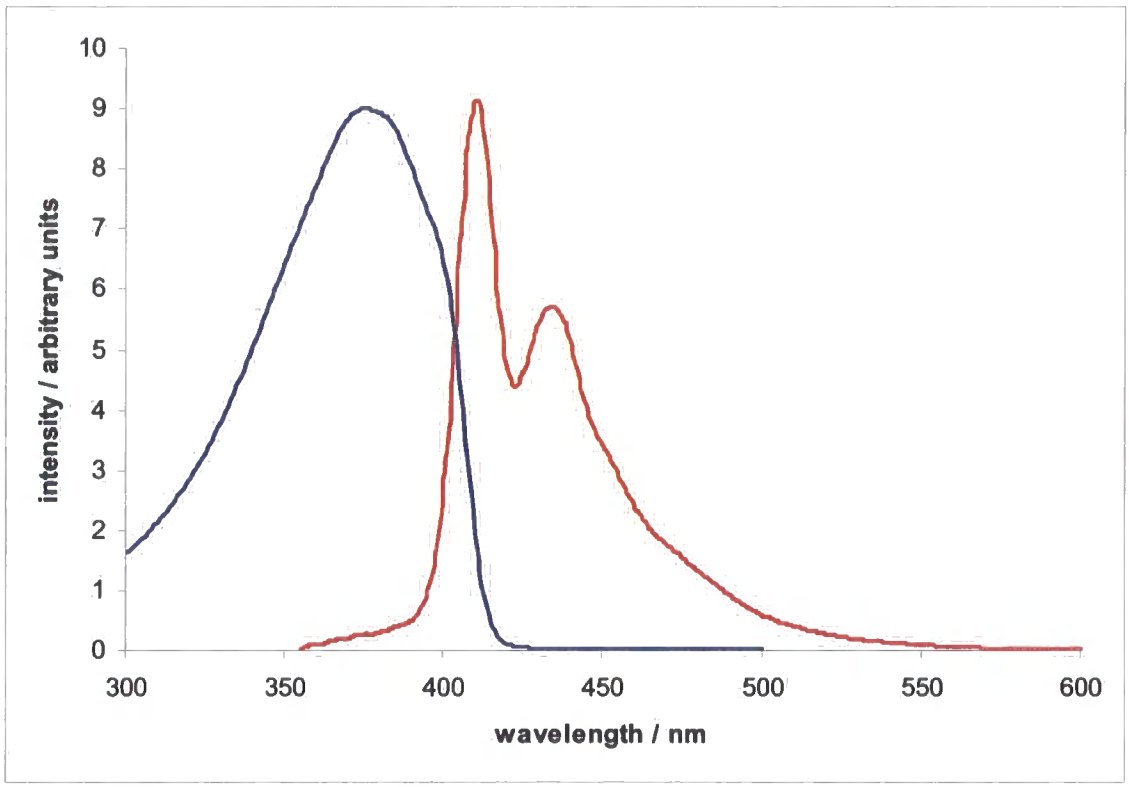

Figure 2.33. Absorption (blue) and fluorescence (red) spectra 3-ring all H (2j)

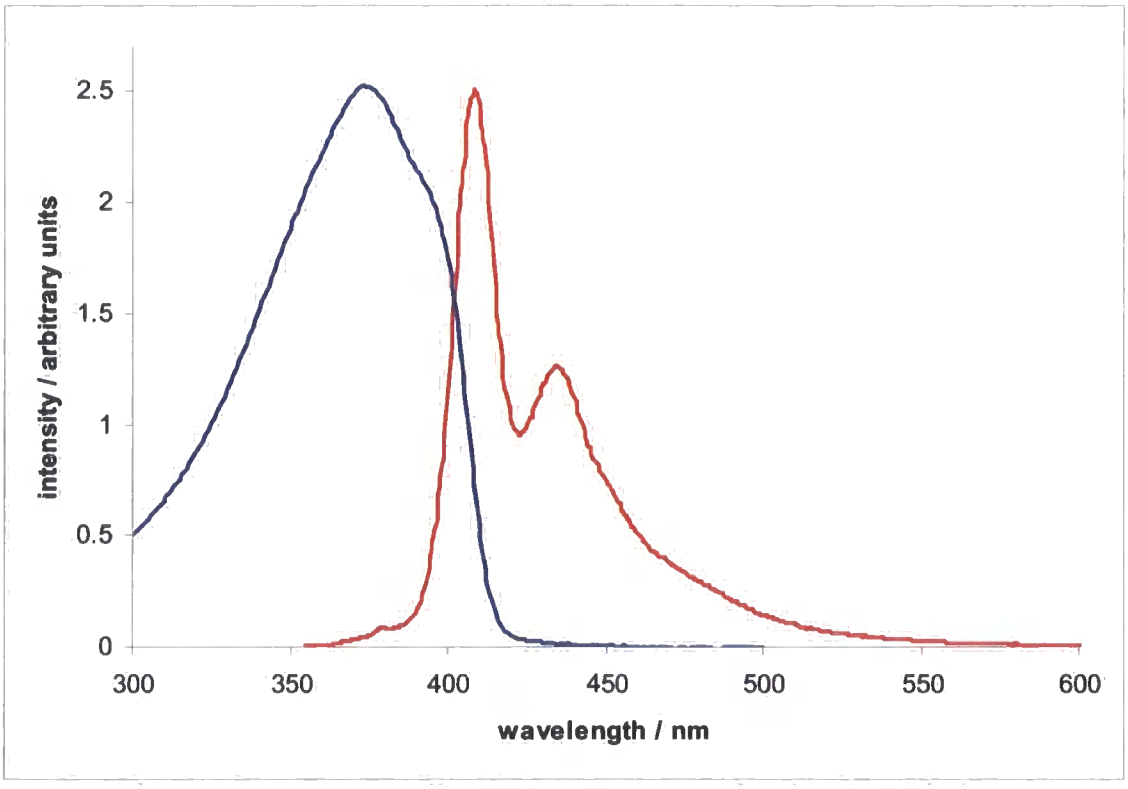

Figure 2.34. Absorption (blue) and fluorescence (red) spectra 3-ring-F4 (2k)

Fused-ring systems

The absorption maxima of compounds containing either naphthalene or anthracene moieties in their backbone are significantly red – shifted with respect to compounds **2a** and **3a**, which have the same conjugation length between the boron atoms, reflecting the lower aromaticity of these units compared to that of benzene. Molar extinction coefficients are also rather larger. Compounds **2d** and **3b** exhibit complex absorption spectra that extend below 300 nm, whereas compound **2e** has a broad absorption band that lacks fine structure; this may be a result of the lower symmetry in this compound. Fluorescence spectra show the opposite effect, with both anthracene – containing compounds having a broad, featureless emission band and the naphthalene - containing compound **2e** having a structured band that is similar to compounds based on benzene units. The presence of vinyl spacers results in a dramatic lowering of fluorescence efficiency; whilst compound **3b** has Φ_F of ca. 0.68, by far the highest of the compounds studied, compound **2d** was very weakly fluorescent, and a quantum yield could not be obtained since fluorescence was too low under the conditions required for accurate measurement. A likely explanation for this dramatic difference is that it is largely a result of the different steric demands; as indicated from the crystal structure of compound **3b** (Section 2.2.2), this compound adopts a twisted conformation in the solid state, with a planar conformation inaccessible due to steric clash with the mesityl groups and hydrogen atoms in the 1 4,5 and 8 positions of the anthracene moiety. This would also be expected to hinder rotation of the $BMes_2$ groups. Since BC_3 rings are coplanar, however, it seems that conjugation is extended to the vacant orbitals situated on the boron atoms. As a result, the conformation is partially locked, and favours a compromise between electronic and steric effects, one that fluoresces efficiently. In compound **2d**, the steric

effects are lessened but still important, being mainly a result of steric clash between anthracene and vinyl H – atoms, but the molecule is less rigid and thus has a greater number of possible conformations. The position of λ_{max}(em) indicates that fluorescence is associated with a conformation in which conjugation extends throughout the molecule, with the low quantum yield indicating that the molecule rarely accesses this electronically favourable configuration. Substitution of a naphthalene unit, as in compound **2e,** for the anthracene ring system in **2d** results in unsymmetric steric demands, with a *cisoid* conformation having considerably less steric strain than *transoid* (Figure 2.35). This enables **2e** to attain a relatively planar conformation much more readily, and is reflected in the much higher fluorescence efficiency.

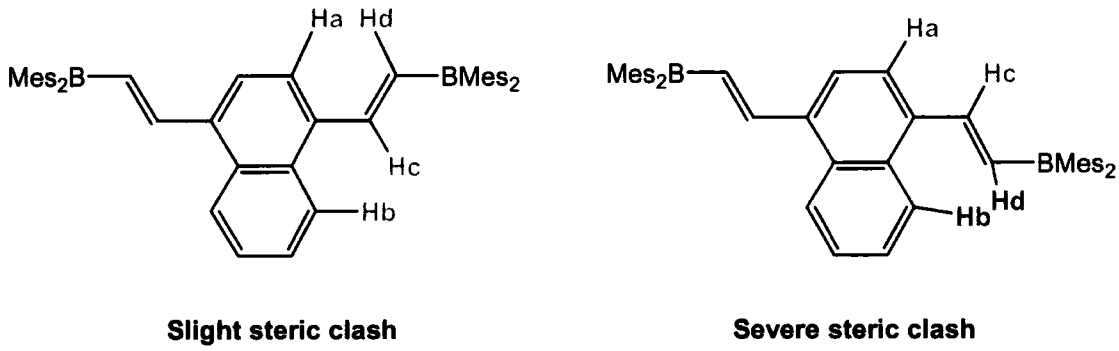

Figure 2.35. Schematic representation of *cisoid* and *transoid* conformations of 2e, showing relative steric favourability.

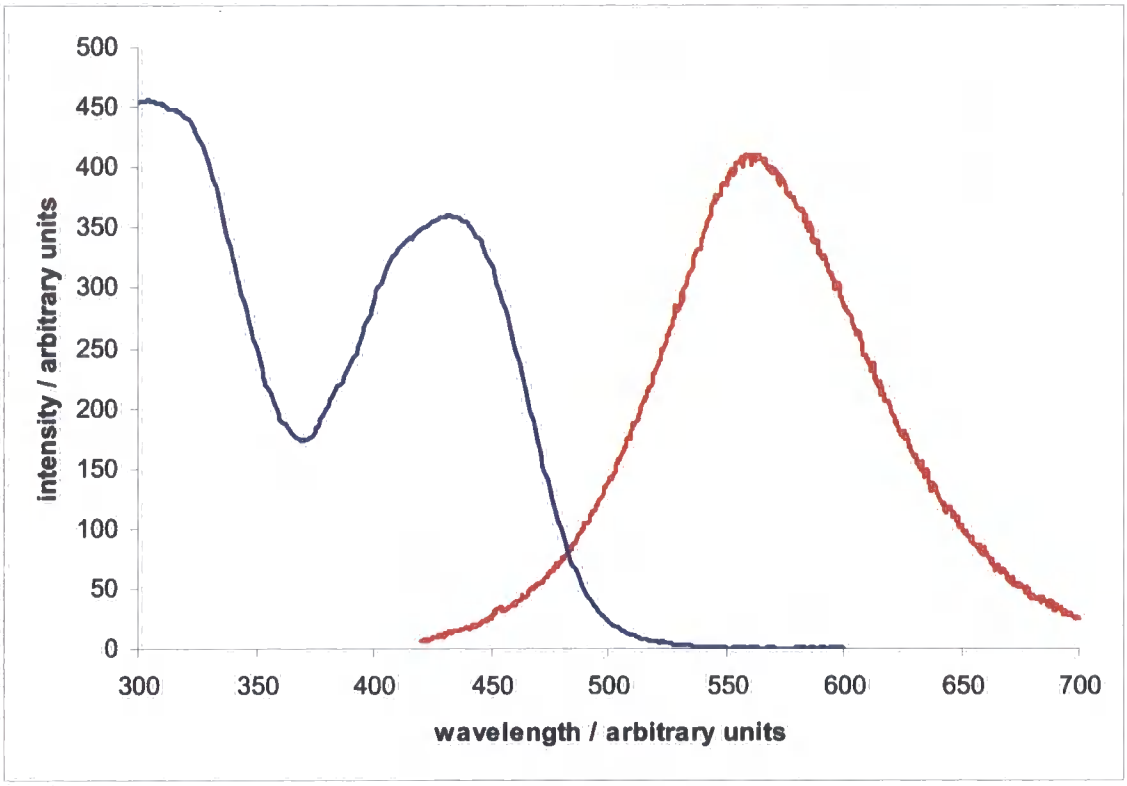

Figure 2.36. Absorption (blue) and fluorescence (red) spectra for 9,10-bis(dimesitylborylvinyl)anthracene (2d).

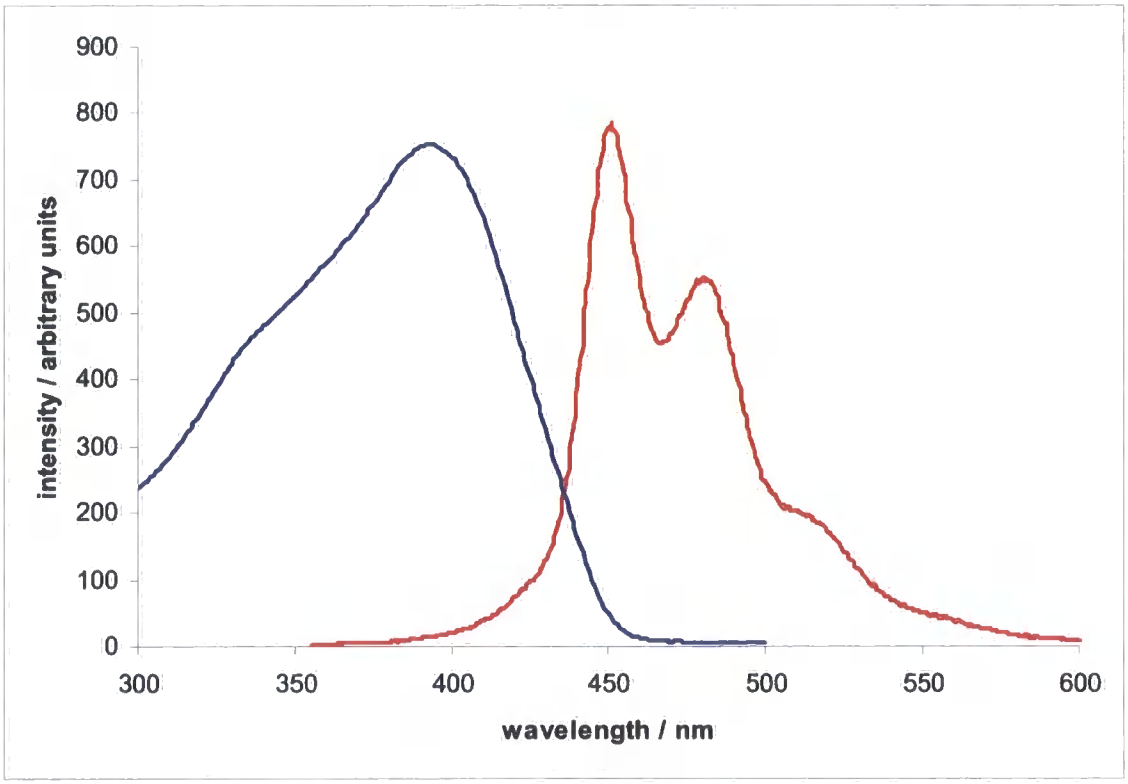

Figure 2.37. Absorption (blue) and fluorescence (red) spectra for 1,4-bis(dimesitylborylvinyl)naphthalene (2e)

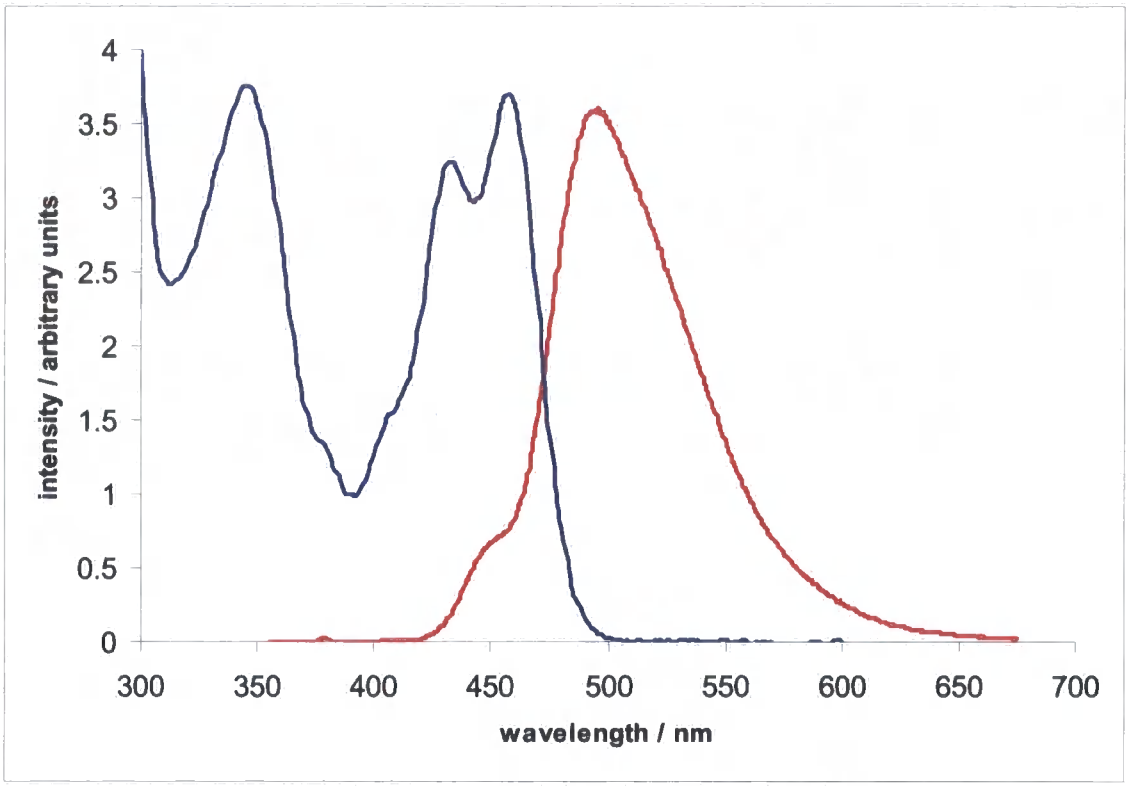

Figure 2.38. Absorption (blue) and fluorescence (red) spectra for 9,10-bis(dimesitylboryl)anthracene (3b).

2.2.5. Electrochemical Properties

The electrochemical behaviour of selected compounds was examined by cyclic voltammetry (CV) in order to determine the reduction potentials and stability of reduced species, properties that are important for electron transport applications. The reduction potentials of compound **3a** have been reported previously, as have those of the related compounds 1,3-bis(dimesitylboryl)benzene (**3d**) and 4,4'-bis(dimesitylboryl)biphenyl (**3e**) , and are reported in Table 2.7, along with that of the monoboryl compound dimesitylborylvinylbenzene (**4a**).

Table 2.7. Reduction potentials of compounds containing the dimesitylboryl group.

Compound	E^{o}_{1} (V)	$E_{½}$ (V)[b]	E^{o}_{2} (V)	$E_{½}$ (V)[b]	ΔE^{o} (V)[a]
2a	-1.53	-1.43[c]	-1.78	-1.69[c]	0.25
2b	-1.74	-1.55			
2c	-1.43	-1.36[c]	-1.56	-1.51[c]	0.13
2h	-1.62	-1.55			
3a		-1.39		-2.08	0.69
3b	-1.65	-1.54	-1.90	-1.77	0.25
3d		-2.02		-2.64	0.62
3e		-1.47		-1.72	0.25
4a	-1.0				

a. Calculated from E^{o} data where available

b. $E_{½}$ measured in THF / $^{t}Bu_4N.ClO_4$

c. Estimated value, given so as to more easily compare compounds to literature values.

E^{o}_{1} is E_{pa}, the voltage at which the cathodic current is greatest in magnitude (current is most negative);

$E_{½}$ is equal to $(E_{pa} + E_{pc})/2$

The monoboryl species **4a** exhibits a single, chemically irreversible, reduction process at –1.0 V. The chemical reversibility was not improved at lower temperatures, or by variation of the working electrode (glassy carbon, **gC** or platinum, **Pt**). In contrast, the bis(boryl) compound **2a** underwent two sequential reductions (E^{o}_{1} = -1.55 V, E^{o}_{2} = -1.75 V) in DCM against a glassy carbon electrode, which became more reversible at lower temperatures. The electrochemical response in THF, including ΔE^{o}, was similar, and reversibility appeared to be improved, but the reductions could not be considered electrochemically reversible since i_{pa} was considerably lower in magnitude than i_{pc}. Repeated attempts to investigate compound **2b** were hindered by its very low solubility in all solvents. It proved impossible to record reproducible cyclic voltammagrams in DCM, whereas a single reduction was observed in THF. Whilst this appeared to be chemically reversible, there was evidence that decomposition was occurring since the apparent concentration vs. ferrocene decreased over time, and several additional reductions were observed in later experiments. For this reason, meaningful discussion of the electrochemical properties of **2b** is not possible. It is worth noting, however, that the fluorine atoms would be expected to remove electron density from the π – system, rendering reduction more facile, but surprisingly this does not appear to be the case. Compound **2c** exhibits two closely spaced sequential reductions, and in this case the reduction waves appear to be fully chemically reversible. The relatively low potential of the second reduction (and correspondingly low value of ΔE^{o}) may indicate that electrons are less delocalised in this compound than in other bis(boryl)s.

It proved impossible to record a CV of **3b** in DCM. On changing to THF, however, two sequential reductions were observed that appear to be chemically reversible at room temperature. It is noticeable that the peak separation is significantly

less than that observed for compound **3a**, which has the same conjugation length between boron atoms. It would appear, therefore, that electron delocalisation is significantly lower in reduced **3b**, but it is unclear what causes this effect.

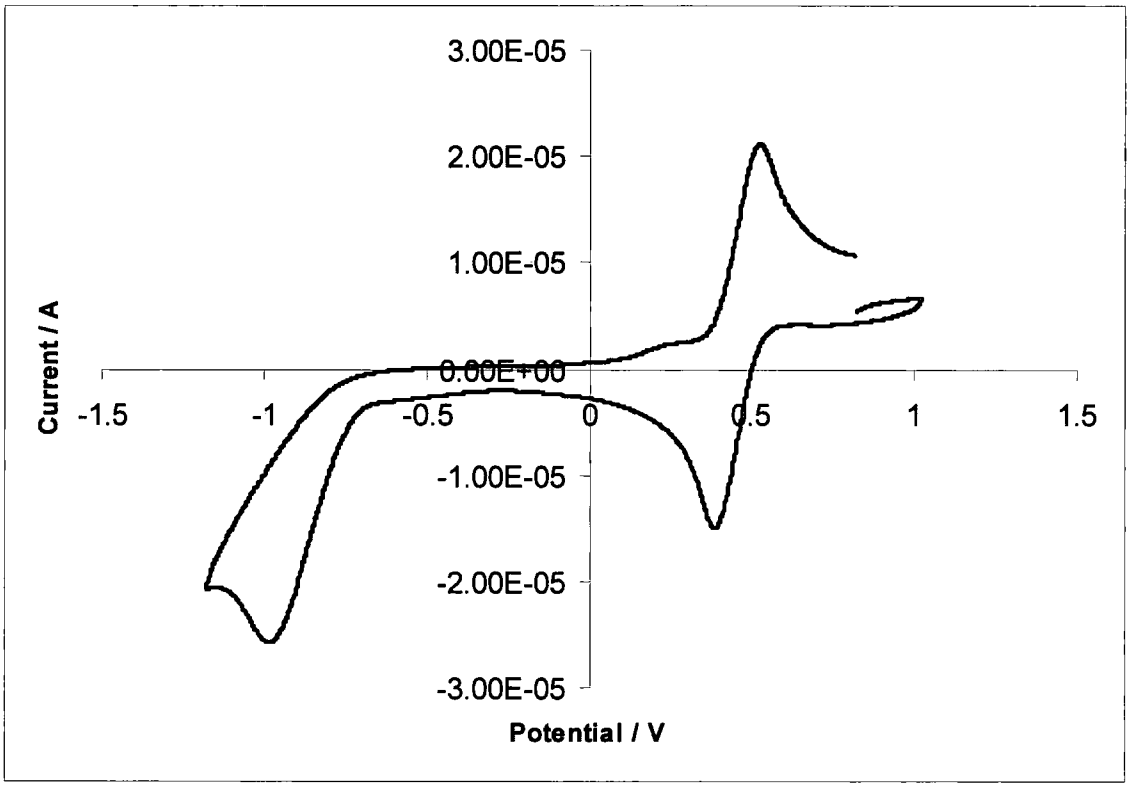

Figure 2.39. Cyclic voltammogram of compound 4a.

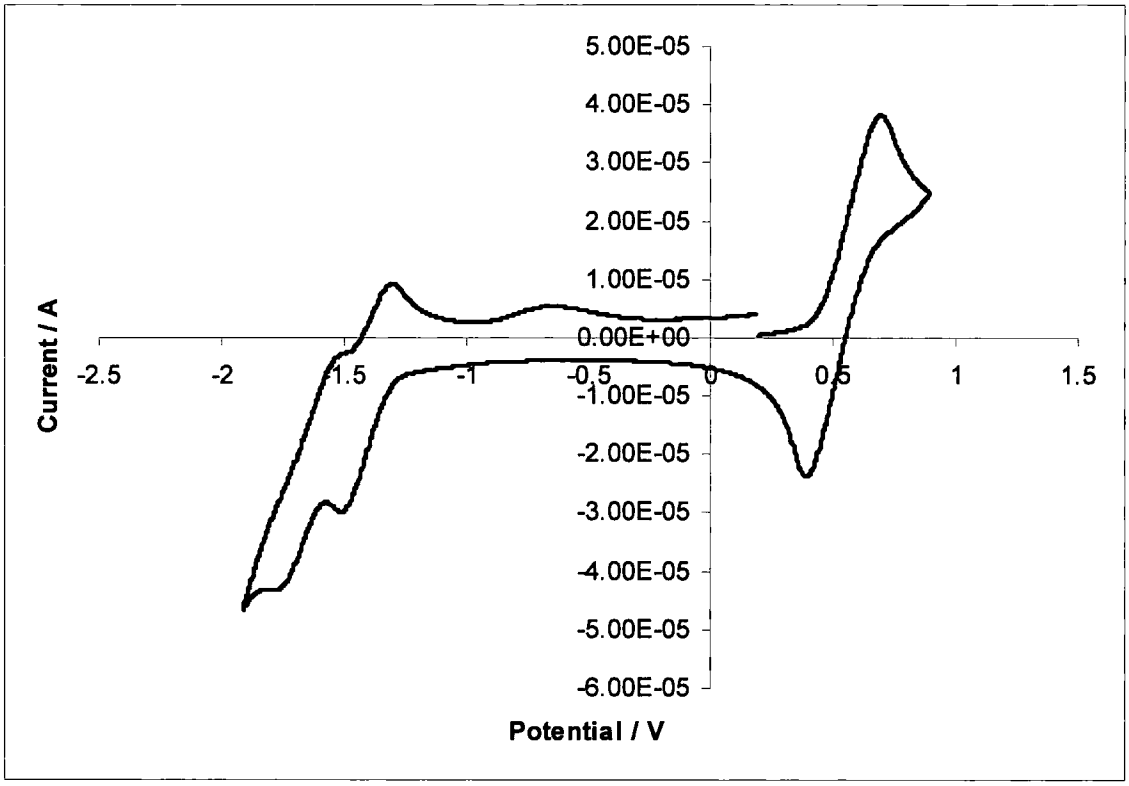

Figure 2.40. Cyclic voltammogram for compound 2a. (THF / 0.1 M $TBABF_4$, 0.2 Vs^{-1})

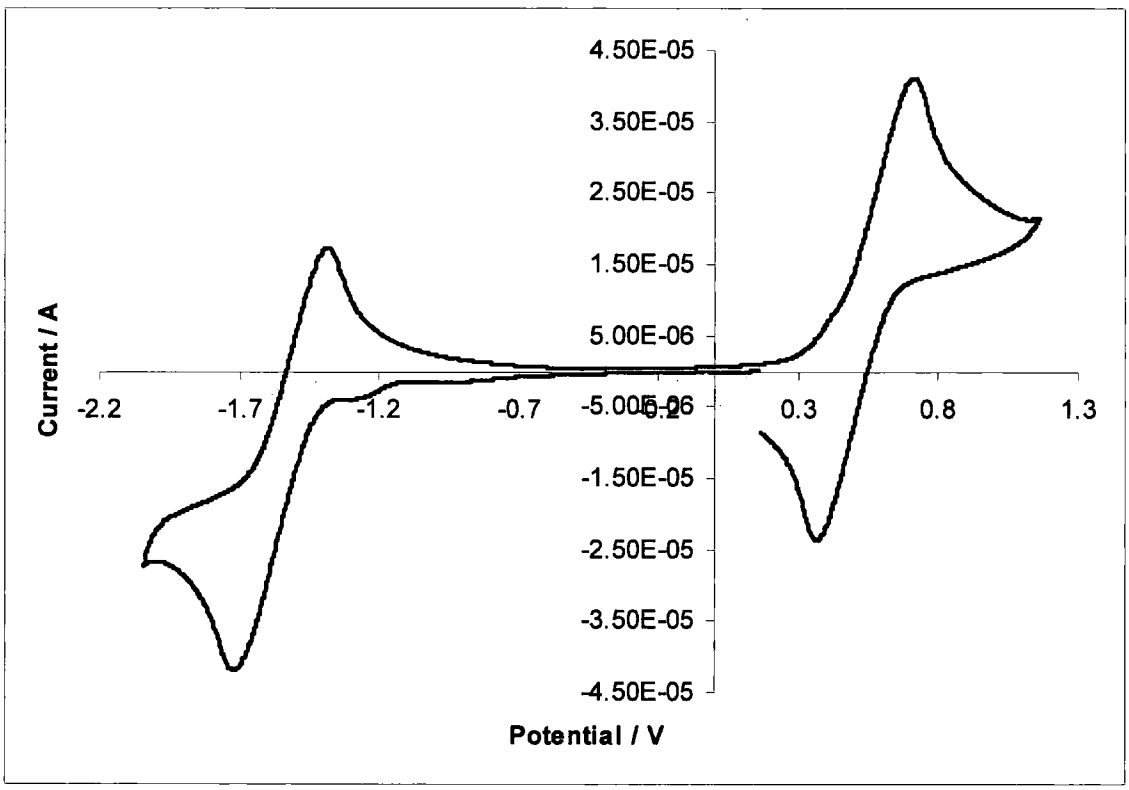

Figure 2.41. Cyclic voltammogram of compound 2b (THF / 0.1 M $TBABF_4$, 0.2 Vs^{-1})

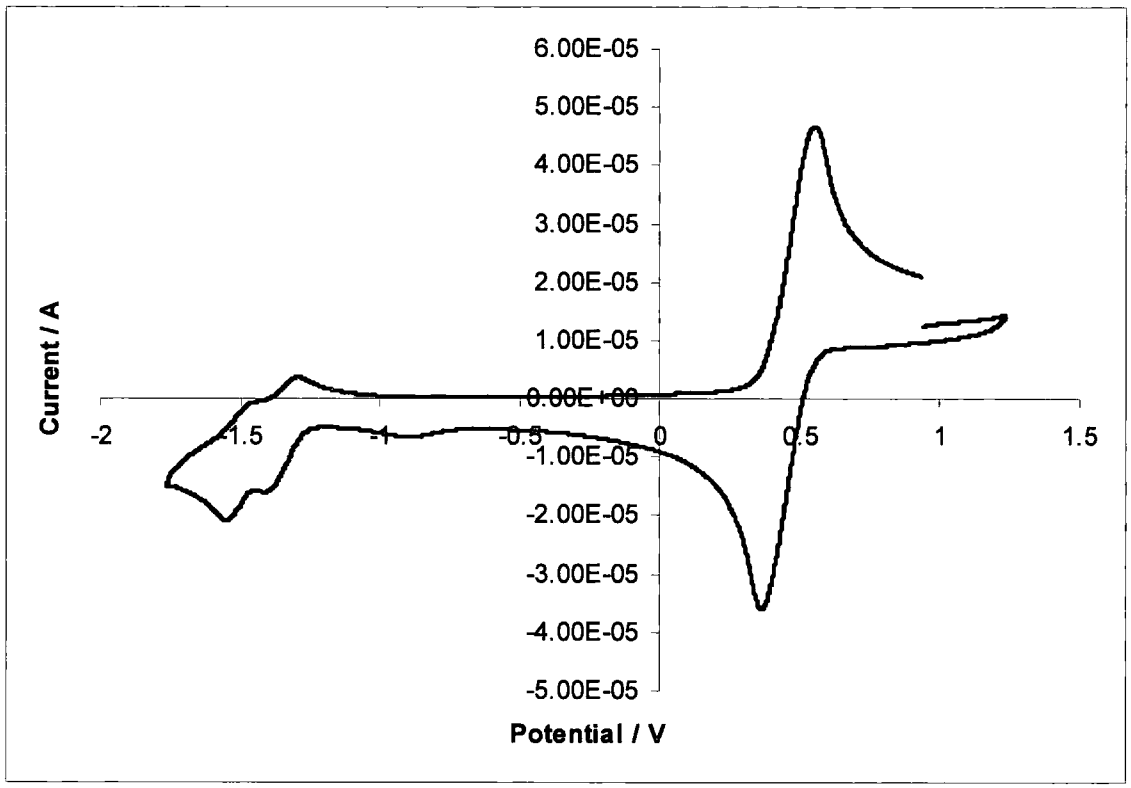

Figure 2.42. Cyclic voltammogram of compound 2c (DCM / 0.1 M $TBABF_4$, 0.2 Vs^{-1})

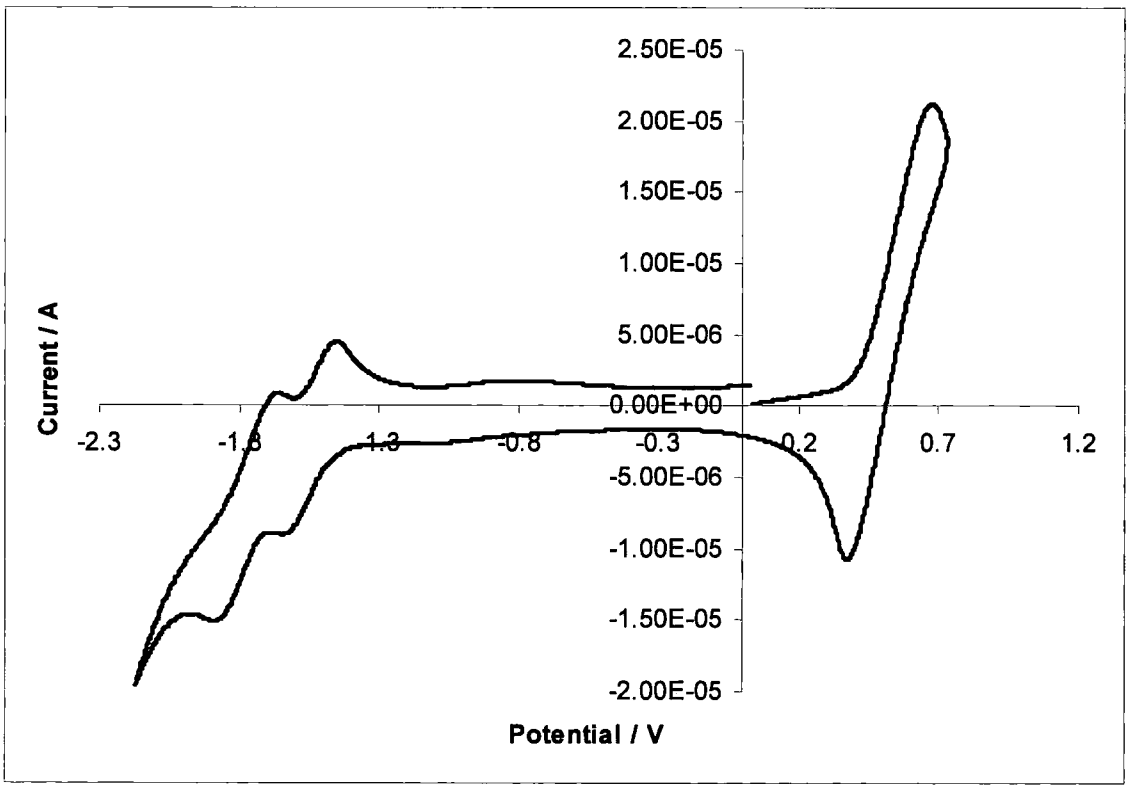

Figure 2.43. Cyclic voltammogram of compound 3b (THF, 0.1M $TBABF_4$, 0.2 Vs^{-1})

Compound **2h** has only a single reduction that appears to be chemically reversible. This may be a two-electron reduction, which would indicate that in the reduced species, the extra electrons reside in localised orbitals (probably the vacant p_z orbitals situated on the boron atoms). Alternatively, the second reduction may occur at lower potential, beyond the experimental limits (ca. –2.5 V). From the Nernst equation, it follows that for a fully reversible reduction, the separation between E_{PA} and E_{PC} should be approximately 59/n mV (where n is the number of electrons involved) so in theory ΔE_P can be used to distinguish between single and multiple electron reductions. In practice, however, it is common for values to deviate significantly from the ideal even for fully reversible processes. The reduction wave for compound **2h** was somewhat broader ($\Delta E_P \approx 130$ mV) than Nernstian, as was that of the internal Fc standard, which is known to be fully electrochemically reversible ($\Delta E_P \approx 150$ mV), so although it seems more likely that it was a two electron reduction, a second one electron reduction beyond experimental limits cannot be ruled out. The increased peak-to-peak separations are likely to be the result of uncompensated solution resistance. The electrochemical reversibility of the reduction was established by the linear relationship between the square root of the scan rate and the peak current, since in a reversible process the peak current (i_p) is proportional to the square root of the scan rate (ν) (Figure 2.45.).

In general, symmetric bis(dimesitylboryl)s exhibit facile reduction due to the influence of the π – electron withdrawing Mes_2B group. The extent of delocalisation in the reduced species and the electrochemical reversibility are highly dependent on the nature of the organic π system, and reduced species appear to be stabilised by coordinating solvents such as THF.

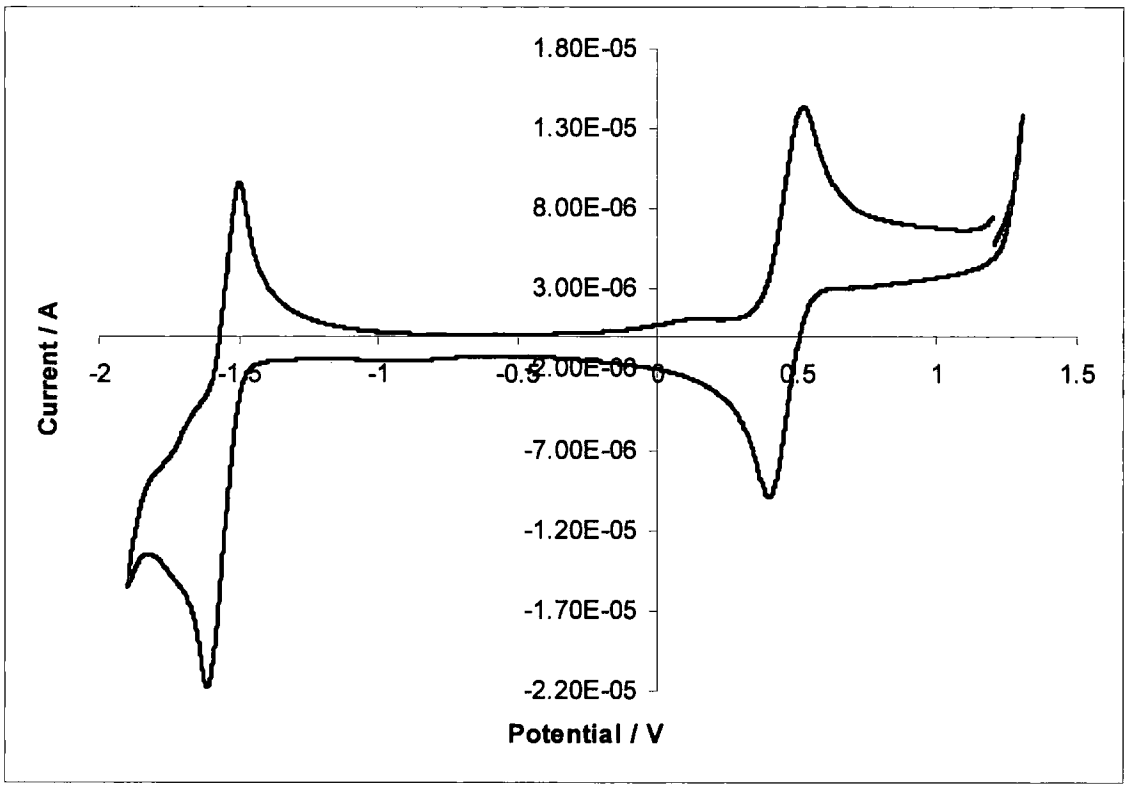

Figure 2.44. Cyclic voltammogram for compound 2h (DCM / 0.1 M $TBABF_4$, 0.2 Vs^{-1})

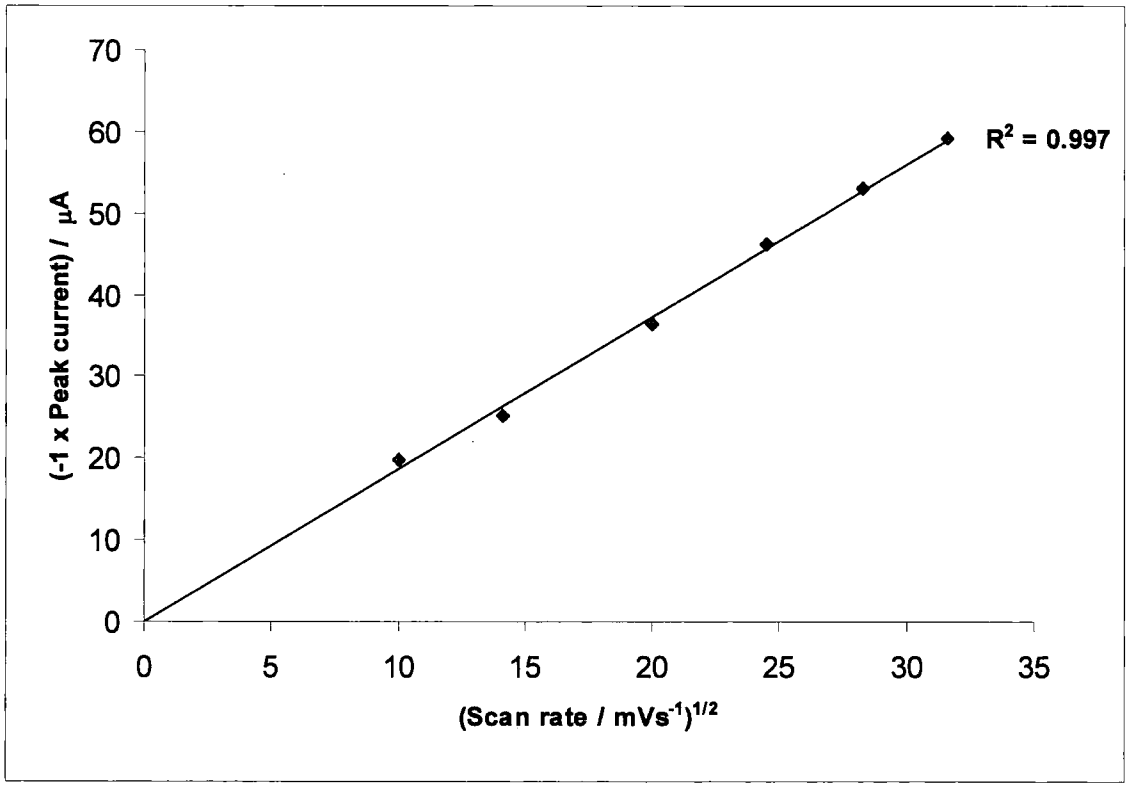

Figure 2.45. Plot of peak current vs. the square root of the scan rate for compound 2h, establishing electrochemical reversibility.

2.3. Conclusions and further work

A series of symmetric bis-boryls of the form Mes_2B-X-$BMes_2$ including a number of new compounds, has been prepared via the hydroboration of bis-terminal acetylenes with dimesitylborane, or via the reaction of dimesitylfluoroborane with aryldilithium reagents. The high yield of most reactions has provided more evidence for the chemoselectivity and regioselectivity of dimesitylborane. Molecular structures of the known compounds **2a** and **2f** and of the new compound **2c** have been determined by single-crystal X-ray diffraction. Optical measurements, including the first determinations of the fluorescence quantum yields of symmetric compounds containing the dimesitylboryl group, have been obtained for all compounds. Both optical and structural data suggest that these molecules contain a highly conjugated π – system that extends to the vacant p_z orbitals on the boron atoms. Electrochemical measurements for selected compounds show that these molecules have low reduction potentials, and suggest that electronic communication is highly dependent upon the nature of the organic π – system. The stability of reduced species was high in most cases, and appeared to be greater in donor solvents such as THF. The thermal stabilities and glass-forming abilities of selected compounds have been investigated by DSC and TGA, revealing that it should be possible to form amorphous films from several of the compounds. The combination of properties (high stability towards air and moisture, blue light emission, low tendency towards crystallisation and favourable reduction potentials) may make them attractive candidates in the rapidly growing field of organic electronics, and in particular for the construction of OLEDs.

In order to assess fully the utility of this class of compound, it will be necessary to construct test devices. A number of important factors may be assessed in this manner. It is essential that amorphous films can be deposited onto appropriate

substrates, and whilst the evidence provided by thermal measurements and by apparent formation of glassy films by solvent evaporation suggests that such materials might be useful, it is not known whether suitable films can be prepared. Since all the compounds investigated appeared to decompose before melting, films would have to be deposited by techniques such as vacuum deposition or spin-coating from solution. The stability of deposited films to repeated heating – cooling cycles would also have to be assessed. Fluorescence quantum yield in solution is a useful guide, but may not be relevant to photoluminescence in the solid state or to electroluminescence.

2.4. Experimental

2.4.1. General Manipulations and Synthetic Techniques

Solvents were distilled under nitrogen from either sodium/benzophenone or calcium hydride. Alkynes were prepared under oxygen-free conditions via standard Schenk techniques. The preparation of dimesitylborane and dimesitylfluoroborane are described in Chapter 5. Hydroborations were carried out in an Innovative Technologies Inc. nitrogen-filled drybox with attached freezer. The compounds 1,4-bis(trimethylsilylethynyl)benzene,[27] 1,4-bis(trimethylsilylethynyl)tetrafluorobenzene,[28,29a] 2,5-bis(trimethylsilyl)thiophene,[29] 4,4'-bis(trimethylsilylethynyl)biphenyl,[30] 4',4''diethynyl-1,4-bis(phenylethynyl)benzene and 4',4''diethynyl-1,4-bis(phenylethynyl)tetrafluorobenzene were prepared previously in the group, and existing samples were used. The compound 4,4'-diethynyl fluorene was prepared according to the literature.[31] The compound 9,10-bis(trimethylsilylethynyl)anthracene[32] was prepared by Miss Judith Magee. The Compound **3b** was prepared by Mr. Zheng Yuan.[33]

NMR experiments were performed on Varian Unity 500, Varian Mercury 200 or Bruker AV 400 instruments. Proton spectra and carbon spectra were referenced to residual protons in the solvent. Boron spectra were referenced to external boron trifluoride diethyletherate. Due to the very broad nature of peaks in the boron spectra of these compounds, it was sometimes impossible to measure a boron spectrum. Purity of acetylenes was assessed by GC-MS.

2.4.2. Preparation of terminal acetylenes

Preparation of 1,4-diethynylbenzene (1a) [27]

In a 100 ml round bottom flask, 1,4-bis(trimethylsilylethynyl)benzene (1.5 g, 5.6 mmol) in methanol (50 ml) and water (2.0 ml) was stirred over Na_2CO_3 (15 g, 140 mmol) for 1h. An aliquot was analysed by GC-MS, and showed that the reaction was complete. The Na_2CO_3 was removed by filtration and a saturated solution of brine (100 ml) was added to the filtrate, which was then extracted with ether (4 x 50 ml). The combined ethereal extracts were dried over $MgSO_4$, filtered through a short pad of silica and the solvent was removed by rotary evaporation to give a white powder, 0.60 g (85 %). A small amount was purified by vacuum sublimation at ambient temperature prior to use.

Preparation of 1,4-diethynyltetrafluorobenzene (1b) [28,29a]

Similar to the preparation of 1,4-diethynylbenzene, 1,4-bis(trimethylsilylethynyl)tetrafluorobenzene (2.0 g, 5.8 mmol) was deprotected by stirring over Na_2CO_3 followed by ether/aqueous phase extraction to give a light brown powder. The powder was dissolved in hexane and passed through a pad of

silica to give a yellow solution. After concentrating and cooling in the freezer overnight, analytically pure (by GC-MS) 1,4-diethynyltetrafluorobenzene was obtained as colourless crystals, 0.74 g (64 %).

Preparation of 2,5-diethynylthiophene (1c) [29]

In contrast to most trimethylsilyl-protected alkynes, stirring over Na_2CO_3 proved to be ineffective in providing the terminal alkyne, so an alternative procedure was used. To a stirred solution of 2,5-bis(trimethylsilylethynyl)thiophene (1.0 g, 3.6 mmol) in methanol (50 ml) was added KOH (0.08 g, 1.4 mmol) in water (2.0 ml), resulting in an immediate brown colouration. After 5 minutes, TLC showed no sign of starting materials. The solution was diluted with ether (100 ml) and water (100 ml) and the ethereal layer collected. The aqueous layer was extracted with ether (3 x 50 ml) and the combined ethereal extracts washed with 0.1 M HCl (aq) and dried over $MgSO_4$. The solution was concentrated to give a brown oil. The oil was dissolved in ethanol (20 ml) and $AgNO_3$ (2.0 g, 11.7 mmol (excess)) in water (2 ml) added, resulting in the formation of a bright yellow precipitate. The solvent was removed by decantation and the precipitate washed with ethanol (2 x 10 ml) and ether (3 x 10 ml) followed by decantation. At no stage was the solvent completely removed from the precipitate. The precipitate was suspended in ether (50 ml) and HCl (aq) added until all precipitate had disappeared, resulting in a pale yellow solution. Water (10 ml) was added, and the ethereal layer was collected, washed with water (3 x 50 ml), and dried over $MgSO_4$ overnight. The solution was concentrated to give a colourless oil. ^1H-

NMR showed that the oil contained an approximately 1:1 molar ratio of diethynylthiophene and ether, from which it was calculated a yield of 0.25 g (52 %).

Preparation of 9,10-diethynylanthracene (1d) [34]

Similar to the preparation of **1a**, 9,10-bis(trimethylsilylethynyl)anthracene (2.5 g, 6.8 mmol) was deprotected by stirring over Na_2CO_3 followed by ether/aqueous phase extraction to give a yellow solution. The solution was dried over $MgSO_4$ and concentrated to give a yellow powder, which rapidly turned orange / red on standing, 0.70 g (45 %, crude yield). Recrystallisation from hexane immediately before use gave yellow needles of 9,10-diethynylanthracene, 0.32 g (21 %).

Preparation of 1,4-diethynylnaphthalene (1e) [35]

To a stirred solution of 1,4-dibromonaphthalene (3.06 g, 10.7 mmol) in triethylamine (150 ml) was added a solution of $Pd(NCC_6H_5)_2Cl_2$ (0.04 g) and $^tBu_3P$ (0.03 g) in toluene (10 ml). After 0.5 h, TMSA (2.5 g, 26 mmol) was added via syringe, and the mixture was stirred overnight at 40 °C. The triethylamine was removed by rotary evaporation and the solid extracted with ether (3 x 70 ml). The ethereal extracts were passed through a short pad of silica gel, concentrated and refrigerated overnight, after which bis(trimethylsilylethynyl)naphthalene (yellow powder) was isolated by filtration in 80 % yield (2.74 g).

A solution of bis(trimethylsilylethynyl)naphthalene (1.15 g, 3.6 mmol) in methanol (50 ml) and DCM (5 ml) was stirred over Na_2CO_3 for 2 h. After ether / aqueous phase extraction, the ethereal extracts were dried over $MgSO_4$ and concentrated to a yellow oil, which crystallised on standing. The colour of the crystals visibly darkened over several minutes. Yield 0.55g (87%).

Preparation of 4,4'-diethynylbiphenyl (1f) [30]

Similar to the preparation of **1a**, 4,4'-bis(trimethylsilylethynyl)biphenyl (1.0 g) was deprotected by stirring over Na_2CO_3 followed by ether/aqueous phase extraction to give an off-white powder. Recrystallisation from hexane gave pure 4,4'-diethynylbiphenyl as colourless crystals, 0.45 g (78 %).

Preparation of *trans*-4,4'diethynylstilbene (1h)

To a 44 % solution of aqueous tetrafluoroboric acid (30 ml, 196 mmol) was added 4-bromoaniline (13.7 g, 80 mmol). The mixture was cooled to 0 °C and a solution of $NaNO_2$ (5.7 g, 82 mmol) in water (30 ml) was added dropwise. The mixture was stirred for 1 h, after which GCMS revealed complete consumption of bromoaniline. The resulting white precipitate was filtered off and dried at the pump, dissolved in minimum volume of acetone and reprecipitated with ether. The preciptate was filtered and washed with ether (2 x 30 ml) and hexane (30 ml) before being suspended in methanol. A reflux condenser was fitted to the flask, and to the suspension was added $Pd(OAc)_2$ (350 mg) and vinyltriethoxysilane (7.6 g, 40 mmol). The reaction was exothermic, heating to reflux without applied heat. After stirring overnight, the mixture was concentrated by rotary evaporation and the product purified by passing through a short pad of silica gel (eluted with hexane / DCM 10:1), to give analytically pure (GC-MS) *trans*-4,4'-dibromostilbene [23] in 40 % yield (5.4 g)

To a solution of *trans*-4,4'-dibromostilbene (1.04 g, 0.07 mmol) in triethylamine (100 ml) was added $(Ph_3P)_2PdCl_2$ (2 mol %) and CuI (2 mol %). The

mixture was stirred under nitrogen for 0.5 h, and trimethylsilylacetylene (1.0 g, 10.2 mmol) was added via syringe. The mixture was stirred overnight and then heated to reflux for 1 h. Triethylamine was removed by rotary evaporation and the resulting solid was extracted with toluene. The toluene extracts were concentrated to dryness and *trans*-4,4'-bis(trimethylsilylethynyl)stilbene was recrystallised from hexane / acetone as a yellow powder in 62 % yield (0.70 g).

A solution of *trans*-4,4'-bis(trimethylsilylethynyl)stilbene (0.5 g, 1.3 mmol) in methanol (50 ml) and water (0.5 ml) was stirred over Na_2CO_3 for 1 h. The mixture was filtered, and the filtrate extracted with ether. The ethereal extracts were dried over $MgSO_4$ and concentrated to a yellow powder, analytically pure **1h** in 95 % yield (0.29 g).

^{1}H NMR (200 MHz, CD_2Cl_2) δ: 7.48 (8H, stilbendiyl, singlet by coincidence), 7.14 (s, 2H, vinyl), 3.21 (s, 2H, alkynyl).

Preparation of 4,4'-diethynyltolan (1i) [24]

To a solution of *p*-bromoiodobenzene (2.5 g, 8.8 mmol) in triethylamine (250 ml) was added $(Ph_3P)_2PdCl_2$ (15 g) and CuI (40 mg). After stirring for 15 m, $HC{\equiv}C(CH_3)_2OH$ (0.8 g, 9.5 mmol) was added via syringe and the mixture was refluxed overnight. Triethylamine was removed by rotary evaporation and the resulting brown oil was adsorbed onto silica gel and extracted with toluene. The toluene solution was concentrated to dryness and 4-(4-bromophenyl)-2-methyl-but-3-yn-2-ol [36] was isolated by vacuum sublimation in 71 % yield (1.5 g).

To a solution of 4-(4-bromophenyl)-2-methylbut-3-yn-2-ol (1.0 g, 4.2 mmol) in triethylamine (150 ml) was added a solution of $(Ph_3P)_2PdCl_2$ (10 mg) and CuI (30 mg) in toluene (10 ml). After 15 m, a solution of 1,4-diethnylbenzene (**1a**) (1.0 g, 7.9

mmol) in triethylamine (20 ml) was added via syringe. After overnight stirring, the mixture was concentrated to dryness and extracted with hot toluene.

To the toluene solution was added KO^{t}Bu (0.5 g). The mixture was heated for 2 h, washed with water and the organic phase separated and dried over $MgSO_4$. Toluene was removed by rotary evaporation and the solid recrystallised from hexane / DCM to give analytically pure **1i** in 83 % yield (0.79 g).

2.4.3. Preparation of Bis(dimesitylborylvinyl)organoboranes

Preparation of 1,4-bis(dimesitylborylvinyl)benzene (2a)

To a solution of 1,4-diethynylbenzene (0.12 g, 0.95 mmol) in THF (15 ml) was added a solution of dimesitylborane (0.50 g, 2.0 mmol) in THF (25 ml) (dropwise with rapid stirring, at room temperature). The colourless mixture was stirred for 2 h, during which time a pale yellow colour evolved. GC-MS revealed no sign of either diethynylbenzene or dimesitylborane. Solvent was removed *in vacuo* and residual THF was removed by stirring in ether followed by removal of solvent *in vacuo* (3 times), resulting in a pale yellow powder. After checking for purity by ^{1}H-NMR, the powder was recrystallised from DCM/hexane as the 1:1 DCM solvate in 75% yield (0.51 g). Crystals suitable for single-crystal XRD were grown by cooling a toluene solution. Large, high quality crystals were also obtained from a hexane solution containing **2a** and *p*-N,N-dimethylaminobenzene.

^{1}H NMR (200 MHz, C_6D_6) δ: 7.53 (d, 2H, $^3J_{H\text{-}H}$ 17.5 Hz, CH vinyl), 7.34 (d, 2H, $^3J_{H\text{-}H}$ 17.9 Hz, CH vinyl), 7.18 (s, 4H, C_6H_4), 6.85 (s, 8H, Mes), 2.35 (s, 24 H, *o*-CH_3), 2.20 (s, 12 H, *p*-CH_3). ^{13}C{^{1}H} NMR (50 Hz, C_6D_6) δ: 142.1, 140.7, 138.7,, 128.7, 23.5, 21.1 (Mes), 152.4 (CH vinyl), 138.2 (B-CH vinyl), 136.0 (B-C_6H_4), 128.8 (C_6H_4). ^{11}B

NMR (96 MHz, $CDCl_3$) 40. *m/z*: 626 (M^+), 506 (- mesitylene) 275, 164. Calculated for $C_{46}H_{52}B_2 \cdot CH_2Cl_2$: C, 79.40; H, 7.65. Found: C, 79.89; H, 7.55%.

Preparation of bis(dimesitylborylvinyl)tetrafluorobenzene (2b)

The electronegativity of the attached fluorine atoms results in a low reactivity of diethynyltetrafluorobenzene towards hydroboration. For this reason, an extended reaction time was required for complete conversion. Similarly to the preparation of bis(dimesitylborylvinyl)benzene, a solution of 1,4-diethynyltetrafluorobenzene (0.18 g, 0.91 mmol) in THF (15 ml) was reacted with a solution of dimesitylborane (0.5 g, 2.0 mmol) in THF (25 ml) for 3 d. The yellow powder was recrystallised from DCM in 87 % yield (0.55 g).

^1H NMR (200 MHz, $CDCl_3$) δ: 7.78 (d, 2H, $^3J_{H-H}$ 18.7 Hz, CH vinyl), 7.08 (d, 2H, $^3J_{H-H}$ 18.7 Hz, CH vinyl), 6.83 (s, 8H, Mes), 2.30 (s, 12 H, *p*-CH_3), 2.18 (s, 24 H, *o*-CH_3). ^{19}F NMR (188 MHz, $CDCl_3$) –144.3. *m/z*: 698 (M^+), 578 (- mesitylene) 448. Calculated for $C_{46}H_{48}B_2F_4$: C, 79.10; H, 6.93. Found: C, 79.25; H, 7.02%.

Preparation of 2,5-bis(dimesitylborylvinyl)thiophene (2c)

Similarly to the preparation of **2a**, a solution of 2,5-diethynylthiophene (0.25 g, 1.9 mmol) in THF (10 ml) and ether (5 ml) was reacted with a solution of dimesitylborane (1.0 g, 4.0 mmol) in THF (25 ml). Over 12 h, the solution evolved an intense yellow colour. After removal of THF, the resulting orange oil was mixed with ether (10 ml) and hexane (20 ml) to precipitate the product as a bright yellow powder in 35 % yield (0.44 g). Crystals suitable for single crystal XRD were grown by refrigeration of DCM/hexane solution.

^{1}H NMR (500 MHz, C_6D_6) δ: 7.29 (d, 2H, $^3J_{H-H}$ 17.4 Hz, CH vinyl), 7.28 (d, 2H, $^3J_{H-H}$ 17.4 Hz, CH vinyl), 6.80 (s, 8H, Mes), 6.26 (s, 2H, C_4H_2S), 2.29 (s, 24 H, *o*-CH_3), 2.18 (s, 12 H, *p*-CH_3). $^{13}C\{^1H\}$ NMR (50 Hz, C_6D_6) δ: 142.4, 140.7, 138.6, 128.7, 23.4, 21.1 (Mes), 146.7 (CH vinyl), 139.4 (B-CH vinyl), 144.3 (B-C_4H_2S), 131.2 (C_4H_2S). ^{11}B NMR (96 MHz, $CDCl_3$) 55. *m/z*: 632 (M^+), 512 (- mesitylene). Calculated for $C_{44}H_{50}B_2S$: C, 83.55; H, 7.97. Found: C, 83.45; H, 8.04%.

Preparation of bis(dimesitylborylvinyl)anthracene (2d)

Similarly to the preparation of bis(dimesitylborylvinyl)benzene, a solution of freshly recrystallised diethynylanthracene (0.226 g, 1.0 mmol) in THF (25 ml) was reacted with a solution of dimesitylborane (0.5 g, 2.0 mmol) in THF (25 ml) for 3 d. Removal of solvent and washing with hexane (4 x 15 ml) gave a red/orange powder, which contained various unidentified impurities (by ^{1}H-NMR). Column chromatography (silica, eluted with 20:1 hexane-acetone) and removal of solvent resulted in an orange powder. It proved impossible to recrystallise this powder in reasonable yield.

^{1}H NMR (400 MHz, C_6D_6) δ: 8.16 (m, 4H, anth), 8.05(d, 2H, $^3J_{H-H}$ 18.1 Hz, CH vinyl), 7.30 (d, 2H, $^3J_{H-H}$ 18.1 Hz, CH vinyl), 7.36 (m, 4H, anth), 6.79 (s, 8H, Mes), 2.27 (s, 24 H, *o*-CH_3), 2.23 (s, 12 H, *p*-CH_3). $^{13}C\{^1H\}$ NMR (100 MHz, $CDCl_3$) δ: 140.9, 138.9, 134.0, 127.8, 22.4, 21.0 (Mes), 149.4 (CH vinyl), 138.8 (B-CH vinyl), 134.3, 127.3, 127.2, 119.3 (anth). *m/z*: 726 (M^+), 606 (- mesitylene). Calculated for $C_{54}H_{56}B_2$: C, 89.26; H, 7.77. Found: C, 90.01; H, 8.24%.

Preparation of 1,4-bis(dimesitylborylvinyl)naphthalene (2e)

To a solution of freshly prepared **1e** (0.10 g, 0.57 mmol) in THF (20 ml) was added solid dimesitylborane (0.265 g, 0.57 mmol). The solution was stirred for 2 d before being concentrated to dryness and washed with hexane (3 x 10 ml). The resulting yellow powder was recrystallised from ether in 64 % yield (0.25 g).

^{1}H NMR (500 MHz, C_6D_6) δ: 8.26 (d, 2H, $^3J_{H-H}$ 17.3 Hz, CH vinyl), 8.01 (broad, 2H, naphth), 7.77, (s, 2H naphth) 7.64 (d, 2H, $^3J_{H-H}$ 17.3 Hz, CH vinyl), 6.94 (broad, 2H, naphth), 6.83 (s, 8H, Mes), 2.36 (s, 24 H, *o*-CH_3), 2.16 (s, 12 H, *p*-CH_3). $^{13}C\{^1H\}$ NMR (100 MHz, C_6D_6) δ: 140.7, 128.3, 128.0, 127.5, 23.5, 21.3 (Mes), 148.8 (CH vinyl), 138.6 (B-CH vinyl), 127.0, 126.5, 125.7, 124.5, 123.9 (naphth). ^{11}B NMR (96 MHz, C_6D_6) 70. *m/z*: 676 (M^+), 556 (- mesitylene). Calculated for $C_{50}H_{54}B_2$: C, 88.76; H, 8.04. Found: C, 88.84; H, 8.10%.

Preparation of 4,4'-bis(dimesitylborylvinyl)biphenyl (2f)

Similarly to the preparation of bis(dimesitylborylvinyl)benzene, a solution of 4,4'-diethynylbiphenyl (0.19 g, 0.94 mmol) in THF (15 ml) was reacted with a solution of dimesitylborane (0.50 g, 2.0 mmol) in THF (25 ml). The pale yellow powder was recrystallised from DCM/hexane in 90% yield (0.62 g). Crystals suitable for single-crystal XRD were obtained by cooling a toluene solution.

^{1}H NMR (200 MHz, $CDCL_3$) δ: 7.63 (8H, singlet by coincidence), 7.51 (d, 2H, $^3J_{H-H}$ 17.9 Hz, CH vinyl), 7.23 (d, 2H, $^3J_{H-H}$ 17.9 Hz, CH vinyl), 6.86 (s, 8H, Mes), 2.33 (s, 12 H, *p*-CH_3), 2.25 (s, 24 H, *o*-CH_3). $^{13}C\{^1H\}$ NMR (50 Hz, C_6D_6) δ: 142.0, 140.6, 138.4, 128.3, 23.3, 21.1 (Mes), 151.4 (CH vinyl), 138.2 (B-CH vinyl), 141.4, 137.0, 128.8, 128.5 (biphenyl). ^{11}B NMR (96 MHz, $CDCl_3$) 46. *m/z*: 702 (M^+), 582 (-

mesitylene) 386. Calculated for $C_{52}H_{56}B_2$: C, 88.89; H, 8.03. Found: C, 88.95; H, 8.00%.

Preparation of 4,4'-bis(dimesitylborylvinyl)fluorene (2g)

Similarly to the preparation of bis(dimesitylborylvinyl)benzene, a solution of 4,4'-diethynylfluorene (0.20 g, 0.94 mmol) in THF (15 ml) was reacted with a solution of dimesitylborane (0.50 g, 2.0 mmol) in THF (25 ml). The pale yellow powder was recrystallised from ether in 86% yield (0.6 g).

^{1}H NMR (200 MHz, C_6D_6) δ: 7.31 (d, 2H, $^3J_{H-H}$ 17.6 Hz, CH vinyl), 7.20 (d, 2H, $^3J_{H-H}$ 17.6 Hz, CH vinyl), 7.01 (s, 2H, fluorenediyl), 6.86 (4H, singlet by coincidence), 6.59 (s, 8H, Mes), 3.08 (s, 2H, CH_2), 2.09 (s, 24 H, *o*-CH_3), 2.25 (s, 12 H, *p*-CH_3). $^{13}C\{^1H\}$ NMR (50 Hz, C_6D_6) δ: 143.0, 140.7, 138.6, 128.2, 23.6, 21.2 (Mes), 153.3 (CH vinyl), 137.5 (B-CH vinyl), 144.6, 140.3,128.7, 128.0, 127.8, 124.9, 31.8 (fluorenediyl). *m/z*: 714 (M^+), 594 (- mesitylene) 468, 248. Calculated for $C_{53}H_{56}B_2$: C, 89.08; H, 7.90. Found: C, 89.01; H, 8.02%.

Preparation of all *trans*-4,4'-bis(dimesitylborylvinyl)stilbene (2h)

Similarly to the preparation of bis(dimesitylborylvinyl)benzene, a solution of *trans*-4,4'-diethynylstilbene (0.23 g, 1.0 mmol) in THF (25 ml) was reacted with a solution of dimesitylborane (0.50 g, 2.0 mmol) in THF (25 ml). The bright yellow powder was recrystallised from DCM/hexane in 82% yield (0.60 g).

^{1}H NMR (200 MHz, CD_2Cl_2) δ: 7.46 (8H, stilbenediyl, singlet by coincidence), 7.33 (d, 2H, $^3J_{H-H}$ 17.6 Hz, CH vinyl), 7.09 (s, 2H, vinyl) 7.04 (d, 2H, $^3J_{H-H}$ 17.6 Hz, CH vinyl), 6.75 (s, 8H, Mes), 2.21 (s, 12 H, *p*-CH_3), 2.10 (s, 24 H, *o*-CH_3). $^{13}C\{^1H\}$ NMR (50 Hz, CD_2Cl_2) δ: 141.4, 137.6, 136.8, 128.0, 22.2, 20.1 (Mes), 151.1 (CH vinyl), 136.5 (B-CH vinyl), 126.1 (stilbenediyl vinyl) 141.4, 138.4, 138.2,137.7,127.8, 127.3

(stilbenediyl). *m/z*: 728 (M^+), 608 (- mesitylene) 480, 248. Calculated for $C_{54}H_{58}B_2$: C, 89.01; H, 8.02. Found: C, 88.94; H, 7.99%.

Preparation of 4,4'-bis(dimesitylborylvinyl)diphenylacetylene (2i)

Similarly to the preparation of bis(dimesitylborylvinyl)benzene, a solution of 4,4'-diethynyltolan (0.23 g, 1.0 mmol) in THF (20 ml) was reacted with a solution of dimesitylborane (0.5 g, 2.0 mmol). The bright yellow powder was recrystallised from DCM / hexane in 75% yield (0.55 g).

^{1}H NMR (400 MHz, $CDCL_3$) δ: 7.44 (8H, tolan, singlet by coincidence), 7.36 (d, 2H, $^3J_{H-H}$ 18.2 Hz, CH vinyl), 7.06 (d, 2H, $^3J_{H-H}$ 18.2 Hz, CH vinyl), 6.76 (s, 8H, Mes), 2.25 (s, 12 H, *p*-CH_3), 2.13 (s, 24 H, *o*-CH_3). $^{13}C\{^1H\}$ NMR (50 Hz, $CDCl_3$) δ: 143.3, 140.0, 138.7, 128.9, 23.3, 21.0 (Mes), 152.1 (CH vinyl), 137.7 (B-CH vinyl), 140.63, 138.6, 131.9, 128.3, 128.0(tolan). *m/z*: 726 (M^+), 606 (- mesitylene), 248. Calculated for $C_{54}H_{56}B_2$: C, 89.26; H, 7.77. Found: C, 89.54; H, 7.95%.

Preparation of 1,4-bis(dimesitylborylvinylphenylethynyl)benzene (2j)

Similarly to the preparation of bis(dimesitylborylvinyl)benzene, a solution of diethynylbis(phenylethynyl)benzene (0.16 g, 0.5 mmol) in THF (15 ml) was reacted with a solution of dimesitylborane (0.25 g, 1.0 mmol) in THF (25 ml). The yellow powder was passed through a pad of silica (initially eluting with hexane, then with DCM) to remove impurities, and recrystallised from DCM in 84 % yield (0.34 g).

^{1}H NMR (400 MHz, CD_2Cl_2) δ: 7.45 (8H, C_6H_4, singlet by coincidence), 7.44 (4H, C_6H_4, singlet by coincidence), 7.37 (d, 2H, $^3J_{H-H}$ 17.6 Hz, CH vinyl), 7.04 (d, 2H, $^3J_{H-H}$ 17.6 Hz, CH vinyl), 6.75 (s, 8H, Mes), 2.21 (s, 12 H, *p*-CH_3), 2.10 (s, 24 H, *o*-CH_3). $^{13}C\{^1H\}$ NMR (50 Hz, $CDCl_3$) δ: 140.6, 139.8, 138.4, 128.6, 23.3, 21.2 (Mes), 151.3 (CH vinyl), 138.6 (B-CH vinyl), 138.6, 131.9, 131.7, 128.3, 128.0, 125.6, 124.2,

123.0 (backbone). *m/z*: 826 (M^+), 606 (- mesitylene), 248. Calculated for $C_{62}H_{60}B_2$: C, 90.07; H, 7.31. Found: C, 89.86; H, 7.54%.

Preparation of 1,4-bis(dimesitylborylvinylphenylethynyl)tetrafluorobenzene (2k)

Similarly to the preparation of bis(dimesitylborylvinyl)benzene, a solution of diethynylbis(phenylethynyl)tetrafluorobenzene (0.10 g, 0.5 mmol) in THF (15 ml) was reacted with a solution of dimesitylborane (0.25 g, 1.0 mmol) in THF (25 ml). After removal of solvent and washing with ether, the yellow powder was passed through a pad of silica (initially eluting with hexane, then with DCM) to remove impurities, and recrystallised from DCM in 84 % yield (0.34 g).

^{1}H NMR (400 MHz, CD_2Cl_2) δ: 7.50 (8H, C_6H_4, singlet by coincidence), 7.41 (d, 2H, $^3J_{H\text{-}H}$ 17.7 Hz, CH vinyl), 7.06 (d, 2H, $^3J_{H\text{-}H}$ 17.7 Hz, CH vinyl), 6.77 (s, 8H, Mes), 2.23 (s, 12 H, *p*-CH_3), 2.11 (s, 24 H, *o*-CH_3). $^{13}C\{^1H\}$ NMR (50 Hz, $CDCl_3$) δ: 144.3, 141.2, 138.4, 128.7, 23.3, 21.5 (Mes), 149.0 (CH vinyl), 137.7 (B-CH vinyl), 139.6, 138.0, 131.2, 127.8, 127.0, 126.8, 126.0, 124.2 (backbone).^{19}F NMR(188 MHz, CD_2Cl_2) 137.9. *m/z*: 898 (M^+), 778 (- mesitylene), 248. Calculated for $C_{62}H_{56}B_2F_4$: C, 82.86; H, 6.28. Found: C, 83.04; H, 6.59%.

Preparation of 1,4-bis(dimesitylboryl)benzene (3a)

To a solution of 1,4-dibromobenzene (0.24 g, 1.0 mmol) in toluene (30 ml) was added ^{n}butyl lithium (2.0 ml of a 1.6 M solution in hexanes, 3.2 mmol). After stirring overnight, the initially colourless solution had become pale yellow, with a large amount of white precipitate. To the suspension was added dimesitylfluoroborane (0.84 g, 3.1 mmol), resulting in the initial disappearance of precipitate. After 4 h, the suspension was passed through a short pad of Celite and concentrated to dryness,

giving a pale yellow powder. The powder was washed with hexane (3 x 10 ml), dissolved in DCM and passed through a short pad of silica. The solution was concentrated to dryness and recrystallised from ether to give a white powder in 78 % yield (0.45 g).

^{1}H NMR (400 MHz, $CDCl_3$) δ: 7.43 (s, 4H, C_6H_4), 6.80 (s, 8H, Mes), 2.30 (s, 12 H, *p*-CH_3), 1.99 (s, 24 H, *o*-CH_3). $^{13}C\{^1H\}$ NMR (100 MHz, $CDCl_3$) 142.0, 140.8, 138.8, 128.2, 23.4, 21.2 (Mes) 148.0 (C-B) 128.1 (C_6H_4). *m/z*: 574 (M^+), 454 (- mesitylene), 248. Calculated for $C_{42}H_{48}B_2$: C, 87.81; H, 8.42. Found: C, 88.01; H, 8.54%.

Preparation of 2,5-bis(dimesitylboryl)thiophene (3c)

Similar to the preparation of **3a**, to a solution of 2,5-dibromothiophene (24 g, 1.0 mmol) in toluene (30 ml) was added three molar equivalents of a solution of ^{n}Buli in hexanes, resulting in the immediate formation of a dense white precipitate. After 0.5 h, dimesitylfluoroborane (0.84 g, 3.1 mmol) was added, resulting in the evolution of a slight yellow colour. After stirring overnight, the solution was filtered and concentrated to a yellow powder. The powder was dissolved in ether and passed through a pad of silica to remove traces of LiF, and the silca was extracted with DCM. The combined extracts were concentrated to dryness and **3a** was recrystallised from ether in 55 % yield (0.32 g).

^{1}H NMR (400 MHz, $CDCl_3$) δ: 7.32 (s, 2H, C_4H_2S), 6.66 (s, 8H, Mes), 2.13 (s, 12 H, *p*-CH_3), 1.95 (s, 24 H, *o*-CH_3). $^{13}C\{^1H\}$ NMR (100 MHz, $CDCl_3$) 140.4, 139.8, 139.2, 127.2, 23.0, 20.7 (Mes) 160.8 (C-B) 141.0 (C_4H_2S). *m/z*: 580 (M^+), 460 (- mesitylene). Calculated for $C_{40}H_{46}B_2S$: C, 82.76; H, 7.99. Found: C, 82.56; H, 8.20%.

2.5 References

[1] Glogowski, M. E.; Williams, J. L. R. *J. Organomet. Chem.* **1981**, *218*, 137 – 146.

[2] For reviews of boron-containing materials for molecular electronic applications, see (a) Entwistle, C.D; Marder, T.B. *Chem. Mater.* **2004**, *16*, 4574 – 4585. (b) Entwistle, C.D.; Marder, T.B. *Angew. Chem. Int. Ed.Engl.* **2002**, *41*, 2927 – 2931. (c) Yuan, Z.; Collings, J. C.; Taylor, N. J.; Marder, T. B.; Jardin, C.; Halet, J-F. *J. Solid State Chem.* **2000**, *154*, 5 – 12.

[3] (a) Yamaguchi, S.; Akiyama, S.; Tamao, K. *J. Am. Chem. Soc.* **2000**, *122*, 6335 – 6336. (b) Yamaguchi, S.; Akiyama, S.; Tamao, K. *J. Am. Chem. Soc.* **2001**, *123*, 11372 – 11375. (c) Yamaguchi, S.; Akiyama, S.; Tamao,K. *J. Organomet. Chem.* **2002**, *652*, 3 – 9. (d) Yamaguchi, S.; Shirasaka, T.; Akiyama, S.; Tamao, K. *J. Am. Chem. Soc.* **2002**, *124*, 8816 – 8817. (e) Yamaguchi, S.; Shirasaka, T.; Tamao, K. *Org. Lett.* **2000**, *2*, 4129 – 4132.

[4] (a) Jai, W-L.; Song, D.; Wang, S. *J. Org. Chem.* **2002**, *68*, 701 – 705. (b) Jia, W.-L.; Bai, D.-R.; M^{c}Cormick, T.; Liu, Q.-D.; Motala, M.; Wang, R.-Y.; Seward, C.; Wang, S. *Chem. Eur. J.* **2004**, *10*, 994 – 1006.

[5] (a) Yuan, Z.; Taylor, N. J.; Marder, T. B.; Williams, I. D.; Kurtz, S. K.; Cheng, L-T.; *J. Chem. Soc., Chem. Communs.* **1990**, 1489 – 1492. (b) Yuan, Z.; Taylor, N. J.; Marder, T. B.; Williams, I. D.; Cheng, L.-T. in *Organic Materials for Non-linear Optics II, Spec. Publ. No. 91* (Eds.: R. A. Hann and D. Bloor), The Royal Society of Chemistry, Cambridge, **1991**, pp. 190 – 194.

[6] Yuan, Z.; Taylor, N. J.; Sun, Y.; Marder, T. B.; Williams, I. D.; Cheng, L.-T.*J. Organomet. Chem.* **1993**, *449*, 27 – 37.

[7] Yuan, Z.; Taylor, N. J.; Ramachandran, R.; Marder, T. B. *Appl. Organomet. Chem.* **1996**, *10*, 305 – 316.

[8] (a) Lequan, M.; Lequan, R. M.; Ching, K. C. *J. Mater.Chem.* **1991**, 1, 997 – 999. (b) Lequan, M.; Lequan, R. M.; Ching, K. C.; Barzoukas, M.; Fort, A.; Lahoucine, H.; Bravic, B.; Chasseau, D.; Gaultier, J. *J. Mater. Chem.* **1992**, *2*, 719 – 725. (c) Lequan, M.; Lequan, R. M.; Chane-Ching, K.; Callier, A.-C.; Barzoukas, M.; Fort, A. *Adv. Mat. Opt. Electron.* **1992**, *1*, 243-247. (d) Branger, C.; Lequan, M.; Lequan, R. M.; Barzoukas, M.; Fort, A. *J. Mater. Chem.*, **1996**, *6*, 555 – 558.

[9] Branger, C.; Lequan, M.; Lequan, R. M.; Large, M.; Kajzar, F. *Chem. Phys. Lett.* **1997**, *272*, 265 – 270.

[10] (a) Williams, J. L. R.; Grisdale, P. J.; Doty, J. C. *J. Org. Chem.* **1971**, *36*, 544 – 549. (b) Doty, J. C.; Babb, B.; Grisdale, P. J.; Glogowski, M.; Williams, J. L. R. *J. Organomet. Chem.* **1972**, *38*, 229 – 236. (c) Glogowski, M. E.; Williams, J. L.

R. *J. Organomet. Chem.* **1981**, *216*, 1 – 8. (d) Glogowski, M. E.; Zumbulyadis, N.; Williams, J. L. R. *J. Organomet. Chem.* **1982**, *231*, 97 – 107.

[11] Allbrecht, K.; Kaiser, V.; Boese, R.; Adams, J.; Kaufmann, D. E. *J. Chem. Soc., Perkin Trans. 2* **2000**, 2153 – 2157.

[12] (a) Liu, Z-Q.; Fang, Q.; Wang, D.; Xue, G., Yu, W-T.; Shao, Z-S.; Jiang, M-H.; *Chem. Commun.* **2002**, 2900 – 2901. (b) Liu, Z-Q.; Fang, Q., Wang, D.; Cao, D-X.; Xue, G.; Yu, W-T.; Lei, H. *Chem. - Eur. J.* **2003**, *9*, 5074 – 5084.

[13] (a) Kaim, W; Schultz, A. *Angew. Chem. Int. Ed.* **1984**, *23*, 615 – 616. (b) Schultz, A.; Kaim, W. *Chem. Ber.* **1989**, *122*, 1863 – 1868. (c) Fiedler, J.; Zalis, S.; Klein, A.; Hornung, F. M.; Kaim, W. *Inorg. Chem.* **1996**, *35*, 3039 – 3043.

[14] (a) Okada, K.; Sugawa, T.; Oda, M.; *J. Chem. Soc., Chem. Commun.* **1992**, 74 – 75. (b) Rajca, A.; Rajca, S.; Desai, S. R.; *J. Chem. Soc. Chem., Commun.* **1995**, 1957 – 1958.

[15] Lichtblau, A.; Kaim, W.; Scultz, A.; Stahl, T. *J. Chem. Soc., Perkin Trans. 2* **1992**, 1497 – 1501.

[16] (a) Noda, T.; Shirota, Y. *J. Am. Chem. Soc.* **1998**, *120*, 9714 – 9715. (b) Makinen, A. J.; Hill, I. G.; Noda, T.; Shirota, Y.; Kafafi, Z. H. *Appl. Phys. Lett.* **2001**, *78*, 670 – 672. (c) Noda, T.; Ogawa, H.; Shirota, Y. *Adv. Mater.* **1999**, *11*, 283 – 285. (d) Noda, T.; Shirota, Y. *J. Luminescence* **2000**, 1168 – 1170. (e) Hamada, Y.; Adachi, C.; Tsutsui, T.; Saito, S. *Jpn. J. Appl. Phys.* **1992**, *31*, 1812 – 1813. (f) Chen, B. J.; Zhang, X. H.; Lin, X. Q.; Kwang, H. L.; Wong, N. B.; Gambling, W. A.; Lee, S.T. *Syn. Met.* **2001**, *118*, 193 – 196. (g) Zhou, J.; Pun, E. Y. B.; Chung, P. S.; Zhang, X. H. *Optics Commun.* **2001**, *191*, 427 – 433.

[17] Kinoshita, M.; Shirota, Y. *Chem. Lett.* **2001**, 614 – 615.

[18] Kinoshita, M.; Fujii, N.; Tsuzuki, T.; Shirota, Y. *Syn. Met.* **2001**, *121*, 1571 – 1572.

[19] (a) Shirota, Y.; Kinoshita, M.; Noda, T.; Okumoto, K.; Takahiro, O. *J. Am. Chem. Soc.* **2000**, *122*, 11021 – 11022. (b) Doi, H.; Kinoshita, M.; Okumoto, K.; Shirota, Y. *Chem. Mater.* **2003**, *15*, 1080 – 1089.

[20] (a) Hooz, J.; Akiyama, S.; Cedar, F.J.; Bennet, M.J.; Tuggle, R.M. *J. Am. Chem. Soc.* **1974**, *96,* 274 (b) Pelter, A.; Singaram, S.; Brown, H.C. *Tetrahedron Lett.* **1983**, *24*, 1433. (c) Entwistle, C.D.; Marder, T.B.; Smith, P.S.; Howard, J.A.K.; Fox, M.A.; Mason, S.A. *J. Organometal. Chem.* **2003**, *680*, 165-172.

[21] See, for example, (a) Nicolaou, K.C.; Webber, S.E.; *J. Chem. Soc., Chem. Commun.*, **1986**, 1816. (b) Hird, M.; Toyne, K.J.; Gray, G.W. *Liq. Cryst.*, **1993**, *14*, 741. (c) Dibowski, H.; Schmidtchen, F.P. *Angew. Chem. Int. Ed.*, **1998**, *37*, 476. (d) W.R. Turner, M.J. Suto, *Tetrahedron Lett.*, **1993**, *34*, 281.

[22] (a) Sonogashira, K.; Tohda, Y.; Hagihara, N. *Tetrahedron Lett.* **1975**, 4467. (b) Nguyen, P.; Yuan, Z.; Agocs, L.; Lesley, G.; Marder, T.B. *Inorg. Chim. Acta* **1994**, *220*, 289 – 296.

[23] Sengupta, S.; Bhattacharya, S.; Sadhukhan, S.K.*J. Chem. Soc. Perkin Trans 1* **1998**, 275 – 278.

[24] Simson, C.D.; Brand, J.D.; Berresheim, A.J.; Przybilla, L.; Raeder, H.J.; Muellen, K. *Chem. Europ. J.*, **2002**, 1424 – 1429.

[25] Williams, A.T.R.; Winfield, S.A.; Miller, J.N. *Analsyt* **1983**, *108*, 1067.

[26] Dhami, S.; de Mello, A.J.; Rumbles, G.; Bishop, S.M.; Phillips, D.; Beeby, A. *Photochem. Photobiol.* **1995**, *61*, 341.

[27] (a) Plater, M.J.; Sinclair, J.P.; Aiken, S.; Gelbrich, T.; Hursthouse, M.B. *Tetrahedron* **2004**, *60*, 6385 – 6394. (b) Pelter, A.; Jones, D.E. *J. Chem. Soc. Perkin Trans. 1* **2000**, 2289 – 2294.

[28] Kahn, M.S.; Al-Mandhary, M.R.A.; Al-Suti, M.K.; Corcoran, T.C.; Al-Mahrooqi, Y.; Attfield, P.J.; Feeder, N.; David, W.I.F.; Shankland, K.; Friend, R.H.; Kohler, A. *New J. Chem.* **2003**, *27*, 140 – 149.

[29] (a) Neenan, T.X.; Whitesides, G.M. *J. Org. Chem.* **1988**, 2489 – 2496. (b) Lewis, J.; Long, N.J.; Raithby, P.R.; Shields, G.P.; Wong, W-Y.; Younus, M. *J. Chem. Soc. Dalton Trans.* **1997**, 4283 – 4288.

[30] Lowe, G.; Droz, A-S.; Park, J.J.; Weaver,G. *Bioorg. Chem.* **1999**, *27*, 477 – 486.

[31] Lewis, J.; Raithby, P.R.; Wong, W-Y. *J. Organomet. Chem.* **1998**, *556*, 219 – 228.

[32] Scott, L.T.; Necula, A. *Tetrahedron Lett.* **1997**, *38*, 1877 – 1880.

[33] Yuan, Z. *PhD thesis, University of Waterloo,* **1993**.

[34] Wong, W-Y.; Lee, A.W.M.; Wang, C-L.; Lu, G-L.; Zhang, H.; Mo, T.; Lam, K-T. *New J. Chem.* **2002**, *26*, 354 – 360.

[35] Rohde, W. *Macromol. Chem.* **1978**, *179*, 1999 – 2008.

[36] Mayr, H.; Halberstadt-Kausch, I.K. *Chem. Ber.* **1982**, *115*, 3479 – 3515.

Chapter 3

Compounds Containing a Single Dimesitylboryl Group: Optical and Structural Properties

3.1. Introduction

A large number of conjugated organic molecules containing a single dimesitylboryl group (where mesityl = 2,4,6-trimethylphenyl; Mes) have been synthesised, with the majority being donor-acceptor type compounds. [1,2,3,4,5,6,7,8,9,10] Several groups have also investigated symmetric compounds of the form Mes_2B-X-$BMes_2$ (where X is a conjugated organic π – system), which have proven to have interesting optical and electrochemical properties. [11,12,13,14,15,16,17,18,19,20] In order to investigate the differences between symmetric compounds with two dimesitylboryl groups and those with a single dimesitylboryl group, and thus the interaction between the two boron centres, several compounds of the form Mes_2B-CH=CH-X were synthesised (where X = a conjugated organic π-system or *ortho*-carborane). A further aim was to investigate how changing the group X affected the properties of these compounds. The compound *p*-dimesitylborylbromobenzene (**5**) has been previously investigated, [1] but the crystal structure is reported here for the first time.

3.2. Results and Discussion

3.2.1. Synthesis

Synthesis of these compounds was achieved in a similar manner to that of symmetric bis(dimesitylborylvinyl) compounds (Scheme 3.1). A solution of

dimesitylborane [21] was added dropwise to a solution of the appropriate terminal alkyne in THF under a nitrogen atmosphere (1:1 Mes_2BH monomer to alkyne) (Scheme 3.1). The triarylborane, compound **5**, [1] was prepared by the reaction of ^nBuLi with 1,4-dibromobenzene in hexane followed by quenching with a slight excess of dimesitylfluoroborane (Scheme 3.2). All compounds were purified by recrystallisation from hexane / dichloromethane.

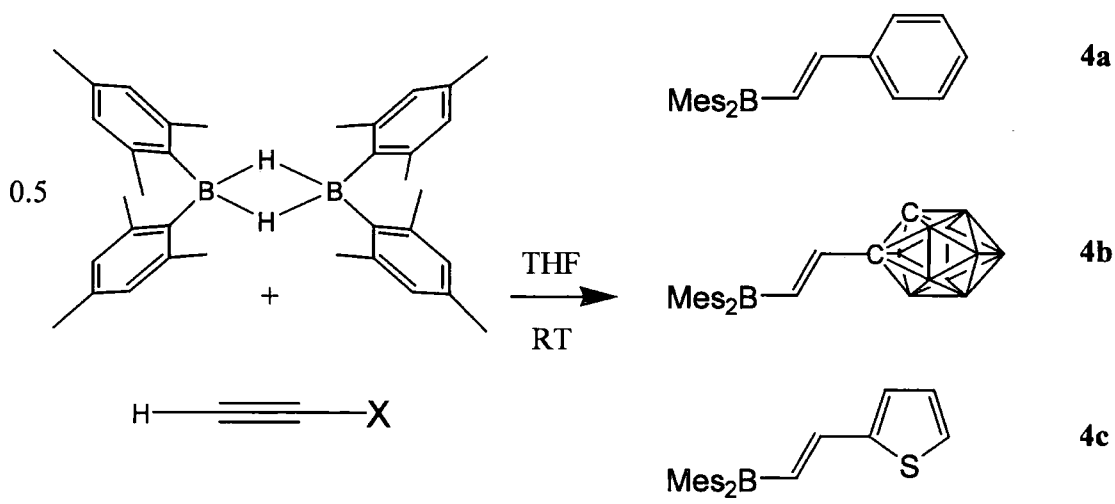

Scheme 3.1. Synthesis of dimesitylvinylboranes, 4a-c. In the diagram of 4b, vertices in the carborane moiety represent boron atoms.

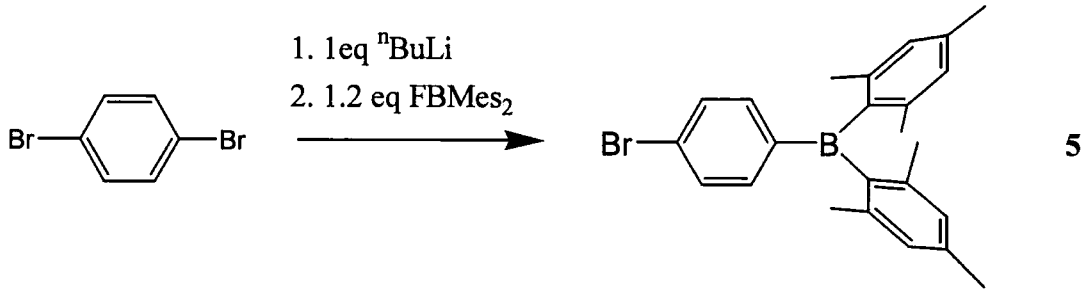

Scheme 3.2. Synthesis of *p*-dimesitylborylbromobenzene (5)

3.2.2. Structural Properties

In general, compounds containing a single dimesitylboryl group were much more easy to crystallise than those containing two such groups. Single crystals of **4a** suitable for XRD were grown by cooling a hexane / DCM solution. Single crystals of **4c** were grown by slow evaporation of a hexane solution. Single crystals of compound **5** were grown by cooling a hexane solution. Whilst these three compounds proved to crystallise much more readily than the analogous bis(boryl)s, and did not include solvent molecules, it proved impossible to obtain crystals of compound **4b**. Selected bond lengths and angles are presented in Tables 3.1 – 3.5.

Table 3.1. Selected bond lengths and angles for compound 4a

Bond lengths (Å)		Bond Angles (°)	
B-C(8)	1.553(18)	C(8)-B-C(11)	118.43(11)
B-C(11)	1.5792(18)	C(8)-B-C(21)	118.29(11)
B-C(21)	1.5741(18)	C(21)-B-C(11)	123.15(10)
C(1)-C(2)	1.395(2)	C(2)-C(1)-C(6)	117.95(13)
C(1)-C(6)	1.3968(19)	C(2)-C(1)-C(7)	122.50(12)
C(1)-C(7)	1.4698(17)	C(6)-C(1)-C(7)	119.53(13)
C(2)-C(3)	1.388(2)	C(3)-C(2)-C(1)	120.83(14)
C(3)-C(4)	1.379(2)	C(4)-C(3)-C(2)	120.46(16)
C(4)-C(5)	1.378(3)	C(5)-C(4)-C(3)	119.70(14)
C(5)-C(6)	1.393(2)	C(6)-C(5)-C(4)	120.17(15)
C(7)-C(8)	1.3403(18)	C(5)-C(6)-C(1)	120.88(16)
		C(8)-C(7)-C(1)	127.20(12)
		C(7)-C(8)-B	123.21(11)

Table 3.2. Selected bond lengths for compound 4c

Bond lengths (Å)			
S(1)-C(5)	1.703(4)	S(2)-C(05)	1.706(4)
S(1)-C(2)	1.726(3)	S(2)-C(02)	1.724(3)
B(1)-C(6)	1.541(5)	B(2)-C(06)	1.545(5)
B(1)-C(11)	1.585(5)	B(2)-C(31)	1.574(5)
B(1)-C(21)	1.586(5)	B(2)-C(41)	1.583(5)
C(1)-C(6)	1.340(4)	C(01)-C(06)	1.339(5)
C(1)-C(2)	1.439(4)	C(01)-C(02)	1.440(5)
C(2)-C(3)	1.374(5)	C(02)-C(03)	1.373(5)
C(3)-C(4)	1.412(5)	C(03)-C(04)	1.412(5)
C(4)-C(5)	1.350(6)	C(04)-C(05)	1.343(6)

Table 3.3. Selected bond angles for compound 4c

Bond angles (°)			
C(5)-S(1)-C(2)	91.95(19)	C(05)-S(2)-C(02)	91.9(2)
C(1)-C(2)-S(1)	122.2(3)	C(01)-C(02)-S(2)	122.9(3)
C(3)-C(2)-S(1)	110.3(3)	C(03)-C(02)-S(2)	110.3(3)
C(4)-C(5)-S(1)	112.2(3)	C(04)-C(05)-S(2)	112.3(3)
C(3)-C(2)-C(1)	127.4(3)	C(03)-C(02)-C(01)	126.8(3)
C(2)-C(3)-C(4)	112.9(4)	C(02)-C(03)-C(04)	112.9(4)
C(5)-C(4)-C(3)	112.6(4)	C(05)-C(04)-C(03)	112.7(4)
C(1)-C(6)-B(1)	124.4(3)	C(01)-C(06)-B(2)	124.5(3)
C(6)-B(1)-C(11)	119.4(3)	C(06)-B(2)-C(31)	119.2(3)
C(6)-B(1)-C(21)	118.8(3)	C(06)-B(2)-C(41)	118.6(3)
C(11)-B(1)-C(21)	121.8(3)	C(31)-B(2)-C(41)	122.2(3)

Table 3.4. Selected bond lengths and angles for compound 5

Bond lengths (Å)		Bond angles (°)	
Br-C(1)	1.849(14)	C(4)-B-C(11)	118.86(12)
B-C(4)	1.571(2)	C(4)-B-C(21)	117.20(12)
B-(C11)	1.578(2)	C(21)-B-C(11)	123.92(12)
B-C(21)	1.572(2)	C(2)-C(1)-C(6)	121.99(13)
C(1)-C(2)	1.382(2)	C(2)-C(1)-Br	118.97(11)
C(1)-C(6)	1.387(2)	C(6)-C(1)-Br	119.03(11)
C(2)-C(3)	1.392(2)	C(1)-C(2)-C(3)	118.70(13)
C(3)-C(4)	1.4004(19)	C(2)-C(3)-C(4)	121.77(18)
C(4)-C(5)	1.404(2)	C(3)-C(4)-C(5)	117.17(13)
C(5)-C(6)	1.390(2)	C(3)-C(4)-B	121.78(12)
		C(5)-C(4)-B	120.99(12)
		C(6)-C(5)-C(4)	122.19(13)
		C(1)-C(6)-C(5)	118.13(13)

Table 3.5. Selected bond torsion angles for compounds 4a, 4c and 5

Torsion angles (°)			
4a		5	
C(11)-B-C(8)-C(7)	-150.08	C(11)-B-C(4)-C(3)	26.54
C(21)-B-C(8)-C(7)	25.98	C(11)-B-C(4)-C(5)	-156.34
B-C(8)-C(7)-C(1)	170.79	C(21)-B-C(4)-C(5)	25.47
C(8)-C(7)-C(1)-C(2)	13.5	C(21)-B-C(4)-C(3)	-151.66
C(8)-C(7)-C(1)-C(6)	-165.02		
4c		4c	
C(11)-B(1)-C(6)-C(1)	161.69	C(31)-B(2)-C(06)-C(01)	-159.21
C(21)-B(1)-C(6)-C(1)	-17.79	C(41)-B(2)-C(06)-C(01)	19.98
B(1)-C(6)-C(1)-C(2)	179.32	B(2)-C(06)-C(01)-C(02)	178.01
C(6)-C(1)-C(2)-C(3)	163.30	C(06)-C(01)-C(02)-C(03)	-172.78
C(6)-C(1)-C(2)-S(1)	-16.08	C(06)-C(01)-C(02)-S(1)	7.57

As with the bis(boryl)s, these compounds have a strongly twisted geometry, with propeller – like configurations about the boron atoms, and bond lengths and angles are similar in these classes of compound. Boron atoms are trigonal planar, with the C-B-C angles adding up to 360°, and π – systems are largely planar and twisted w.r.t. the BC_3 plane.

In compound **4a**, which crystallised in space group $P2_1/c$, the vinyl group deviates from planarity by ca. 9°, and the phenyl group and BC_3 plane are twisted w.r.t. one another by ca. 37.2°. This results in a structure that is considerably more twisted than the related bis(boryl) compound **2a**, in which the two BC_3 planes are

twisted w.r.t. the central C_6H_4 unit by ca. 2° and ca. 15.1° respectively and the vinyl groups are much closer to planarity. Since steric factors about the vinyl groups are identical for these two molecules, this data may therefore suggest that conjugation is improved by the presence of two dimesitylboryl units or that crystal packing effects are significant at least in this case.

Compound **4c** crystallised in space group $P\bar{1}$, with two independent molecules in the unit cell that have slightly different torsion angles but are otherwise largely similar. The vinyl groups in each independent molecule are closer to planarity than in compound **4a**, deviating by ca. 0.7 and 2 ° respectively. This may be explained by the observation that the vinyl groups are positioned so as to avoid steric clash between H atoms on C(3) and C(6) (figure 3.2) , similar to the *cisoid* form of the related bis(boryl) compound **2c**. It is noticeable that the angle between the vinyl and thiophenyl planes differs considerably in the two independent molecules of **4c** (C(6)-C(1)-C(2)-S(1) = -16.08°, vs. C(06)-C(01)-C(02)-S(2) = 7.57°), and this results in a marked difference in the angle between the thiophenyl and BC_3 planes. In one molecule, the value is ca. 35.5°, similar to compound **4a**, whereas the other molecule has higher overall planarity and the angle is only ca. 26.3°. Since the molecules are chemically equivalent, this must be attributed to crystal packing effects, and once more highlights the fact that the solid - state configuration can only be a guide to the most likely configuration in solution.

Compound **5** also crystallised in space group $P\bar{1}$, but with a single independent molecule in the unit cell. The absence of a vinyl spacer between the boron atom and the π – system results in more severe steric demands about the boron atom, such that the BC_3 plane is twisted w.r.t. the bromophenyl plane by ca. 25.8°. Whilst this value is much greater for than for BC_3 – vinyl planes, the aryl and BC_3

moieties in compound **5** are, perhaps surprisingly, closer to planarity than the dimesitylvinylboranes **4a** and **4c**. Since the bromine atom is a weak π – electron donor, compound **5** may be thought of as a D-π-A system; these have previously been shown to adopt increasingly planar geometries with increasing π – donor strength. [3,4]

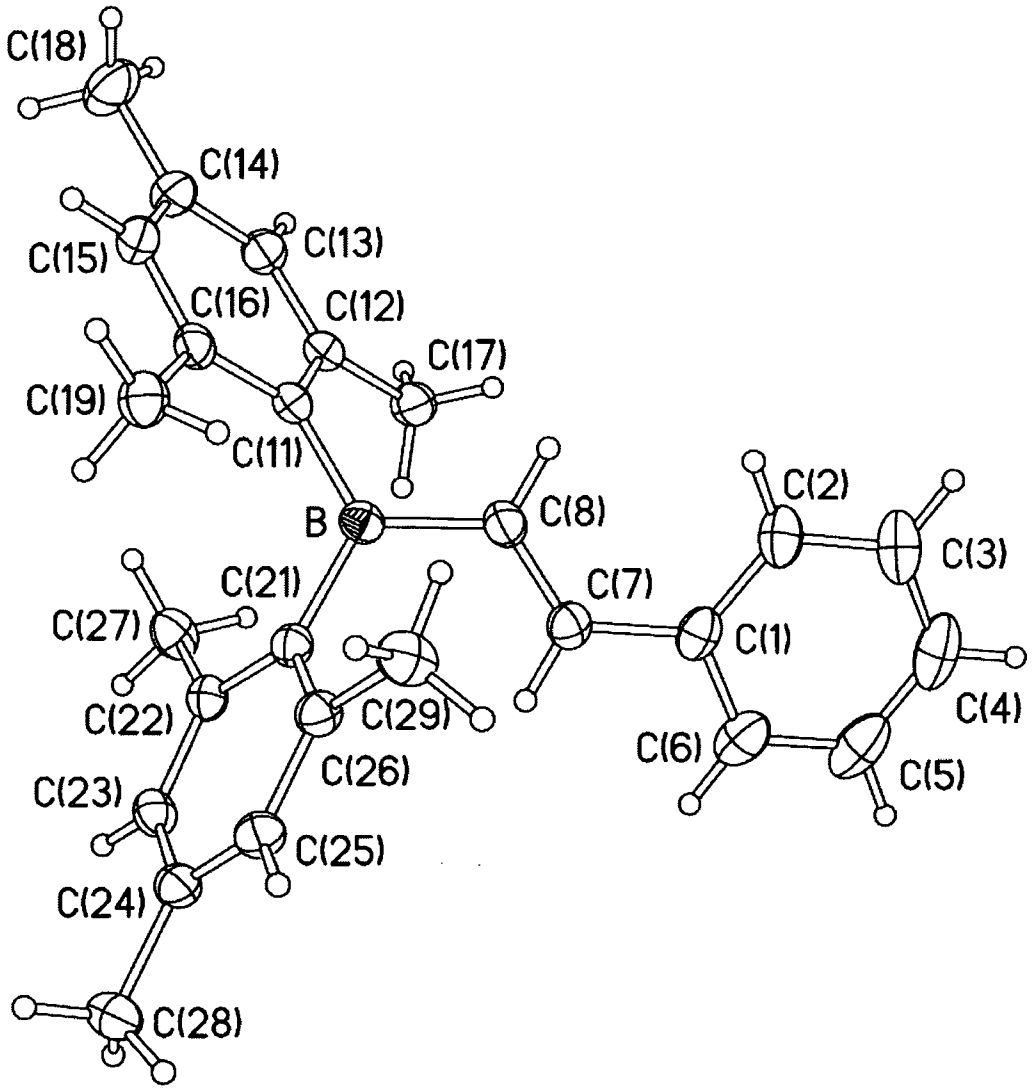

Figure 3.1. ORTEP diagram of the molecular structure of dimesitylborylvinylbenzene (4a) (50% thermal ellipsoids)

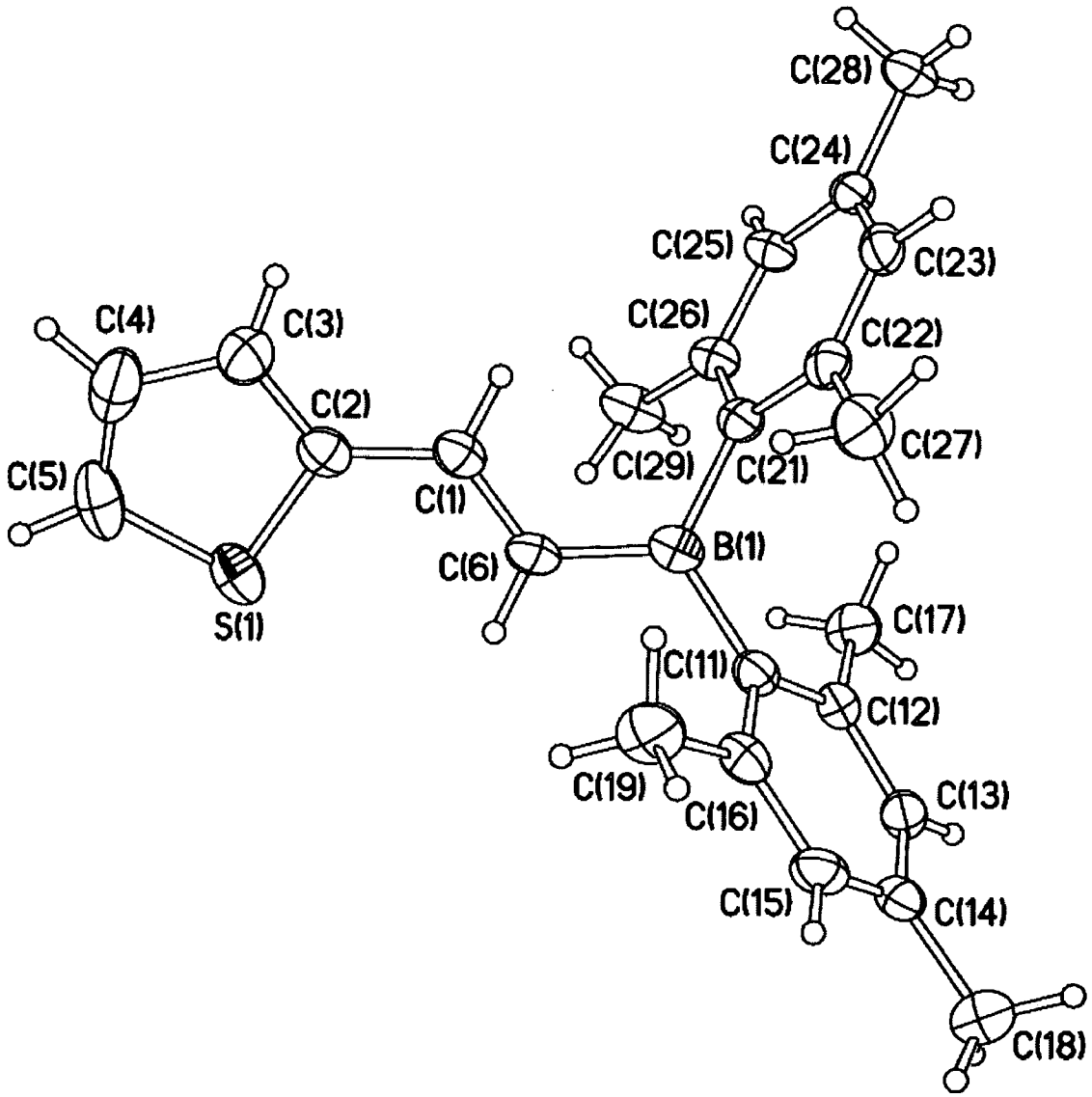

Figure 3.2. ORTEP diagram of the molecular structure of dimesitylborylvinylthiophene (4c) (50% thermal ellipsoids)

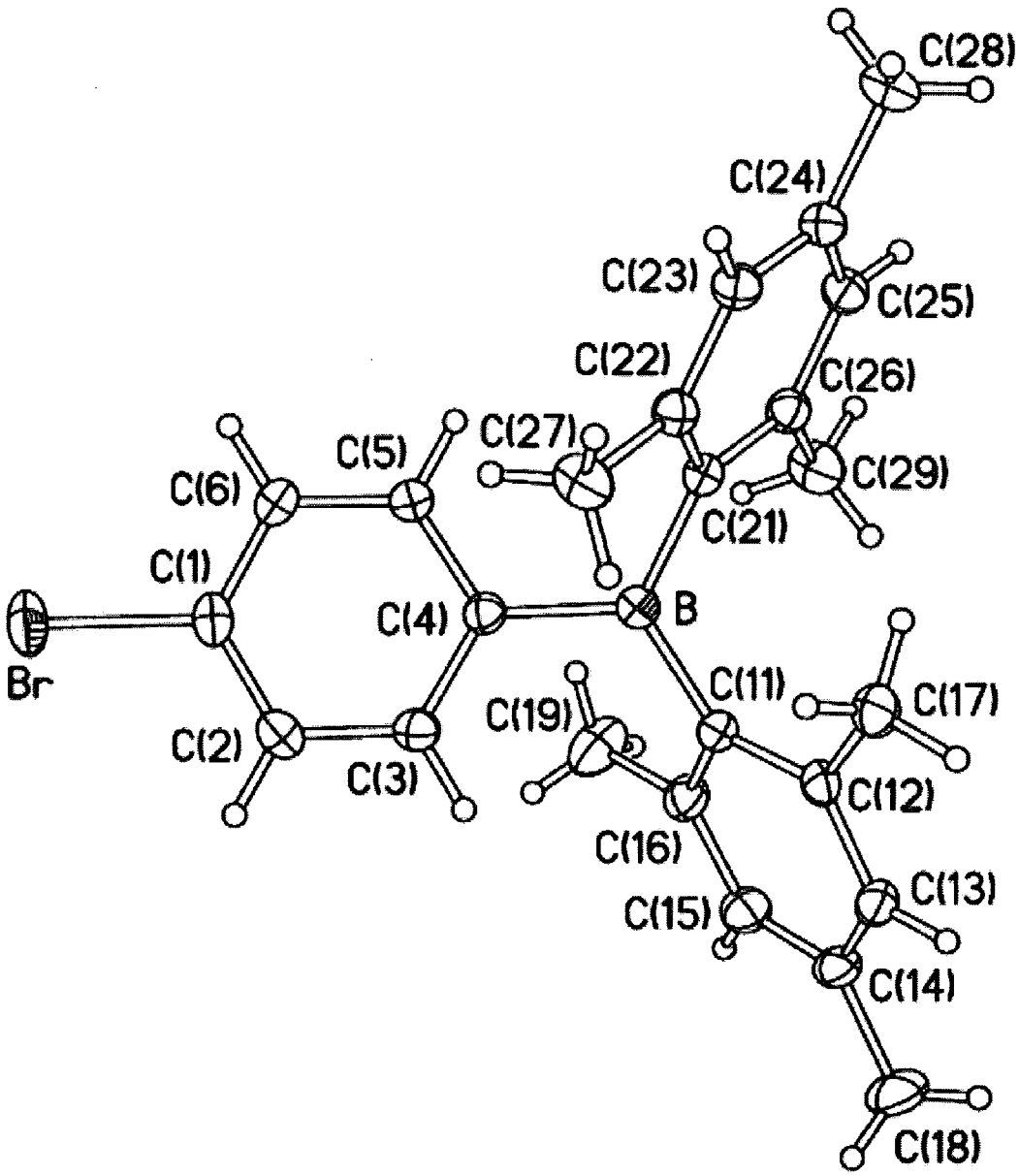

Figure 3.3. ORTEP diagram of the molecular structure of *p*-dimesitylborylvinylbromobenzene (5) (50% thermal ellipsoids)

3.2.3. Thermal properties

The thermal properties of compounds **4a** and **4c** were examined by DSC and TGA. Compound **4a** melts at 146 °C (144 – 147 °C by melting point apparatus; 140 – 149 °C by DSC, 10 °C min^{-1}). DSC revealed an exothermic event immediately prior to melting, this being tentatively attributed to a rearrangement that must relieve strain and result in a lower energy morphology. No recrystallisation was observed on cooling. Upon heating, an initial loss of weight (ca. 6 %) due to desorption of solvent or moisture occurred from 70 – 150 °C, followed by sublimation at T > 150 °C. Compound **4c** exhibits a sharp melting point at 115 °C (114 – 116 °C by melting point apparatus; 112 – 117 °C by DSC, 10 °C min^{-1}). No recrystallisation was observed on cooling back to room temperature. Unlike compound **4a** or related bis(boryl)s, there was no evidence for loss of adsorbed solvent or moisture. At temperatures above ca. 200 °C, TGA showed a steady weight loss, with a final mass of ca. 12 % remaining at 295 °C after which no further weight loss was observed. Since the residue would be expected to consist of a mixture of boric acid and boron oxide, which would result in a final mass of approximately 17 - 20 %, the weight loss is attributed mainly to sublimation, with some decomposition occurring at higher temperatures. In both cases, the observation of white powder in the chimney of the TGA apparatus after experiments proved that sublimation rather than simply decomposition had occurred. Whilst neither TGA nor DSC analysis of compound **4b** was undertaken, a sample in a sealed melting point tube was observed to decompose at ca. 145 °C.

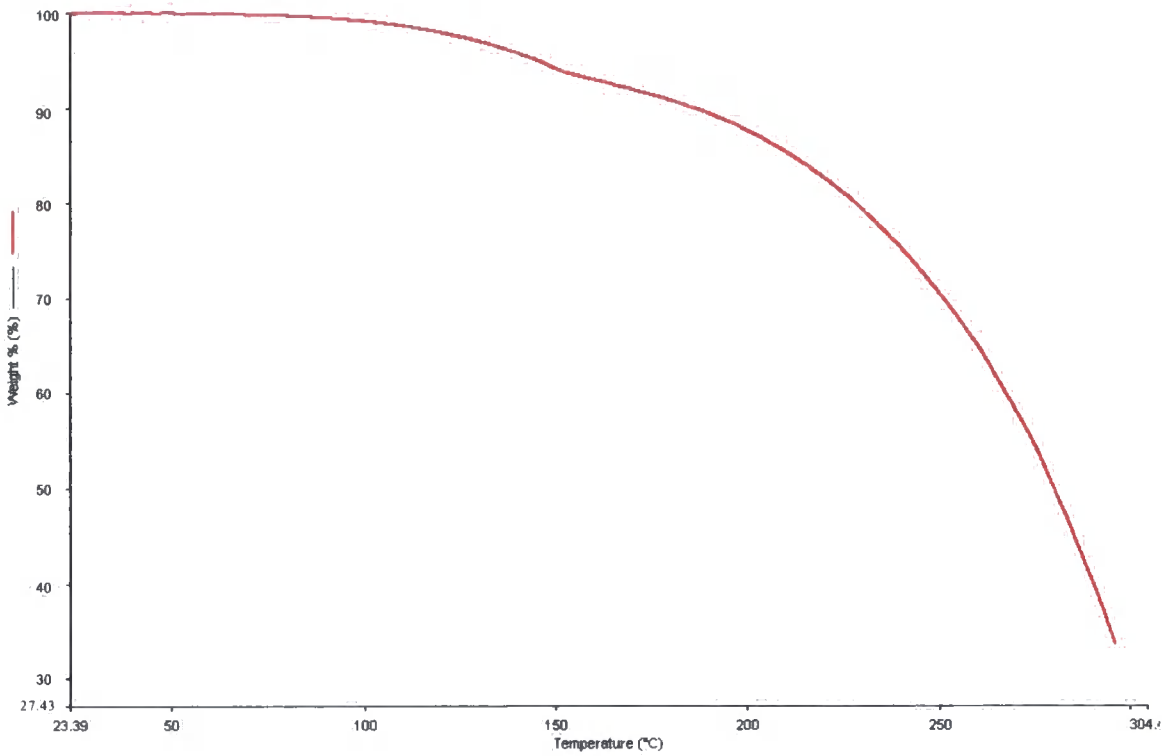

Figure 3.4. Weight loss as a funtion of temperature for compound 4a (heating rate 10 °C min^{-1})

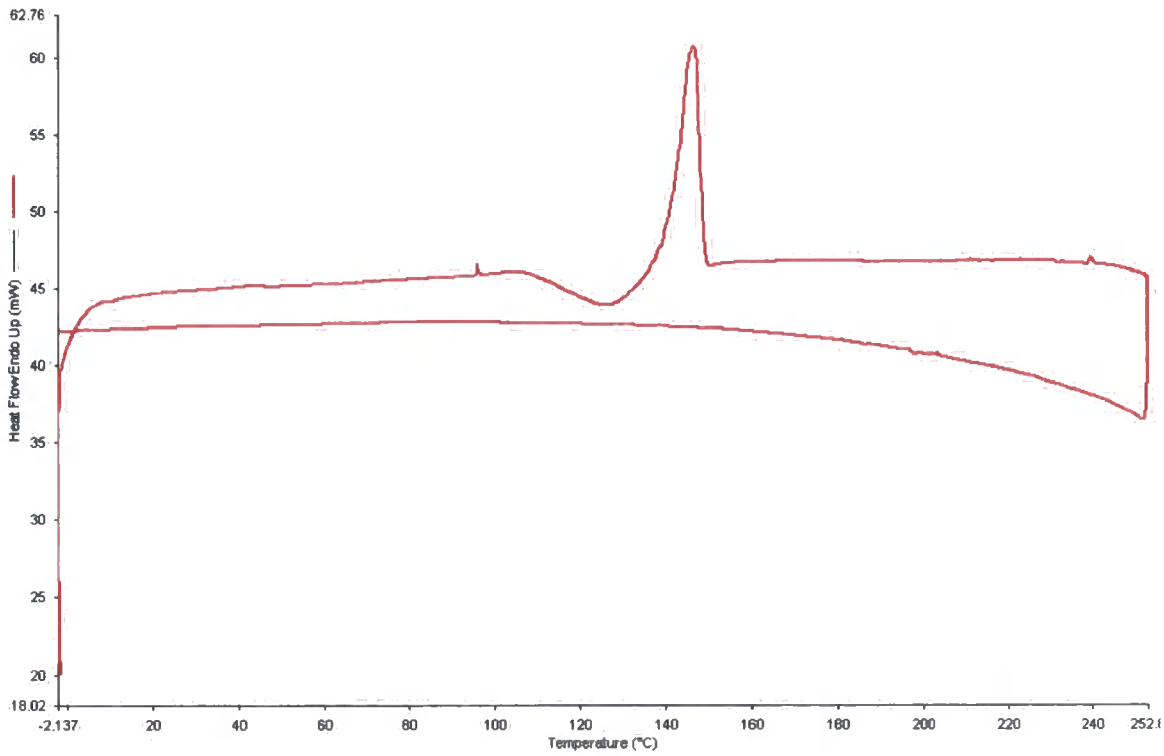

Figure 3.5. DSC curve for compound 4a (heating rate 10 °C min^{-1})

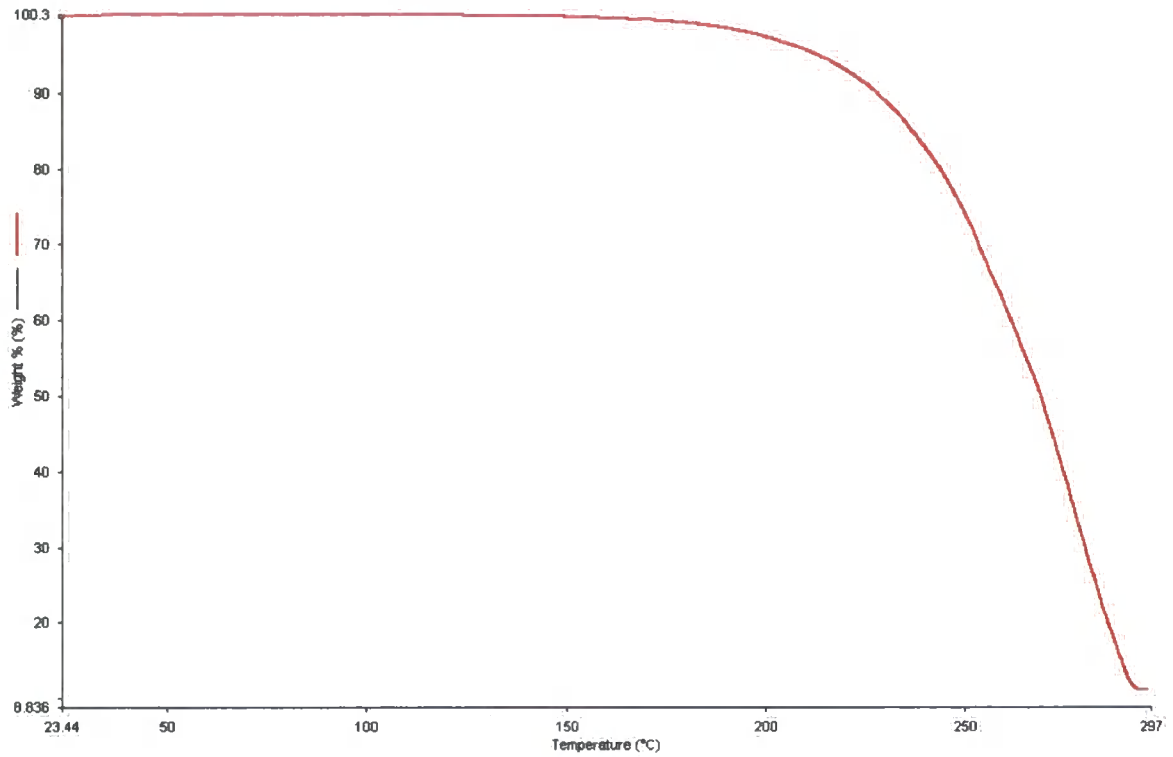

Figure 3.6. Weight loss as a funtion of temperature for compound 4c (heating rate 10 °C min^{-1})

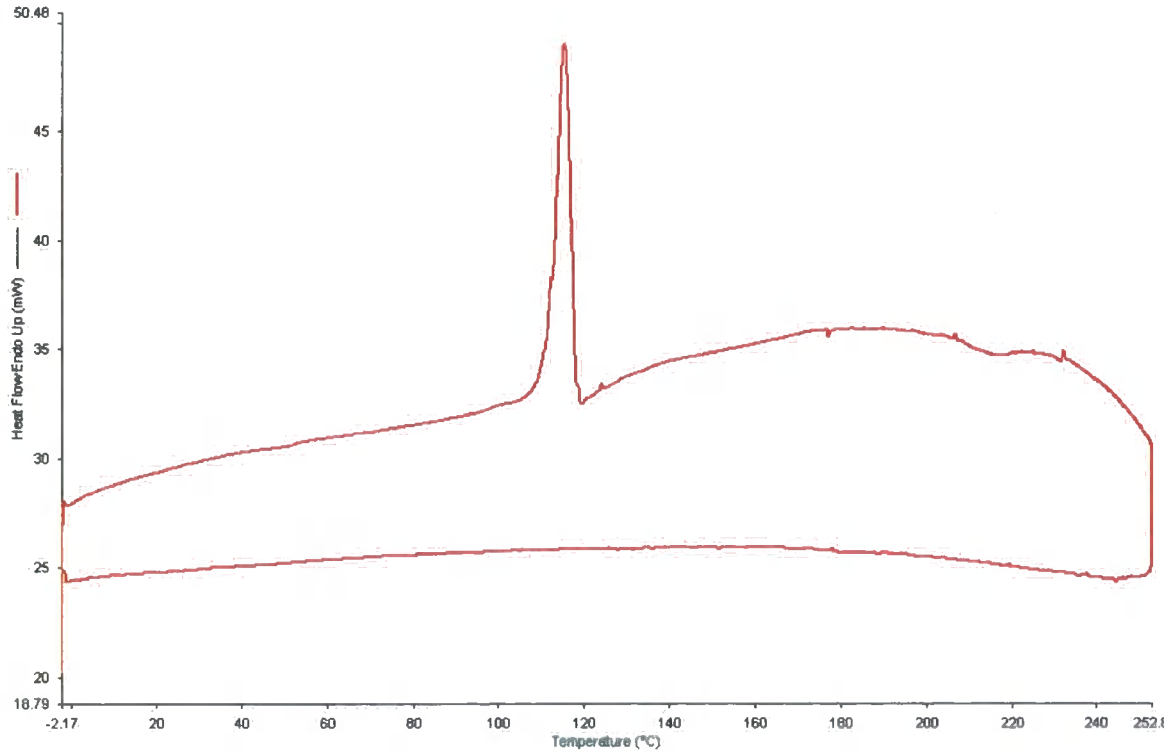

Figure 3.7. DSC curve for compound 4c (heating rate 10 °C min^{-1})

3.2.4. Optical Properties

In common with other compounds containing the dimesitylboryl group, all compounds exhibited an intense absorption in the UV region (ca. 205 nm), attributed to $\pi - \pi^*$ transitions associated with the unconjugated mesityl groups. Compound **4a** had a broad absorption with λ_{max} = 335 nm (ε (335 nm) = 23000 $dm^3mol^{-1}cm^{-1}$ [22]) and a conspicuous high - energy shoulder (290 nm). Compound **4b** exhibited a broad, featureless absorption at similar energy (λ_{max} = 332 nm), but with much lower intensity than that of **4a** (ε (332 nm) = 12000 $dm^3mol^{-1}cm^{-1}$). The absorption maximum of compound **4c** was shifted to lower energy by ca. 15 nm, with λ_{max} = 352 nm. The extinction coefficient was similar to that of compound **4a** at 27000 $dm^3mol^{-1}cm^{-1}$. The positions of fluorescence maxima were similar for compounds **4a**, **b** and **c** (λ_{max}(em) = 398, 408 and 406 nm respectively, but the fluorescence intensities were markedly different for the carborane, compound **4b**. Whilst **4a** and **4c** were very only very weakly fluorescent, as can be observed by the low signal to noise ratios in their fluorescence spectra, compound **4b** exhibited an unexpectedly high quantum yield of 0.021±0.001. This must be a reflection of the difference between the "σ – aromaticity" of the carborane moiety and the π – delocalisation in the thiophenyl or phenyl groups, perhaps because the spherical distribution of electrons in the carboranyl group allows for conjugation in more conformations than in systems where conjugation (and therefore fluorescence) can only occur from only a relatively planar conformation. This result indicates that carborane moieties may be useful in the preparation of linear optical materials; both theoretical [23,24] and experimental [25,26] results have already suggested that boron clusters can enhance nonlinear optical activity. In general, the optical data suggest that mono(dimesitylboryl)s are inherently less efficient fluorophores than related bis(boryl)s, except in cases where the dimesitylboryl group

is conjugated with a strong π – donor. It also supports the assertion that in conjugated, symmetric bis(boryls)s, the presence of two three – coordinate boron atoms leads to an overall increase in planarity and thus to more desirable optical properties, though the increase in conjugation length cannot be discounted.

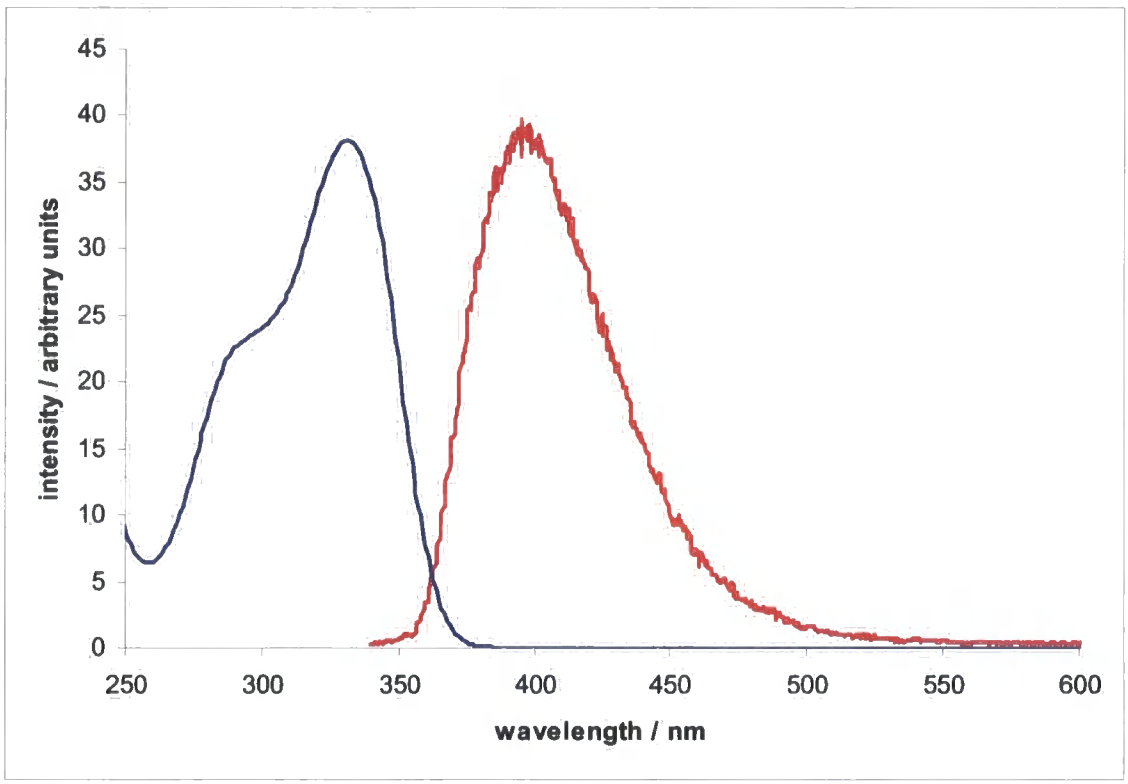

Figure 3.8. Absorption (blue) and fluorescence (red) spectra for compound 4a

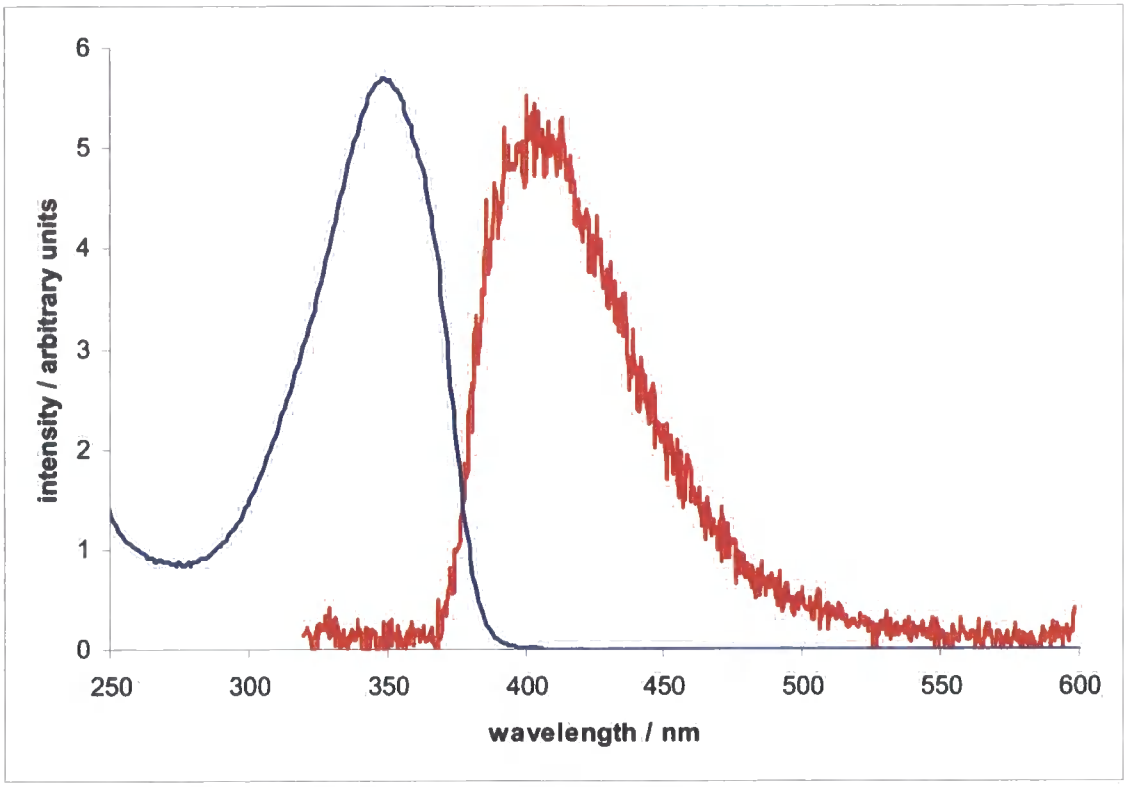

Figure 3.9 Absorption and fluorescence spectra for compound 4c

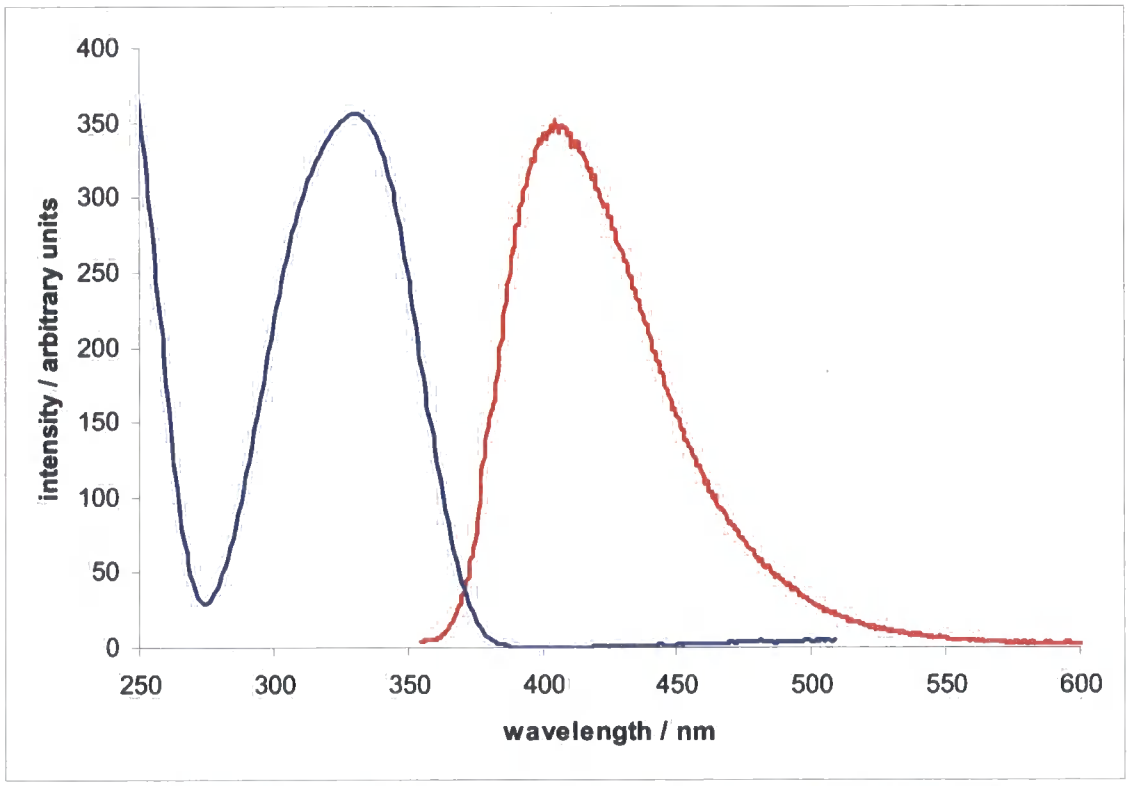

Figure 3.10. Absorption (blue) and fluorescence (red) spectra for compound 4b

3.3. Conclusions and suggested further work

Several compounds containing a single dimesitylboryl group have been prepared, including the new compounds dimesitylborylvinyl-*ortho*-dodecacarborane (**4b**) and dimesitylborylvinylthiophene (**4c**). Compound **4b** constitutes the first report of a molecule containing both dimesitylboryl and carboranyl moieties. We present here the first structural analyses of the compounds dimesitylborylvinylthiophene (**4b**) and *p*-(dimesitylborylvinyl)bromobenzene (**5**) as well as that of the previously solved dimesitylborylvinylbenzene (**4a**)(all bond lengths and angles being within experimental error for the two structures). [27] In addition, thermal analysis has been conducted for two of the compounds (**4a**,**c**) by TGA and DSC and optical data have been collected for the vinylboranes.

Structural data show that in the solid state, a single dimesitylboryl unit does not lead to significant conjugation with adjacent organic π – systems, since these compounds are much more twisted than their symmetric bis(boryl) counterparts, and provides further evidence that the presence of two such units can lead to greater overall planarity and thus effectively enhance conjugation. In addition, mono(boryl) species that lack a suitable π – donor do not appear to have attractive optical properties. The presence of an *ortho*-carborane leads to a significant increase in fluorescence efficiency, and suggests that related compounds of the form Mes_2B-carborane-$BMes_2$ or donor – accepter systems containing boron clusters may have useful linear optical properties. The compounds **4a** and **4c** appear to sublime readily, and so might be able to be deposited as films for functions such as electron transport, [11-14] but the propensity of these compounds to crystallise readily could be a major disadvantage in such applications.

3.4. Experimental

3.4.1. General

All solvents were dried over and distilled under nitrogen from appropriate drying agents. Hydroborations were performed in an Innovative Technology Inc. nitrogen-filled glovebox. NMR spectra were recorded on a Bruker A400 at 400 MHz (^{1}H) and 100 MHz (^{13}C), and were referenced to residual protonated solvent. Boron spectra were recorded on a Varian Mercury 300 at 160 MHz and referenced to external $BF_3 \bullet OEt_2$. Elemental analyses were performed in house. The purity of starting materials and intermediates was verified by GC-MS. The compounds phenylacetylene and p-dibromobenzene were purchased from Aldrich Chemical Company and 2-bromothiophene was purchased from Lancaster Chemical Company; all were used without further purification. The compound ethynyl-*ortho*-carborane[28] was supplied by Dr. M.A. Fox. Compound **5** was synthesised according to literature procedures. [1]

3.4.2. Synthesis

3.4.2.1. Synthesis of 2-ethynylthiophene [29]

To a mixture of 2-bromothiophene (24.5 g, 0.15 mol), $(Ph_3P)_2PdCl_2$ (1.1 g, 1.6 mmol) one equivalent of CuI in diethylamine (250 ml) was added trimethylsilylacetylene (17.7 g, 0.18 mol). The solution was stirred overnight at room temperature during which time a dense white precipitate formed. GC-MS revealed no remaining bromothiophene. The mixture was filtered through a pad of silica and concentrated to a colourless liquid by rotary evaporation. Residual diethylamine was removed by ether / water solvent extraction and the combined ethereal layers dried

over $MgSO_4$ and concentrated by rotary evaporation and purified by distillation under reduced pressure to give 2-trimethylsilylethynylthiophene, 22.0 g (92%).

A mixture of 2-trimethylsilylethynylthiophene (1.0 g, 5.5 mmol), methanol (40 ml) and water (0.5 ml) was stirred over Na_2CO_3 for 2 h. The mixture was filtered and the filtrate extracted with ether (4 x 60 ml). The combined ethereal extracts were dried over $MgSO_4$ and concentrated by rotary evaporation to give 2-ethynylthiophene (colourless oil) in 65 % yield (0.39 g, 3.6 mmol).

3.4.2.2. Synthesis of dimesitylborylvinylbenzene (4a)

To a stirred solution of phenylacetylene (0.11 g, 1.1 mmol) in THF (25 ml) was added a solution of dimesitylborane (0.5 g, 1.0 mmol) dropwise via syringe. After 3 h, the mixture was concentrated to dryness and residual THF was removed by adding small portions of ether followed by evaporation to give a white powder. The powder was washed with hexane (3 x 5 ml) and recrystallised from DCM / hexane to give **4a** (colourless crystals of suitable quality for XRD) in 85% yield (0.51 g).

^{1}H NMR (400 MHz, C_6D_6) δ: 7.50 (d, 1H, $^3J_{H\text{-}H}$ 18.0 Hz, CH vinyl) 7.38 (d, 1H, $^3J_{H\text{-}H}$ 18.0 Hz, CH vinyl), 7.25 (m, 3H, phenyl), 7.00 (m, 2H, phenyl), 6.84 (s, 4H, Mes), 2.43 (s, 12 H, *o*-CH_3), 2.32 (s, 6H, *p*-CH_3). $^{13}C\{^1H\}$ NMR (100 MHz, $CDCl_3$) δ: 142.1, 140.9, 138.8, 128.5, 23.5, 21.1 (Mes), 152.7 (CH vinyl), 138.1 (B-CH vinyl), 137.8, 129.8, 129.0, 128.4 (phenyl). ^{11}B NMR (96 MHz, $CDCl_3$) δ: 69. *m/z*: 352 (M^+), 232 (- mesitylene). Calculated for $C_{26}H_{29}B$: C, 88.64; H, 8.30. Found: C, 88.59; H, 8.25%.

3.4.2.3. Synthesis of dimesitylborylvinyl-*ortho*-carborane (4b)

To a stirred solution of 2-ethynyl-*ortho*-carborane (0.084 g, 0.5 mmol) in THF (25 ml) was added a solution of dimesitylborane (0.25 g, 0.5 mmol) dropwise via syringe. After stirring overnight, the mixture was concentrated to dryness to give a colourless oil. Residual THF was removed by adding small portions of ether followed by evaporation to give a white powder. The powder was washed with hexane (2 x 5 ml) and ether (5 ml) and recrystallised from DCM / hexane to give **4c** (white powder) in 63% yield (0.21 g).

^{1}H NMR (400 MHz, C_6D_6) δ: 6.91 (d, 1H, $^{3}J_{H-H}$ 16.7 Hz, CH vinyl), 6.81 (s, 4H, Mes), 7.34 (d, 1H, $^{3}J_{H-H}$ 17.0 Hz, CH vinyl), 2.94 (s, 1H), 2.87 (s, 1H), 2.75 (s, 2H), 2.52 (s, 2H), 2.21 (s, 2H), 2.05 (s, 2H) (carboranyl; one carboranyl proton could not be observed since the peak was apparently obscured by the methyl protons), 2.13 (s, 12 H, *o*-CH_3), 2.10 (s, 6H, *p*-CH_3). $^{13}C\{^{1}H\}$ NMR (400 MHz, $CDCl_3$) δ: 143.1, 140.9, 140.7, 128.5, 23.3, 21.2 (Mes), 145.8 (CH vinyl), 139.7 (B-CH vinyl), 74.9, 59.2 (carboranyl). $^{11}B\{^{1}H\}$ NMR (96 MHz, $CDCl_3$) δ: 71 (Mes_2B), -2.1, -3.7, -8.2, -11.4, -11.9, -12.9 (carborane). *m/z*: 418 (M^+), 298 (- mesitylene). Calculated for $C_{22}H_{35}B_{11}$: C, 63.15; H, 8.43. Found: C, 63.54; H, 8.60%.

3.4.2.4. Synthesis of 2-dimesitylborylvinylthiophene (4c)

To a stirred solution of 2-ethynylthiophene (0.11 g, 1.0 mmol) in THF (25 ml) was added a solution of dimesitylborane (0.5 g, 1.0 mmol) dropwise via syringe. After 2 h, the mixture was concentrated to dryness and residual THF was removed by adding small portions of ether followed by evaporation to give a white powder. The powder was washed with hexane (2 x 5 ml) and recrystallised from DCM / hexane to

give **4c** (white powder) in 70% yield (0.43 g). Single crystals of sufficient quality for XRD were grown by the slow evaporation of a hexane solution.

^{1}H NMR (400 MHz, C_6D_6) δ: 7.46 (d, 1H, $^3J_{H-H}$ 16.7 Hz, CH vinyl) 7.34 (d, 1H, $^3J_{H-H}$ 16.7 Hz, CH vinyl), 6.81 (s, 4H, Mes), 6.75 (d, 1H, $^3J_{H-H}$ 4.9 Hz, thienyl), 6.53 (m, 2H, thienyl), 2.28 (s, 12 H, *o*-CH_3), 2.18 (s, 6H, *p*-CH_3). $^{13}C\{^1H\}$ NMR (100 MHz, C_6D_6) δ: 144.9, 140.8, 130.2, 128.9, 23.6, 21.5 (Mes), 145.2 (CH vinyl), 138.6 (B-CH vinyl), 128.3, 128.2, 128.1, 127.9 (thienyl). ^{11}B NMR (96 MHz, $CDCl_3$) δ: 68. *m/z*: 358 (M^+), 238 (- mesitylene). Calculated for $C_{24}H_{27}BS$: C, 80.44; H, 7.59. Found: C, 80.49; H, 7.77%.

References

[1] Doty, J. C.; Babb, B.; Grisdale, P. J.; Glogowski, M.; Williams, J. L. R. *J. Organomet. Chem.* **1972**, *38*, 229 – 236.

[2] (a) Glogowski, M. E.; Williams, J. L. R. *J. Organomet. Chem.* **1981**, *216*, 1 – 8. (b) Glogowski, M. E.; Zumbulyadis, N.; Williams, J. L. R. *J. Organomet. Chem.* **1982**, *231*, 97 – 107.

[3] (a) Yuan, Z.; Taylor, N. J.; Marder, T. B.; Williams, I. D.; Kurtz, S. K.; Cheng, L.-T.; *J. Chem. Soc., Chem. Commun.* **1990**, 1489 – 1492. (b) Yuan, Z.; Taylor, N. J.; Marder, T. B.; Williams, I. D.; Cheng, L.-T. in *Organic Materials for Non-linear Optics II, Spec. Publ. No. 91* (Eds.: R. A. Hann and D. Bloor), The Royal Society of Chemistry, Cambridge, **1991**, pp. 190 – 194. (c) Yuan, Z.; Collings, J. C.; Taylor, N. J.; Marder, T. B.; Jardin, C.; Halet, J.-F. *J. Solid State Chem.* **2000**, *154*, 5 – 12.

[4] Yuan, Z.; Taylor, N. J.; Sun, Y.; Marder, T. B.; Williams, I. D.; Cheng, L.-T.*J. Organomet. Chem.* **1993**, *449*, 27 – 37.

[5] (a) Lequan, M.; Lequan, R. M.; Ching, K. C. *J. Mater. Chem.* **1991**, 1, 997 – 999. (b) Lequan, M.; Lequan, R. M.; Ching, K. C.; Barzoukas, M.; Fort, A.; Lahoucine, H.; Bravic, B.; Chasseau, D.; Gaultier, J. *J. Mater. Chem.* **1992**, *2*, 719 – 725. (c) Lequan, M.; Lequan, R. M.; Chane-Ching, K.; Callier, A.-C.; Barzoukas, M.; Fort, A. *Adv. Mat. Opt. Electron.* **1992**, *1*, 243-247. (d) Branger, C.; Lequan, M.; Lequan, R. M.; Barzoukas, M.; Fort, A. *J. Mater. Chem.*, **1996**, *6*, 555 – 558.

[6] (a) Shirota, Y.; Kinoshita, M.; Noda, T.; Okumoto, K.; Takahiro, O. *J. Am. Chem. Soc.* **2000**, *122*, 11021 – 11022. (b) Doi, H.; Kinoshita, M.; Okumoto, K.; Shirota, Y. *Chem. Mater.* **2003**, *15*, 1080 – 1089.

[7] Allbrecht, K.; Kaiser, V.; Boese, R.; Adams, J.; Kaufmann, D. E. *J. Chem. Soc., Perkin Trans. 2* **2000**, 2153 – 2157.

[8] (a) Liu, Z.-Q.; Fang, Q.; Wang, D.; Xue, G., Yu, W.-T.; Shao, Z.-S.; Jiang, M.-H.; *Chem. Commun.* **2002**, 2900 – 2901. (b) Liu, Z.-Q.; Fang, Q., Wang, D.; Cao, D.-X.; Xue, G.; Yu, W.-T.; Lei, H. *Chem. - Eur. J.* **2003**, *9*, 5074 – 5084.

[9] Yamaguchi, S.; Shirasaka, T.; Tamao, K. *Org. Lett.* **2000**, *2*, 4129 – 4132.

[10] Jia, W.-L.; Bai, D.-R.; M^{c}Cormick, T.; Liu, Q.-D.; Motala, M.; Wang, R.-Y.; Seward, C.; Wang, S. *Chem. Eur. J.* **2004**, *10*, 994 – 1006.

[11] Kaim, W; Schultz, A. *Angew. Chem. Int. Ed.* **1984**, *23*, 615 – 616.

[12] Schultz, A.; Kaim, W. *Chem. Ber.* **1989**, *122*, 1863 – 1868.

[13] Fiedler, J.; Zalis, S.; Klein, A.; Hornung, F. M.; Kaim, W. *Inorg. Chem.* **1996**, *35*, 3039 – 3043.

[14] Lichtblau, A.; Kaim, W.; Scultz, A.; Stahl, T. *J. Chem. Soc., Perkin Trans. 2* **1992**, 1497 – 1501.

[15] Yuan, Z.; Taylor, N. J.; Ramachandran, R.; Marder, T. B. *Appl. Organomet. Chem.* **1996**, *10*, 305 – 316.

[16] Shirota, Y. *J. Mater. Chem.* **2000**, *10*, 1 – 25.

[17] (a) Noda, T.; Shirota, Y. *J. Am. Chem. Soc.* **1998**, *120*, 9714 – 9715. (b) Makinen, A. J.; Hill, I. G.; Noda, T.; Shirota, Y.; Kafafi, Z. H. *Appl. Phys. Lett.* **2001**, *78*, 670 – 672.

[18] (a) Noda, T.; Ogawa, H.; Shirota, Y. *Adv. Mater.* **1999**, *11*, 283 – 285. (b) Noda, T.; Shirota, Y. *J. Luminescence* **2000**, 1168 – 1170.

[19] Chen, B. J.; Zhang, X. H.; Lin, X. Q.; Kwang, H. L.; Wong, N. B.; Gambling, W. A.; Lee, S.T. *Synth. Met.* **2001**, *118*, 193 – 196.

[20] Zhou, J.; Pun, E. Y. B.; Chung, P. S.; Zhang, X. H. *Optics Commun.* **2001**, *191*, 427 – 433.

[21] (a) Hooz, J.; Akiyama, S.; Cedar, F. J.; Bennet, M. J.; Tuggle, R.M. *J. Am. Chem. Soc.* **1974**, *96*, 274 (b) Pelter, A.; Singaram, S.; Brown, H. C. *Tetrahedron Lett.* **1983**, *24*, 1433. (c) Entwistle, C. D.; Marder, T. B.; Smith, P. S.; Howard, J. A. K.; Fox, M. A.; Mason, S. A. *J. Organomet. Chem.* **2003**, *680*, 165-172.

[22] A lower value of ca. 18000 $dm^3mol^{-1}cm^{-1}$ has been previously recorded for this compound (Reference 27).

[23] Abe, J.; Nemoto, N.; Nagase, Y.; Shirai, Y.; Iyoda, T. *Inorg. Chem.* **1998**, *37*, 172-173.

[24] (a) Lamrani, M.; Hamasaki, R.; Mitsuichi, M.; Miyashita, T.; Yamamoto, Y. *Chem. Commun.* **2000**, 1595-1596. (b) Hamasaki, R.; Ito, M.; Lamrani, M.; Mitsuishi, M.; Miyashita, T.; Yamamoto, Y. *J. Mater. Chem.*, **2003**, *13*, 21-26.

[25] Grüner, B.; Janoušek, Z.; King, B. T.; Woodford, J. N.; Wang, C. H.; Všetecka, V.; Michl, J. *J. Am. Chem. Soc.* **1999**, *121*, 3122-3126.

[26] (a) Littger, R.; Taylor, J.; Rudd, G.; Newlon, A.; Allis, D.; Kotiah, S.; Spencer, J. T. in *Contemporary Boron Chemistry*, M. G. Davidson, A. K. Hughes, T. B. Marder, K. Wade (Eds.) Spec. Publ. No. 253, The Royal Society of Chemistry, Cambridge **2000**, 67-76. (b) Allis, D. G.; Spencer, J. T. *J. Organomet. Chem.* **2000**, *614*, 309-314. (c) Allis, D. G.; Spencer, J. T. *Inorg. Chem*, **2001**, *40*, 3373-3380.

[27] Yuan, Z. *Ph.D. Thesis, University of Waterloo, Waterloo, Ontario, Canada,* **1993**.

[28] Zakharkin, L.; Kovderov, A.I.; Olshevskaya, V.A. *Bull. Acad. Sci. USSR, Div. Chim. Sci. (Engl transl)* **1986**, *35*, 1260 – 1266.

[29] (a) Wu, R.; Schumm, J.S.; Pearson, D.L.; Tour, J.M. *J. Org. Chem.* **1996**, *61*, 6906 – 6921. (b) Rossi, R.; Carpita, A.; Lezzi, A. *Tetrahedron* **1984**, *40*, 2773 – 2780.

Chapter 4

Reaction of dimesitylborane with 2,5-diethynylpyridine: Unexpected formation of the novel tris-hydroboration product, 1-{dimesitylboryl}-2-{Z-1-dimesitylborylethylidene}-5-{E-dimesitylborylvinyl}-1,2-dihydropyridine.

4.1. Introduction

Compounds containing three – coordinate boron, usually in the form of the dimesitylboryl or other sterically demanding group, have been widely investigated for such purposes as fluoride ion sensors, [1,2] NLO active materials, [3,4,5,6,7,8] single [9,10] and two - photon [11] fluorescence. The electronic and structural properties of compounds containing two or more such groups have also been investigated. [5,12,13,14] Perhaps the most promising applications of stabilized, three-coordinate organoboranes lie in the field of molecular electronics, where the research groups of Shirota [15,16,17,18] and others [19,20] have shown these to be useful as both emitters and charge transporters.

Chujo *et al.* have synthesized a number of polymers containing three – coordinate boron in the main chain. [21] For example, hydroboration polymerization [22] of dialkynes with mesitylborane $\{MesBH_2\}_2$ (Mes = 2,4,6-trimethylphenyl) was used to generate polymers of the form $\{(Mes)B\text{-}CH{=}CH\text{-}X\text{-}CH{=}CH\}_n$ (where X = an organic π – system such as phenylenediyl, C_6H_4) that are related to the small molecules investigated by Marder *et al.* [5] In a later publication, hydroboration of 2,5-diethynylpyridine was reported to result in a low molecular weight polymer having a complex emission

spectrum (λ_{max} = 416, 495 and 593 nm) that was thermally stable up to 240 °C. [23] The group also reported having prepared the model, monomeric compound (Mes)B(CH=CH-2-pyridine)$_2$, but only the absorption maximum was given. In general, reaction of dimesitylborane,[24] $\{Mes_2BH\}_2$, with dialkynes of the form HC≡C-X-C≡CH cleanly provides compounds of the form E,E-Mes_2B-CH=CH-X-CH=CH-$BMes_2$ [5] (Scheme 4.1). As a part of our studies on compounds of this form, we attempted to synthesise the compound 2,5-bis(dimesitylborylvinyl)pyridine (**2m**) , initially using the same synthetic methodology as in the preparation of 1,4-bis(dimesitylborylvinyl)benzene (**2a**). This compound proved inaccessible, however, and instead, the title compound (**6**) was formed.

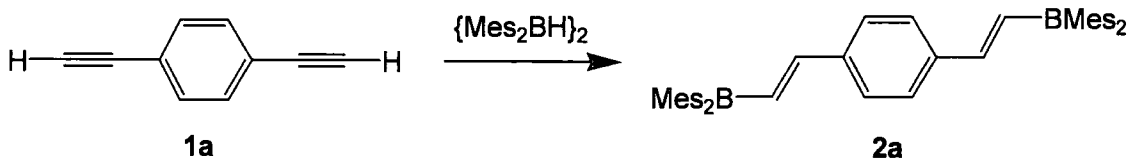

Scheme 4.1. Reaction of dimesitylborane with 1,4-diethynylbenzene, forming compound 2a.

4.2. Results and discussion

4.2.1 Synthesis

Dropwise addition of one molar equivalent of dimesitylborane dimer to a solution of 2,5-diethynylpyridine (**1m**) in THF resulted in the immediate formation of a dark brown solution, from which a brown – black intractable solid precipitated over several minutes. Attempts to purify this material were hampered by its low solubility in common organic solvents. Both TLC and NMR spectroscopy indicated that it consisted of a complex mixture of unreacted dimesitylborane, together with unidentified organoboryl

species and oligomers of diethynylpyridine. It was postulated, therefore, that dimesitylborane somehow induced the polymerization of diethynylpyridine. To prevent this undesired reaction from occurring, a solution of **1m** was added dropwise to a solution of one equivalent of dimesitylborane in THF, so as to maintain a low concentration of the alkyne in the reaction mixture. After overnight stirring and reaction work – up, a yellow - orange powder was isolated. Although this appeared to consist of a single component (by TLC), the ^{1}H-NMR spectrum was considerably more complex than that expected for **2m**, and mass spectrometry did not show the expected molecular ion of m/z = 627, with higher mass peaks also present. In addition, CHN analysis also differed considerably from calculated percentages for **2m**, with the nitrogen percentage being noticeably low (calculated for **2m** N = 2.23 %; observed N = 1.46 %). X-ray crystallography eventually revealed that the reaction had instead proceeded via a different stoichiometry, producing compound **6** (Scheme 4.2).

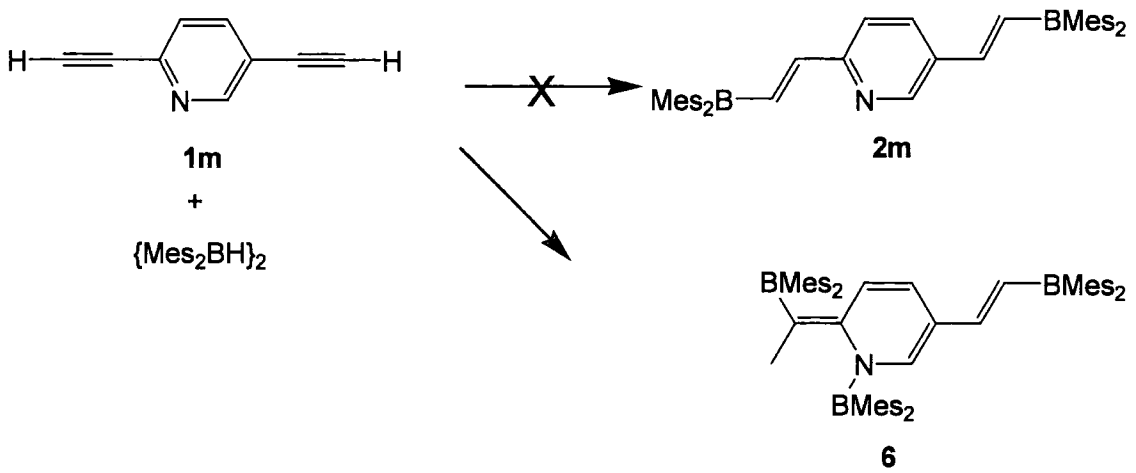

Scheme 4.2. The expected and observed reactions of dimesitylborane with 2,5-diethynylpyridine.

The complexity of the ^{1}H NMR spectrum can be explained by the presence of three distinct $BMes_2$ groups, with the $BMes_2$ group bound to nitrogen having restricted rotation due to a partial boron – nitrogen double bond, resulting in six peaks in the methyl region and four peaks in the aryl region. Such restricted rotation has been observed in the NMR spectra of products (**7a-c**) arising from the reaction of Mes_2BF·pyridine with organolithium reagents, as illustrated in Scheme 4.3. [25] In addition, the vinyl protons gave rise to a singlet (by coincidence) rather than the expected, characteristic, pair of doublets. Even with the use of DEPT and HSQC, it was impossible to unambiguously assign all peaks in the ^{13}C NMR spectrum. The CHN analysis is also much closer to the expected values for compound **6**, with discrepancies explained by the presence of acetone and hexane, both of which were observed in the unit cell of the crystal (1.5 and 0.5 molecules per unit cell respectively), which were not fully removed even by prolonged evacuation. Since some desolvation, presumably from less crystalline material, was observed under ambient temperature and pressure, the CHN analysis did not correspond exactly to the composition of solvated **6** as estimated from XRD or NMR. The higher mass ions observed in the MS are explained by the molecular ion $(M-1)^+$ (m/z = 876) and fragment ions.

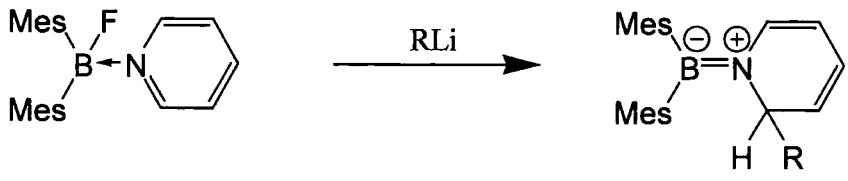

Scheme 4.3. Reaction of Mes_2BF·pyridine with organolithium reagents (R = Ph (7a), , Bu, (7b) 3-pyridyl (7c)).

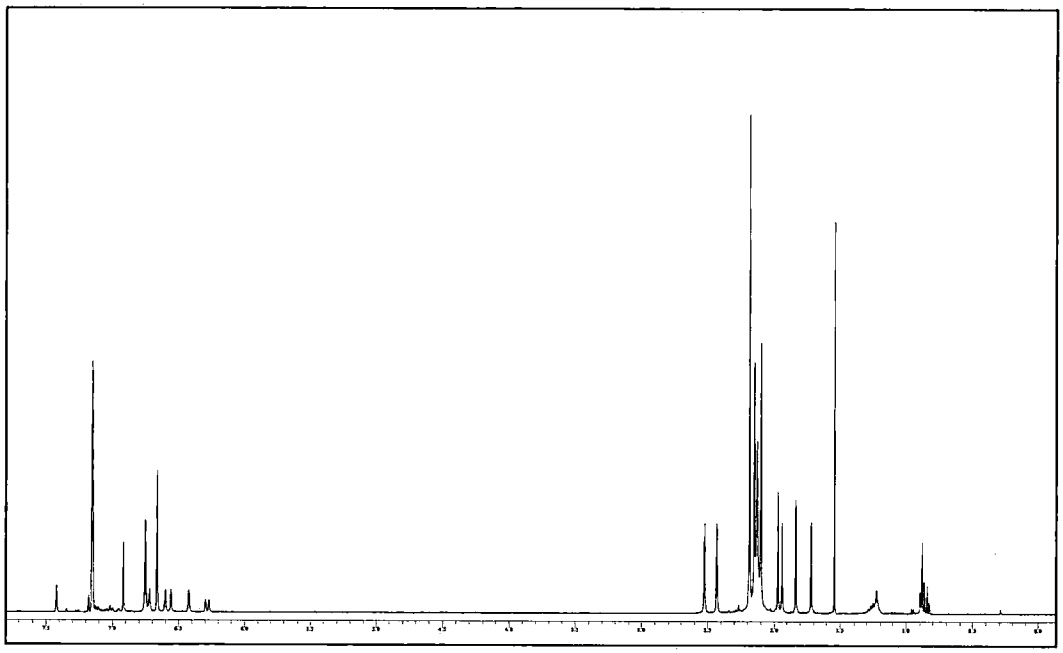

Figure 4.1. ^{1}H-NMR spectrum of Compound 6 (400 MHz, C_6D_6).

4.2.2. Structural properties.

Selected bond lengths and angles are presented in Table 4.1. The molecular structure of compound **6** is presented in Figure 4.2. The 1,2-dihydropyridine ring is unusually puckered: whilst C(2), C(3), C(4) and C(5) are coplanar, N(1) and C(6) deviate from this plane by 0.52 and 0.27 Å respectively. Whilst B(1) and B(2) have trigonal planar geometries, both N(1) and B(3) are somewhat pyramidalised, with a torsion angle of approximately 19.5° around the N-B bond (C(6)-N(1)-B(3)-C(61) = 21.5°, C(2)-N(1)-B(3)-C(51) = 17.5°). This feature diminishes the n(N)→p_z(B) overlap, resulting in a relatively long B-N bond length of 1.453(3) Å, somewhat longer than that found in the related compound **7a** (1.428(4) Å). The severe steric interactions in **6** are evident from

the C(9)-C(2)-N(1)-B(3) torsion angle of –49.9(2) °. The bond lengths and angles of the two Mes_2B-C groups are similar to those found in symmetric bis(dimesitylboryl)s.

Table 4.1. Selected bond lengths (Å) and bond angles (°) for compound 6.

Bond lengths (Å)		Bond angles (Å)	
N(1)-C(6)	1.409(2)	C(8)-B(1)-C(11)	118.70(2)
N(1)-C(2)	1.451(2)	C(8)-B(1)-C(21)	118.00(2)
N(1)-B(3)	1.453(3)	C(11)-B(2)-C(21)	123.35(19)
C(2)-C(9)	1.376(3)	C(9)-B(2)-C(31)	123.04(17)
C(9)-C(10)	1.507(3)	C(9)-B(2)-C(41)	115.40(17)
C(9)-B(2)	1.573(3)	C(31)-B(2)-C(41)	121.51(17)
C(2)-C(3)	1.452(3)	C(51)-B(3)-N(1)	121.19(18)
C(3)-C(4)	1.341(3)	C(61)-B(3)-N(1)	118.45(17)
C(4)-C(5)	1.444(3)	C(51)-B(3)-C(61)	120.10(17)
C(5)-C(6)	1.350(3)	B(3)-N(1)-C(2)	125.50(16)
C(5)-C(7)	1.452(3)	B(3)-N(1)-C(6)	118.18(16)
C(7)-C(8)	1.389(3)		
C(8)-B(1)	1.546(3)		

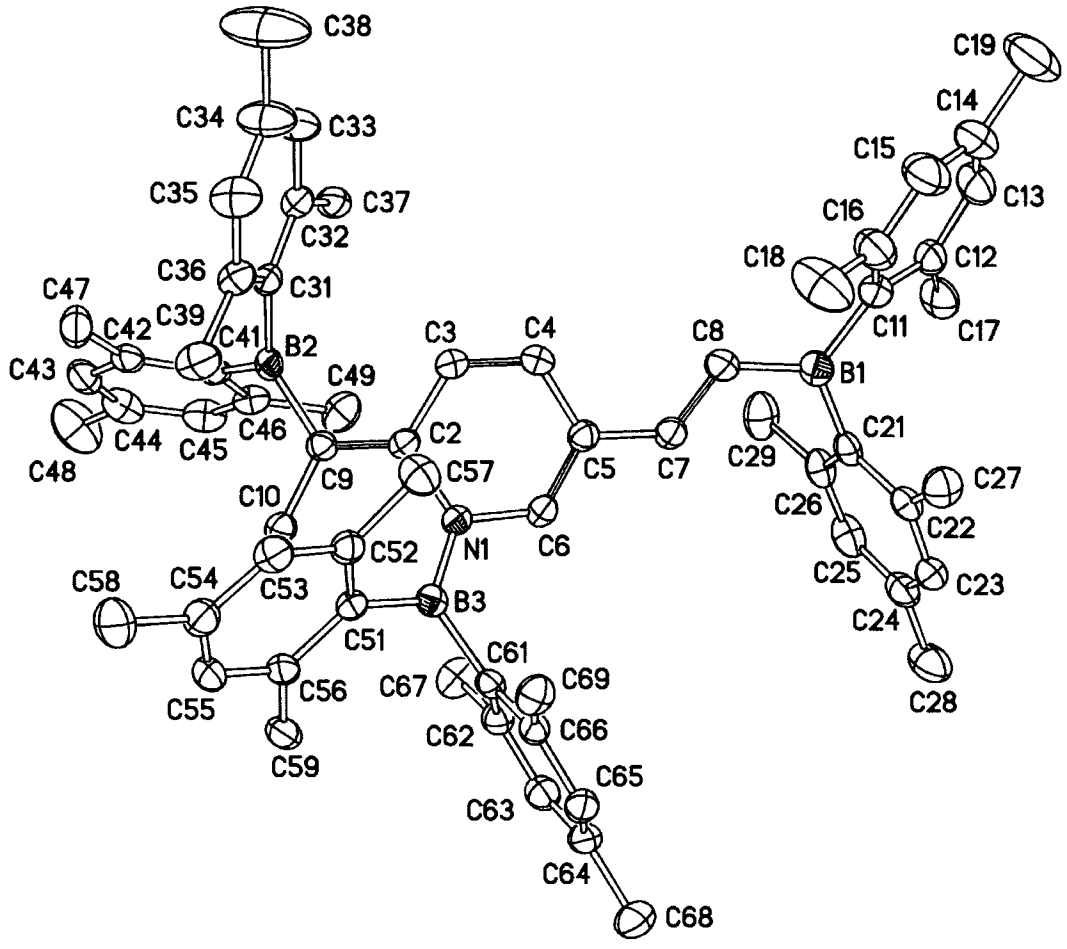

Figure 4.2. Molecular structure of compound 5, with thermal ellipsoids at 50% probability and hydrogen atoms omitted for clarity.

4.2.3. Thermal characteristics.

Thermogravimetric analysis (TGA) revealed that the thermal properties of compound **6** were rather similar to those of the related symmetric bis(dimesitylboryl)s. An initial loss of weight (ca. 5 %) attributed to desorption of solvent and / or moisture was observed from T = 90 °C to T = 120 °C, followed by decomposition at higher temperature (2 % weight loss at 170 °C) (Figure 4.3). Using a sufficiently high scan rate

(10 °C min^{-1}), it was possible to observe a broad melt by DSC (230 – 247 °C), with the broadness attributed to the presence of decomposition products (Figure 4.4). No glass transitions were observed, with the other apparent features in the DSC curve being due to fluctuations in the nitrogen pressure.

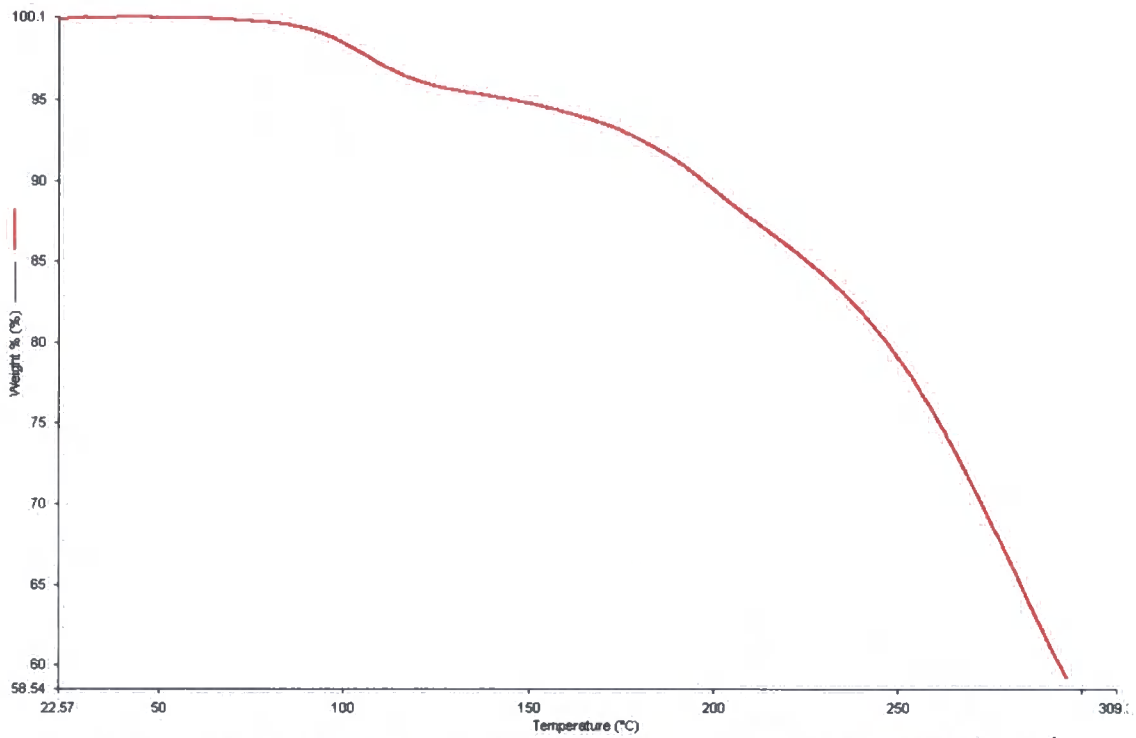

Figure 4.3. Weight loss as a function of temperature for compound 5 (scan rate 10 °Cmin^{-1}).

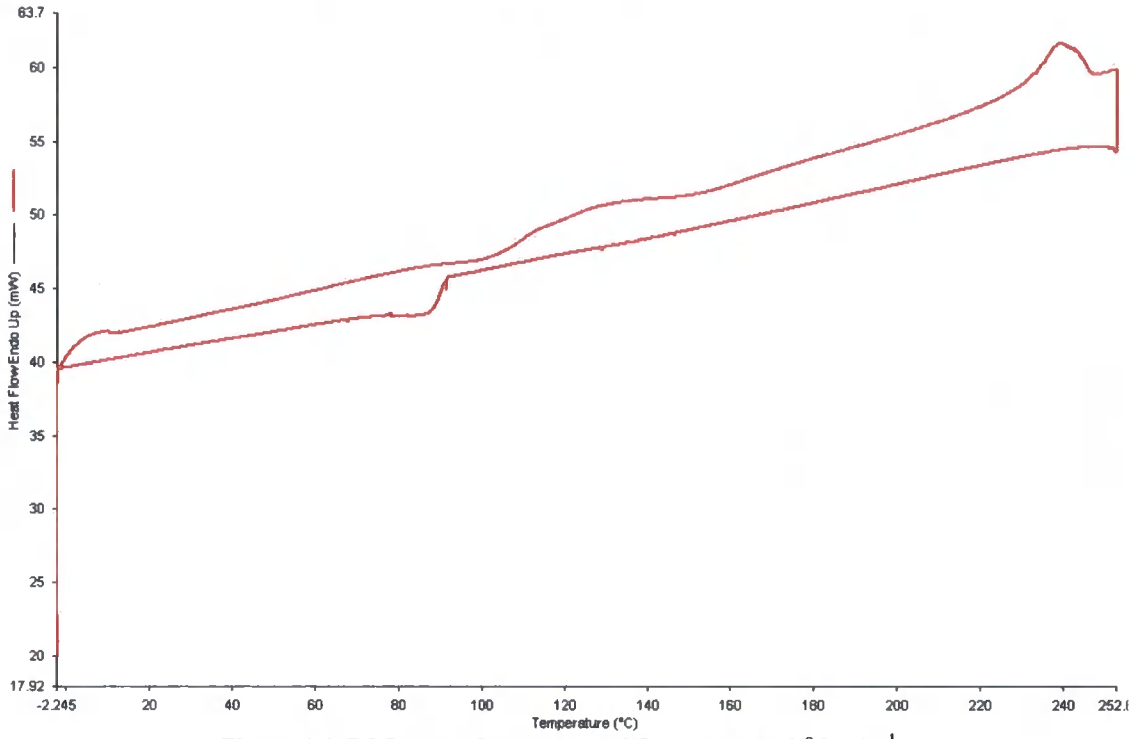

Figure 4.4. DSC curve for compound 5 (scan rate 10 °C min^{-1}).

4.2.4. Optical properties.

In common with other compounds containing the dimesitylboryl group, compound **6** exhibits an intense absorption at ca. 205 nm, assigned to $\pi - \pi^*$ transitions originating in the mesityl groups, with a lower energy absorption band assigned to the conjugated π backbone (Figure 4.5). This latter absorption occurs at lower energy than in related bis(boryl)s (λ_{max} = 428 nm), possibly due to the fact that the central pyridinyl moiety is not aromatic. It is accompanied by a distinct peak at higher energy (λ_{max} = 332 nm). Due to the spacing between these features (ca 100 nm, 7000 cm^{-1}), it seems unlikely that this is the result of vibrational splitting of a single absorption band such as has been observed in symmetric bis(boryl)s, and is more likely to be due to the complex nature of the π – system in this compound, but the exact nature of the electronic structure is unclear

at this time. It is also possible that it originates from a distinct chromophore involving the Mes_2BN group, which is not conjugated with the other Mes_2B groups. It is interesting to note that the position of absorption maximum is similar to the pyridine – based organoboron polymer reported by Chujo *et al* (λ_{max} = 450 nm), but whilst that polymer was highly fluorescent, compound **6** was not found to be fluorescent.

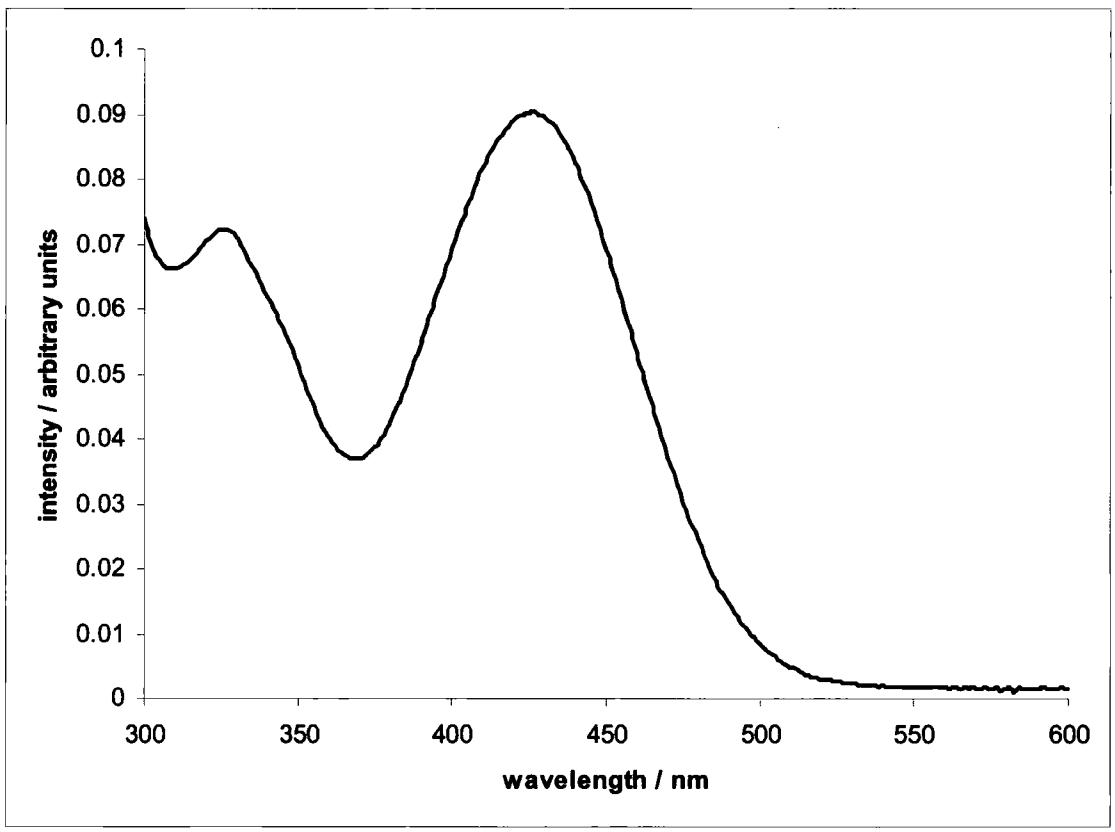

Figure 4.5. UV-visible absorption spectrum of compound 5 in cyclohexane solution.

4.2.5. Suggested reaction mechanism and computational analysis.

The molecular structure of compound **6** indicates that it was formed by the expected *cis* addition of Mes_2BH across the ethynyl group *meta* to nitrogen, with two other hydroborations occurring at the other side of the molecule: (i) a formal 1,2-Markovnikov addition, placing boron on C_α and hydrogen on C_β and (ii) a formal 1,4-hydroboration, placing boron on the nitrogen atom and another hydrogen on C_β. Whilst the mechanism is not yet clear, a suggested reaction mechanism is illustrated in Scheme 4.4. Dr. M.A. Fox has also performed *ab initio* calculations on the optimized geometry of the suggested intermediates (Table 4.2).

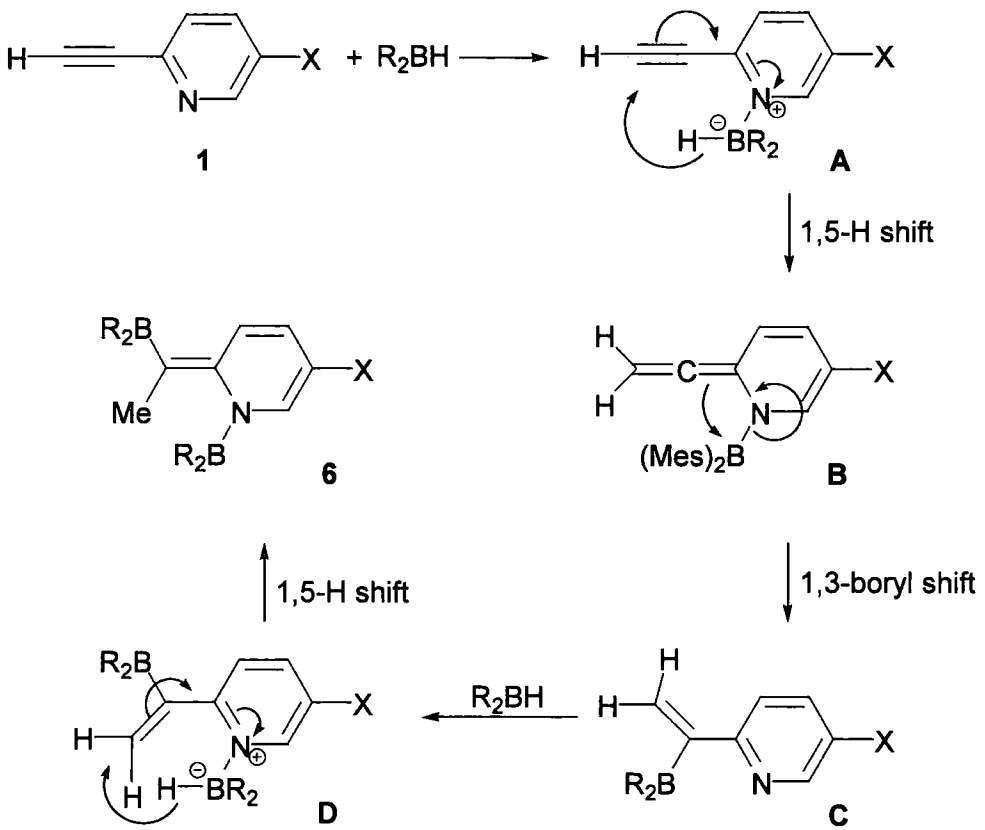

Scheme 4.4. Suggested reaction mechanism in the formation of compound 6. For synthesis, X = C≡CH, R = Mes; for calculations, X = H, R = 2,6-$Me_2C_6H_3$.

It seems likely that initial coordination of Mes_2BH to the pyridine moiety takes place, generating Intermediate **A**, [25] followed by a 1,5-hydride shift from boron to the terminal carbon of the 2-ethynyl group to form the propadiene **B**. Hydroboration of the propadiene moiety would be expected to place boron on the terminal carbon due to steric factors, [24b] but a 1,3-boryl shift allows for re-aromatisation of the pyridine ring (Intermediate **C**) and better accounts for the observed position of the Mes_2B groups in compound **6**. Coordination of a second molecule of Mes_2BH to pyridine (Intermediate **D**), with rotation of the C–C bond α to nitrogen, may then be followed by another 1,5-hydride shift to form the final product, **6**. The calculated energies of the intermediates decrease from **A** to **B** to **C**, indicating that the 1,5-hydride and 1,3-boryl shifts are thermodynamically favourable, and the model compound **6** (X = H, R = 2,6-$Me_2C_6H_3$) is substantially lower in energy than its isomer, Intermediate **D**.

Table 4.2. Calculated energies of Intermediates A-D and of model compound 6.

Compound	Total Energy / au	Rel. Energy / kcalmol^{-1}
Energies of intermediates A – C, at RHF / 6-31G*		
A	- 964.01257	+ 46.9
B	- 964.04040	+ 28.4
C	- 964.08290	0.0
Energies of isomers D, and model of 5, at RHF / 3-21G*		
D	- 1596.81221	+ 24.2
Model of 5	- 1526.84852	0.0

4.3. Conclusions

Attempted synthesis of the compound 2,5-bis(dimesitylborylvinyl)pyridine led instead to the isolation of the novel tris(boryl), compound **6**, which has been characterized by NMR spectroscopy, CHN analysis, mass spectrometry and single crystal X-ray diffraction. The optical and thermal characteristics of **6** have been investigated, and a suggested reaction mechanism for its formation has been evaluated by computational methods. The formation of **6** involves the rarely reported hydroboration of a pyridine, [26] and may cast doubt on the reported hydroboration polymerization of diethynlpyridine by Chujo *et al.*[23]

4.4. Experimental section.

4.4.1. General considerations

NMR spectra were recorded on a Bruker A400 at 400 MHz (^{1}H) and 100 MHz (^{13}C), and were referenced to residual C_6D_5H. Elemental analyses were performed in house. *Ab initio* geometry optimizations were carried out by Dr. M.A. Fox, using the Gaussian98 software package.[27] A crystal of compound **6** was cooled to 120 K using an Oxford Cryosytems Cryostream, [28] and reflections were collected on a Bruker SMART-CCD 6K diffractometer, [29,30] The structure was solved by direct methods and refined by full matrix least squares based on F^2 for all data using SHELXL-97 software.[31]

4.4.2. Preparation of 2,5-diethynylpyridine[32]

To a solution of 2,5-dibromopyridine (5.0 g, 21 mmol), $(Ph_3P)_2PdCl_2$ (0.3 g, 2 mol %) and one equivalent of CuI in triethylamine was added trimethylsilylacetylene (5.0

g, 51 mmol). After heating to 40 °C for 4 h, the mixture was concentrated to dryness by rotary evaporation and extracted with hexane (3 x 100 ml). The combined extracts were passed through a short column of neutral alumina, concentrated and refrigerated overnight. The resulting 2,5-bis(trimethylsilyl)pyridine (colourless crystalline solid) was removed by filtration (4.5 g, 78 %).

A solution of 2,5-bis(trimethylsilyl)pyridine (2.0 g, 7.4 mmol) in methanol (50 ml) and water (5 ml) was stirred over Na_2CO_3 for 2 h. The solid was removed by filtration, the filtrate was extracted with ether (5 x 50 ml) and the combined extracts were dried over $MgSO_4$. The solvent was removed by rotary evaporation and the resulting white powder was recrystallised from hexane to give **1m** in 65 % yield (0.61 g).

4.4.3. Preparation of 1-{dimesitylboryl}-2-{Z-1-dimesitylborylethylidene}-5-{E-dimesitylborylvinyl}-1,2-dihydropyridine (6).

To a stirred solution of dimesitylborane (0.50 g, 2.0 mmol in THF (20 ml) was added dropwise a solution of 2,5-diethynylpyridine (0.13 g, 1.0 mmol) in THF (15 ml) over 2 h. The solution immediately developed a bright yellow colour, darkening to orange after complete addition of the alkyne. After stirring overnight at RT, the solvent was removed *in vacuo* and the resulting orange powder suspended in ether (10 ml) and concentrated to dryness (x 3) to remove residual THF and washed with cold hexane (3 x 5 ml). Crude yield 0.54 g, 92 %. Pure **6** was obtained by column chromatography (silica, first with hexane, then hexane / acetone, 9:1) followed by recrystallization from hexane / acetone, 0.35 g, 60 %.

^{1}H NMR (400 MHz, C_6D_6) δ: 7.43 (d, 1H, $^{4}J_{H\text{-}H}$ 1.6 Hz, H-a), 7.19 (d, 1H, $^{3}J_{H\text{-}H}$ 9.6 Hz, He partially obscured by C_6D_5H), 6.93 (2H, H-b,c, singlet by coincidence), 6.76 (4H, Mes- a), 6.67 (s, 4H, Mes-b), 6.73, 6.61, 6.57, 6.43 (4 s, 4H, Mes-c), 6.30 (dd, 1H, $^{3}J_{H\text{-}H}$ 9.6 Hz, $^{4}J_{H\text{-}H}$ 1.6 Hz, H-d), 2.54, 2.44, 1.98, 1.95, 1.85, 1.73 (6 s, 18H, $BMes_2$-c), 2.20-2.11 (m, 39 H, $BMes_2$-a,b, C=C-Me), 1.55, (s, residual acetone), 1.2, 0.85 (m, residual hexanes). m/z (EI): 876 $(M\text{-}1)^{+}$, 756 (- mesitylene), 612.

CHN: Calculated for $C_{63}H_{74}B_3N$ C 86.21 %, H 8.50 %, N 1.60 %; Found for $C_{63}H_{74}B_3N(acetone)_n(hexane)_m$ C 85.47 %, H 8.84 %, N 1.46 %. (the values of n and m are unknown, since this depended on the extent of desolvation at the time of analysis).

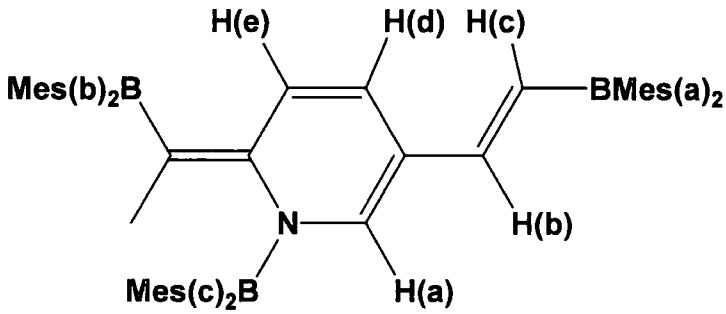

4.5. References

[1] (a) Yamaguchi, S.; Akiyama, S.; Tamao, K. *J. Am. Chem. Soc.* **2000**, *122*, 6335. (b) Yamaguchi, S.; Akiyama, S.; Tamao, K. *J. Am. Chem. Soc.* **2001**, *123*, 11372. (c) Yamaguchi, S.; Akiyama, S.; Tamao, K. *J. Organomet. Chem.* **2002**, *652*, 3. (d) Yamaguchi, S.; Shirasaka, T.; Akiyama, S.; Tamao, K. *J. Am. Chem. Soc.* **2002**, *124*, 8816. (e) Yamaguchi, S.; Shirasaka, T.; Tamao, K. *Org. Lett.* **2000**, *2*, 4129.

[2] (a) Jai, W-L.; Song, D.; Wang, S. *J. Org. Chem.* **2002**, *68*, 701. (b) Jia, W.-L.; Bai, D.-R.; M^{c}Cormick, T.; Liu, Q.-D.; Motala, M.; Wang, R.-Y.; Seward, C.; Wang, S. *Chem. Eur. J.* **2004**, *10*, 994.

[3] (a) Yuan, Z.; Taylor, N. J.; Marder, T. B.; Williams, I. D.; Kurtz, S. K.; Cheng, L-T.; *J. Chem. Soc., Chem. Commun.* **1990**, 1489. (b) Yuan, Z.; Taylor, N. J.; Marder, T. B.; Williams, I. D.; Cheng, L.-T. in *Organic Materials for Non-linear Optics II, Spec. Publ. No. 91* (Eds.: R. A. Hann and D. Bloor), The Royal Society of Chemistry, Cambridge, **1991**, pp. 190 – 194.

[4] Yuan, Z.; Taylor, N. J.; Sun, Y.; Marder, T. B.; Williams, I. D.; Cheng, L.-T. *J. Organomet. Chem.* **1993**, *449*, 27.

[5] Yuan, Z.; Taylor, N. J.; Ramachandran, R.; Marder, T. B. *Appl. Organomet. Chem.* **1996**, *10*, 305.

[6] (a) Lequan, M.; Lequan, R. M.; Ching, K. C. *J. Mater. Chem.* **1991**, 1, 997. (b) Lequan, M.; Lequan, R. M.; Ching, K. C.; Barzoukas, M.; Fort, A.; Lahoucine, H.; Bravic, B.; Chasseau, D.; Gaultier, J. *J. Mater. Chem.* **1992**, *2*, 719. (c) Lequan, M.; Lequan, R. M.; Chane-Ching, K.; Callier, A.-C.; Barzoukas, M.; Fort, A. *Adv. Mat. Opt. Electron.* **1992**, *1*, 243. (d) Branger, C.; Lequan, M.; Lequan, R. M.; Barzoukas, M.; Fort, A. *J. Mater. Chem.*, **1996**, *6*, 555.

[7] Branger, C.; Lequan, M.; Lequan, R. M.; Large, M.; Kajzar, F. *Chem. Phys. Lett.* **1997**, *272*, 265.

[8] Zhou, J.; Pun, E. Y. B.; Chung, P. S.; Zhang, X. H. *Optics Commun.* **2001**, *191*, 427.

[9] (a) Glogowski, M. E.; Williams, J. L. R. *J. Organomet. Chem.* **1981**, *218*, 137. (b) Williams, J. L. R.; Grisdale, P. J.; Doty, J. C. *J. Org. Chem.* **1971**, *36*, 544. (c) Doty, J. C.; Babb, B.; Grisdale, P. J.; Glogowski, M.; Williams, J. L. R. *J. Organomet. Chem.* **1972**, *38*, 229. (d) Glogowski, M. E.; Williams, J. L. R. *J. Organomet. Chem.* **1981**, *216*, 1. (e) Glogowski, M. E.; Zumbulyadis, N.; Williams, J. L. R. *J. Organomet. Chem.* **1982**, *231*, 97.

[10] Allbrecht, K.; Kaiser, V.; Boese, R.; Adams, J.; Kaufmann, D. E. *J. Chem. Soc., Perkin Trans. 2* **2000**, 2153.

[11] (a) Liu, Z-Q.; Fang, Q.; Wang, D.; Xue, G., Yu, W-T.; Shao, Z-S.; Jiang, M-H.; *J. Chem. Soc. Chem. Commun.* **2002**, 2900. (b) Liu, Z-Q.; Fang, Q., Wang, D.; Cao, D-X.; Xue, G.; Yu, W-T.; Lei, H. *Chem. Eur. J.* **2003**, *9*, 5074.

[12] (a) Kaim, W; Schultz, A. *Angew. Chem. Int. Ed.* **1984**, *23*, 615. (b) Schultz, A.; Kaim, W. *Chem. Ber.* **1989**, *122*, 1863. (c) Fiedler, J.; Zalis, S.; Klein, A.; Hornung, F. M.; Kaim, W. *Inorg. Chem.* **1996**, *35*, 3039.

[13] (a) Okada, K.; Sugawa, T.; Oda, M.; *J. Chem. Soc., Chem. Commun.* **1992**, 74. (b) Rajca, A.; Rajca, S.; Desai, S. R.; *J. Chem. Soc. Chem., Commun.* **1995**, 1957.

[14] Lichtblau, A.; Kaim, W.; Scultz, A.; Stahl, T. *J. Chem. Soc., Perkin Trans. 2* **1992**, 1497.

[15] (a) Noda, T.; Shirota, Y. *J. Am. Chem. Soc.* **1998**, *120*, 9714. (b) Makinen, A. J.; Hill, I. G.; Noda, T.; Shirota, Y.; Kafafi, Z. H. *Appl. Phys. Lett.* **2001**, *78*, 670. (c) Noda, T.; Ogawa, H.; Shirota, Y. *Adv. Mater.* **1999**, *11*, 283. (d) Noda, T.; Shirota, Y. *J. Luminescence* **2000**, 1168.

[16] Kinoshita, M.; Shirota, Y. *Chem. Lett.* **2001**, 614.

[17] Kinoshita, M.; Fujii, N.; Tsuzuki, T.; Shirota, Y. *Syn. Met.* **2001**, *121*, 1571.

[18] (a) Shirota, Y.; Kinoshita, M.; Noda, T.; Okumoto, K.; Takahiro, O. *J. Am. Chem. Soc.* **2000**, *122*, 11021. (b) Doi, H.; Kinoshita, M.; Okumoto, K.; Shirota, Y. *Chem. Mater.* **2003**, *15*, 1080.

[19] Hamada, Y.; Adachi, C.; Tsutsui, T.; Saito, S. *Jpn. J. Appl. Phys.* **1992**, *31*, 1812.

[20] Chen, B. J.; Zhang, X. H.; Lin, X. Q.; Kwang, H. L.; Wong, N. B.; Gambling, W. A.; Lee, S.T. *Syn. Met.* **2001**, *118*, 193.

[21] (a) Matsumi, K.; Chujo, Y. in *Contemporary Boron Chemistry, Spec. Publ. No. 253* (Eds.: M. G. Davidson, A. K. Hughes, T. B. Marder, K. Wade), The Royal Society of Chemistry, Cambridge, **2000**, pp. 51 – 58. (b) Chujo, Y.; Takiza, N.; Sakurai, T. *J. Chem. Soc., Chem. Commun.* **1994**, 227 – 228. (c) Chujo, Y. *J. Macromol. Sci. Pure* **1994**, *A3*, 1647 – 1655. (d) Chujo, Y.; Sakarai, T.; Takizawa, N. *Polym. Bull.* **1994**, *33*, 623 – 628. (e) Chujo, Y.; Morimoto, M.; Tomita, I. *Polym. J.* **1994**, *27*, 90 – 97. (f) Matsumi, N.; Chujo, Y. *Polym. Bull.* **1997**, *39*, 295 – 302. (g) Matsumi, N.; Chujo, Y. *Polym. Bull.* **1997**, *38*, 531 – 536. (h) Chujo, Y. *Macromol. Symp.* **1997**, *118*, 111 – 116. (i) Matsumi, N.; Chujo, Y. *Macromolecules* **1998**, *31*, 3155 – 3157. (j) Miyata, M.; Matsumi, N.; Chujo, Y. *Polym. Bull.* **1999**, *42*, 505 – 510. (k) Chujo, Y.; Sasaki, Y.; Kinomura, N.; *Polymer* **2000**, *41*, 5047 – 5051. (l) Miyata, M.; Meyer, F.; Chujo, Y. *Polym. Bull.* **2001**, *46*, 23 – 28. (m) Matsumi, N.; Chujo, Y.

Polym. J. **2001**, *33*, 383 – 386. (n) Miyata, M.; Chujo, Y. *Polym. J.* **2002**, *34*, 967 – 969.

[22] Matsumi, N.; Chujo, Y. *J. Am. Chem. Soc.* **1998**, *120*, 5112 – 5113.

[23] Matsumi, N.; Miyata, M.; Chujo, Y. *Macromolecules* **1999**, *32*, 4467.

[24] (a) Hooz, J.; Akiyama, S.; Cedar, F.J.; Bennet, M.J.; Tuggle, R.M. *J. Am. Chem. Soc.* **1974**, *96,* 274 (b) Pelter, A.; Singaram, S.; Brown, H.C. *Tetrahedron Lett.* **1983**, *24*, 1433. (c) Entwistle, C.D.; Marder, T.B.; Smith, P.S.; Howard, J.A.K.; Fox, M.A.; Mason, S.A. *J. Organometal. Chem.* **2003**, *680*, 165.

[25] Okada, K.; Sujuki, R.; Oda, M. *J. Chem. Soc. Chem. Commun.* **1995**, 2069.

[26] For a recent report of formal 1,4-hydroboration of pyridine, see Braunschweig, H.; Colling, M.; Hu, C. *Inorg. Chem.* **2003**, *42*, 941.

[27] Gaussian 98, Revision A.9, Frisch, M.J.; Trucks, G.W.; Schlegel, H.B.; Scuseria, G.E.; Robb, M.A.; Cheeseman, J.R.; Zakrzewski, V.G.; Montgomery, J.A. Jr.; Stratmann, R.E.; Burant, J.C.; Dapprich, S.; Millam, J.M.; Daniels, A.D.; Kudin, K.N.; Strain, M.C.; Farkas, O.; Tomasi, J.; Barone, J.; Cossi, M.; Cammi, R.; Mennucci, B.; Pomelli, C.; Adamo, C.; Clifford, S.; Ochterski, J.; Petersson, G.A.; Ayala, P.Y.; Cui, Q.; Morokuma, K.; Malick, D.K.; Rabuck, A.D.; Raghavachari, K.; Foresman, J.B.; Cioslowski, J.; Ortiz, J.V.; Baboul, A.G.; Stefanov, B.B.; Liu, G.; Liashenko, A.; Piskorz, P.; Komaromi, I.; Gomperts, R.; Martin, R.L.; Fox, D.J.; Keith, T.; Al-Laham, M.A.; Peng, C.Y.; Nanayakkara, A.; Challacombe, M.; Gill, P.M.W.; Johnson, B.; Chen, W.; Wong, M.W.; Andres, J.L.; Gonzalez, C.; Head-Gordon, M.; Replogle, E.S.; and Pople, J.A.; Gaussian, Inc., Pittsburgh PA, 1998.

[28] Cosier, J.; Glazer, A.M. *J Appl. Cryst.* **1986**, *19*, 105.

[29] Bruker SMART-V5.625. Data Collection Software. Siemens Analytical X-ray Instruments Inc., Madison, Wisconsin, USA.

[30] Bruker SAINT-V6.28A. Data Reduction Software. Siemens Analytical X-ray Instruments Inc., Madison, Wisconsin, USA.

[31] Sheldrick, G.M.; SHELXL-97: University of Göttingen, **1997**

[32] Gelman, D.; Tsvelikhovsky, D.; Molander. G.A.; Blum, J. *J. Org. Chem.* **2002**, *67*, 6287-6290.

Chapter 5

Dimesitylborane Monomer-Dimer Equilibrium in Solution, the Solid-State Structure of the Dimer by Single Crystal Neutron and X-Ray Diffraction and Structural Comparisons with Related Compounds.

5.1. Introduction

Dimesitylborane, first synthesised in 1974 by Hooz *et al.*, is a sterically hindered diarylborane. [1] Its chemistry was investigated by Pelter *et al.*[2], who found it to be relatively unreactive, reacting only slowly with alkenes at room temperature but rapidly with alkynes, thus allowing the selective monohydroboration of compounds having both alkene and alkyne moieties. In addition, hydroborations were found to be very sensitive to substrate steric effects, with preferential reaction with terminal alkenes or alkynes in the presence of disubstituted acetylenic or vinylic compounds. In the context of the present work, there was no evidence for hydroboration of the central vinyl bond of *trans*-1,4'-diethynylstilbene. The resulting triorganoboranes contained almost exclusively terminal dimesitylboryl groups. The regio- and steriospecificity of dimesitylborane hydroborations has led to its use in the synthesis of air and moisture stable three-coordinate organoboranes and, in particular, the synthesis of conjugated organic materials where the organic π system interacts with the vacant p-orbital situated on boron. [3,4,5,6] Hydrolysis is prevented by the sterically demanding mesityl groups, which block the approach of nucleophiles by

forming a "cage" around the vacant p-orbital with their *ortho* methyl groups. Such materials have been shown to have interesting optical and electronic properties, and are promising candidates for use in a wide range of organic electronic devices. [3,4,5,6,7,8,9,10,11,12,13]

During our research into the properties of conjugated organic materials containing the dimesitylboryl group, we noticed that the NMR spectra of dimesitylborane always contained minor peaks that did not correspond to dimeric dimesitylborane. These peaks remained after repeated recrystallisations and washings, indicating that they were not the result of any impurity. Further investigation suggested that in solution, dimesitylborane dimer exists in equilibrium with its monomer (Scheme 5.1.). Although it is generally accepted that diboranes react with unsaturated compounds via a π-complex involving monomeric borane, [14] there is little direct experimental evidence to support this, with bis(pentafluorophenyl)borane [15] and 10-trimethylsilyl-9-borabicyclodecane-H (10-TMS-9-BBD-H) [16] (Figure 5.2) being the only other experimentally observed cases of monomer-dimer equilibrium in solution for an organoborane. Monomeric organoboranes are rare, two known examples being the exceptionally hindered di(2,4,6-tri-isopropylphenyl)borane (ditripylborane) [17] and bis(2,3-dimethyl-2-butyl)borane (dithexylborane). [18] Dioxaborolanes such as catecholborane (HBcat, cat = 1,2-$O_2C_6H_4$), commonly used in hydroborations, are also monomeric [19,20] (Figure 5.1). We therefore decided to investigate this equilibrium by variable concentration and variable temperature multinuclear NMR spectroscopy, and by ^{11}B NMR in supercritical carbon dioxide ($scCO_2$). We have also used computational methods to predict the structures, binding energy of the dimer and ^{11}B NMR chemical shifts of both monomer and dimer, and

have reinvestigated the solid-state structure of dimesitylborane (first solved from X-ray data by Power *et al.* in 1990) [17] by X-ray and neutron diffraction. This study represents one of few cases where neutron diffraction has been used to solve the structure of a compound containing one or more B-H bonds,[21,22] and is the only simple diborane (6) compound to have been studied. We have also obtained the structure of the related compound dimesitylfluoroborane ($(Mes)_2BF$).

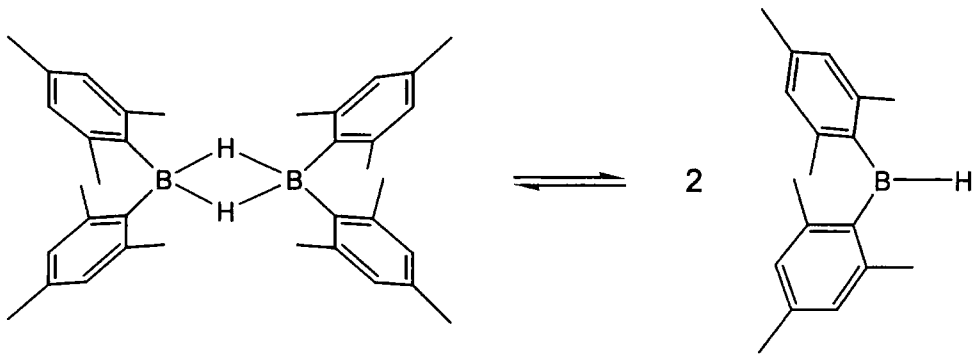

Scheme 5.1. Schematic representation of dimesitylborane dissociation.

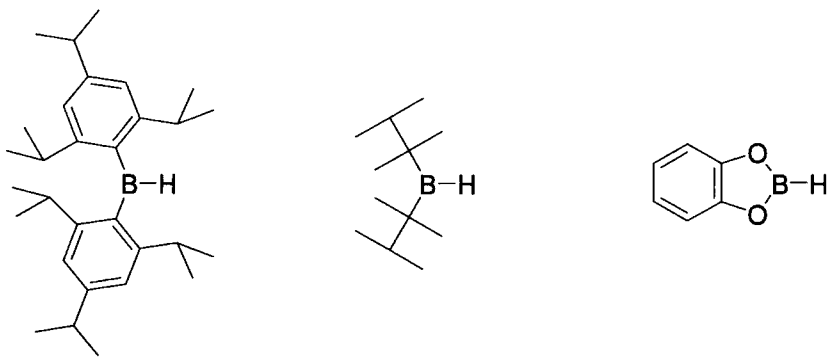

Figure 5.1. Monomeric boranes ditripylborane, dithexylborane and catecholborane.

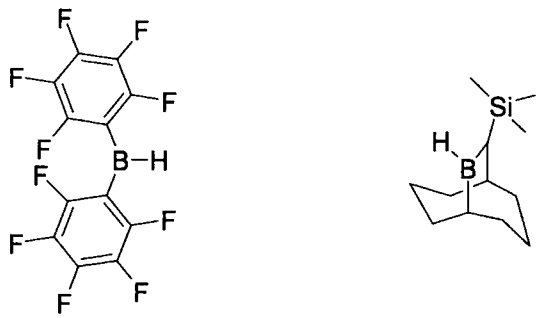

Figure 5.2. Monomeric forms of boranes known to exist in both monomeric and dimeric forms in solution, bis(pentafluorophenyl)borane and 10-trimethylsilyl-9-borabicyclodecane-H.

5.2. Results and Discussion

5.2.1 NMR results

The $^{11}B\{^1H\}$ NMR spectrum of dimesitylborane in d_8-toluene or d_6-benzene at room temperature shows two broad peaks corresponding to monomer (73.3 ppm) and dimer (25.9 ppm). Even without proton decoupling, neither of the peaks show any splitting in their ^{11}B NMR spectrum, almost certainly because of the broadness of the peaks, which is attributed to a combination of slow tumbling due to steric bulk (resulting in inhomogeneity) and the presence of the quadrupolar boron nucleus (resulting in highly efficient relaxation). In the case of the dimesitylborane monomer, these factors are compounded by the fact that the boron atom is three-coordinate, but the steric bulk is much reduced when compared to the dimer. At room temperature, the peak width at half height is approximately 380 Hz (monomer) and 770 Hz (dimer). The broad peak at ca. 50 ppm corresponds to traces of dimesitylborinic acid (Mes_2BOH, <1%) formed by hydrolysis of dimesitylborane by traces of water.

In THF solution, the NMR spectrum again shows two peaks, corresponding to monomer and dimer. The dimer peak is shifted upfield by approximately 3 ppm to 22.9 ppm, whilst the monomer peak is shifted upfield by approximately 8 ppm to 65.1 ppm. This is in contrast to bis(pentafluorophenyl)borane, which forms the isolable complex $(C_6F_5)_2BH{\bullet}THF$ (^{11}B, δ = -1.6), which is a very weak hydroborating agent.[15] Dimesitylborane may be recrystallised from THF, the resulting solid having no THF present by ^1H-NMR, and hydroborations proceed efficiently in THF solution. However, solutions of dimesitylborane in THF have a higher proportion of monomer than those of the same overall concentration of dimesitylborane in aromatic solvents (approximately double the proportion for a 0.1 M solution at ambient temperature), indicating that some stabilisation of the monomer by coordination to THF does occur.

There may be some contribution in the form of a labile complex, which must be short-lived on the NMR timescale, as evidenced by the greater upfield shift of the monomer peak position compared to that of the dimer, though it should be noted that differences in solvation alone may be enough to explain this effect.

Proton-NMR chemical shifts are presented in Table 5.1, and a typical proton spectrum is shown in Figure 5.3. Without boron decoupling, the monomer B-H peak is not visible and the dimer B-H peak is considerably broadened. The dimer shows evidence of hindered rotation of the mesityl groups, with the aryl-H and *ortho*-methyl-H peaks each giving rise to two singlets; the corresponding groups appear as single peaks in the monomer indicating that reduced steric crowding allows free rotation about the B-C bonds. Though well resolved, the low intensity of the monomer B-H resonance under most conditions precluded its use in calculations. The methyl group region is slightly crowded but the aryl region is well resolved at 500 MHz, so this region was used to quantify the ^{1}H-NMR spectra.

Table 5.1. $^{1}H\{^{11}B\}$ NMR chemical shifts and relative intensities in C_6D_6 at ambient temperature.

	B-H	Aryl	Methyl
Dimer	4.26, s, 2H	6.66, s, 4H; 6.54, s, 4H	2.19, s, 12H; 2.16, s, 12H; 2.01, s, 12H
Monomer	8.17, s, 1H	6.75, s, 4H	2.24, s, 12H; 2.10, s, 6H

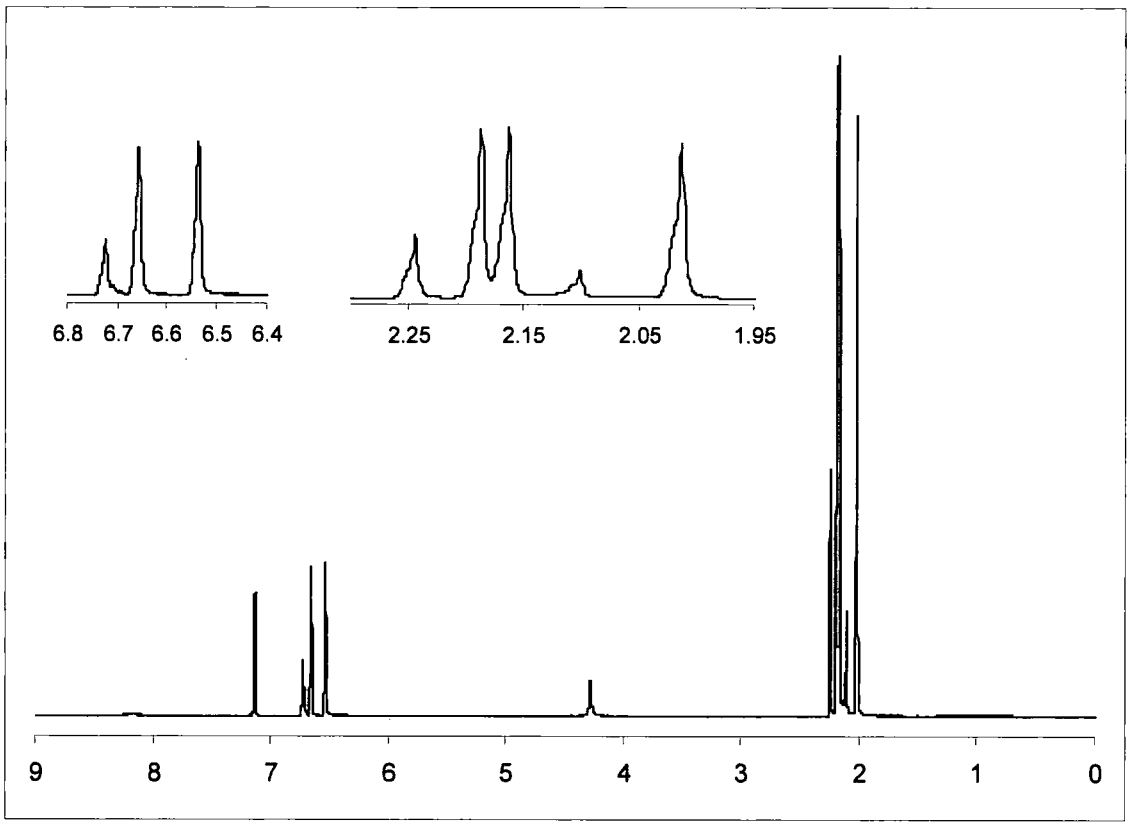

Figure 5.3. $^{1}H\{^{11}B\}$ NMR spectrum of dimesitylborane

5.2.2 Variable concentration NMR study

To examine the effect of varying the concentration on the position of the monomer-dimer equilibrium, a series of solutions was prepared by successive dilution and examined by $^{11}B\{^{1}H\}$ and $^{1}H\{^{11}B\}$ NMR spectroscopy (Figures 5.4. and 5.5.). As the total concentration of dimesitylborane is reduced, the relative concentration of the monomer increases as expected, since dissociation is expected to be a first-order process whereas association is expected to be second-order. From this experiment, the ambient temperature dissociation constant, K_{diss}, was calculated from the total concentration of dimesitylborane and the percentage of monomer present in a given solution, and was found to be $(3.2 \pm 0.4) \times 10^{-3}$ mol dm^{-3} (combined ^{1}H and ^{11}B data).

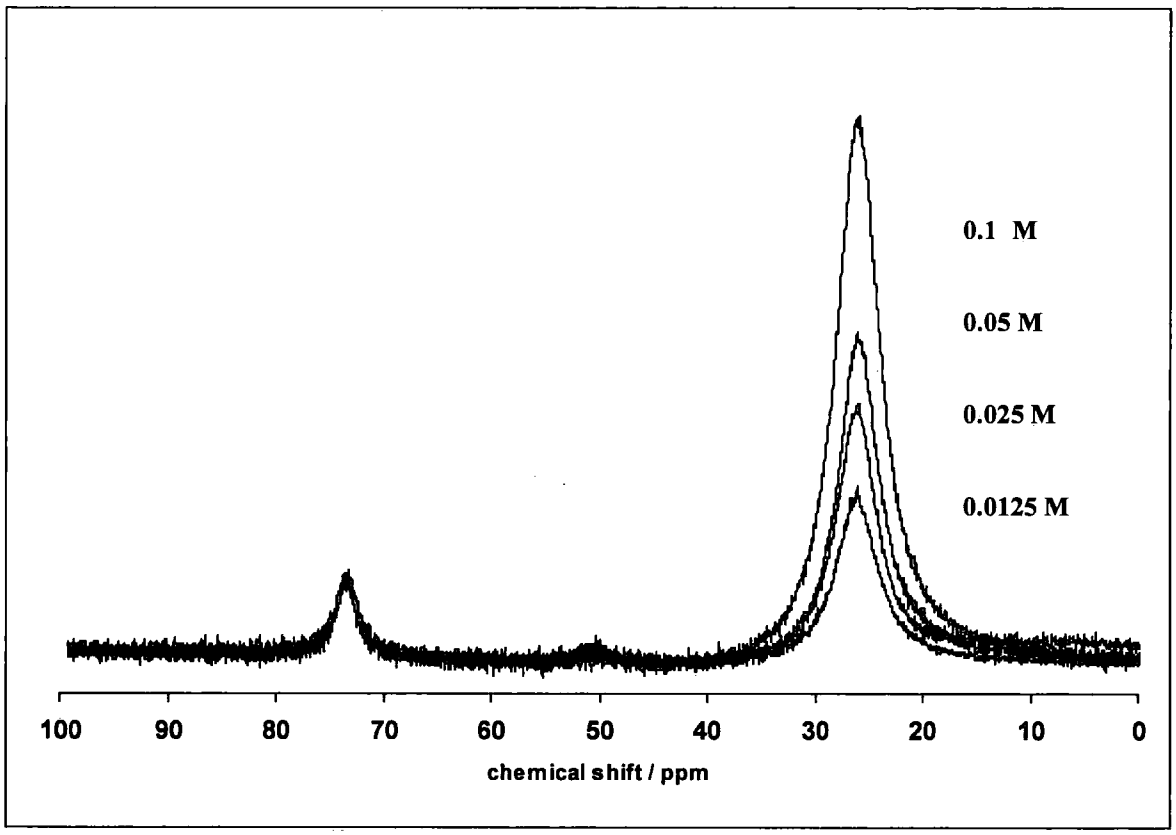

Figure 5.4. Effect of varying dimesitylborane concentration on $^{11}B\{^1H\}$ spectra, normalised to monomer intensity.

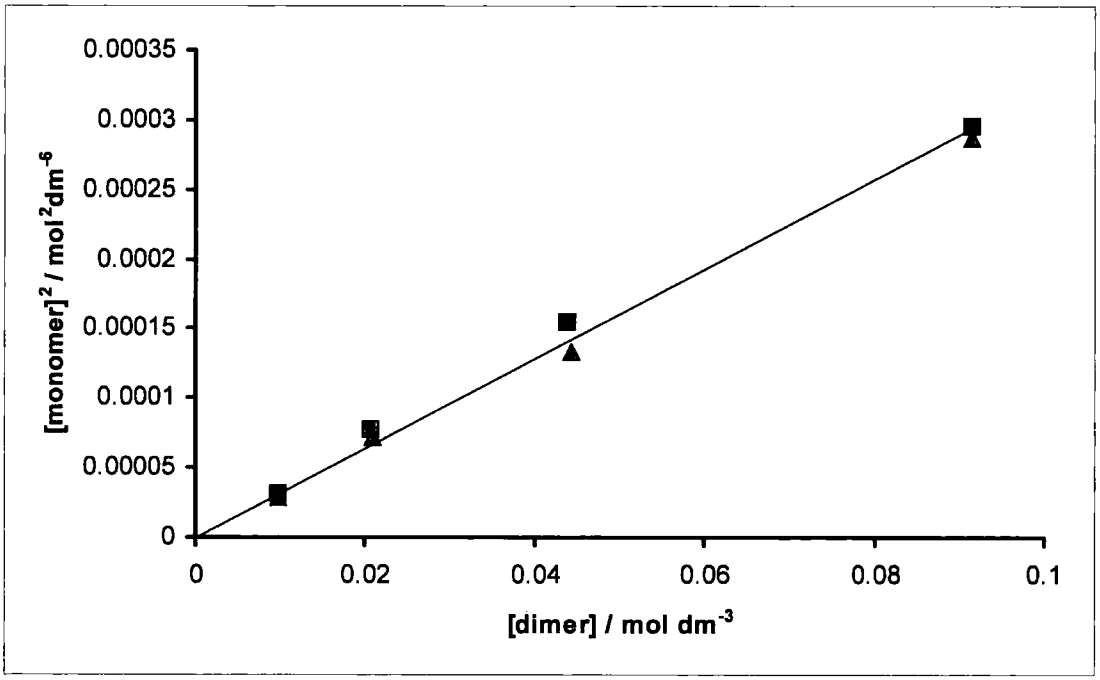

Figure 5.5. Plot of concentration (monomer) ^{2} vs. concentration (dimer), ^{11}B-data (▲) and ^1H-data (■).

5.2.3 Variable temperature NMR study

A solution of dimesitylborane in deuterated toluene was examined by variable temperature NMR spectroscopy from 203 K to 333 K (Figure 5.6). As temperature increases, the proportion of monomer increases from approximately zero at 253 K to ca. 50 percent at 333 K. The line width in the $^{11}B\{^1H\}$ NMR spectrum was also strongly temperature dependent, decreasing from 3000 Hz (dimer, 203 K) to 640 Hz (dimer, 333 K). The monomer/dimer peaks showed no evidence of coalescence even at 333 K, indicating a very slow rate of exchange. A van't Hoff plot of $-\ln[K_{diss}(T)]$ vs. 1/T (Figure 5.7) was used to determine the enthalpy of dissociation, ΔH_{diss}, which was found to be 70 kJ mol^{-1}. The value of ΔS for dissociation (from a plot of $\Delta G/T$ vs. 1/T) was calculated to be 212 J $K^{-1}mol^{-1}$, similar to that found for 10-TMS-9-BBD-H (-198 J K^{-1} mol^{-1} for association of monomer),[16] though it should be noted that the relatively small temperature range may lead to correspondingly large errors in the calculation.

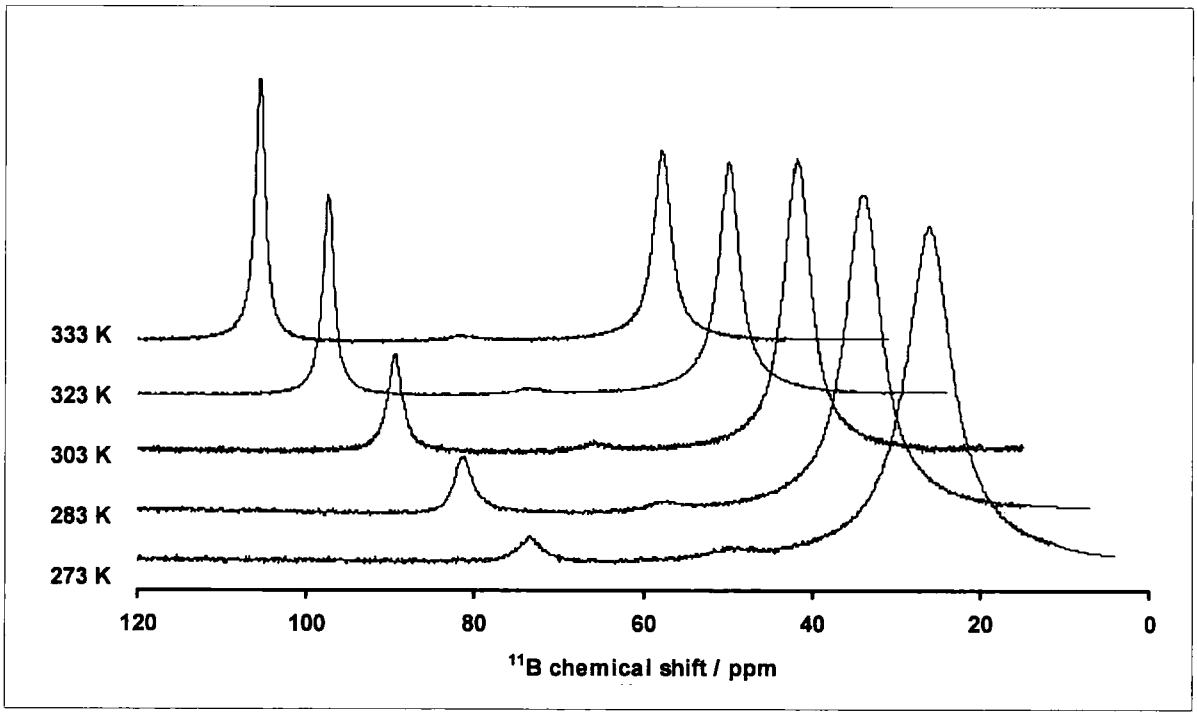

Figure 5.6. Effect of varying temperature on the $^{11}B\{^1H\}$ spectrum of dimesitylborane.

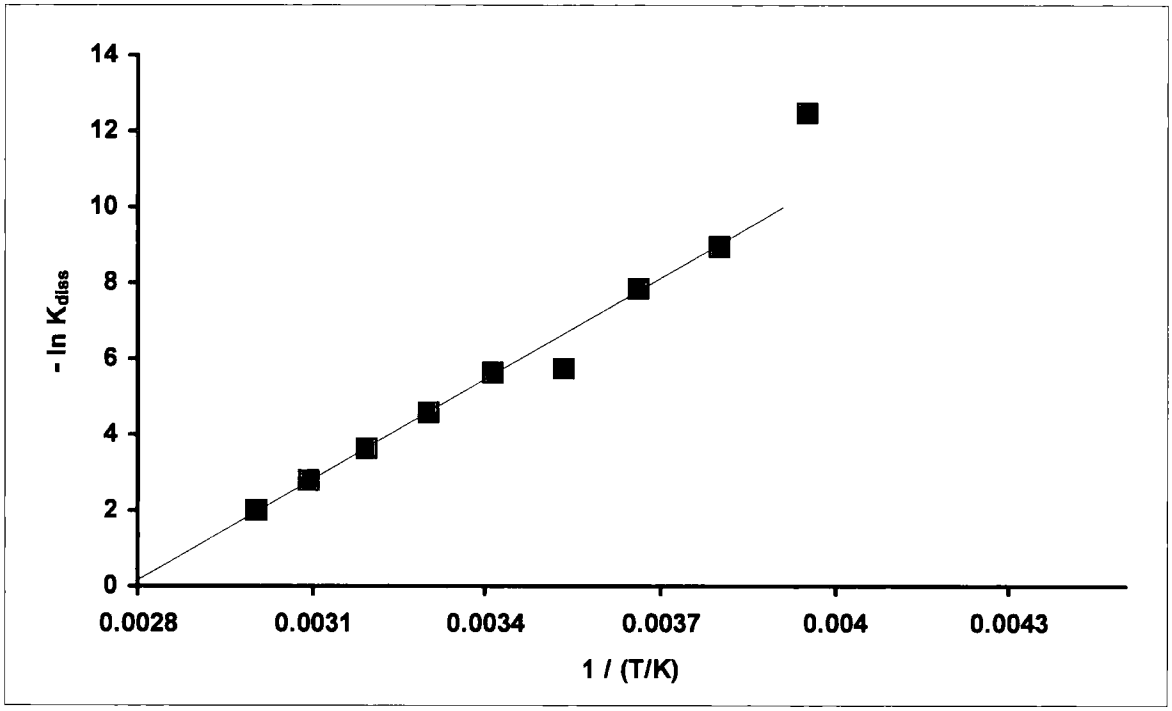

Figure 5.7. van't Hoff plot showing variation of K_{diss} with temperature.

5.2.4. NMR study of dimesitylborane in supercritical carbon dioxide

Supercritical carbon dioxide ($scCO_2$) is a fluid with properties intermediate between those of a liquid and a gas. It is formed under certain conditions of temperature and pressure, and is becoming widely used as a more environmentally benign alternative to traditional organic solvents.[23] One of the most useful properties of $scCO_2$ is its extremely low viscosity, which should result in increased tumbling speeds for solute molecules and a corresponding decrease in NMR line widths. Since much of the broadness of dimesitylborane ^{11}B-NMR peaks in traditional solvents is attributed to the slow tumbling speed of these bulky molecules, we decided to investigate whether a reduction in line widths would result from recording spectra in $scCO_2$. We were also interested in observing whether the position of monomer –

dimer equilibrium would be changed, and whether dimesitylborane would coordinate to or react with CO_2. To this end, we performed some preliminary studies in collaboration with Dr. Jonathon Iggo at the University of Liverpool, who operates a multinuclear NMR spectrometer capable of recording spectra in $scCO_2$.

The work was hampered by the unusual sensitivity of dimesitylborane to traces of moisture under the conditions employed in these experiments, and by the apparently low solubility of dimesitylborane and its hydrolysis products (resulting in low signal-to-noise ratios). It was necessary to use relatively large samples (ca. 250 mg) in order to scavenge water without converting all dimesitylborane to hydrolysis products, which contributed to the low resolution of proton spectra due to the inhomogeneous nature of the mixtures obtained. For this reason, proton spectra did not yield useful information and will not be further discussed here.

Initial experiments showed no evidence for the presence of dimesitylborane, with a single resonance at ca. 49 ppm. Despite increased precautions to exclude moisture, this was always the dominant species present; analysis of samples after the $scCO_2$ experiments revealed this to be primarily Mes_2BOH and $Mes_2B\text{-}O\text{-}BMes_2$, which have similar chemical shifts. With greater precautions with regard to moisture removal, it was possible to observe peaks attributed to monomeric (72.4 ppm) and dimeric dimesitylborane (31.3 ppm) (Figure 5.8). Without proton decoupling, the peak at 31.3 ppm split to a doublet with J(B-H) = 111 Hz, which is in the range expected for terminal B-H bonds (Figure 5.9). Proton coupling was not observed for the dimer, probably because of a lower coupling constant. Under all conditions investigated (45 - 90 °C), the intensity of the monomer peak was approximately equal to or greater than the intensity of dimer peak; it is tempting, therefore, to suggest that in $scCO_2$ the position of equilibrium is shifted towards monomer formation w.r.t.

conventional solvents, but the low signal to noise ratio means that this can only be a tentative assessment. At temperatures above 90 °C peaks attributed to dimesitylborane disappeared, with only Mes_2BOH remaining. Higher temperatures (> 140 °C) resulted in the loss of all peaks, suggesting that even Mes_2BOH was decomposed to insoluble products such as boric acid ($B(OH)_3$).

The low stability to hydrolysis of dimesitylborane in $scCO_2$ might be explained by the presence of acids such as H_2CO_3 and $[HCO_3]^-$ as shown in equations 1 and 2. Water can also be generated by the dehydration of two molecules of Mes_2BOH to form $Mes_2B\text{-}O\text{-}BMes_2$, both of which were detected in the residue remaining after the $scCO_2$ experiments. It is also possible that a reactive complex formed by reaction with CO_2 may be involved.

$$H_2O + CO_2 \rightleftharpoons H_2CO_3 \rightleftharpoons H^+ + [HCO_3]^- \rightleftharpoons 2H^+ + [CO_3]^{2-} \quad \textbf{(1)}$$

$$R_2BH + H^+ \longrightarrow H_2 + [R_2B]^+ \xrightarrow{H_2O} R_2BOH + H^+ \quad \textbf{(2)}$$

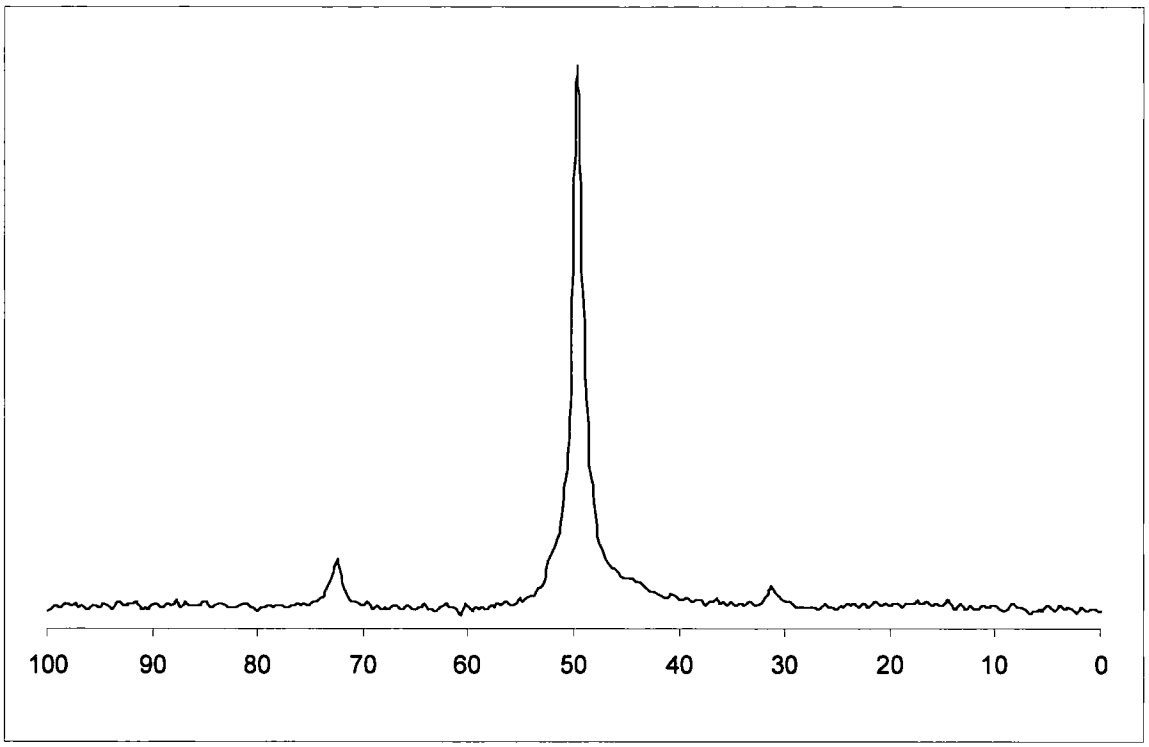

Figure 5.8. $^{11}B\{^1H\}$ NMR spectrum of dimesitylborane in $scCO_2$ (348 K, 190 bar) showing both monomer and dimer resonances and decomposition products.

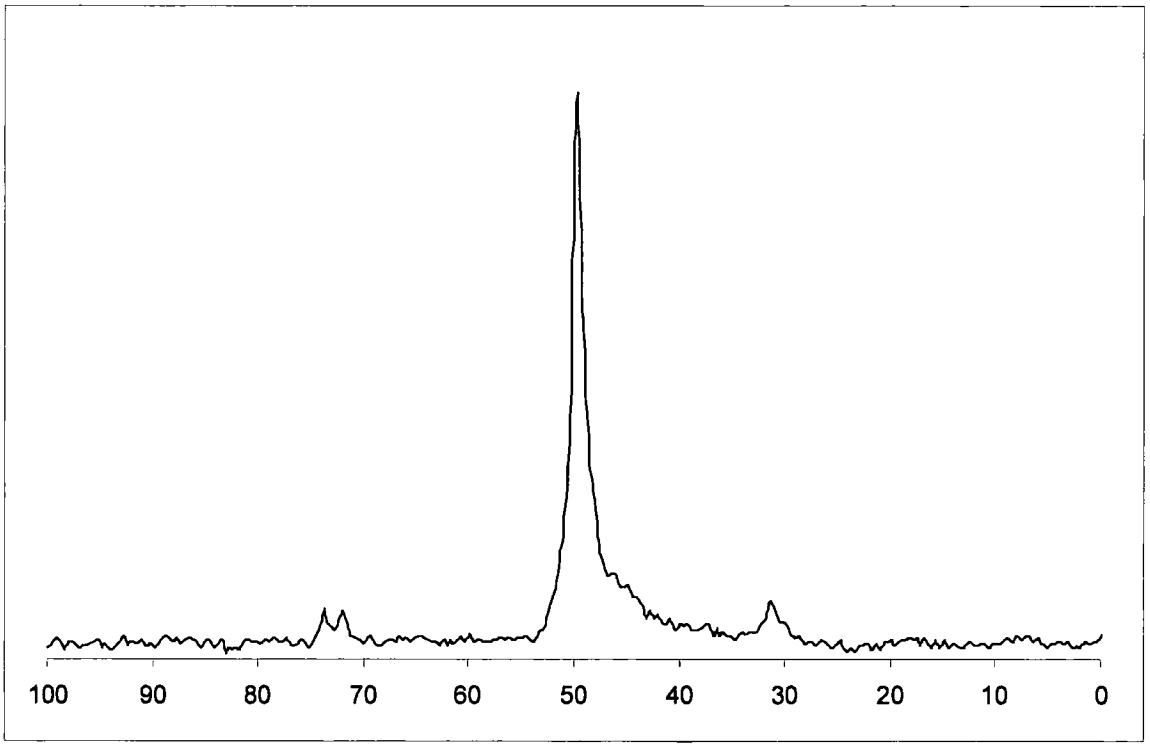

Figure 5.9. ^{11}B NMR spectrum of dimesitylborane in $scCO_2$ (348 K, 190 bar) demonstrating B-H coupling in the monomer.

5.2.5 Neutron and X-ray crystallography

The solid-state structure of dimesitylborane dimer was determined by single crystal neutron at 20 K and X-ray diffraction at 120 K (Figure 5.10). Important geometrical parameters are listed in Table 5.2. The B–H bond length determined by X-ray diffraction is significantly shorter than the length determined from neutron diffraction, consistent with the errors associated with locating the hydrogen atom by X-ray diffraction.[24] This is also apparent from the reduced B-H-B angle and the larger e.s.d.s in the X-ray data, and results in a contraction of the apparent B_2H_2 unit when determined by X-ray diffraction. This contraction of the B_2H_2 unit is also evident in X-ray crystal structures determined for related diborane(6) derivatives.[15,17,25-33] Geometrical values concerning the heavy atoms in the dimesitylborane dimer are within experimental error for both the neutron and X-ray structures. The B_2H_2 system in dimesitylborane is very close to D_{2h} symmetry, although only the two-fold rotational axis through H1 and H2 is crystallographically imposed.

The location of hydrogens determined by gas-phase electron diffraction is considered to be accurate, and several diboranes have been studied by this technique.[34,35,36] Values for tetramethyldiborane ($Me_4B_2H_2$) and diborane(6) (B_2H_6) are included in Table 2 for comparison.[34,35] Although data is limited, there is an apparent trend in the structural parameters of the B_2H_2 unit on going from the bulky mesityl groups, to the less bulky methyl groups and finally, to hydrogens as the terminal groups, with the B···B distances becoming shorter and the H-B-H angles becoming larger. An interesting point in this series is that the B-H bond lengths remain largely unchanged.

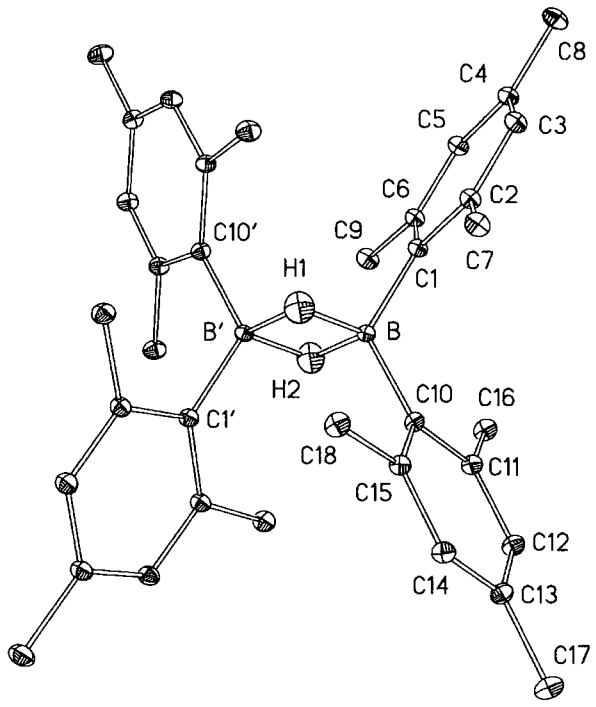

Figure 5.10. ORTEP diagram of the molecular structure of $[Mes_2BH]_2$ (neutron data, 50% thermal ellipsoids) with all hydrogen atoms except the bridging hydrogens omitted for clarity. Bridging hydrogens are also represented by 50% thermal ellipsoids.

A search of the Cambridge Structural Database reveals that forty structures of compounds containing boron have been solved using neutron diffraction. Of these, the majority are salts containing anions such as BF_4^- or BPh_4^-. Of the remaining compounds, twelve contain B–H bonds [37,38,39,40,41,42,43,44,45] including only three that contain B–H–B bridging bonds such as those occurring in the dimesitylborane dimer. Decaborane [46] exhibits a range of bridging B-H distances from 1.321 to 1.354 Å. In contrast, the B-H-B bridge in the compound [8-dimethylamino-1-(dimethylammonio)naphthalene]$^+$ [10,11-μ-H-7,8-dicarba-nido-undecaborate]$^-$ is unsymmetric, with a short bond length of 1.253 Å and a significantly longer bond of

1.469 Å.[22] In the heptahydroborate anion $[H_3\text{-}B\text{-}H\text{-}BH_3]^-$, the B-H-B is also unsymmetric, with rather short bond lengths of 1.324 and 1.216 Å.[47] From this limited data set, it appears that the symmetric dimesitylborane dimer has bridging B-H bond lengths that lie close to the midpoint of the range of values exhibited by B–H–B bridged compounds.

Table 5.2. Selected bond lengths and angles for the borane dimers $R_4B_2H_2$ by X-ray (R = Mes), neutron (R = Mes) and electron diffraction (R = Me, H) methods.

$R_4B_2H_6$	R = Mes X-Ray	R = Mes Neutron	R = Me Electron	R = H Electron
B–H (Å)	1.280(15) 1.288(16)	1.340(2) 1.342(2)	1.36(4)	1.339(4)
B---B (Å)	1.856(3)	1.855(2)	1.84(1)	1.775(4)
B–C (Å)	1.5959(19) 1.5972(19)	1.5959(13) 1.6000(14)	1.590(3)	
B-H-B (°)	93	87.7	85	83
H-B-H (°)	87.5(10)	92.46(14)	95(3)	97.0(3)
C-B-C (°)	123.43(11)	123.70(8)	120.0(13)	

5.2.6 Computational studies

Computational studies were carried out by Dr. Mark A. Fox. While the fully optimized geometry of the dimesitylborane dimer at the computationally intensive MP2/6-31G* level of theory is desirable for comparison with our experimental data, it could not be achieved due to computing limitations. Nevertheless, the optimized geometry of the dimer at the HF/6-31G* level is in fairly good agreement with the observed structural data. Calculated (GIAO) boron NMR shifts generated from the HF/6-31G* optimized geometries of the dimesitylborane monomer and dimer are 68.7

and 25.3 ppm in agreement with observed shifts of 73.3 and 25.9 ppm in aromatic solvents and 65.1 and 22.9 ppm in THF.

Unlike for the dimesitylborane dimer, we were able to carry out MP2/6-31G* geometry optimizations of the dimesitylborane monomer and the related dimesitylfluoroborane. Selected geometric parameters for these compounds are listed in Table 5.3 and the fully optimized geometry of the monomer is shown in Figure 5.11 and that of Mes_2BF in Figure 5.12. Comparison of the optimised geometry of the dimesitylborane monomer with the structures of dimesitylfluoroborane (by optimized geometry and by X-ray diffraction[48]) and ditripylborane (by X-ray diffraction[17]) in Table 4.3 reveals a very good agreement between the optimized and X-ray geometries of the fluoroborane and that there is little difference in the geometry around the boron atom in all cases. The geometries appear to be dominated by the steric effects of the mesityl groups rather than electronic or steric effects from the similarly sized fluorine or hydrogen atoms. Replacing a mesityl group with the bulkier tripyl group causes an increase in the C–B–C angle due to even greater steric congestion. The experimental value of the B-H bond length in the ditripylborane is, as expected by X-ray diffraction, shorter than that for the optimized geometry of the dimesitylborane monomer. The ^{11}B NMR shift computed (at the GIAO-B3LYP/6-311G* level) for the MP2/6-31G* optimized geometry of the dimesitylborane monomer is 70.6 ppm, confirming this geometry to be present in solution.

Table 5.3. Selected bond lengths and angles for the MP2/6-31G* optimised dimesitylborane monomer and dimesitylfluoroborane and for the structures of dimesitylfluoroborane and ditripylborane solved by X-ray diffraction.

	Mes_2BH calc	Mes_2BF calc	Mes_2BF X-ray	$Trip_2BH$ X-ray
B-X (Å)	1.202	1.354	1.339(2)	1.13(4)
B-C (Å)	1.557	1.563	1.568(2) 1.570(2)	1.564(6) 1.570(6)
C-B-C (°)	124.21	125.66	125.39(14)	128.0(4)
C-B-X (°)	117.90 117.88	117.17	116.82(14) 117.79(14)	116(2) 116(2)

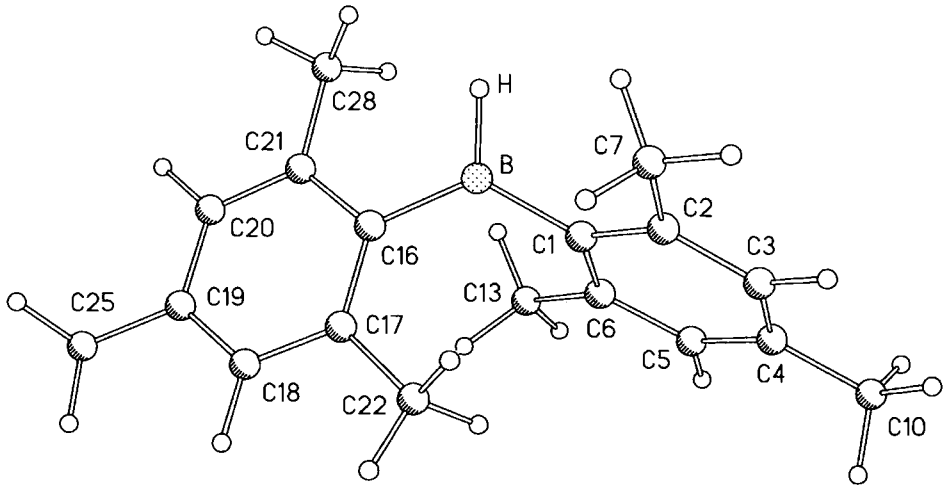

Figure 5.11. Ball and stick diagram of the optimised geometry of Mes_2BH at the MP2/6-31G* level.

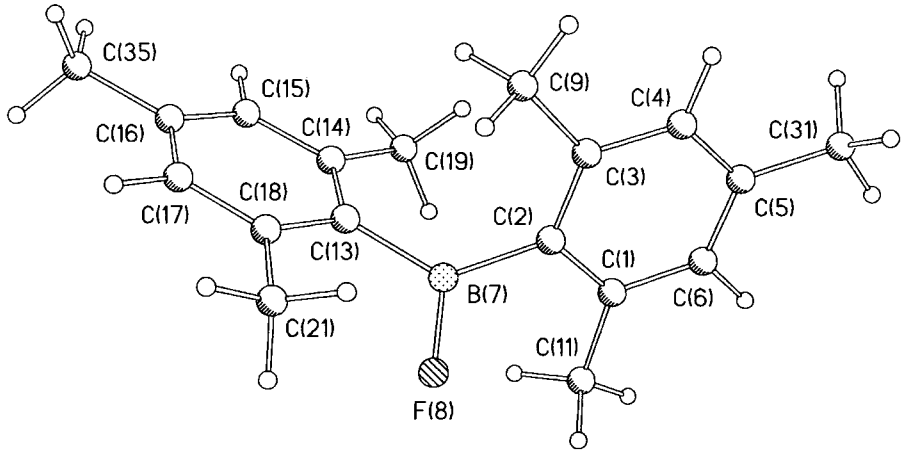

Figure 5.12. Ball and stick diagram of the optimised geometry of Mes_2BF at the MP2/6-31G* level.

Table 5.4 lists the binding energies for a selection of boranes that are either known in the monomeric form or commonly used in hydroboration. These were calculated from the energies of monomeric and dimeric species for which geometries were optimized at the HF/6-31G* level.[49] The binding energy of the dimesitylborane dimer was computed to be 79 $kJmol^{-1}$, which indicates the dimesitylborane monomer to be the more stable form thermodynamically in the gas-phase. It is stressed here that this value is only useful for comparing with related boranes since a low level of theory was used.[49] The trends in the binding energies are in broad agreement with the monomeric and dimeric species reported experimentally.[1517,27,28,34,35,50] It is clear from Table 5.4. that the trend towards monomeric species on going from dimesitylborane to ditripylborane is due to steric factors.

Table 5.4. Total and binding energies for selected boranes at the HF/6-31G* level of theory. A positive sign in the binding energy indicates that the dimer is lower in energy than the separated monomers.

R	R_2BH (au)	$R_4B_2H_2$ (au)	Binding Energy ($kJmol^{-1}$)	Known species
tripyl	-1188.12265	dissociates	-	Monomer
R_2 = cat	-404.62598	dissociates	-	Monomer
thexyl	-494.79999	dissociates	-	Monomer
R_2BH = 9-TMS-10-BBD	-782.59496	-1565.15523	-91.06	Dimer / Monomer
mesityl	-719.72702	-1439.42378	-79.42	Dimer / Monomer
phenyl	-485.52413	-971.03316	-39.62	Not known
C_6F_5	-1473.96407	-2947.92446	-9.68	Dimer / Monomer
methyl	-104.49136	-208.99327	27.70	Dimer
R_2BH = 9-BBN	-336.35384	-672.72162	36.59	Dimer
H	-26.39001	-52.812401	85.01	Dimer

5.3. Conclusions

We show here by NMR spectroscopy that the dimesitylborane monomer exists in equilibrium with the known dimesitylborane dimer. The presence of relatively large amounts of monomer in dimesitylborane solutions can be attributed mainly to steric factors, with the change from four to three-coordination on forming the monomer relieving congestion. The low reactivity of dimesitylborane, despite the high proportion of monomer, may be due to steric bulk, inhibiting the formation of a π-complex with unsaturated substrates, or due to a labile complex with donor solvents such as THF. NMR experiments in $scCO_2$ provided a value for the B-H coupling of

the monomer. Neutron diffraction was carried out on a diborane(6) compound for the first time, providing a more accurate geometry for the BH_2B unit in a solid state structure of a diborane(6) compound than could be achieved by X-ray diffraction. By *ab initio* computations, the geometry of the dimesitylborane monomer was optimised at the MP2/6-31G* level and confirmed by the computed boron NMR shift. The trend in the calculated binding energies between the monomer and dimer in selected boranes is in good agreement with their known tendencies to exist as monomeric and / or dimeric species.

5.4. Experimental

5.4.1 General

All solvents were dried over and distilled under nitrogen from appropriate drying agents. NMR solutions were made up in an Innovative Technology Inc. nitrogen-filled glovebox. NMR spectra were acquired on a Varian Unity Inova 500 MHz spectrometer. Proton spectra were recorded at 500 MHz and referenced to residual protonated solvent. Boron spectra were recorded at 160 MHz and referenced to external $BF_3 \cdot OEt_2$.

5.4.2 Synthesis

5.4.2.1. Preparation of dimesitylfluoroborane

Dimesitylfluoroborane was prepared via a modified literature procedure.[51] The compounds bromomesitylene and boron trifluoride-diethyl etherate were obtained from Lancaster Chemical Company and were dried over and distilled from calcium hydride prior to use.

An oven-dried, three necked, 500 ml round-bottomed flask was fitted with a reflux condenser and a dropping funnel. Dry magnesium turnings (2.0 g, 82 mmol) and a magnetic stir-bar were added to the flask, a vacuum take-off was fitted, and the apparatus was purged of oxygen by evacuation/nitrogen refill. The flask was charged with THF (100 ml) and a crystal of iodine. The dropping funnel was charged with bromomesitylene (15.0 g, 75.4 mmol) and THF (150 ml) and several millilitres were admitted to the reaction flask. The unstirred reaction mixture was warmed with a hot air gun until initiation occurred, after which the bromomesitylene solution was added dropwise with rapid stirring so as to maintain a gentle reflux. The mixture was heated to relux for 3 h, cooled to room temperature and diluted with THF (100 ml). An aliquot was quenched with ethanol and showed no remaining bromomesitylene by GC-MS.

An oven-dried, three necked, one litre round-bottomed flask was fitted with a mechanical stirrer, a reflux condenser and a dropping funnel and purged by evacuation / nitrogen refill. The flask was charged with boron trifluoride-diethyl etherate (5.0 g, 36 mmol) and cooled to 0 °C with an ice bath. The previously prepared Grignard solution was transferred to the dropping funnel via cannula and added dropwise with vigorous stirring to the reaction vessel, resulting in a dense white precipitate. After complete addition, the reaction mixture was allowed to warm to room temperature overnight.

The mixture was allowed to settle and the supernatant liquid was transferred via cannula to a one litre, round-bottomed flask with vacuum take-off. The residue was extracted with hexane (5 x 50 ml) and the combined extracts were transferred to a second one litre round-bottomed flask with vacuum take-off via filter cannula and concentrated *in vacuo* to give a white solid, 9.2 g (95 %) which was used without

further purification. High quality crystals for X-ray diffraction were obtained by slow evaporation of an ether solution.

^{1}H NMR ($CDCl_3$) 6.66 (s, 4H, aryl), 2.29 (s, 6H, *o*-methyl), 2.28 (6H, *o*-methyl), 2.10 (6H, *p*-methyl). $^{19}F\{^{1}H\}$ NMR ($CDCl_3$) −14.5 (s). $^{11}B\{^{1}H\}$ NMR ($CDCl_3$) 53 (s, broad).

5.4.2.2. Preparation of dimesitylborane

Dimesitylborane was prepared by the reduction of dimesitylfluoroborane with lithium aluminium hydride.

In the glovebox, a suspension of lithium aluminium hydride (0.14 g, 2.5 mmol) in dimethoxyethane (100 ml) was added dropwise to a solution of dimesitylfluoroborane (2.68 g, 10 mmol) and the mixture was stirred overnight at room temperature, resulting in a dense white precipitate. An aliquot was taken and examined by ^{11}B NMR and ^{19}F NMR, which revealed no remaining dimesitylfluoroborane. The reaction mixture was allowed to settle for 3 h and the supernatant liquid removed via syringe. The residue was extracted with toluene (4 x 50 ml) and the combined extracts filtered through a pad of Celite and concentrated *in vacuo* to give a colourless solid. The solid was recrystallised from a mixture of THF and diethyl ether and washed with diethyl ether and hexane to give colourless crystals, 2.30 g (92 %).

5.4.3. NMR experiments in $scCO_2$

NMR spectra were recorded on a Bruker AM 200 SWB spectrometer equipped with a home – built high pressure NMR cell and sapphire NMR tube. ^{1}H NMR spectra were referenced to external tetramethylsilane (0.0 ppm). ^{11}B NMR spectra were

referenced to external $KBF_{4\ (aq)}$ (-2.0 ppm). High purity carbon dioxide was passed through a centrifugal drier and then over activated molecular sieves before pressurising the sample chamber. The sample was mixed by raising and lowering the temperature (and pressure) to encourage convection currents.

5.4.4. Computational methods

All *ab initio* computations were carried out with the Gaussian 98 package.[52] The structures of the dimesitylborane dimer and monomer were optimized at the HF/6-31G* level with no symmetry constraints. Frequency calculations were computed on these optimized geometries at the HF/6-31G* level for imaginary frequencies. Optimisation of the HF/6-31G* geometry for the monomer was then carried out at the computationally intensive MP2/6-31G* level of theory. Theoretical ^{11}B chemical shifts were referenced to B_2H_6 (16.6 ppm)[53] and converted to the usual $BF_3{\cdot}OEt_2$ scale: $\delta(^{11}B) = 123.4 - \sigma(^{11}B)$ at the RHF/6-31G*//RHF/6-31G* level and $\delta(^{11}B) = 102.83 - \sigma(^{11}B)$ at GIAO-B3LYP/6-311G*//MP2/6-31G*.

5.4.5. Neutron Structure Determinations

A clear rod shaped crystal of dimensions 0.9 x 1.4 x 5.2 mm^3 was glued with Kwikfill to a 1 mm V pin, and cooled slowly to 20 K using an Air Products 201 Helium Displex[54] cryorefrigerator on the D19 instrument[55] at the ILL (equipped with both a 4 ° x 64 ° 'banana' detector and a 20 ° x 20 ° square detector). Reflections were collected on both detectors quasi-simultaneously using equatorial and normal beam geometry, and scaled together empirically using common reflections. Three standard reflections showed no change in intensity during the data collection. Reflections were integrated using the 'Retreat' software. [56] Neutron structure refinement was carried out using SHELXL-97.

[57] Neutron coherent scattering lengths were taken from ref. 58. The initial difference Fourier map showed clearly the positions of the ordered hydrogen atoms, though the presence of residual density in the difference map around the methyl group of C(16), coupled with very large ADP's, led to a disordered model for this group. Full anisotropic refinement for all atoms was then carried out.

Crystal data for dimesitylborane: C_{36} H_{46} B_2. M=500.00, pale yellow block, 6.25 mm^3 Monoclinic, Space group *P2/n* (No. 10), a = 12.2778(8), b = 7.7353(6), c = 16.5979(2) Å, ß= 109.836°, V= 1482.81(18) $Å^3$, Z = 2, D_c = 1.120 Mg/m^3, F_{000} = 156, ILL D19, neutron radiation, λ = 1.3186(1) Å, T = 20(2)K, $2\theta_{max}$ = 132.28°, 10868 reflections collected, 3342 unique (R_{int} = 0.0391). Final *GoF* = 1.134, *R1* = 0.0354, *wR2* = 0.0833, *R* indices based on 3078 reflections with I >2σ (I) (refinement on F^2), 409 parameters, 0 restraints. Absorption corrections (μ = 4.44 cm^{-1}) were applied with the program d19abs, based on the ILL version of the CCSL system.[59]

5.4.6. X-ray Structure Determinations

A colourless block shaped crystal of dimensions 0.3 x 0.2 x 0.12 mm^3 was oil mounted onto a hair and flash cooled to 120 K under nitrogen gas flow, Oxford Cryosytems Cryostream. [60] 16175 reflections (2.58 < θ < 28.46 °) were collected on a Brucker SMART-CCD 6K diffractometer [61,62] (ω-scans, 0.3 ° $frame^{-1}$) yielding 3817 unique data. The structure was solved by direct methods and refined by full matrix least squares based on F^2 for all data using SHELXL-97 [57] software. All non-hydrogen atom were refined with anisotropic displacement factors, hydrogen atoms were placed geometrically at calculated positions and refined with a ridged model. Though the presence of residual electron density in the difference map around the methyl groups of C(13), C(14), C(15) and C(16), a disordered model for these groups was employed.

Final *GoF* = 1.042, *R1* = 0.0501, *wR2* = 0.1441, *R* indices based on 2855 reflections with $I > 4\sigma(I)$ (192 parameters).

a = 12.2566(6), *b* = 7.7598(4), *c* = 16.7075(9) Å, ß = 109.5960(10)°, *V*= 1496.99(13) $Å^3$, Monoclinic, space group *P2/n* (No. 10), Mo-Kα, λ = 071073 Å, D_c = 1.110 Mg/m^3.

5. 5. References

[1] Hooz, J.; Akiyama, S.; Cedar, F.J.; Bennet, M.J.; Tuggle, R.M. *J. Am. Chem. Soc.* **1974**, *96*, 274.

[2] Pelter, A.; Singaram, S.; Brown, H.C. *Tetrahedron Lett.* **1983,** *24,* 1433.

[3] Yuan, Z.; Taylor, N.J.; Ramachandran, R.; Marder, T.B. *Appl. Organomet. Chem.* **1996**, *10,* 305.

[4] Yuan, Z; Taylor, N.J.; Marder, T.B.; Williams, I.D.; Kurtz, S.K.; Cheng, L.T. *J. Chem. Soc., Chem. Commun.* **1990**, 1489.

[5] Matsumi, N.; Naka, K.; Chujo, Y. *J. Am. Chem. Soc.* **1998**, *120*, 5112.

[6] Matsumi, N.; Miyata, M.; Chujo, Y. *Macromolecules* **1999**, *32*, 4467.

[7] Glagowski, M.E.; Williams, J.L.R. *J. Organomet. Chem.* **1981**, *216*, 1.

[8] Fiedler, J.; Zalis, S.; Klein, A.; Hornung, F.M.; Kaim, W. *Inorg. Chem.* **1996**, *35*, 3039.

[9] Lequan, M.; Lequan, R.M.; Ching, K.C. *J. Mater. Chem.* **1992**, *2*, 719.

[10] Kinoshita, M.; Shirota, Y. *Chem. Lett.* **2001**, 614.

[11] Yamaguchi, S.; Akiyama, S.; Tamao, K. *Org. Lett.* **2000**, *2*, 4129.

[12] Liu, Z.; Fang, Q.; Wang, D.; Xue, G.; Yu, W.; Shao, Z.; Jiang, M. *Chem. Commun.* **2002**, 2900.

[13] For reviews, see (a) Entwistle, C.D.; Marder, T.B., *Chem. Mater.* **2004**, in the press. (b) Entwistle, C.D.; Marder, T.B. *Angew. Chem. Intl. Ed. Eng.* **2002**, *41*, 2927. (c) Yuan, Z.; Collings, J.C.; Taylor, N.J.; Marder, T.B.; Jardin, C.; Halet, J-F. *J. Solid State Chem.* **2000**, *154*, 5.

[14] Chandrasekharan, J.; Brown, H.C. *J. Org. Chem.* **1985**, *50*, 518.

[15] Parks, D.J.; Piers, W.E.; Yap, G.P.A. *Organometallics* **1998**, *17*, 5492.

[16] Soderquist, J.A.; Matos, K.; Burgos, C.H.; Lai, C.; Vacquer, J.; Medina, J.R.; *Contemporary Boron Chemistry,* Spec. Publ. No. 253 (Eds.: Davidson, M.G.; Hughes, A.K.; Marder, T.B.; Wade, K.;), The Royal Society of Chemistry, Cambridge (2000) p. 472.

[17] Bartlett, R.A.; Rasika Dias, H.V.; Olmstead, M.M.; Power, P.P.; Weese, K.J. *Organometallics* **1990**, *9*, 146.

[18] Negishi, E.; Katz, J.J.; Brown, H.C. *J. Am. Chem. Soc.* **1972**, *94*, 4025.

[19] Aldridge, S.; Calder, R.J.; Rossin, A.; Dickinson, A.A.; Willock, D.J.; Jones, C.; Evans, D.J.; Steed, J.W.; Light, E.M.; Coles, S.J.; Hursthouse, M.B. *J. Chem. Soc., Dalton Trans.* **2002**, 2020.

[20] Lane, C.F.; Kabalka, G.W. *Tetrahedron* **1976**, *32*, 981.

[21] Ho, N.N.; Bau, R.; Plecnik, C.; Shore, S.G.; Wang, X.; Schultz, A.J. *J. Organomet. Chem.* **2002**, *654*, 216.

[22] Fox, M.A.; Goeta, A.E.; Howard, J.A.K.; Hughes, A.K.; Johnson, A.L.; Keen, D.A.; Wade, K.; Wilson, C.C. *Inorg. Chem.* **2001**, *40*, 173.

[23] For recent reviews of the use of $scCO_2$, see: (a) Noyori, R., Guest Ed., *Chem. Rev.* **1999**, *99*, 353. (b) Oakes, R.S.; Clifford, A.A.; Rayner, C.M. *J. Chem. Soc., Perkin Trans.* **2001**, *1*, 917.

[24] Jones, D.S.; Lipscomb, W.N. *Acta Crystallogr.* **1970**, *A26*, 196.

[25] Smith, H.W.; Lipscomb, W.N. *J. Chem. Phys.* **1965**, *43*, 1060.

[26] Liu, J.; Meyers, E.A.; Shore, S.G. *Inorg. Chem.* **1998**, *37*, 496.

[27] Brauer, D.J.; Krüger, C. *Acta Crystallogr.* **1973**, *B29*,1684.

[28] Köster, R.; Willemsen, H.G. *Liebigs Ann. Chem.* **1974**, 1843.

[29] Al-Juaid, S.S.; Eaborn, C.; Hitchcock, P.B.; Kundu, K.K.; Molla, M.E.; Smith, J.D. *J. Organomet.Chem.* **1990**, *385*, 13.

[30] Paetzold, P.; Geret, L.; Boese, R. *J. Organomet. Chem.* **1990**, *385*, 1.

[31] Yalpani, M.; Boese, R.; Köster, R. *Chem. Ber.* **1987**, *120*, 607.

[32] Wadepohl, H.; Arnold, U.; Pritzkow, H. *Angew. Chem. Int. Ed. Engl.* **1997**, *36*, 974.

[33] Mennekes, T.; Paetzold, P.; Boese, R. *Angew. Chem. Int. Ed. Engl.* **1990**, *29*, 899.

[34] Carroll, B.L.; Bartell, L.S. *J. Am. Chem. Soc.* **1965**, *42*, 1135.

[35] Carroll, B.L.; Bartell, L.S. *Inorg. Chem.* **1968**, *7*, 219.

[36] Hedberg, L.; Hedberg, K.; Kohler, D.; Ritter, D.M.; Schomaker, W. *J. Am. Chem. Soc.* **1980**, *102*, 3430.

[37] Corey, E.J.; Cooper, N.J.; Canning, W.M.; Lipscomp, W.N.;, Koetzle, T.F. *Inorg. Chem.* **1982**, *21*, 192.

[38] Lawrence, S.H.; Shore, S.G.; Koetzle, T.F.; Huffman, J.C.; Wei, C-Y.; Bau, R. *Inorg. Chem.* **1985**, *24*, 3171.

[39] Klooster, W.T.; Koetzle, T.F.; Siegbahn, P.E.M.; Richardson, T.B.; Crabtree, R.H. *J. Am. Chem. Soc.* **1999**, *121*, 6337.

[40] Bernstein, E.R.; Hamilton, W.C.; Kiederling, T.A.; La Placa, S.J.; Lippard, S.J.; Mayerele, J.J. *Inorg. Chem.* **1972**, *11*, 3009.

[41] Broach, R.W.; Cheung, I-S.; Marks, T.J.; Williams, J.M. *Inorg. Chem.* **1983**, *22*, 1081.

[42] Kahn, S.A.; Morris, J.H.; Harman, M.; Hursthouse, M.B. *J. Chem. Soc., Dalton Trans.* **1992**, 119.

[43] Johnson, P.L.; Cohen, S.A.; Marks, T.J.; Williams, J.M. *J. Am. Chem. Soc.* **1978**, *100*, 2709.

[44] Takusagawa, F.; Fumigalli, A.; Koetzle, T.F.; Shore, S.G.; Schimitikons, T.; Fratini, A.V.; Morse, K.W.; Wei, C-Y.; Bau, R. *J. Am. Chem. Soc.* **1981**, *103*, 5165.

[45] Singh, P.; Zotolla, M.; Huang, S.; Shaw, B.R.; Pedersen, L.G. *Acta Crystallogr.* **1996**, *C52*, 52.

[46] Brill, R.; Dietrich, H.; Dierks, H. *Acta Crystallogr.* **1971**, *B27*, 2003.

[47] Kahn, S.I.; Chiang, M.Y.; Bau, R.; Koetzle, T.F.; Shore, S.G.; Lawrence, S.H. *J. Chem. Soc., Dalton Trans.* **1986**, 1753.

[48] Cornet, S.M.; Dillon, K.B.; Entwistle, C.D.; Fox, M.A.; Goeta, A.E.; Goodwin, H.P.; Marder, T.B. and Thompson, A.L., *J. Chem. Soc., Dalton Trans.* **2003**, 4395.

[49] DeFrees, D.J.; Raghavachari, K.; Schlegel, H.B.; Pople, J.A.; Schleyer, P.v.R. *J. Phys. Chem.* **1987**, *91*, 1857.

[50] Koster, R.; Benedikt, G. *Angew. Chem. Int. Ed. Engl.* **1963**, *2*, 323.

[51] Pelter, A.; Smith, K.; Brown, H.C. *"Borane Reagents," Best Synthetic Methods,* Academic Press, London, **1988**, p. 428.

[52] Gaussian 98, Revision A.9, Frisch, M.J.; Trucks, G.W.; Schlegel, H.B.; Scuseria, G.E.; Robb, M.A.; Cheeseman, J.R.; Zakrzewski, V.G.;

Montgomery, J.A. Jr.; Stratmann, R.E.; Burant, J.C.; Dapprich, S.; Millam, J.M.; Daniels, A.D.; Kudin, K.N.; Strain, M.C.; Farkas, O.; Tomasi, J.; Barone, J.; Cossi, M.; Cammi, R.; Mennucci, B.; Pomelli, C.; Adamo, C.; Clifford, S.; Ochterski, J.; Petersson, G.A.; Ayala, P.Y.; Cui, Q.; Morokuma, K.; Malick, D.K.; Rabuck, A.D.; Raghavachari, K.; Foresman, J.B.; Cioslowski, J.; Ortiz, J.V.; Baboul, A.G.; Stefanov, B.B.; Liu, G.; Liashenko, A.; Piskorz, P.; Komaromi, I.; Gomperts, R.; Martin, R.L.; Fox, D.J.; Keith, T.; Al-Laham, M.A.; Peng, C.Y.; Nanayakkara, A.; Challacombe, M.; Gill, P.M.W.; Johnson, B.; Chen, W.; Wong, M.W.; Andres, J.L.; Gonzalez, C.; Head-Gordon, M.; Replogle, E.S.; and Pople, J.A.; Gaussian, Inc., Pittsburgh PA, 1998.

[53] Onak, T.P.; Landesman, H.L.; Williams, R.E. *J. Phys. Chem.* **1959**, *63*, 1533.

[54] Archer, J.M.; Lehmann, M.S. *J. Appl. Cryst.* **1986**, *21*, 471.

[55] Thomas, M.; Stansfield, R.F.D.; Berneron, M.; Filhol, A.; Greenwood, G.; Jacobe, J.; Feltin, D.; Mason, S.A. *"Position-Sensitive Detection of Thermal Neutrons,"* P. Convert, J.B. Forsyth, Eds., Academic Press: London, **1983**, p 344.

[56] Wilkinson, C.; Khamis, H.W.; Stansfield, R.F.D.; McIntyre, G.J. *J. Appl. Cryst.* **1988**, *21*, 471.

[57] Sheldrick, G.M.; SHELXL-97: University of Göttingen, **1997**.

[58] Sears, V.F. *Neutron News* **1992** *3* 26.

[59] Matthewman, J.C.; Thompson, P.; Brown, P.J. *J. Appl. Cryst.* **1982**, *15*, 167.

[60] Cosier, J.; Glazer, A.M. *J Appl. Cryst.* **1986**, *19*, 105.

[61] Bruker SMART-V5.625. Data Collection Software. Siemens Analytical X-ray Instruments Inc., Madison, Wisconsin, USA.

[62] Bruker SAINT-V6.28A. Data Reduction Software. Siemens Analytical X-ray Instruments Inc., Madison, Wisconsin, USA.